



TECHNISCHE
UNIVERSITÄT
DARMSTADT

Modulation of the FKBP51 structure by protein engineering and isolation of conformation-locking antibodies and affibodies

at the Department of Chemistry
of the Technischen Universität Darmstadt

submitted in fulfilment of the requirement for the degree
Doctor rerum naturalium
(Dr. rer. nat.)

Doctoral Thesis

By

Jorge Alberto Lerma Romero

from Mexico City, Mexico

First reviewer: Prof. Dr. Harald Kolmar

Second reviewer: Prof. Dr. Felix Hausch

Darmstadt, 2024

Lerma Romero, Jorge Alberto: Modulation of the FKBP51 structure by protein engineering and isolation of conformation-locking antibodies and affibodies

Darmstadt, Technische Universität Darmstadt,

Year thesis published in TUprints: 2024

URN: urn:nbn:de:tuda-tuprints-265635

URL: <https://tuprints.ulb.tu-darmstadt.de/26563>

Date of submission: 08 November 2023

Day of the oral examination: 22 January 2024

In Copyright:

<https://rightsstatements.org/page/InC/1.0/>

Publications derived from this work

Lerma Romero, JA., Meyners, C., Christmann, A., Reinbold, L. M., Charalampidou, A., Hausch, F., & Kolmar, H. (2022). Binding pocket stabilization by high-throughput screening of yeast display libraries. *Frontiers in Molecular Biosciences*, 9, 1023131. <https://doi.org/10.3389/fmolb.2022.1023131>

Lerma Romero JA & Kolmar, H. (2023). Accessing Transient Binding Pockets by Protein Engineering and Yeast Surface Display Screening. *Methods in molecular biology* (Clifton, N.J.). 2681. 249-274. 10.1007/978-1-0716-3279-6_14.

Lerma Romero JA, Meyners C, Rupp N, Hausch F, Kolmar H (2023). A protein engineering approach towards understanding FKBP51 conformational dynamics and mechanisms of ligand binding. *Protein Engineering, Design and Selection*; gzad014, <https://doi.org/10.1093/protein/gzad014>

Contributions to Publications & Conferences

Publications

Schneider H, Englert S, Macarrón Palacios A, **Lerma Romero JA**, Ali A, Avrutina O, Kolmar H. Synthetic Integrin-Targeting Dextran-Fc Hybrids Efficiently Inhibit Tumor Proliferation In Vitro. *Front Chem.* 2021 Jul 22;9:693097. doi: 10.3389/fchem.2021.693097. PMID: 34368077; PMCID: PMC8339797.

Conferences

Lerma Romero JA, Meyners C, Christmann A, Hausch F, Kolmar H. FKBP51 transient binding pocket stabilization by protein engineering (poster). PEGS Europe, Barcelona (Spain) (14–16 November 2022).

Lerma Romero JA, Meyners C, Hausch F, Kolmar H. Conformation locking scFvs for the research and discovery of FKBP51 selective ligands (presentation and poster). PEGS Europe, Lisbon (Portugal) (14–16 November 2023).

Table of contents

Publications derived from this work	iii
Contributions to Publications & Conferences	iii
Table of contents	iv
Scientific Novelty & Significance	ii
Zusammenfassung und wissenschaftlicher Erkenntnisgewinn.....	v
Individual Contributions by J.A. Lerma Romero for Cumulative Section.....	viii
1 Introduction	1
1.1 <i>Challenges of drug discovery for protein families</i>	1
1.2 <i>Allostery</i>	2
1.3 <i>Transient binding pockets</i>	4
1.4 <i>Protein engineering</i>	4
1.4.1 <i>Directed evolution</i>	5
1.4.2 <i>Random mutagenesis</i>	6
1.4.3 <i>Site-saturation mutagenesis</i>	6
1.4.4 <i>Combinatorial and iterative mutagenesis</i>	7
1.5 <i>Display technologies</i>	7
1.5.1 <i>Yeast surface display</i>	8
1.6 <i>Fluorescence-activated cell sorting (FACS)</i>	10
1.7 <i>Antigen binding molecules for research</i>	10
1.7.1 <i>Single-chain variable fragments (scFvs)</i>	12
1.7.2 <i>Affibody molecules</i>	13
1.8 <i>FK506-binding proteins (FKBPs) and FKBP51</i>	14
1.8.1 <i>The role of immunophilins in the transcriptional activity of glucocorticoid receptor</i>	15
1.8.2 <i>FKBP51 and FKBP52</i>	16
1.8.3 <i>FKBP51 in disease</i>	17
1.9 <i>FKBP51 transient binding pocket and selective inhibitors</i>	18
2 Objective	19
3 References.....	20
4 Cumulative Section	37
4.1 <i>Binding pocket stabilization by high-throughput screening of yeast display libraries</i>	37
4.2 <i>Accessing Transient Binding Pockets by Protein Engineering and Yeast Surface Display Screening</i>	69
4.3 <i>A protein engineering approach towards understanding FKBP51 conformational dynamics and mechanisms of ligand binding</i>	96
4.4 <i>Conformation locking scFvs and affibodies for the research of FKBP51 transient binding pocket</i>	117
5 Acknowledgments	172
6 Curriculum Vitae.....	174
7 Erklärung laut Promotionsordnung	175

Scientific Novelty & Significance

Proteins are biomolecules with an intrinsic flexibility that enables them to carry out their functions by interacting with other proteins, substrates, cells, and many other molecules. The structural flexibility of a protein influences ligand-protein binding, and for some therapeutic targets, this feature can limit the access to its binding site. This presents a constraint for the development of novel molecules to inhibit or activate a target protein.

The FK506 binding protein 51 (FKBP51) is a member of the immunophilin family, and it is linked to several psychiatric and stress-related disorders, among many other reported diseases. Various members of the FKBP family possess an FK1 domain with a highly conserved active site (or orthosteric site). This is not only specific for FKBP51, but it is common to find largely conserved orthosteric sites across protein families. Due to small differences in the amino acid sequence of FKBP51 compared to other members of its family, this protein exhibits higher flexibility than other FKBP51s, which translates into a higher number of possible conformers. One of these reported conformers forms a transient binding pocket that can potentially accommodate FKBP51-selective ligands without interacting with other members of this protein family. This doctoral thesis focuses on the development of research tools to shift the conformational ensemble of FKBP51 from the native low-energy state (closed conformation) to a conformer with a stabilized transient binding pocket that can bind conformation-specific ligands.

The first part of this work focuses on a protein engineering and screening strategy that was used to successfully identify FKBP51 variants with a favored open conformation of a transient binding pocket. To that end, the amino acids of the FKBP51 FK1 domain were systematically modified by random and Site Saturation Mutagenesis (SSM) to spot FKBP51 mutants that change the distribution of the protein to an open conformation, favoring the binding of two reported conformation-specific ligands. Firstly, random mutagenesis was used to mutate the FK1 domain-encoding gene of FKBP51. With this genetic material, a Yeast Surface Display (YSD) library presenting a pool of mutagenesis variants was created and screened via high throughput Fluorescence-Activated Cell Sorting (FACS). From this first library, a specific region of the protein that destabilizes the FKBP51 binding pocket was identified. Subsequently, an SSM of the identified region spanning glycine-64 to serine-69 was applied, and a second YSD library was created and screened *via* FACS. From this SSM library, key residues for the destabilization of the FKBP51 binding pocket were identified. Three mutants with enhanced affinity to conformation-specific ligands (G64S, F67E, and D68Y) were characterized by fluorescence polarization and crystallography, and demonstrated to facilitate a cryptic site formation which enables the binding of the open conformation ligands.

In subsequent experiments, these three improved FKBP51 variants were used as a starting point to create libraries with multiple mutations to further optimize the affinity to open conformation ligands. Additional SSM libraries based on combinatorial and iterative mutagenesis yielded over 20 FKBP51 variants with two or more mutations that improved ligand binding. Moreover, variants with a mutated position K121 confirmed the

importance of this loop region which was not identified in the initial experiments. From all four different libraries, over 30 unique FKBP51 muteins with one or multiple exchanged amino acids were found.

FKBP51 is one of the many proteins with a reported transient binding pocket. Cryptic sites in a protein represent a unique opportunity to design high-affinity ligands that bind selectively to the target protein without interacting with structurally similar proteins and consequently, avoid off-target effects. Our protein engineering-based research used FKBP51 as a model to test the possibilities and potential benefits of protein engineering methods coupled with a cell display system such as yeast surface display (YSD) and FACS to identify variants with enhanced binding to open conformation ligands. These methods were described in detail and are transferable to other proteins that, similarly to FKBP51, exhibit a transient binding pocket. This step-wise methodology can be used to systematically modify a target protein to shift a population from a native state with a low-populated conformer with a cryptic site, to a population with an open conformation that permits the binding of selective ligands.

The second part of this study focused on the use of chicken-derived single-chain variable fragments (scFvs) as conformation-locking molecules to stabilize the open conformation of FKBP51 and facilitate the screening of novel selective inhibitors. An allosteric effector, in this case an scFv, would be able to redistribute the protein conformational ensembles, optimally favoring a low-populated conformation found in the unbound state.

Because of the large evolutionary distance between humans and avians, chickens have a stronger immune response to human proteins than conventional murine immunizations to develop antibodies. For this reason, a *Gallus gallus* specimen was immunized with the FK1 domain of FKBP51. From the splenic RNA of the immunized animal, a pool of scFvs was synthesized and used to create a YSD library. This library was then screened in different campaigns to obtain either high-affinity binders, conformation locking, or blocking scFvs.

While no blocking scFvs were found, the conformation-locking screening campaign generated six different scFvs, and one of them showed potential allosteric effects on FKBP51 which influenced the binding of canonical and conformation-selective ligands. Multiple fluorescence polarization (FP) and biolayer interferometry (BLI) assays were able to demonstrate the effect of the isolated clone T32, as a conformation-locking scFv. The allosteric effects of T32 were orthogonally assessed by Hydrogen/Deuterium exchange Mass Spectrometry (HDX-MS), which revealed the binding epitope on FKBP51 and a clear conformational change in the region of the binding pocket.

Moreover, the same goal was pursued by transferring the search of high-affinity binders and allosteric effectors to the screening of affibody molecules. These small molecules are derived from the Z-domain of *Staphylococcus aureus*. An affibody consists of a 3-helical structure where selected amino acids on two of their helices are randomized to create a synthetic library that acts as an antibody-mimicking molecule able to deliver high-affinity binders for many target proteins. An *Escherichia coli* display library expressing affibodies was screened with the

FK1 domain of FKBP51. Six screening rounds by magnetic-activated cell sorting (MACS) and FACS yielded four affibodies which bind FKBP51 and one of them with potential effects on ligand intake.

Either by the use of FKBP51 muteins or interactions with an scFv, methods for the stabilization of the transient binding pocket of FKBP51 represent an invaluable set of research tools to characterize the molecular dynamics of the binding pocket and provide an alternative to find new FKBP51 selective ligands on a fragment screening basis. Moreover, both scFvs and affibodies as FKBP51 binders have the potential to be conjugated to detection reagents and make them effective resources for the biochemical characterization of FKBP51 selectively. The results presented in this thesis yielded biomolecules with potential applications in the research and characterization of FKBP51 and the search for high affinity and selective ligands that bind to the cryptic pocket of FKBP51.

Zusammenfassung und wissenschaftlicher Erkenntnisgewinn

Proteine sind Biomoleküle mit einer inhärenten Flexibilität, die es ihnen ermöglicht, ihre Funktionen durch Interaktion mit anderen Proteinen, Substraten, Zellen und vielen anderen Molekülen zu erfüllen. Die strukturelle Flexibilität eines Proteins kann die Liganden-Protein-Bindung beeinflussen, und bei einigen therapeutischen Zielmolekülen kann dies den Zugang der Liganden zu ihrer Bindungsstelle einschränken. Dies stellt ein Hindernis für die Entwicklung neuer Moleküle zur Hemmung oder Aktivierung eines Zielproteins dar.

Das FK506-bindende Protein 51 (FKBP51) gehört zur Immunophilin-Familie und wird mit verschiedenen psychiatrischen und stressbedingten Störungen sowie mit vielen anderen Krankheiten in Verbindung gebracht. Verschiedene Proteine der FKBP-Familie verfügen über eine FK1-Domäne mit einer hochkonservierten aktiven Stelle (oder orthosterischen Stelle). Dies ist nicht spezifisch für FKBP, sondern es kommt recht häufig vor, dass man weitgehend konservierte orthosterische Stellen innerhalb einer Proteinfamilie findet. Aufgrund kleiner Unterschiede in der Aminosäuresequenz von FKBP51 weist dieses Protein eine höhere Flexibilität als andere FKBP auf, was sich in einer größeren Anzahl möglicher Konformere niederschlägt. Eines dieser bekannten Konformere bildet eine transiente Bindungstasche, die möglicherweise selektive Liganden von FKBP51 aufnehmen kann, ohne mit anderen Mitgliedern dieser Proteinfamilie zu interagieren. Der Schwerpunkt dieser Doktorarbeit liegt in der Entwicklung von Forschungsinstrumenten, um das Konformationsensemble von FKBP51 vom nativen Niedrigenergiezustand (geschlossene Konformation) in ein Konformer mit einer stabilisierten transienten Bindungstasche zu überführen, die konformationsspezifische Liganden binden kann.

Der erste Teil dieser Arbeit befasst sich mit einer Protein-Engineering- und *Screening*-Strategie, die zur erfolgreichen Identifizierung von FKBP51-Varianten mit einer bevorzugt offenen Konformation der transienten Bindungstasche. Zu diesem Zweck wurden die Aminosäuren der FKBP51 FK1-Domäne systematisch durch Zufalls- und Sättigungsmutagenese (SSM) verändert, um FKBP51-Muteine zu finden, die das konformationelle Gleichgewicht des Proteins in Richtung einer offenen Konformation ändern, wodurch die Bindung von konformationsspezifischen Liganden begünstigt wird. Zunächst wurde das Gen, das für die FK1-Domäne von FKBP51 kodiert, mittels Random Mutagenese mutiert. Mit diesem genetischen Material wurde eine Yeast Surface Display (YSD)-Bibliothek mit einem Pool von Mutagenese-Varianten erstellt und mittels Fluoreszenz-aktivierter Zellsortierung (FACS) mit hohem Durchsatz durchmustert. Aus dieser ersten Bibliothek wurde eine spezifische Region im Protein identifiziert, die die FKBP51-Bindungstasche destabilisiert. Anschließend wurde eine SSM der identifizierten Region, die sich von G64 bis S69 erstreckt, angewandt, und eine zweite YSD-Bibliothek erstellt, die ebenfalls mittels FACS gescreent wurde. Aus dieser SSM-Bibliothek wurden Schlüsselreste für die Destabilisierung der FKBP51-Bindungstasche identifiziert. Drei Muteine mit erhöhter Affinität zu konformationsspezifischen Liganden (G64S, F67E und D68Y) wurden charakterisiert und es wurde nachgewiesen, dass sie die Bildung einer kryptischen Stelle erleichtern, die die Bindung von Liganden in offener Konformation ermöglicht.

In nachfolgenden Experimenten wurden diese drei verbesserten FKBP51-Varianten als Ausgangspunkt für die Erstellung von Bibliotheken mit weiteren Mutationen verwendet, um die Affinität zu Liganden mit offener Konformation weiter zu optimieren. Additive SSM-Bibliotheken, die auf kombinatorischer und iterativer Mutagenese basieren, ergaben über 20 FKBP51-Varianten mit zwei oder mehr Mutationen, die die Ligandenbindung verbesserten. Darüber hinaus bestätigten Varianten mit einer mutierten Position K121 die Bedeutung dieser Schleifenregion, die in den ersten Experimenten nicht identifiziert werden konnte. In allen vier verschiedenen Bibliotheken wurden über 30 einzigartige FKBP51-Mutante mit einer oder mehreren ausgetauschten Aminosäuren gefunden.

FKBP51 ist eines von vielen Proteinen mit einer kryptischen Bindungstasche. Kryptische Stellen in einem Protein bieten eine einzigartige Gelegenheit, Liganden mit hoher Affinität zu entwickeln, die selektiv an das Zielprotein binden, ohne mit strukturell ähnlichen Proteinen zu interagieren, und folglich Off-Target-Effekte zu vermeiden. Unsere auf Protein-Engineering basierende Forschung nutzte FKBP51 als Modell, um die Möglichkeiten und potenziellen Vorteile von Protein-Engineering-Methoden in Verbindung mit einem Zell-Display-System wie Yeast Surface Display (YSD) und FACS zu testen, um Varianten mit verstärkter Bindung an Liganden mit offener Konformation zu identifizieren. Diese Methoden sind auf andere Proteine übertragbar, die ähnlich wie FKBP51 eine transiente Bindungstasche aufweisen. Mit dieser schrittweisen Methodik kann ein Zielprotein systematisch modifiziert werden, um eine Population von einem nativen Zustand mit einem schwach besiedelten Konformer und einer kryptischen Stelle in eine Population mit einer offenen Konformation zu verschieben, die die Bindung selektiver Liganden ermöglicht.

Der zweite Teil dieser Studie konzentrierte sich auf die Verwendung von aus Hühnern gewonnenen einkettigen variablen Fragmenten (scFvs) als konformationsverriegelnde Moleküle, um die offene Konformation von FKBP51 zu stabilisieren und das Screening neuartiger selektiver Hemmstoffe zu erleichtern. Ein allosterischer Effektor, in diesem Fall ein scFv, wäre in der Lage, das Konformationsensemble des Proteins umzuverteilen und dabei eine niedrig besiedelte Konformation im ungebundenen Zustand optimal zu begünstigen.

Aufgrund des großen evolutionären Abstands zwischen Menschen und Vögeln haben Hühner eine stärkere Immunreaktion auf menschliche Proteine, als es bei der herkömmlichen Immunisierung von Mäusen zur Entwicklung von Antikörpern der Fall ist. Aus diesem Grund wurde ein *Gallus gallus* Exemplar mit der FK1-Domäne von FKBP51 immunisiert. Aus der Milz-RNA des immunisierten Tieres wurde ein Pool von scFvs synthetisiert und zur Erstellung einer YSD-Bibliothek verwendet. Diese Bibliothek wurde dann in verschiedenen Kampagnen gescreent, um entweder hochaffine Binder, konformationssperrende oder blockierende scFvs zu erhalten.

Während keine blockierenden scFvs gefunden wurden, brachte die Conformation-Locking-Screening-Kampagne sechs verschiedene scFvs hervor, von denen einer (bezeichnet als Kandidat T32) potenzielle allosterische Effekte auf FKBP51 hatte, die die Bindung von kanonischen und konformationsselektiven Liganden beeinflussten. Mehrere Fluoreszenzpolarisations- (FP) und Biolayer-Interferometrie- (BLI)

Experimente konnten die Wirkung von T32 als konformationsbindendes scFv nachweisen. Diese Wirkung von T32 wurde nachfolgend orthogonal durch Wasserstoff-/Deuterium-Austausch-Massenspektrometrie (HDX-MS) untersucht, welche das Bindungssepitop auf FKBP51 und eine deutliche Konformationsänderung im Bereich der Bindungstasche durch allosterische Effekte des T32 scFv aufzeigte.

Darüber hinaus wurde das gleiche Ziel verfolgt, indem die Suche nach hochaffinen Bindern und allosterischen Effektoren auf das Screening von Affibody-Molekülen übertragen wurde. Diese kleinen Moleküle sind von der Z-Domäne von *Staphylococcus aureus* abgeleitet. Ein Affibody besteht aus einer β -Helix-Struktur, bei der ausgewählte Aminosäuren auf zwei ihrer Helices randomisiert sind, um eine synthetische Bibliothek zu schaffen, die als Antikörper-ähnliches Molekül fungiert und hochaffine Binder für viele Zielproteine liefern kann. Eine *Escherichia coli* Display-Bibliothek, die Affibodies exprimiert, wurde mit der FK1-Domäne von FKBP51 gescreent. Sechs Screening-Runden durch magnetisch aktivierte Zellsortierung (MACS) und FACS ergaben vier Affibody, die FKBP51 binden, und einen davon mit potenzieller Wirkung auf die Ligandenaufnahme.

Methoden zur Stabilisierung der transienten Bindungstasche von FKBP51, entweder durch die Verwendung von FKBP51-Muteinen oder durch Wechselwirkungen mit einem scFv, stellen ein unschätzbares Forschungsinstrumentarium zur Charakterisierung der molekularen Dynamik der Bindungstasche dar und bieten eine Alternative zur Suche nach neuen selektiven FKBP51-Liganden im Rahmen eines Fragmentscreenings. Darüber hinaus können sowohl scFvs als auch Affibodies als FKBP51-Binder an jedes beliebige Nachweisreagenz konjugiert werden, was sie zu effektiven Ressourcen für die biochemische Charakterisierung von FKBP51 macht. Die in dieser Arbeit vorgestellten Ergebnisse haben Biomoleküle hervorgebracht, die bei der Erforschung und Charakterisierung von FKBP51 und bei der Suche nach hochaffinen und selektiven Liganden, die an die kryptische Tasche von FKBP51 binden, eingesetzt werden können.

Individual Contributions by J.A. Lerma Romero for Cumulative Section

1) Lerma Romero JA, Meyners C, Christmann A, Reinbold LM, Charalampidou A, Hausch F, Kolmar H. Binding pocket stabilization by high-throughput screening of yeast display libraries. *Front Mol Biosci.* 2022 Nov 7;9:1023131. doi: 10.3389/fmolb.2022.1023131. PMID: 36419931; PMCID: PMC9676650.

Contributions by J.A. Lerma Romero:

- Generation and screening of YSD libraries
- Cloning, expression and purification of all FKBP51 variants
- Characterization of muteins together with Meyners C
- Writing of original manuscript draft
- Generation of figures

The contribution of J.A. Lerma Romero totaled 80%. C. Meyners contributed 10% for his support in characterization experiments. The remaining 10% were distributed between A. Christmann, L.M. Reinbold, A. Charalampidou, F. Hausch, and H. Kolmar for support with experiments, reading and correcting the manuscript.

2) Lerma Romero JA, Kolmar H. Accessing Transient Binding Pockets by Protein Engineering and Yeast Surface Display Screening. *Methods Mol Biol.* 2023;2681:249-274. doi: 10.1007/978-1-0716-3279-6_14. PMID: 37405652.

Contributions by J.A. Lerma Romero:

- Experimental design
- Performing experiments and reproducibility experiments
- Writing of original manuscript draft
- Generation of figures

The contribution of J.A. Lerma Romero totaled 90%. The remaining 10% was contributed by H. Kolmar for reading and correcting the manuscript.

3) Lerma Romero JA, Meyners C, Rupp N, Hausch F, Kolmar H. A protein engineering approach towards understanding FKBP51 conformational dynamics and mechanisms of ligand binding. *Protein Engineering, Design and Selection.* 2023; gzad014. <https://doi.org/10.1093/protein/gzad014>. PMID: 37903068

Contributions by J.A. Lerma Romero:

- Generation and screening of YSD libraries
- Cloning, expression and purification of all FKBP51 variants
- Characterization of muteins together with Meyners C
- Writing of original manuscript draft
- Generation of figures

The contribution of J.A. Lerma Romero totaled 90%. The remaining 10% were distributed between C. Meyners N. Rupp, F. Hausch, and H. Kolmar for support with experiments, reading and correcting the manuscript.

1 Introduction

1.1 Challenges of drug discovery for protein families

Broadly explained, the drug discovery process starts by recognizing a disease for which adequate medical treatment is poor or nonexistent. Once a disease and its potential therapeutic target have been properly identified and validated, the drug development process begins [1]. According to the Food and Drug Administration (FDA), the drug development process can be divided into five stages: discovery and development, preclinical research, clinical research, authority review, and post-market safety monitoring [2].

One of the main challenges during the drug discovery and development process is finding ligands that selectively bind to the intended target receptor while avoiding binding to closely related off-target receptors. This is essential to prevent harmful side effects [3]. Before getting into the drug discovery process, it is essential to study the molecular dynamics of the target protein and identify the protein-ligand model that best fits the particular case. The binding of an inhibitor to the target protein's surface pocket can be explained by three key concepts: the lock-and-key model, induced-fit, and conformational selection (Figure 1) [4].

In order to describe the connection between an enzyme and its substrate, Fischer proposed the lock-and-key model in 1894. One of the first models of protein-ligand binding which compared a lock to a rigid protein binding pocket, and a key to a rigid ligand [5]. When protein crystal structures revealed the existence of diverse pocket geometries for the same protein co-crystallized with various ligands, the shortcomings of this model became apparent [4, 6].

In 1958, Koshland proposed a model that took protein flexibility into consideration, in which the protein binding site adjusts by way of an "induced fit" to bind the appropriate ligand, but only after it is bound [7, 8]. To clarify how the interaction of an allosteric ligand alters the conformation of a protein binding site, a different model known as "conformational selection" was first used. In this model, also known as the "population-shift model", the protein in its unbound state can adopt several conformations, and a ligand binds preferentially to one of these pre-existing conformations. This drives the equilibrium of the protein population toward the binding conformation [8–10]. Moreover, a mix of these two models had been used to describe the binding mechanism of some proteins (Figure 1) [11].

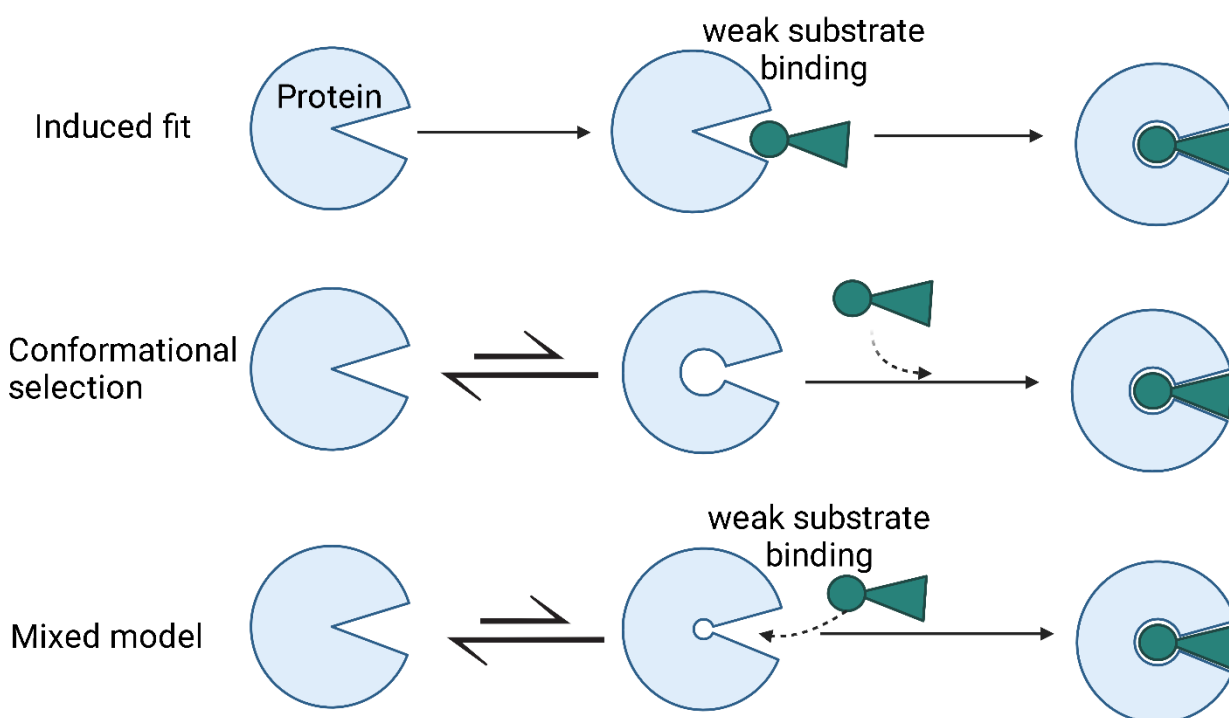


Figure 1. Schematic representation of the induced fit, conformational selection and mixed model for protein-ligand binding. The induced fit model proposes a pocket reconfiguration after ligand binding, while conformational selection suggests the coexistence of multiple conformers of a protein, and a ligand can bind to one of them. Figure generated with Biorender.com

Typically, the primary goal of drug design is developing or discovering a molecule that binds to a target of interest with high affinity [12]. One obstacle for drug design is to avoid off-target interactions, which is especially difficult to circumvent if the target protein has a highly similar sequence, few structural differences, or similar orthosteric binding pockets [13, 14]. This problem is especially present when the therapeutic target is part of a large protein family, which is the case for many current target proteins like adenosine receptors of the GPCR subfamily [13], chemokine receptors [15], the kinase family [16], FKBP51 of the FK506 binding proteins [17–19], among other numerous targets with homologs that bind non-specifically one substrate. Hence, family or subtype selectivity has received substantial attention in the development of novel medications [14].

Despite early discoveries defining proteins as static and rigid structures, they are more commonly viewed as dynamic polymers that exist as an ensemble of different conformations in an equilibrium [6, 20]. The significance of protein flexibility in the selectivity and specificity of small molecule binding has lately come to light, with an increasing number of studies devoted to the investigation of transient pockets [9, 21–24] or allosteric modulators [25–30] as an alternative method to selectively target challenging receptors.

1.2 Allostery

Allostery can be defined as the modulation of a target protein when another molecule binds to a site different from the functional site, also called the orthosteric site [25, 28]. As a consequence of this interaction, the target

protein may undergo conformational and/or dynamic changes that ultimately affect the binding of a substrate to its orthosteric site or the function of the protein [25, 31, 32].

Because proteins are flexible molecules, they exist in various closely related conformations called an ensemble. All these conformers swap on various timescales resulting in populations with diverse conformations distributed in different proportions. The interaction of an allosteric effector with the protein does not create new conformations, but shifts the distribution and interconversion rates of the existing conformational ensembles [33–36]. This ensemble redistribution can ultimately affect the overall kinetics of the affected protein because the modification of the orthosteric binding site can activate or inhibit the binding of a ligand [4, 33].

Allosteric modulators can be very diverse. Some molecules like ions, lipids, cAMP, drugs, different proteins, RNA, or DNA can interact non-covalently with the allosteric site [37]. On the other hand, there are covalent modifications, like posttranslational modifications and point mutations, that can cause structural changes as well [22, 38, 39]. Even the modification of the physical environment (e.g., light exposure, irradiation, and pH) can trigger conformational alterations in a protein [26, 32, 40].

One of the main advantages of using allosteric modulators over the direct interaction of a molecule at the orthosteric site is the higher selectivity, which is especially useful as subtype selectivity within protein families. Normally, the orthosteric site is highly conserved across different proteins of the same family, and if one single member of a protein family is to be targeted, the outcome of the design of orthosteric inhibitors might be reduced efficacy, or poor selectivity [25, 29]. Allosteric sites generally offer extraordinary levels of selectivity since they are less evolutionarily conserved and there is less pressure for conservation throughout a protein family [27, 29, 32]. Additionally, compared to competing inhibitors targeting the orthosteric site, the effect of allosteric modulators can be used to either increase or decrease enzyme activity, resulting in a more effective regulatory action [25, 33, 36, 41].

There are many examples of allosteric proteins. Hemoglobin, aspartate transcarbamylase, phosphofructokinase, GPCRs, and ion channels are some of the numerous examples of proteins presenting allosteric activity after binding of an effector molecule [25, 29, 42, 43]. The allosteric modulation of a protein may trigger diverse effects on its structure. The protein can undergo substantial conformational changes that either cause the active site to open or close, allowing the protein to perform its function or turning off its activity. The conformational change can be mayor, for example resulting in hinge motion at the border of two domains to create or open a binding pocket, or it can be minor, like the rotation of a single side chain to allow the entrance of another molecule to the binding pocket [41, 44]. Additionally, changes to electrostatic properties of the active site or control of complex formation (e.g., multimerization) are other ways in which allosteric changes can be observed in a protein [41]. Some of these conformational changes can be very similar to the ones observed by proteins that present transient binding pockets. In this case, the structural changes last for a fraction of a second and do not require the interaction with another molecule to happen [4].

1.3 Transient binding pockets

Allosteric modulation is not the only method to target single members of closely related proteins with virtually identical binding pockets. According to several studies, the subtype selectivity of orthosteric ligands may be influenced by changes in conformational dynamics among various protein families [45–48]. Specifically, the creation of transient binding pockets, also called cryptic pockets, that cannot be detected with crystallography in the apo-state (unbound-state) of a protein [3, 49].

The number of potential molecular targets for many diseases has increased dramatically in recent years, mainly due to the great progress in sequencing the human genome [50]. Unfortunately, plenty of these potential targets are deemed undruggable, which means that they are inaccessible to the standard substrate-competitive drug development [51]. Proteins without an apparent surface pocket have become new potential targets for drug development. These proteins that had previously been thought to be undruggable may actually contain hidden druggable pockets, which doubles the size of the druggable human proteome [9, 52]. Transient binding pockets can be classified into five different categories depending on the type of modification that the protein undergoes: subpocket, adjacent pocket, breathing motion, channel/tunnel, and allosteric pocket [4].

Identifying transient binding pockets is a difficult task, as this conformation is a rare event that may occur in less than 1% of cases in some proteins [53]. These pockets are metastable in thermodynamic equilibrium, which means that they appear mostly in thermodynamically unstable states [9]. Cryptic pocket discovery by computational methods is strongly reliant on the ability of simulation approaches to disclose the protein movements necessary for pocket opening. However, the computational cost required for these simulations is an obstacle that makes molecular dynamics modeling unpractical for this purpose [4, 21].

While cryptic pockets are not visible in the apo-state of a protein, they emerge in ligand-bound structures [54]. Numerous studies state that the formation of these cryptic sites after ligand binding is driven by two well-known mechanisms: induced-fit and conformational selection [10, 18, 55]. Even though ligands seem to be required for cryptic pocket opening, other methods like large-scale fragment screening, site-directed tethering, machine learning, atomistic simulations, allosteric mutations, or antibodies can be used for their identification [56–59]. The use of transient binding pockets to target specific members of a large protein family has already been successfully applied for GPCRs [3], tyrosine kinases [47], IL-2 [60, 61], and P38 mitogen-activated protein kinase [62], among others.

1.4 Protein engineering

Protein engineering is defined as the process of designing and creating new synthetic proteins by substitution, insertion, or deletion of nucleotides in the genetic material coding for a naturally occurring amino acid sequence [63]. These modifications to the protein can alter its function or properties, tailoring a protein with specific characteristics for any purpose [64]. The application of protein engineering techniques is broad and can be used

for the development of protein-based tools with medical, industrial, agricultural, and environmental applications [64–69].

Protein engineering is broadly divided into three branches: *de novo* design, rational design, and directed evolution [70]. *De novo* design of proteins, which originally referred to the creation of new proteins entirely from scratch, has now broadened its spectrum to incorporate computer techniques to modify natural proteins [71, 72]. Rational design aims to reduce the sequence space to be randomized. For this reason, this method requires previous knowledge of the molecular basis of the protein attribute (structure–function relationship) for the protein of interest [71, 73]. Finally, directed evolution tries to simulate natural evolution by inserting random mutations in the target gene and screening via high-throughput methods to find proteins with improved functionality. Contrary to rational approaches, directed evolution does not require any information on the protein structure [64, 74].

Today, synthetic proteins may be engineered *in silico* or *in vitro* through directed evolution [75]. *In silico* protein design and engineering refers to the search for new proteins or mutations in a protein that will improve its properties or function assisted by computational methods such as bioinformatics molecular docking, molecular dynamics simulations, and *de novo* design [76–78]. Computational techniques for directed evolution have many advantages but have certain limitations too. For instance, the number of different sequences that computational approaches can explore is significantly larger than that explored by experimental methods in a laboratory. However, it is still difficult to estimate a protein's biophysical characteristics as a result of mutations, such as changes in stability and ligand-binding affinity, as it would require extensive calculations and computational power [79–81]. Even with all the advantages that structure-based protein design offers, over 95% of protein engineering is done via screening, which involves introducing random mutations to naturally occurring proteins and isolating those that improve a particular characteristic of the protein [82, 83].

Experimentally, directed evolution starts with the mutagenesis of the genetic material coding for the protein to be modified, followed by one or several screening steps, to finally decide which parental genes will advance to the next evolution round [84]. In order to investigate the sequence space of a gene, diverse randomization approaches are utilized for the creation of libraries. Some exemplary methods to randomize genetic material are error-prone PCR, Site-saturation mutagenesis (SSM), site-directed mutagenesis (SDM), and cassette mutagenesis [85, 86].

1.4.1 Directed evolution

Directed evolution is based on repeated rounds of creating a diversified population, and selecting a fraction of it, which improves the desired function [85, 87]. As mentioned above, evolutionary methods do not require any previous knowledge of the protein to be randomized, which can be an advantage over rational design methods [74]. On the other hand, the whole mutational space of a typical protein cannot be covered, as the number of

variants in the library will quickly outgrow the feasible library size for any reported library construction technique [86].

If it is previously known which region of the protein is responsible for the activity or property to be optimized, targeted mutagenesis is probably the first logical step to create a library that contains enhanced variations [86, 88]. On the contrary, if such information is not available, random mutagenesis offers a better chance to find improved protein variants and identify structure–function correlations of the protein [22, 89, 90].

1.4.2 Random mutagenesis

Random mutagenesis is a directed evolution method to randomly create point mutations into whole genes. The randomization of the genetic material can be done by different techniques such as chemical mutagens DNA, using mutator strains, error-prone PCR, rolling circle error-prone PCR, or saturation mutagenesis, among others [91–95].

Of all these methods, error-prone PCR is the most popular. This method relies on the use of DNA polymerases with a high error frequency, potentiated by changing the conditions of the reaction, like an increased Mn^{2+} or Mg^{2+} concentration to disturb the base-pairing process, unequal dNTP concentration to promote misincorporation, or increased polymerase concentration [96–98].

This method allows to control the DNA segment that is to be mutated by simply designing primers flanking the desired fragment. Moreover, it grants a certain degree of control of the mutation rate, as the number of PCR cycles and template concentration regulate the average number of mutations per DNA fragment [98, 99]. Error-prone PCR is an invaluable tool that not only focuses on the optimization of enzymes for any industrial process but it is also a method for producing variations that provide information on the link between a protein sequence, structure, and function [95, 97, 100].

1.4.3 Site-saturation mutagenesis

Focused mutagenesis is a semi-rational protein engineering method that can be used together with directed evolution methods to design a synergistic approach to obtain a protein with enhanced characteristics [101, 102]. Libraries generated with semi-rational methods are able to produce successful results because they mutate particular residues based on prior structural or functional understanding [102–105]. After obtaining some mechanistic and structural data either experimentally or by computationally-guided mutagenesis strategies, specific regions in the protein that influence its properties can be identified. These regions can then be selected to be randomized [105, 106]. When the activity of a protein is the property to be modified, the catalytic region is frequently the target for activity optimization *via* mutagenesis. However, it has been shown that mutagenesis at residues far from the active site may also be used to improve the protein binding properties [39, 107–109].

SSM is a focused semi-rational approach where all 20 natural amino acids can be randomized at specific residues in or close to the active site of a protein. The mutation of these strategically appointed amino acids might result in significant gains in activity compared to the mutagenesis of the full sequence [106, 108, 110]. By focusing on specific residues, a significantly smaller library with high functional proteins might be obtained, which simultaneously reduces the work and time dedicated to high-throughput methods for the screening of the resulting library [105].

1.4.4 Combinatorial and iterative mutagenesis

Both random and rational mutagenesis strategies can be applied for the first engineering steps of a protein, but after several variants are identified *via* these methods, fine-tuning of the protein activity can be achieved by combinatorial or iterative mutagenesis approaches [111, 112].

As the name suggests, combinatorial mutagenesis is a protein engineering strategy for systematically generating variants with multiple mutations with improved properties compared to individual mutations [113, 114]. However, saturation mutagenesis of multiple residues in a protein can also cause a number of technical challenges, such as protein unfolding. To avoid these complications while covering the whole desired region, this technique can be repeated in an iterative manner [115, 116].

Iterative mutagenesis is a mix of both techniques, rational design and combinatorial randomization where the best mutants of a focused library are used as the template for another set of saturation mutagenesis experiments [111, 115]. This iterative process can continue until the selected property is optimized to a desired point or until the additional mutations do not result in an improvement of the protein [117, 118].

1.5 Display technologies

In 2018, the Nobel Prize in Chemistry was shared between Frances H. Arnold for the directed evolution of enzymes, and George P. Smith and Sir Gregory P. Winter for the phage display of peptides and antibodies [119]. Frances H. Arnold conducted the first experiments on directed evolution of enzymes in 1993, and in 1999, she published a directed evolution approach to optimize the thermostability of the psychrophilic protease subtilisin S4 after manually picking over 2000 clones from their random mutagenesis and SSM libraries together with Kentaro Miyazaki [119, 120]. This research was complemented by George P. Smith and Sir Gregory P. Winter as they used phage display for the directed evolution of antibodies [119, 121, 122]. Since then, directed evolution and display technologies have gone hand in hand to develop optimized engineered proteins [22, 123–128].

Display technology is a set of techniques that allows the creation and screening of large biomolecule libraries, being genotype-phenotype coupling an important feature of these systems [129–131]. Display libraries can be very diverse in type and size, but all of them are built up in a very similar modular configuration which consists

of a displayed element (e.g. protein or RNA/DNA aptamers), a linker, and the corresponding genetic code for the displayed molecule [130, 132].

The surface presentation of biomolecules for selection purposes was first shown in 1985 with phage display of antibodies [133]. Since then, phage display and other technologies based on the same principle have been developed and improved. Today, a variety of *in vivo* and *in vitro* display methods are available to study a wide spectrum of protein-ligand interactions [134]. The capacity to physically connect the displayed molecule to its associated genotype is possible for all five types of display systems: phage display, cell display, ribosome display, mRNA display, and DNA display [130, 135].

1.5.1 Yeast surface display

Yeast surface display is a cell-based display system. As such, a single vector encoding a protein genetically linked to a cell-surface anchor protein is employed to transform each individual cell. The protein is then transported to the extracellular space by the anchor protein's signal sequence to be finally displayed on the cell surface [136].

The use of yeast cells for the display of proteins has many advantages over other systems. Firstly, with yeast belonging to eukaryotic expression systems, they are able to process post-translational modifications including disulfide bonds which aid in efficient protein folding and activity of proteins that cannot be expressed by other systems like bacterial or phage display [130, 135–138]. Furthermore, the technical and time requirements are still lower than other eukaryotic display systems such as mammalian cells [136, 139–142]. Besides, the use of epitope tags to measure the display of the protein of interest allows a 2D selection of cells with high expression levels and high affinity binding to a target molecule. This selection process can be easily done *via* fluorescence-activated cell sorting (FACS), due to the compatibility of these two technologies [126, 128, 136, 143, 144].

The yeast *Saccharomyces cerevisiae* is generally used for the creation of yeast display libraries. It is one of the most commonly used microorganisms in bio-industrial processes as it is a "generally regarded as safe" (GRAS) microorganism approved for food and pharmaceutical production, and it can grow at high density in affordable culture medium [145–147]. Moreover, novel optimized transformation methods allow the creation of high-diversity libraries that exceed 10^{10} clones [143].

The protein of interest (POI) can be displayed on the cell surface using a variety of yeast anchor proteins such as agglutinin (Ag α 1 and Aga1), flocculin Flo1, Sed1, Cwp1, Cwp2, Tip1, and Tir1/Srp1 [137, 139]. The sexual agglutinins, a-agglutinin, and α -agglutinin, are cell surface glycoproteins participating in the aggregation of cells during the mating process expressed on the mating type "a" and " α " yeast cells, respectively. [137, 148]. The a-agglutinin system is often employed as the method of choice for protein display on *S. cerevisiae*. This system consists of two subunits: Aga1p and Aga2p. The Aga2p subunit attaches to Aga1p via two disulfide bonds before being released to the cell surface while the Aga1p subunit anchors to the cell wall via a β -glucan covalent link (Figure 2) [137, 149, 150].

The C-terminus of Aga2p is the region accessible to molecules of the extracellular space. Thus, the protein of interest to be displayed is fused to the C-terminus of Aga2p. However, some proteins require a free N-terminus for correct function or substrate binding. For those cases, the orientation of the fusion protein can be changed [139, 149, 151].

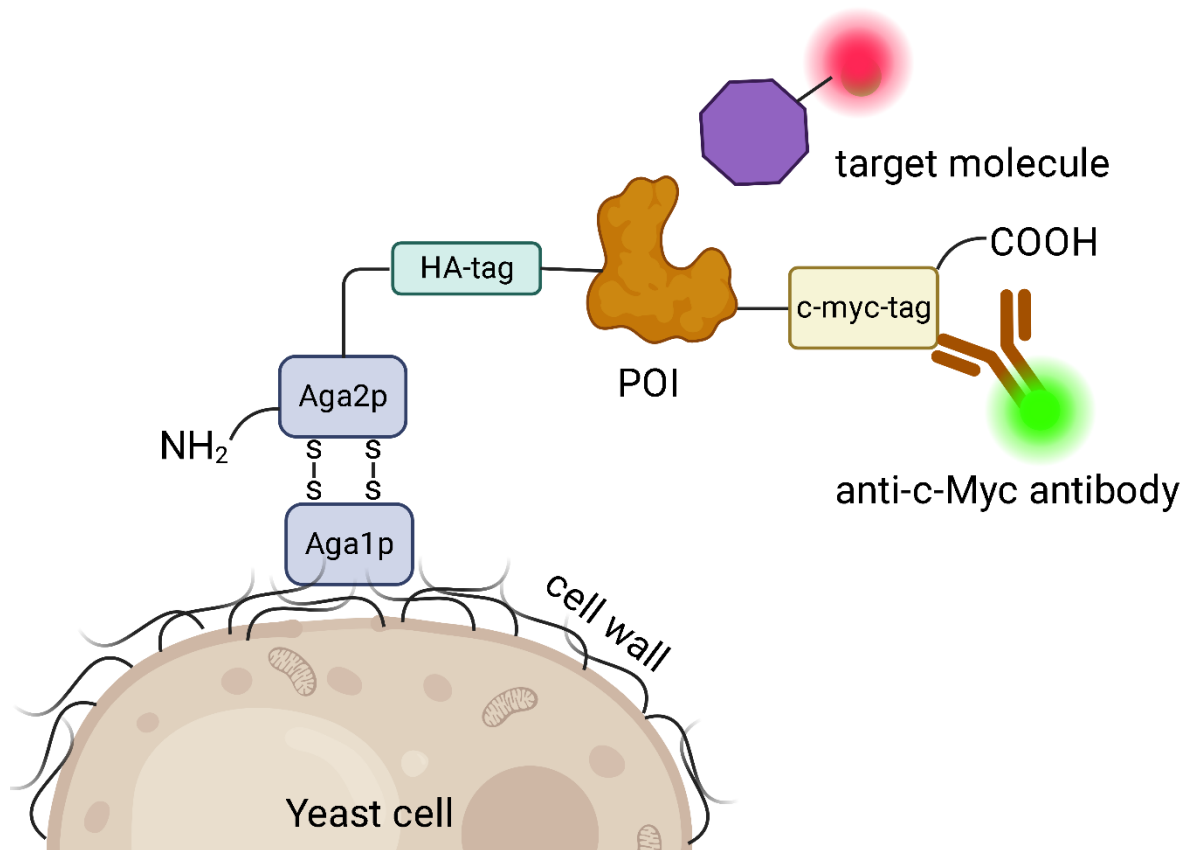


Figure 2. Schematic representation of the yeast surface display (YSD) presenting a protein of interest (POI) via the α -agglutinin Aga2p subunit. A HA-tag or myc-tag may be used for determining correct display of the POI. Created with BioRender.com.

Today, different kinds of proteins have been successfully expressed and selected with yeast surface display in conjunction with a sorting strategy. Many of them are antibodies, antibody fragments, antibody mimetics, or binding proteins such as the fragment antigen-binding region of antibodies (Fab) [152–154], single-chain variable fragments (scFv) [155, 156], camelid single domain antibodies (VHHs) [157, 158], the variable domain of cartilaginous fish IgNAR antibodies (vNAR) [159, 160], Immunoglobulin G [161], lamprey variable lymphocyte receptors (VLRs) [162], fibronectins [163], human kringle domains [164, 165], or Designed Ankyrin Repeat Proteins (DARPs) [166].

Yeast surface display is often used for the expression of all the examples mentioned above due to the advantageous eukaryotic post-translational processing that yeast cells provide. However, further proteins have been successfully displayed on the yeast surface with the goal of engineering one or multiple of their properties. Some

examples of these proteins are the FK506-binding protein 51 (FKBP51) [22], horseradish peroxidase [167], glucose oxidase [168], β -lactamase [169], or epidermal growth factor receptor (EGFR) [170], among others [171].

1.6 Fluorescence-activated cell sorting (FACS)

The screening of yeast libraries using with fluorescence-activated cell sorting (FACS) has numerous advantages and is frequently used for sorting of protein-binding molecules and directed evolution libraries [172, 173].

Flow cytometers are equipped with one or multiple lasers to allow the quick analysis of individual cells. The optical detectors of the device can collect information on a cell's size by measuring visible light forward scatter (FSC), and the internal complexity or granularity are determined with the side scatter (SSC) [173, 174]. Moreover, the multiple laser system of the flow cytometer can distinguish between over 18 different fluorescent signals depending on the number of lasers in the device [174]. The fluorescent signals are obtained by the expression of fluorescent proteins such as Green Fluorescent Protein (GFP) or Red fluorescent protein (DsRed), staining the target molecule with fluorescent dyes (e.g. PE, APC or FITC) or staining with fluorescently conjugated antibodies like Anti-c-Myc-APC to label c-Myc tagged proteins, or anti-Mouse-IgG-PE as a secondary antibody to label mouse immunoglobulins [174]. At a flow rate of 10,000 or more cells/second, the cells in a FACS are individually analyzed and separated depending on the measured light scattering and fluorescent signals [173, 175].

1.7 Antigen binding molecules for research

Over the past 30 years, monoclonal antibodies (mAbs) have become one of the most effective class of biomolecules for the treatment of diverse diseases and diagnostic purposes [176]. According to the last data recorded in November 2022, around 175 antibodies are in regulatory review or approved and approximately 1,200 are currently in clinical studies [177].

Antibodies consist of four polypeptide chains that form the crystallizable fragment (Fc) domains responsible for the interaction with innate immune receptors, and the antigen-binding fragment (Fab) domain, which is the part of the antibody that can bind antigens with high affinity and specificity [178]. If the functions of the Fc domain of an antibody are not required, Fabs, scFvs, nanobodies or antibody-mimicking molecules such as affibodies can be used (Figure 3) [179–181].

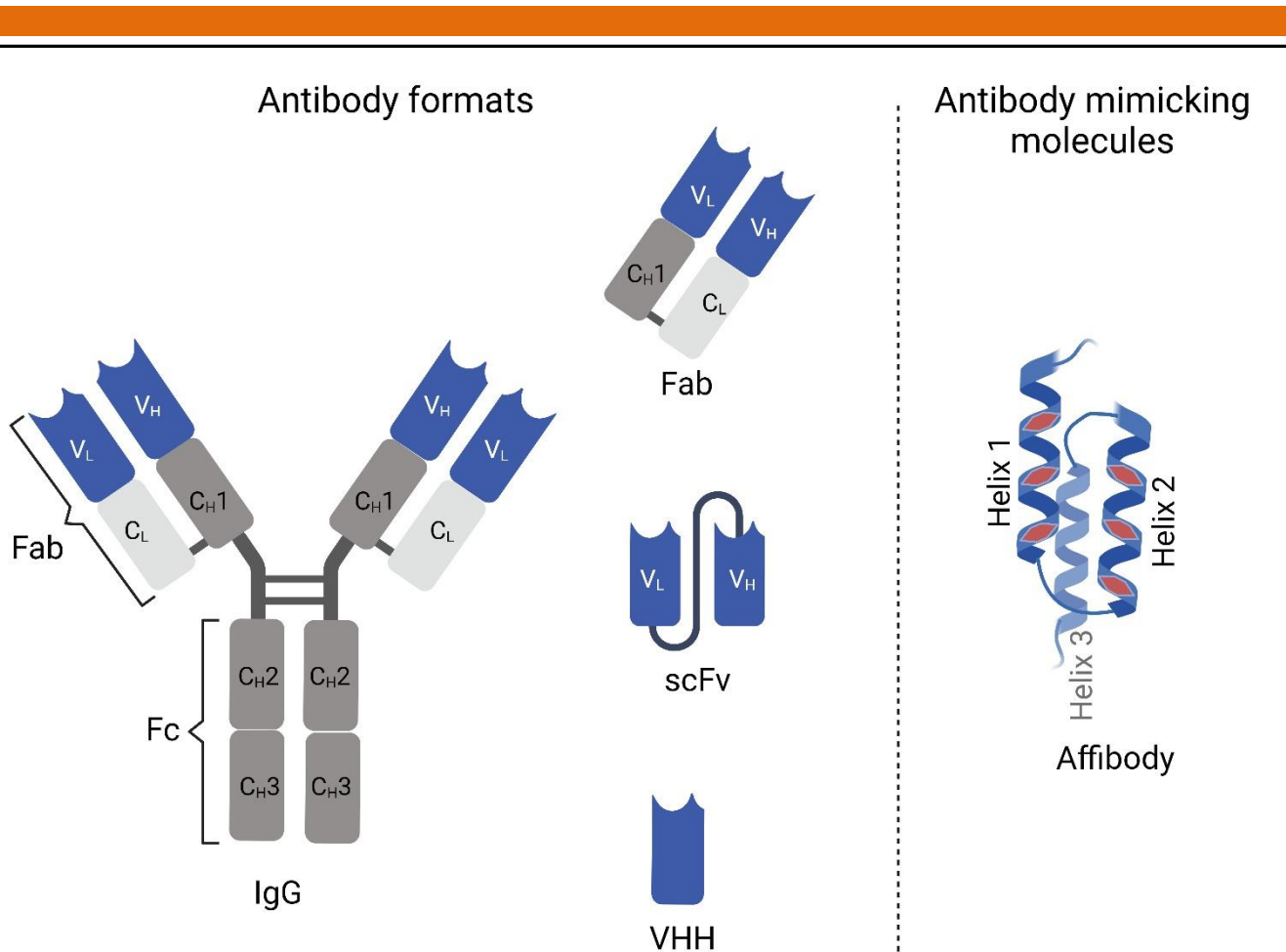


Figure 3. Representation of an IgG and some of the antibody fragments that can be derived from it. Besides, affibodies as antibody mimicking molecule with research or clinical applications. Figure generated with Biorender.com

All the above-mentioned antigen-binding molecules have been largely applied as therapeutics. Nonetheless, they have also been exploited as research and development tools across many areas. These include the use of Fabs, scFvs, affibodies, DARPin or VHHs as protein crystallization chaperones [181–185], Fabs and VHHs as conformation-locking antibodies [186–188], affibodies and scFvs for biomolecular imaging, [189, 190] immunoblotting, and immunodetection [191], among many others.

1.7.1 Single-chain variable fragments (scFvs)

ScFvs are heterodimers formed by an immunoglobulin heavy (V_H) and light chain (V_L) variable regions fused by a linker. It has been shown that scFvs retain both the affinity and specificity when compared to their IgG counterparts [192, 193]. Nevertheless, the avidity of a full-length antibody is greater because of its bivalency compared to the one-armed binding of a scFv [192, 193].

One of their greatest advantages over full-length antibodies is that scFvs can be expressed with high yields using bacterial expression systems [194]. Moreover, scFvs can be displayed on the surface of various expression systems such as mammalian, yeast, insect, and plant cells [155, 156, 195–197]. Compared to full-length antibodies, the smaller scFvs enable better and faster tumor penetration when used for cancer therapy [198, 199]. If used as targeting molecules, the scFvs can be coupled with drugs and radionuclides to quickly deliver the cargo. In addition, the reduced size results in rapid clearance from the blood which helps reducing the exposure of healthy tissue to toxic compounds [200, 201].

Chicken antibodies

One of the many methods to obtain monoclonal antibodies against a specific antigen is to use the selected antigen for animal immunizations. While mice or rats are the most common options, other animals can provide different antibody formats with different characteristics. For example, camelid VHHs [157, 158], cartilaginous fish antibodies (IgNAR)[159, 160], lamprey variable lymphocyte receptors (VLRs) [162, 202] or avian antibodies (IgY) [203–205], among others.

Mouse systems are often used for the isolation of mAbs against a target of interest due to their biochemical and biophysical similarity to human antibodies [206]. However, these biological similarities between species can sometimes be disadvantageous, as mice or other mammals may have highly homologous proteins to a desired human epitope, therefore limiting the epitope diversity that can be obtained by the immunization of these animals as these will not be recognized as antigens [207]. Due to their evolutionary distance from mammals, avian proteins share less sequence homology with human proteins. For this reason, chicken immunizations are a suitable alternative and have been successful in finding high-affinity antibodies against human antigens, as these animals can present strong immune responses to highly conserved mammalian antigens that are poorly immunogenic in mice or other mammalian hosts [205, 207–209].

While most mammals express five classes of immunoglobulins (IgD, IgM, IgG, IgA, and IgE), avian species express only three (IgM, IgA, and IgY) [210, 211]. IgY is a monomeric antibody which is not only found in birds but in reptiles and amphibians too [212]. For many years, IgY was identified as “avian IgG” due to their similarities. However, some years later it was clear that IgY is a different isotype which was probably the precursor of the mammalian IgG and IgE, as these two mammalian isotypes have some resemblances in structure and function to IgYs [212, 213].

Like most immunoglobulins, IgYs consist of two heavy and two light chains. The IgY heavy chain has five domains: one variable (V_H) and four constant domains (C_H), one additional C_H domain compared to IgGs [212, 214]. Besides, it is the most common kind in chicken sera, and it is found in high concentrations in the yolk sacs of oviparous animals, which makes it an efficient and cheap method to produce and isolate antibodies [204, 205, 213]. Because IgYs include sections made up of chicken sequences that would be potentially immunogenic in therapeutic applications, several humanization methods such as CDR grafting and framework shuffling are available to overcome this issue [155, 203, 215, 216].

1.7.2 Affibody molecules

Affibodies are small (~ 6.5 kDa) affinity proteins based on the engineered version of the B-domain (Z-domain) of the immunoglobulin-binding region of *Staphylococcus aureus* protein A [179, 217, 218]. Structurally, an affibody is a three-helix protein of around 58 amino acids (Figure 2). This binding molecule is commonly obtained from a synthetic library where 13 positions in helices one and two are randomized and screened against a target molecule [179, 219].

Similar to scFvs, affibodies try to provide a simple alternative to the otherwise complex but widely used IgG. The poor heat stability and the expensive and laborious manufacturing process of antibodies might be avoided if the large domains that provide IgGs additional immunological functions and binding with complement factors and Fc-receptors are not required [217]. Affibodies have many diagnostics and research applications. For example, affibodies as imaging tracers in oncology can deliver higher contrast, excellent sensitivity, and faster analyses thanks to improved tissue penetration, rapid blood clearance, and reduced nontarget-specific accumulation in tumors when compared to full-length antibodies [179, 220]. Moreover, affibodies have been successfully applied in optical and magnetic resonance imaging, fluorescence-based imaging, quantum dot-based imaging, and near-infrared imaging [217, 221–223].

Affibodies have not only been proven useful in imaging techniques, but also as protein inhibitors, targeted payload delivery vehicles, intercalators of neurotoxic peptides, and nanoparticle-based drug delivery modules [217, 224–227].

1.8 FK506-binding proteins (FKBPs) and FKBP51

The FK506 binding protein 51 (FKBP51) is a 51-kDa protein encoded by the *FKBP5* gene and is one of the many members of the FK506 binding proteins (FKBPs) family [228]. FKBPs are highly conserved in eukaryotes and are key in critical cellular signaling pathways such as calcium and Notch signaling pathways. Moreover, they play a role in stress-related disorders like peritraumatic dissociation, posttraumatic stress disorder (PTSD), immune-related diseases, inflammation, steroid hormone receptor-associated tumorigenesis, Alzheimer's disease, reproductive development, among others [229–233].

FKBPs, together with the cyclosporin A-binding cyclophilins are members of the immunophilin family. They all have a peptidylprolyl isomerase (PPIase) activity that catalyzes the cis-trans conversion of peptidylprolyl bonds (Figure 4) [234, 235]. The FKBPs PPIase site can bind the immunosuppressant drugs rapamycin and FK506, and inhibit its activity [234, 236].

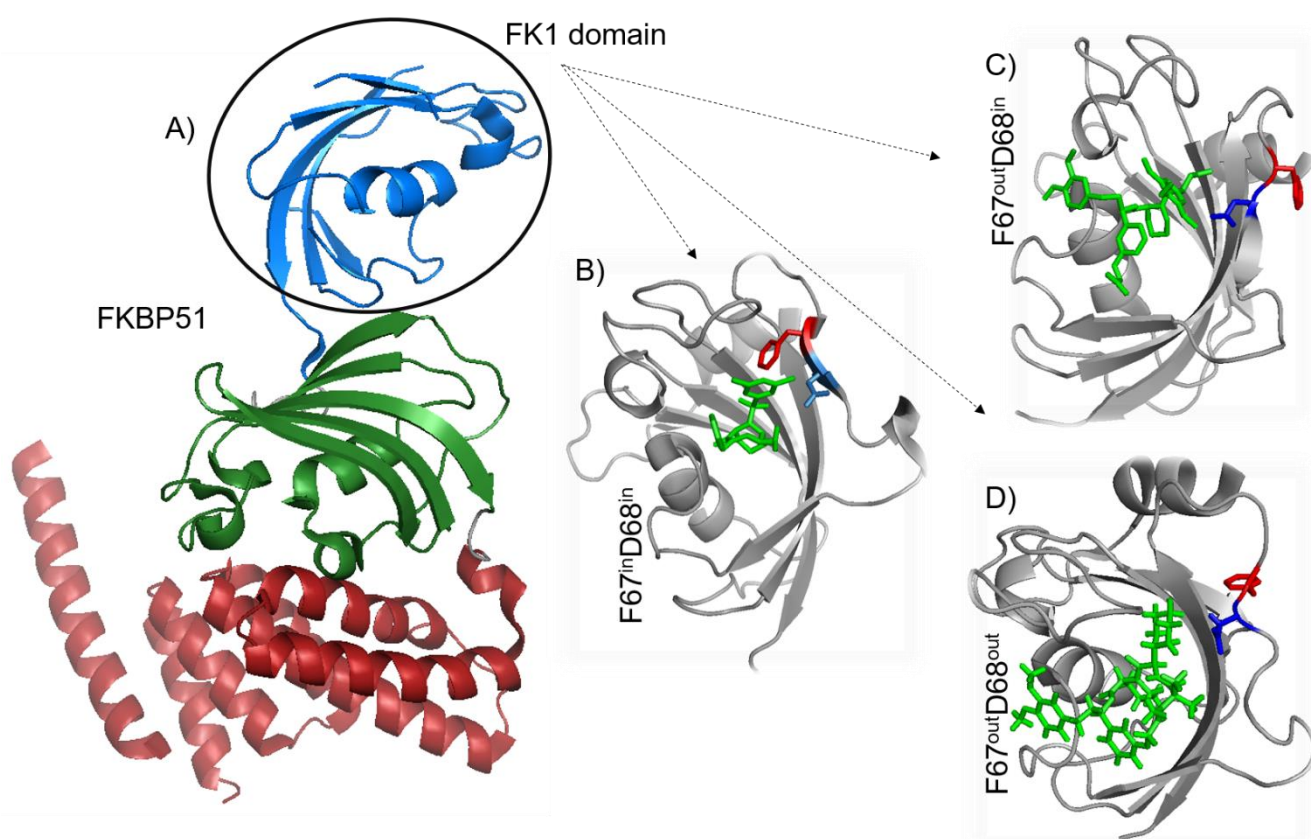


Figure 4. Crystal structure of A) FKBP51 (PDB: 1kt0). The FK1 domain is depicted in blue, FK2 domain in green and TRP domain in red. B) FK1 domain (16-140) in complex with FK431 (PDB: 5OBK) with a F67ⁱⁿ/D68ⁱⁿ-conformation C) FK1 domain (16-140) in complex with iFit1 (PDB: 4TW6) with a F67^{out}/D68ⁱⁿ-conformation and C) FK1 domain (16-140) in complex with macrocyclic ligand (PDB: 7AWF) with a F67^{out}/D68^{out}-conformation. In B) C) and D), the FK1 domain is depicted in grey, the bound ligand in green, F67 and D68 in red and blue sticks, respectively.

1.8.1 The role of immunophilins in the transcriptional activity of glucocorticoid receptor

FKBP51, FKBP52, and Cyclophilin 40 (Cyp40) are immunophilins involved in the assembly of high-affinity steroid receptor complexes like the progesterone receptor (PR) or glucocorticoid receptor (GR). These receptors must be assembled in a specific order with their other components such as heat shock proteins (Hsp), as well as a number of other Hsp-binding co-chaperones [234, 236].

In the absence of steroids, the receptors are in a mature complex with a Hsp90 dimer, the Hsp90-binding protein p23, and any of the three Hsp90 co-chaperone immunophilins (FKBP51, FKBP52, or Cyp40). However, these complexes constantly disassemble and reassemble, resulting in the presence of intermediate complexes, but only mature receptor complexes (PR and GR) are able to bind their respective hormones with high efficiency and affinity [237, 238]. There are several final receptor-Hsp90 heterocomplexes, and each one is unique based on the immunophilins that reside in the tetratricopeptide repeat (TPR) acceptor site on Hsp90 [239, 240].

The mature GR complex is located in the cytoplasm, and after hormone binding, the GR moves into the nucleus to either increase or reduce the transcription of glucocorticoid response element genes [241, 242]. However, the transcriptional activity of the GR varies greatly depending on the immunophilin assembled in the complex. Following hormone exposure, GR transcriptional activity is diminished by overexpression of FKBP51 caused by the decrease of the binding affinity of GR to glucocorticoids [243, 244]. On the other hand, FKBP52 overexpression promotes GR-dependent transcription attributed to its higher binding affinity to cortisol [244, 245]. However, it is thought that steroid binding to the FKBP51-bound receptor causes an immunophilin exchange to FKBP52 [244]. Hormone binding strength is not the only factor affecting GR transcription activity. The nuclear translocation is different depending again on the immunophilin in the GR complex. To be transported into the nucleus, the binding to dynein via the PPIase domain of the immunophilin is necessary. While FKBP52 can bind dynein, followed by nuclear translocation of the complex, the FKBP51 PPIase domain cannot bind dynein, impeding nuclear translocation of the GR complex into the nuclear space [241, 246]. Furthermore, GR activation substantially increases the expression FKBP51, which results in an intracellular ultrashort negative-feedback loop that may desensitize GR following initial steroid stimulation (Figure 5) [247–249].

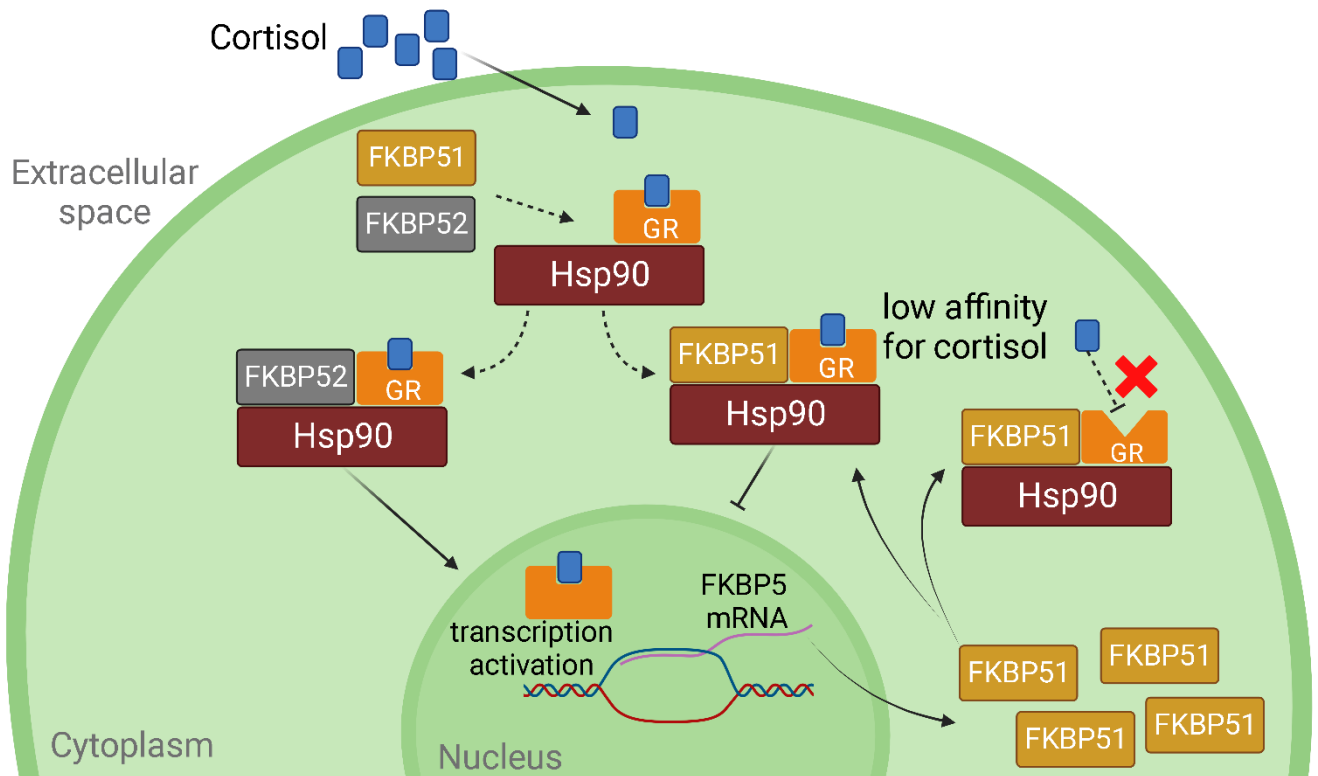


Figure 5. Biochemical pathway and interactions between the components of the glucocorticoid receptor (GR), heat shock protein 90 (Hsp90), and the effect of FKBP51 as a negative regulator of steroid hormone receptors. Figure generated with biorender.com

1.8.2 FKBP51 and FKBP52

Members of the FKBP family are named based on their molecular mass. The smallest FKBP (e.g. FKBP12) consist mostly of a PPIase motif in a single FK domain, while bigger FKBP are made up of different functional domains. For instance, FKBP51, FKBP52, and other major FKBP consist of two FKBP12-like domains (FK1 and FK2) and the TPR domain (Figure 4) [234].

Both human FKBP51 and FKBP52 are expressed constitutively in a variety of cell and tissue types including brain, kidney, colon, skeletal muscle, liver, placenta, heart, and peripheral blood [250–252]. They share 60% amino acid sequence identity and 75% similarity [233, 235, 253].

The N-terminal FK1 domain of FKBP51 and FKBP52 is formed by five antiparallel β -strands curved around a central α -helix (Figure 4) [234]. It is responsible for the PPIase activity of the proteins which can be inhibited by the immunosuppressive drugs FK506 and rapamycin. Moreover, this domain plays an essential role in the control of steroid hormone signaling. [234, 245, 254, 255].

Although structurally similar to FK1, the FK2 domain does not present PPIase activity and it is unable to bind FK506. The precise function of the FK2 domain of FKBP has not been entirely elucidated. Nonetheless, it is possible that the small differences in the binding pocket orientation of the FK2 domain of related FKBP resulting in distinct interaction with steroid receptors. For instance, it has been observed that this difference in the

orientation of FK2 in FKBP51 favors the binding of PR complexes over FKBP52. In the presence of FKBP51, hormone binding is suppressed, whereas in the presence of FKBP52, it is potentiated [233, 234, 256]. The TPR domains are all-helical structures responsible for Hsp90 binding to the FKBP5s [257–260]. TPR motifs consist of 3–16 tandem-repeats of 34 amino acid residues. They have been found in a wide range of species, and proteins containing TPRs are involved in transcription regulation and protein transportation [229, 260, 261]. FKBP51 and FKBP52 possess a three-unit repeat of the TPR domain [261].

Despite the close sequence similarity between these two proteins, their functions and structural dynamics differ greatly. While FKBP52 is a positive regulator of the GR, PR, and androgen receptor (AR), FKBP51 is a negative regulator of steroid hormone receptors [245, 255, 262]. This modulation of steroid hormone receptor activity may result in significant physiological consequences such as cortisol resistance when FKBP51 is overexpressed [263, 264]. One key difference between FKBP51 and FKBP52 is how their FK1 domain influences its activity [241, 245]. Because of the few distinct amino acids of the PPIase pocket, the binding pocket of each protein interacts differently in the GR, resulting in conformational changes of the GR ligand binding domain which directly affect the binding affinity to hormones [233, 245]. While FKBP52 potentiates hormone binding, FKBP51 represses it [233]. Moreover, it has been demonstrated that due to these differences in the binding pocket of the FK1 domain, FKBP5s bind substrates with different affinities [265, 266].

1.8.3 FKBP51 in disease

Over the years, FKBP51 and FKBP52 have been correlated to a number of diseases, including as endocrine-related disorders, stress-related diseases, metabolic diseases, prostate and breast cancer, and male and female infertility [233].

Both FKBP51 and FKBP52, together with Hsp90 and other co-chaperones, have been studied for their involvement in protein misfolding and aggregation disorders like Alzheimer's disease. FKBP51 prevents tau clearance and reduces its phosphorylation, while higher levels of FKBP52 correlate with reduced tau stability [267–269]. Interestingly, FKBP51 has been shown to be either overexpressed or downregulated in different types of cancer. For instance, melanoma, lymphoma, prostate cancer, and brain cancer have been reported to be correlated with elevated levels of FKBP51 [261, 270–273]. On the other hand, it has also been demonstrated that FKBP51 is downregulated in testicular cancer, colon cancer, and pancreatic cancer [261, 274].

In humans, the hypothalamus pituitary adrenal axis is the neuroendocrine connection between a stress-triggering situation and the body's physiological response to it [275]. While the normal physiological response is a short-term glucocorticoid release, a chronic state of stress creates an imbalanced cortisol level [276, 277]. This has multiple consequences due to the biological connection that exists between stress and metabolic disorders, which can be translated into an increased risk for obesity and metabolic-related disorders such as diabetes [278]. The negative regulation of the GR by FKBP51 has significant effects on the control of the stress response since GRs are responsible to end it. Additionally, increased *FKBP5* mRNA levels are linked to high levels of

circulating cortisol and FKBP51 level is increased by the effects of an intracellular negative feedback loop [243, 279–282].

1.9 FKBP51 transient binding pocket and selective inhibitors

As previously discussed in the context of GR signaling, FKBP51 and FKBP52 are present in different types of cells. Because of their opposing roles and their involvement in disease, it is vital to have inhibitors that can distinguish between these two proteins with high affinity.

The immunosuppressive drug FK506 interacts with similar affinity with the FK1-domain of FKBP51 and FKBP52. Because the FK1 domain is the main determinant of how differently FKBP51 and FKBP52 affect GR function, this domain has been studied as a potential therapeutic target [233, 254]. Despite a high degree of structural similarity, sequence variances in specific regions of the FK1 domain of both proteins are sufficient for different conformational dynamics [234, 283].

The iFit class ligands were the first molecules to selectively bind FKBP51 [18]. This selectivity is attributed to conformational changes in the FKBP51 FK1 domain after binding of iFit ligands, which can be classified as an induced-fit binding mechanism. When the crystal structure of the bound and apo-state of the protein were compared, it came to light that the complex of FKBP51 with SAFit1 (member of the iFit ligands) causes the displacement of the F67 side chain to accommodate the cyclohexyl moiety of SAFit1. The displaced F67 interacts with FKBP51 residues K58, K60, and F129, thus stabilizing the F67^{out} conformation. These contacts are not possible in FKBP52 as the residues T58, W60, and V129 are bulkier and do not allow comparable rearrangements [18]. As mentioned in section 1.2, proteins are flexible molecules that exist in several closely related conformations swapping on various timescales resulting in populations with diverse distributions [33, 34]. The F67^{out} conformer of FKBP51 exists in the apo-state, but it is only populated to approximately 0.4% (Figure 4) [17].

After the discovery of the transient binding pocket of FKBP51, a great amount of effort was put into the research of this immunophilin conformational dynamics and mechanisms of ligand binding. NMR and mutagenesis experiments with FKBP51 determined the importance of the β_{4-5} interconnecting loop and residues in the β_{3a} strand near F67 for the stabilization of this conformer with a flipped-out phenylalanine at position 67 [17, 22]. Nevertheless, due to allosteric effects, residues located far from the FK1 binding pocket exhibit increased dynamics, opposite to the strong reduction of conformational dynamics after the FK[431] (FK506-like ligand) binding [17].

These SAFit-like ligands have a 10,000-fold superior affinity to FKBP51 over FKBP52 [18, 284]. Nevertheless, they bind FKBP12 and its isoform FKBP12.6 as well. For this reason, a new set of SAFit-derived macrocyclic ligands were synthesized and tested [285–287]. These macrocyclic ligands, exactly like SAFit1, caused a F67 displacement upon binding. Surprisingly, this was not the only structural difference. The highly dynamic β_{3a}

strand was altered again, but this time the D68 was displaced too (F67^{out} D68^{out} conformation). The carbonyl group of the macrocyclic compounds 13a, 13d and, 13h reported by Voll *et al.*, 2021, takes the position of D68 and acts as a hydrogen bond acceptor for Y57 [285].

Additionally, fluorescently labeled tracers derived from the SAFit and macrocyclic tracers are available as tools for biochemical characterization and screening methods: SAFit-FL, a fluorescein-labeled analog of the iFit ligand class that binds preferentially to the F67^{out}/D68ⁱⁿ-conformation of FKBP51. Mcyc-TA_(out/out) (compound 14 in Voll *et al.*, 2021), a TAMRA conjugated macrocyclic analog of the SAFit class ligands that binds preferentially to an F67^{out}/D68^{out} conformation. And finally, a TAMRA labeled FK [431]-TA_(in/in) which binds the F67ⁱⁿ/D68ⁱⁿ-conformation of FKBP51 [18, 254, 285].

SAFit1 and SAFit2, the two best compounds of the iFit ligand class, selectively inhibited FKBP51 over FKBP52 with potential antidepressant-like effects *in vivo* [284, 288]. Unfortunately, the physicochemical properties of these two compounds do not comply with the normal central nervous system drugs, and for this reason, they are considered to be a research tool to find more appropriate molecules able to bind in a similar manner to FKBP51 while having more drug-like characteristics to have a higher chance to succeed in clinical trials [289, 290]. Although the macrocyclic analogs of SAFit are believed to have better drug-like characteristics, further optimization is necessary for *in vivo* experiments [287]. Optimized or completely new ligands that take advantage of the high conformational plasticity of FKBP51 are necessary to obtain ligands with high selectivity to FKBP51 over other members of the FKBP family while having optimal drug-like properties.

2 Objective

FKBP51 is a protein member of the immunophilins associated to several psychiatric and stress-related disorders, among many other reported diseases. The FKBP family is comprised of several highly conserved proteins in mammals. Some of them have high sequence identity and structural similarity. This is a concern when inhibitors targeted to one specific member of the FKBP family are able to bind to other proteins, causing off-target effects. Specially, FKBP51 and FKBP2 have a very similar structure, but with opposing biological functions. It is of great importance to create FKBP51 selective inhibitors that bind with high affinity and selectivity to this protein over other members of the FKBP family to avoid unwanted effects in *in vivo* experiments and subsequent clinical trials.

The structural flexibility of a protein may influence ligand-protein binding, and for some therapeutic targets, this property can limit access to its binding site. This presents a constraint for the development of novel molecules to inhibit or activate a target protein. Protein engineering tools together with yeast surface display and flow cytometry are a set of methods that can deliver FKBP51 mutants with enhanced affinity to ligands which bind preferentially to the transient binding pocket of FKBP51, without interacting (or interacting with low affinity) with FKBP52 and other FKBP.

The first goal of this work was to create different mutant libraries of the FK1 domain of FKBP51. Gene randomization was achieved by diverse protein engineering techniques such as directed evolution, Site Saturation Mutagenesis, Site-Directed Mutagenesis, Iterative, and Combinatorial Mutagenesis. The resulting randomized gene pools were used to create Yeast Surface Display libraries that were screened via FACS utilizing two reported ligands that bind preferentially to the open conformation of FKBP51. The identified mutants were characterized by fluorescence polarization, thermal stability assays, and some of the best variants were crystallized in apo- and bound-state with the open conformation ligands.

These FKBP51 mutants with improved affinity to open conformation ligands will lead to a better understanding of the FKBP51 transient binding pocket dynamics, protein-ligand binding mechanisms, and will provide invaluable information for drug design and development of novel molecules developed to inhibit FKBP51. Moreover, the methods used in this work can be transferred to stabilize binding pockets of diverse therapeutic proteins.

The stabilization of a specific protein conformation can be achieved by different methods. Additionally, to protein engineering, it was hypothesized that protein-protein interactions could be an alternative way to accomplish the same goal. Aiming to stabilize the FKBP51 open conformation, the second goal of this thesis was to identify chicken-derived single chain variable domains acting as conformation-locking molecules or high-affinity binders for *in vitro* experiments.

Gallus gallus specimens were immunized with the FK1 domain of FKBP51. The extracted spleen RNA was used to create a Yeast Surface Display library of scFvs, which was then screened against FKBP51 to obtain high-affinity binders. In subsequent FACS campaigns, FKBP51-binding scFvs were screened to find those that facilitate the binding of conformation-specific ligands upon scFv binding. ScFvs as conformation-locking molecules have the potential to be invaluable tools to screen new fragment libraries that bind specifically to the open conformation of FKBP51 over the native closed conformation, being with high probability, specific to FKBP51 over other proteins of the FKBP family.

Parallel to these experiments, derived from the need for antibodies with higher affinity and FKBP51 specificity than those currently on the market, the third goal of this work was to identify scFvs and antibodies with high affinity and specificity to FKBP51 over other members of the FKBP family as research tools. These two protein-binding molecules can be used in research as biomarkers or labeling the target protein for identification and characterization.

3 References

1. Spedding M (2006) New directions for drug discovery. *Dialogues Clin Neurosci* 8:295–301. <https://doi.org/10.31887/DCNS.2006.8.3/mspedding>

2. U.S. Food & Drug Administration (2018) The Drug Development Process. <https://www.fda.gov/patients/learn-about-drug-and-device-approvals/drug-development-process>
3. Hollingsworth SA, Kelly B, Valant C, et al (2019) Cryptic pocket formation underlies allosteric modulator selectivity at muscarinic GPCRs. *Nat Commun* 10:1–9. <https://doi.org/10.1038/s41467-019-11062-7>
4. Stank A, Kokh DB, Fuller JC, Wade RC (2016) Protein Binding Pocket Dynamics. *Acc Chem Res* 49:809–815. <https://doi.org/10.1021/acs.accounts.5b00516>
5. Fischer E (1894) Einfluss der Configuration auf die Wirkung der Enzyme. *Berichte der deutschen chemischen Gesellschaft* 27:2985–2993. <https://doi.org/10.1002/cber.18940270364>
6. James LC, Tawfik DS (2003) Conformational diversity and protein evolution – a 60-year-old hypothesis revisited. *Trends Biochem Sci* 28:361–368. [https://doi.org/10.1016/S0968-0004\(03\)00135-X](https://doi.org/10.1016/S0968-0004(03)00135-X)
7. Koshland DE (1958) Application of a Theory of Enzyme Specificity to Protein Synthesis. *Proceedings of the National Academy of Sciences* 44:98–104. <https://doi.org/10.1073/pnas.44.2.98>
8. Arora K, Brooks CL (2007) Large-scale allosteric conformational transitions of adenylate kinase appear to involve a population-shift mechanism. *Proceedings of the National Academy of Sciences* 104:18496–18501. <https://doi.org/10.1073/pnas.0706443104>
9. Umezawa K, Kii I (2021) Druggable Transient Pockets in Protein Kinases. *Molecules* 26:651. <https://doi.org/10.3390/molecules26030651>
10. Csermely P, Palotai R, Nussinov R (2010) Induced fit, conformational selection and independent dynamic segments: an extended view of binding events. *Trends Biochem Sci* 35:539–546. <https://doi.org/10.1016/j.tibs.2010.04.009>
11. Hamers-Casterman C, Atarhouch T, Muyldermans S, et al (1993) Naturally occurring antibodies devoid of light chains. *Nature* 363:446–448. <https://doi.org/10.1038/363446a0>
12. Gleeson MP, Hersey A, Montanari D, Overington J (2011) Probing the links between in vitro potency, ADMET and physicochemical parameters. *Nat Rev Drug Discov* 10:197–208. <https://doi.org/10.1038/nrd3367>
13. Mattedi G, Deflorian F, Mason JS, et al (2019) Understanding Ligand Binding Selectivity in a Prototypical GPCR Family. *J Chem Inf Model* 59:2830–2836. <https://doi.org/10.1021/acs.jcim.9b00298>
14. Huggins DJ, Sherman W, Tidor B (2012) Rational Approaches to Improving Selectivity in Drug Design. *J Med Chem* 55:1424–1444. <https://doi.org/10.1021/jm2010332>
15. Hochberg MC (2003) Comparison of the efficacy of the tumour necrosis factor blocking agents adalimumab, etanercept, and infliximab when added to methotrexate in patients with active rheumatoid arthritis. *Ann Rheum Dis* 62:13ii–1316. https://doi.org/10.1136/ard.62.suppl_2.ii13
16. Graczyk PP (2007) Gini Coefficient: A New Way To Express Selectivity of Kinase Inhibitors against a Family of Kinases. *J Med Chem* 50:5773–5779. <https://doi.org/10.1021/jm070562u>
17. Jagtap PKA, Asami S, Sippel C, et al (2019) Selective Inhibitors of FKBP51 Employ Conformational Selection of Dynamic Invisible States. *Angewandte Chemie International Edition* 58:9429–9433. <https://doi.org/10.1002/anie.201902994>
18. Gaali S, Kirschner A, Cuboni S, et al (2015) Selective inhibitors of the FK506-binding protein 51 by induced fit. *Nat Chem Biol* 11:33–37. <https://doi.org/10.1038/nchembio.1699>
19. Kang CB, Hong Y, Dhe-Paganon S, Yoon HS (2008) FKBP Family Proteins: Immunophilins with Versatile Biological Functions. *Neurosignals* 16:318–325. <https://doi.org/10.1159/000123041>
20. Smith Z, Ravindra P, Wang Y, et al (2020) Discovering Protein Conformational Flexibility through Artificial-Intelligence-Aided Molecular Dynamics. *J Phys Chem B* 124:8221–8229. <https://doi.org/10.1021/acs.jpcc.0c03985>

21. Kokh DB, Czodrowski P, Rippmann F, Wade RC (2016) Perturbation Approaches for Exploring Protein Binding Site Flexibility to Predict Transient Binding Pockets. *J Chem Theory Comput* 12:4100–4113. <https://doi.org/10.1021/acs.jctc.6b00101>
22. Lerma Romero JA, Meyners C, Christmann A, et al (2022) Binding pocket stabilization by high-throughput screening of yeast display libraries. *Front Mol Biosci* 9. <https://doi.org/10.3389/fmolb.2022.1023131>
23. Frembgen-Kesner T, Elcock AH (2006) Computational Sampling of a Cryptic Drug Binding Site in a Protein Receptor: Explicit Solvent Molecular Dynamics and Inhibitor Docking to p38 MAP Kinase. *J Mol Biol* 359:202–214. <https://doi.org/10.1016/j.jmb.2006.03.021>
24. Kokh DB, Richter S, Henrich S, et al (2013) TRAPP: A Tool for Analysis of Transient Binding Pockets in Proteins. *J Chem Inf Model* 53:1235–1252. <https://doi.org/10.1021/ci4000294>
25. Peracchi A, Mozzarelli A (2011) Exploring and exploiting allostery: Models, evolution, and drug targeting. *Biochimica et Biophysica Acta (BBA) - Proteins and Proteomics* 1814:922–933. <https://doi.org/10.1016/j.bbapap.2010.10.008>
26. Nussinov R, Tsai CJ (2013) Allostery in disease and in drug discovery. *Cell* 153:293–305. <https://doi.org/10.1016/j.cell.2013.03.034>
27. Burford NT, Clark MJ, Wehrman TS, et al (2013) Discovery of positive allosteric modulators and silent allosteric modulators of the μ -opioid receptor. *Proc Natl Acad Sci U S A* 110:10830–10835. <https://doi.org/10.1073/pnas.1300393110>
28. Wodak SJ, Paci E, Dokholyan N V., et al (2019) Allostery in Its Many Disguises: From Theory to Applications. *Structure* 27:566–578. <https://doi.org/10.1016/j.str.2019.01.003>
29. Wenthur CJ, Gentry PR, Mathews TP, Lindsley CW (2014) Drugs for Allosteric Sites on Receptors. *Annu Rev Pharmacol Toxicol* 54:165–184. <https://doi.org/10.1146/annurev-pharmtox-010611-134525>
30. Hardy JA, Wells JA (2004) Searching for new allosteric sites in enzymes. *Curr Opin Struct Biol* 14:706–715. <https://doi.org/10.1016/j.sbi.2004.10.009>
31. Wu N, Strömich L, Yaliraki SN (2022) Prediction of allosteric sites and signaling: Insights from benchmarking datasets. *Patterns* 3:100408. <https://doi.org/10.1016/j.patter.2021.100408>
32. Byun JA, VanSchouwen B, Akimoto M, Melacini G (2020) Allosteric inhibition explained through conformational ensembles sampling distinct “mixed” states. *Comput Struct Biotechnol J* 18:3803–3818. <https://doi.org/10.1016/j.csbj.2020.10.026>
33. Goodey NM, Benkovic SJ (2008) Allosteric regulation and catalysis emerge via a common route. *Nat Chem Biol* 4:474–482. <https://doi.org/10.1038/nchembio.98>
34. Nussinov R, Ma B (2012) Protein dynamics and conformational selection in bidirectional signal transduction. *BMC Biol* 10:2. <https://doi.org/10.1186/1741-7007-10-2>
35. Kumar S, Tsai CJ, Nussinov R (2000) Factors enhancing protein thermostability. *Protein Eng* 13:179–191
36. Suplatov D, Švedas V (2015) Study of functional and allosteric sites in protein superfamilies. *Acta Naturae* 7:34–45. <https://doi.org/10.32607/20758251-2015-7-4-34-45>
37. Nussinov R, Tsai CJ, Xin F, Radivojac P (2012) Allosteric post-translational modification codes. *Trends Biochem Sci* 37:447–455. <https://doi.org/10.1016/j.tibs.2012.07.001>
38. Sinha N, Nussinov R (2001) Point mutations and sequence variability in proteins: Redistributions of preexisting populations. *Proceedings of the National Academy of Sciences* 98:3139–3144. <https://doi.org/10.1073/pnas.051399098>

39. Wu S, Acevedo JP, Reetz MT (2010) Induced allostery in the directed evolution of an enantioselective Baeyer–Villiger monooxygenase. *Proceedings of the National Academy of Sciences* 107:2775–2780. <https://doi.org/10.1073/pnas.0911656107>
40. Strickland D, Moffat K, Sosnick TR (2008) Light-activated DNA binding in a designed allosteric protein. *Proceedings of the National Academy of Sciences* 105:10709–10714. <https://doi.org/10.1073/pnas.0709610105>
41. Laskowski RA, Gerick F, Thornton JM (2009) The structural basis of allosteric regulation in proteins. *FEBS Lett* 583:1692–1698. <https://doi.org/10.1016/j.febslet.2009.03.019>
42. Chamberlain TC, Cheung ST, Yoon JSJ, et al (2020) Interleukin-10 and Small Molecule SHIP1 Allosteric Regulators Trigger Anti-inflammatory Effects through SHIP1/STAT3 Complexes. *iScience* 23:101433. <https://doi.org/10.1016/j.isci.2020.101433>
43. Kumar S, Ma B, Tsai C-J, et al (2008) Folding and binding cascades: Dynamic landscapes and population shifts. *Protein Science* 9:10–19. <https://doi.org/10.1110/ps.9.1.10>
44. Skora L, Mestan J, Fabbro D, et al (2013) NMR reveals the allosteric opening and closing of Abelson tyrosine kinase by ATP-site and myristoyl pocket inhibitors. *Proceedings of the National Academy of Sciences* 110. <https://doi.org/10.1073/pnas.1314712110>
45. Agafonov R V, Wilson C, Otten R, et al (2014) Energetic dissection of Gleevec’s selectivity toward human tyrosine kinases. *Nat Struct Mol Biol* 21:848–853. <https://doi.org/10.1038/nsmb.2891>
46. Wang T, Bisson WH, Mäser P, et al (2014) Differences in Conformational Dynamics between Plasmodium falciparum and Human Hsp90 Orthologues Enable the Structure-Based Discovery of Pathogen-Selective Inhibitors. *J Med Chem* 57:2524–2535. <https://doi.org/10.1021/jm401801t>
47. Aleksandrov A, Simonson T (2010) Molecular Dynamics Simulations Show That Conformational Selection Governs the Binding Preferences of Imatinib for Several Tyrosine Kinases. *Journal of Biological Chemistry* 285:13807–13815. <https://doi.org/10.1074/jbc.M110.109660>
48. Berndt A, Miller S, Williams O, et al (2010) The p110 δ structure: mechanisms for selectivity and potency of new PI(3)K inhibitors. *Nat Chem Biol* 6:117–124. <https://doi.org/10.1038/nchembio.293>
49. Moroni E, Paladino A, Colombo G (2015) The Dynamics of Drug Discovery. *Curr Top Med Chem* 15:2043–2055. <https://doi.org/10.2174/1568026615666150519102950>
50. Hopkins AL, Groom CR (2002) The druggable genome. *Nat Rev Drug Discov* 1:727–730. <https://doi.org/10.1038/nrd892>
51. Kuzmanic A, Bowman GR, Juarez-Jimenez J, et al (2020) Investigating Cryptic Binding Sites by Molecular Dynamics Simulations. *Acc Chem Res* 53:654–661. <https://doi.org/10.1021/acs.accounts.9b00613>
52. Cimermanic P, Weinkam P, Rettenmaier TJ, et al (2016) CryptoSite: Expanding the Druggable Proteome by Characterization and Prediction of Cryptic Binding Sites. *J Mol Biol* 428:709–719. <https://doi.org/10.1016/j.jmb.2016.01.029>
53. Eyrisch S, Helms V (2007) Transient pockets on protein surfaces involved in protein-protein interaction. *J Med Chem* 50:3457–3464. <https://doi.org/10.1021/jm070095g>
54. Xia Z, Karpov P, Popowicz G, et al (2022) What Features of Ligands Are Relevant to the Opening of Cryptic Pockets in Drug Targets? *Informatics* 9. <https://doi.org/10.3390/informatics9010008>
55. Oleinikovas V, Saladino G, Cossins BP, Gervasio FL (2016) Understanding Cryptic Pocket Formation in Protein Targets by Enhanced Sampling Simulations. *J Am Chem Soc* 138:14257–14263. <https://doi.org/10.1021/jacs.6b05425>

-
56. Lawson ADG (2012) Antibody-enabled small-molecule drug discovery. *Nat Rev Drug Discov* 11:519–525. <https://doi.org/10.1038/nrd3756>
 57. Erlanson DA, Braisted AC, Raphael DR, et al (2000) Site-directed ligand discovery. *Proceedings of the National Academy of Sciences* 97:9367–9372. <https://doi.org/10.1073/pnas.97.17.9367>
 58. Ludlow RF, Verdonk ML, Saini HK, et al (2015) Detection of secondary binding sites in proteins using fragment screening. *Proceedings of the National Academy of Sciences* 112:15910–15915. <https://doi.org/10.1073/pnas.1518946112>
 59. Mizukoshi Y, Takeuchi K, Tokunaga Y, et al (2020) Targeting the cryptic sites: NMR-based strategy to improve protein druggability by controlling the conformational equilibrium. *Sci Adv* 6:. <https://doi.org/10.1126/sciadv.abd0480>
 60. Arkin MR, Randal M, DeLano WL, et al (2003) Binding of small molecules to an adaptive protein–protein interface. *Proceedings of the National Academy of Sciences* 100:1603–1608. <https://doi.org/10.1073/pnas.252756299>
 61. Hyde J, Braisted AC, Randal M, Arkin MR (2003) Discovery and Characterization of Cooperative Ligand Binding in the Adaptive Region of Interleukin-2. *Biochemistry* 42:6475–6483. <https://doi.org/10.1021/bi034138g>
 62. Pargellis C, Tong L, Churchill L, et al (2002) Inhibition of p38 MAP kinase by utilizing a novel allosteric binding site. *Nat Struct Biol* 9:268–272. <https://doi.org/10.1038/nsb770>
 63. Engqvist MKM, Rabe KS (2019) Applications of Protein Engineering and Directed Evolution in Plant Research. *Plant Physiol* 179:907–917. <https://doi.org/10.1104/pp.18.01534>
 64. Brustad EM, Arnold FH (2011) Optimizing non-natural protein function with directed evolution. *Curr Opin Chem Biol* 15:201–210. <https://doi.org/10.1016/j.cbpa.2010.11.020>
 65. Gibson DG, Young L, Chuang R-Y, et al (2009) Enzymatic assembly of DNA molecules up to several hundred kilobases. *Nat Methods* 6:343–345. <https://doi.org/10.1038/nmeth.1318>
 66. Urlacher VB, Eiben S (2006) Cytochrome P450 monooxygenases: perspectives for synthetic application. *Trends Biotechnol* 24:324–330. <https://doi.org/10.1016/j.tibtech.2006.05.002>
 67. Sutherland T, Horne I, Weir K, et al (2004) Enzymatic bioremediation: from enzyme discovery to applications. *Clin Exp Pharmacol Physiol* 31:817–821. <https://doi.org/10.1111/j.1440-1681.2004.04088.x>
 68. Porter JL, Rusli RA, Ollis DL (2016) Directed Evolution of Enzymes for Industrial Biocatalysis. *ChemBioChem* 17:197–203. <https://doi.org/10.1002/cbic.201500280>
 69. Kumar A, Singh S (2013) Directed evolution: tailoring biocatalysts for industrial applications. *Crit Rev Biotechnol* 33:365–378. <https://doi.org/10.3109/07388551.2012.716810>
 70. Singh RK, Lee J-K, Selvaraj C, et al (2017) Protein Engineering Approaches in the Post-Genomic Era. *Curr Protein Pept Sci* 19:. <https://doi.org/10.2174/1389203718666161117114243>
 71. Korendovych I V., DeGrado WF (2020) De novo protein design, a retrospective. *Q Rev Biophys* 53:e3. <https://doi.org/10.1017/S0033583519000131>
 72. Pan X, Kortemme T (2021) Recent advances in de novo protein design: Principles, methods, and applications. *Journal of Biological Chemistry* 296:100558. <https://doi.org/10.1016/j.jbc.2021.100558>
 73. Song Z, Zhang Q, Wu W, et al (2023) Rational design of enzyme activity and enantioselectivity. *Front Bioeng Biotechnol* 11:. <https://doi.org/10.3389/fbioe.2023.1129149>
 74. Bloom JD, Arnold FH (2009) In the light of directed evolution: Pathways of adaptive protein evolution. *Proceedings of the National Academy of Sciences* 106:9995–10000. <https://doi.org/10.1073/pnas.0901522106>
 75. Davydova EK (2022) Protein Engineering: Advances in Phage Display for Basic Science and Medical Research. *Biochemistry (Moscow)* 87:S146–S167. <https://doi.org/10.1134/S0006297922140127>

76. Baammi S, Daoud R, El Allali A (2023) In silico protein engineering shows that novel mutations affecting NAD⁺ binding sites may improve phosphite dehydrogenase stability and activity. *Sci Rep* 13:1878. <https://doi.org/10.1038/s41598-023-28246-3>
77. Thomas S, George JJ (2018) In Silico Protein Engineering: Methods and Tools. In: *Recent Trends in Science and Technology*. pp 73–80
78. Burnside D, Schoenrock A, Moteshareie H, et al (2019) In Silico Engineering of Synthetic Binding Proteins from Random Amino Acid Sequences. *iScience* 11:375–387. <https://doi.org/10.1016/j.isci.2018.11.038>
79. Wang DD, Zhu M, Yan H (2021) Computationally predicting binding affinity in protein–ligand complexes: free energy-based simulations and machine learning-based scoring functions. *Brief Bioinform* 22:. <https://doi.org/10.1093/bib/bbaa107>
80. Montanucci L, Martelli PL, Ben-Tal N, Fariselli P (2019) A natural upper bound to the accuracy of predicting protein stability changes upon mutations. *Bioinformatics* 35:1513–1517. <https://doi.org/10.1093/bioinformatics/bty880>
81. Pucci F, Rooman M (2016) Towards an accurate prediction of the thermal stability of homologous proteins. *J Biomol Struct Dyn* 34:1132–1142. <https://doi.org/10.1080/07391102.2015.1073631>
82. Walker SP, Yallapragada VVB, Tangney M (2021) Arming Yourself for The In Silico Protein Design Revolution. *Trends Biotechnol* 39:651–664. <https://doi.org/10.1016/j.tibtech.2020.10.003>
83. Perkel JM (2019) The computational protein designers. *Nature* 571:585–587. <https://doi.org/10.1038/d41586-019-02251-x>
84. Voskarides K (2021) Directed Evolution. The Legacy of a Nobel Prize. *J Mol Evol* 89:189–191. <https://doi.org/10.1007/s00239-020-09972-y>
85. Bloom JD, Arnold FH (2009) In the light of directed evolution: Pathways of adaptive protein evolution. *Proceedings of the National Academy of Sciences* 106:9995–10000. <https://doi.org/10.1073/pnas.0901522106>
86. Packer MS, Liu DR (2015) Methods for the directed evolution of proteins. *Nat Rev Genet* 16:379–394. <https://doi.org/10.1038/nrg3927>
87. Tizei PAG, Csibra E, Torres L, Pinheiro VB (2016) Selection platforms for directed evolution in synthetic biology. *Biochem Soc Trans* 44:1165–1175. <https://doi.org/10.1042/BST20160076>
88. Li A, Qu G, Sun Z, Reetz MT (2019) Statistical Analysis of the Benefits of Focused Saturation Mutagenesis in Directed Evolution Based on Reduced Amino Acid Alphabets. *ACS Catal* 9:7769–7778. <https://doi.org/10.1021/acscatal.9b02548>
89. Tachioka M, Sugimoto N, Nakamura A, et al (2016) Development of simple random mutagenesis protocol for the protein expression system in *Pichia pastoris*. *Biotechnol Biofuels* 9:199. <https://doi.org/10.1186/s13068-016-0613-z>
90. Labrou N (2010) Random Mutagenesis Methods for In Vitro Directed Enzyme Evolution. *Curr Protein Pept Sci* 11:91–100. <https://doi.org/10.2174/138920310790274617>
91. Kotzia GA, Labrou NE (2009) Engineering thermal stability of l-asparaginase by in vitro directed evolution. *FEBS Journal* 276:1750–1761. <https://doi.org/10.1111/j.1742-4658.2009.06910.x>
92. Fujii R (2004) One-step random mutagenesis by error-prone rolling circle amplification. *Nucleic Acids Res* 32:e145–e145. <https://doi.org/10.1093/nar/gnh147>
93. Greener A, Callahan M, Jerpseth B (1997) An efficient random mutagenesis technique using an *E. coli* mutator strain. *Mol Biotechnol* 7:189–195. <https://doi.org/10.1007/BF02761755>

94. Deshler JO (1992) A simple method for randomly mutating cloned DNA fragments by using chemical mutagens and the polymerase chain reaction. *Genet Anal* 9:103–106. [https://doi.org/10.1016/1050-3862\(92\)90048-A](https://doi.org/10.1016/1050-3862(92)90048-A)
95. Lerma Romero JA, Kolmar H (2023) Accessing Transient Binding Pockets by Protein Engineering and Yeast Surface Display Screening. In: Zielonka S, Krah S (eds) *Methods in Molecular Biology*. Humana, New York, NY, pp 249–274
96. Eckert KA, Kunkel TA (1991) DNA polymerase fidelity and the polymerase chain reaction. *Genome Res* 1:17–24. <https://doi.org/10.1101/gr.1.1.17>
97. McCullum EO, Williams BAR, Zhang J, Chaput JC (2010) Random Mutagenesis by Error-Prone PCR. pp 103–109
98. Wilson DS, Keefe AD (2001) Random Mutagenesis by PCR. In: *Current Protocols in Molecular Biology*. John Wiley & Sons, Inc., Hoboken, NJ, USA
99. Vanhercke T, Ampe C, Tirry L, Denolf P (2005) Reducing mutational bias in random protein libraries. *Anal Biochem* 339:9–14. <https://doi.org/10.1016/j.ab.2004.11.032>
100. Cirino PC, Mayer KM, Umeno D (2003) Generating Mutant Libraries Using Error-Prone PCR. In: Arnold F, Georgiou G (eds) *Directed Evolution Library Creation*. Humana Press, New Jersey, pp 3–10
101. Dennig A, Shivange A V., Marienhagen J, Schwaneberg U (2011) OmniChange: The Sequence Independent Method for Simultaneous Site-Saturation of Five Codons. *PLoS One* 6:e26222. <https://doi.org/10.1371/journal.pone.0026222>
102. Brouk M, Nov Y, Fishman A (2010) Improving Biocatalyst Performance by Integrating Statistical Methods into Protein Engineering. *Appl Environ Microbiol* 76:6397–6403. <https://doi.org/10.1128/AEM.00878-10>
103. Chica RA, Doucet N, Pelletier JN (2005) Semi-rational approaches to engineering enzyme activity: combining the benefits of directed evolution and rational design. *Curr Opin Biotechnol* 16:378–384. <https://doi.org/10.1016/j.copbio.2005.06.004>
104. Fox RJ, Huisman GW (2008) Enzyme optimization: moving from blind evolution to statistical exploration of sequence–function space. *Trends Biotechnol* 26:132–138. <https://doi.org/10.1016/j.tibtech.2007.12.001>
105. Lutz S (2010) Beyond directed evolution—semi-rational protein engineering and design. *Curr Opin Biotechnol* 21:734–743. <https://doi.org/10.1016/j.copbio.2010.08.011>
106. Tang L, Gao H, Zhu X, et al (2012) Construction of “small-intelligent” focused mutagenesis libraries using well-designed combinatorial degenerate primers. *Biotechniques* 52:149–158. <https://doi.org/10.2144/000113820>
107. Zhang Y, Liu M, Wang H, et al (2022) Focused mutagenesis in non-catalytic cavity for improving catalytic efficiency of 3-ketosteroid- Δ 1-dehydrogenase. *Molecular Catalysis* 531:112661. <https://doi.org/10.1016/j.mcat.2022.112661>
108. Morley KL, Kazlauskas RJ (2005) Improving enzyme properties: when are closer mutations better? *Trends Biotechnol* 23:231–237. <https://doi.org/10.1016/j.tibtech.2005.03.005>
109. Clayden J, Lund A, Vallverdú L, Helliwell M (2004) Ultra-remote stereocontrol by conformational communication of information along a carbon chain. *Nature* 431:966–971. <https://doi.org/10.1038/nature02933>
110. Dalby PA (2003) Optimising enzyme function by directed evolution. *Curr Opin Struct Biol* 13:500–505. [https://doi.org/10.1016/S0959-440X\(03\)00101-5](https://doi.org/10.1016/S0959-440X(03)00101-5)
111. Ji J, Fan K, Tian X, et al (2012) Iterative Combinatorial Mutagenesis as an Effective Strategy for Generation of Deacetoxycephalosporin C Synthase with Improved Activity toward Penicillin G. *Appl Environ Microbiol* 78:7809–7812. <https://doi.org/10.1128/AEM.02122-12>

112. Ji J, Tian X, Fan K, Yang K (2012) New strategy of site-directed mutagenesis identifies new sites to improve *Streptomyces clavuligerus* deacetoxycephalosporin C synthase activity toward penicillin G. *Appl Microbiol Biotechnol* 93:2395–2401. <https://doi.org/10.1007/s00253-011-3566-y>
113. Choi GCG, Zhou P, Yuen CTL, et al (2019) Combinatorial mutagenesis en masse optimizes the genome editing activities of SpCas9. *Nat Methods* 16:722–730. <https://doi.org/10.1038/s41592-019-0473-0>
114. Parker AS, Griswold KE, Bailey-Kellogg C (2011) Optimization of Combinatorial Mutagenesis. *Journal of Computational Biology* 18:1743–1756. <https://doi.org/10.1089/cmb.2011.0152>
115. Reetz MT, Carballeira JD (2007) Iterative saturation mutagenesis (ISM) for rapid directed evolution of functional enzymes. *Nat Protoc* 2:891–903. <https://doi.org/10.1038/nprot.2007.72>
116. Belsare KD, Andorfer MC, Cardenas FS, et al (2017) A Simple Combinatorial Codon Mutagenesis Method for Targeted Protein Engineering. *ACS Synth Biol* 6:416–420. <https://doi.org/10.1021/acssynbio.6b00297>
117. Reetz MT, Puls M, Carballeira JD, et al (2007) Learning from Directed Evolution: Further Lessons from Theoretical Investigations into Cooperative Mutations in Lipase Enantioselectivity. *ChemBioChem* 8:106–112. <https://doi.org/10.1002/cbic.200600359>
118. Reetz MT, Wang L-W, Bocola M (2006) Directed Evolution of Enantioselective Enzymes: Iterative Cycles of CASTing for Probing Protein-Sequence Space. *Angewandte Chemie International Edition* 45:1236–1241. <https://doi.org/10.1002/anie.200502746>
119. NobelPrize.org (2023) Nobel Prize Outreach AB 2023. www.nobelprize.org/prizes/chemistry/2018/press-release/. Accessed 11 Aug 2023
120. Miyazaki K, Arnold FH (1999) Exploring Nonnatural Evolutionary Pathways by Saturation Mutagenesis: Rapid Improvement of Protein Function. *J Mol Evol* 49:716–720. <https://doi.org/10.1007/PL00006593>
121. Hoogenboom HR, Griffiths AD, Johnson KS, et al (1991) Multi-subunit proteins on the surface of filamentous phage: methodologies for displaying antibody (Fab) heavy and light chains. *Nucleic Acids Res* 19:4133–4137. <https://doi.org/10.1093/nar/19.15.4133>
122. Winter G, Griffiths AD, Hawkins RE, Hoogenboom HR (1994) Making Antibodies by Phage Display Technology. *Annu Rev Immunol* 12:433–455. <https://doi.org/10.1146/annurev.iy.12.040194.002245>
123. Scott DJ, Kummer L, Egloff P, et al (2014) Improving the apo-state detergent stability of NTS1 with CHES for pharmacological and structural studies. *Biochimica et Biophysica Acta (BBA) - Biomembranes* 1838:2817–2824. <https://doi.org/10.1016/j.bbamem.2014.07.015>
124. Tu R, Martinez R, Prodanovic R, et al (2011) A Flow Cytometry–Based Screening System for Directed Evolution of Proteases. *SLAS Discovery* 16:285–294. <https://doi.org/10.1177/1087057110396361>
125. Cheng F, Kardashliev T, Pitzler C, et al (2015) A Competitive Flow Cytometry Screening System for Directed Evolution of Therapeutic Enzyme. *ACS Synth Biol* 4:768–775. <https://doi.org/10.1021/sb500343g>
126. Yi L, Gebhard MC, Li Q, et al (2013) Engineering of TEV protease variants by yeast ER sequestration screening (YESS) of combinatorial libraries. *Proceedings of the National Academy of Sciences* 110:7229–7234. <https://doi.org/10.1073/pnas.1215994110>
127. Dorr BM, Ham HO, An C, et al (2014) Reprogramming the specificity of sortase enzymes. *Proceedings of the National Academy of Sciences* 111:13343–13348. <https://doi.org/10.1073/pnas.1411179111>
128. Chen I, Dorr BM, Liu DR (2011) A general strategy for the evolution of bond-forming enzymes using yeast display. *Proceedings of the National Academy of Sciences* 108:11399–11404. <https://doi.org/10.1073/pnas.1101046108>
129. Bradbury A (1999) Display technologies expand their horizons. *Trends Biotechnol* 17:137–138. [https://doi.org/10.1016/S0167-7799\(98\)01289-X](https://doi.org/10.1016/S0167-7799(98)01289-X)

-
130. Li M (2000) Applications of display technology in protein analysis. *Nat Biotechnol* 18:1251–1256. <https://doi.org/10.1038/82355>
 131. Galán A, Comor L, Horvatić A, et al (2016) Library-based display technologies: where do we stand? *Mol Biosyst* 12:2342–2358. <https://doi.org/10.1039/C6MB00219F>
 132. Patel DJ, Suri AK (2000) Structure, recognition and discrimination in RNA aptamer complexes with cofactors, amino acids, drugs and aminoglycoside antibiotics. *Reviews in Molecular Biotechnology* 74:39–60. [https://doi.org/10.1016/S1389-0352\(99\)00003-3](https://doi.org/10.1016/S1389-0352(99)00003-3)
 133. Smith GP (1985) Filamentous Fusion Phage: Novel Expression Vectors That Display Cloned Antigens on the Virion Surface. *Science* (1979) 228:1315–1317. <https://doi.org/10.1126/science.4001944>
 134. Marintcheva B (2018) Phage Display. In: *Harnessing the Power of Viruses*. Elsevier, pp 133–160
 135. Sergeeva A, Kolonin M, Molldrem J, et al (2006) Display technologies: Application for the discovery of drug and gene delivery agents. *Adv Drug Deliv Rev* 58:1622–1654. <https://doi.org/10.1016/j.addr.2006.09.018>
 136. Cherf GM, Cochran JR (2015) Applications of Yeast Surface Display for Protein Engineering. pp 155–175
 137. Kondo A, Ueda M (2004) Yeast cell-surface display-applications of molecular display. *Appl Microbiol Biotechnol* 64:28–40. <https://doi.org/10.1007/s00253-003-1492-3>
 138. Teymennet-Ramírez K V., Martínez-Morales F, Trejo-Hernández MR (2022) Yeast Surface Display System: Strategies for Improvement and Biotechnological Applications. *Front Bioeng Biotechnol* 9. <https://doi.org/10.3389/fbioe.2021.794742>
 139. Könnig D, Kolmar H (2018) Beyond antibody engineering: directed evolution of alternative binding scaffolds and enzymes using yeast surface display. *Microb Cell Fact* 17:32. <https://doi.org/10.1186/s12934-018-0881-3>
 140. King D, Bowers P, Kehry M, Horlick R (2014) Mammalian Cell Display and Somatic Hypermutation In Vitro for Human Antibody Discovery. *Curr Drug Discov Technol* 11:56–64. <https://doi.org/10.2174/15701638113109990037>
 141. Waldmeier L, Hellmann I, Gutknecht CK, et al (2016) Transpo-mAb display: Transposition-mediated B cell display and functional screening of full-length IgG antibody libraries. *MAbs* 8:726–740. <https://doi.org/10.1080/19420862.2016.1160990>
 142. Breous-Nystrom E, Schultze K, Meier M, et al (2014) Retrocyte Display® technology: Generation and screening of a high diversity cellular antibody library. *Methods* 65:57–67. <https://doi.org/10.1016/j.ymeth.2013.09.003>
 143. Benatuil L, Perez JM, Belk J, Hsieh CM (2010) An improved yeast transformation method for the generation of very large human antibody libraries. *Protein Engineering, Design and Selection* 23:155–159. <https://doi.org/10.1093/protein/gzq002>
 144. Wójcik M, Telzerow A, Quax W, Boersma Y (2015) High-Throughput Screening in Protein Engineering: Recent Advances and Future Perspectives. *Int J Mol Sci* 16:24918–24945. <https://doi.org/10.3390/ijms161024918>
 145. Ueda M, Tanaka A (2000) Cell surface engineering of yeast: Construction of arming yeast with biocatalyst. *J Biosci Bioeng* 90:125–136. [https://doi.org/10.1016/S1389-1723\(00\)80099-7](https://doi.org/10.1016/S1389-1723(00)80099-7)
 146. Matsumoto T, Fukuda H, Ueda M, et al (2002) Construction of Yeast Strains with High Cell Surface Lipase Activity by Using Novel Display Systems Based on the Flo1p Flocculation Functional Domain. *Appl Environ Microbiol* 68:4517–4522. <https://doi.org/10.1128/AEM.68.9.4517-4522.2002>
 147. Schreuder MP, Mooren ATA, Toschka HY, et al (1996) Immobilizing proteins on the surface of yeast cells. *Trends Biotechnol* 14:115–120. [https://doi.org/10.1016/0167-7799\(96\)10017-2](https://doi.org/10.1016/0167-7799(96)10017-2)
 148. Lipke PN, Kurjan J (1992) Sexual agglutination in budding yeasts: structure, function, and regulation of adhesion glycoproteins. *Microbiol Rev* 56:180–194. <https://doi.org/10.1128/mr.56.1.180-194.1992>

149. Boder ET, Wittrup KD (1997) Yeast surface display for screening combinatorial polypeptide libraries. *Nat Biotechnol* 15:553–557. <https://doi.org/10.1038/nbt0697-553>
150. Kapteyn JC, Van Den Ende H, Klis FM (1999) The contribution of cell wall proteins to the organization of the yeast cell wall. *Biochimica et Biophysica Acta (BBA) - General Subjects* 1426:373–383. [https://doi.org/10.1016/S0304-4165\(98\)00137-8](https://doi.org/10.1016/S0304-4165(98)00137-8)
151. Wang Z, Mathias A, Stavrou S, Neville DM (2005) A new yeast display vector permitting free scFv amino termini can augment ligand binding affinities. *Protein Engineering, Design and Selection* 18:337–343. <https://doi.org/10.1093/protein/gzi036>
152. Rosowski S, Becker S, Toleikis L, et al (2018) A novel one-step approach for the construction of yeast surface display Fab antibody libraries. *Microb Cell Fact* 17:3. <https://doi.org/10.1186/s12934-017-0853-z>
153. Krah S, Grzeschik J, Rosowski S, et al (2018) A Streamlined Approach for the Construction of Large Yeast Surface Display Fab Antibody Libraries. pp 145–161
154. Fiebig D, Bogen JP, Carrara SC, et al (2022) Streamlining the Transition From Yeast Surface Display of Antibody Fragment Immune Libraries to the Production as IgG Format in Mammalian Cells. *Front Bioeng Biotechnol* 10:. <https://doi.org/10.3389/fbioe.2022.794389>
155. Elter A, Bogen JP, Hinz SC, et al (2021) Humanization of Chicken-Derived scFv Using Yeast Surface Display and NGS Data Mining. *Biotechnol J* 16:2000231. <https://doi.org/10.1002/biot.202000231>
156. Bogen JP, Grzeschik J, Krah S, et al (2020) Rapid Generation of Chicken Immune Libraries for Yeast Surface Display. In: *Methods Mol Biol*. pp 289–302
157. Monegal A, Ami D, Martinelli C, et al (2009) Immunological applications of single-domain llama recombinant antibodies isolated from a naïve library. *Protein Engineering, Design and Selection* 22:273–280. <https://doi.org/10.1093/protein/gzp002>
158. Arbabi Ghahroudi M, Desmyter A, Wyns L, et al (1997) Selection and identification of single domain antibody fragments from camel heavy-chain antibodies. *FEBS Lett* 414:521–526. [https://doi.org/10.1016/S0014-5793\(97\)01062-4](https://doi.org/10.1016/S0014-5793(97)01062-4)
159. Grzeschik J, Hinz SC, Könning D, et al (2017) A simplified procedure for antibody engineering by yeast surface display: Coupling display levels and target binding by ribosomal skipping. *Biotechnol J* 12:1600454. <https://doi.org/10.1002/biot.201600454>
160. Macarrón Palacios A, Grzeschik J, Deweid L, et al (2020) Specific Targeting of Lymphoma Cells Using Semisynthetic Anti-Idiotypic Shark Antibodies. *Front Immunol* 11:. <https://doi.org/10.3389/fimmu.2020.560244>
161. Horwitz AH, Chang CP, Better M, et al (1988) Secretion of functional antibody and Fab fragment from yeast cells. *Proceedings of the National Academy of Sciences* 85:8678–8682. <https://doi.org/10.1073/pnas.85.22.8678>
162. Hong X, Ma MZ, Gildersleeve JC, et al (2013) Sugar-Binding Proteins from Fish: Selection of High Affinity “Lambodies” That Recognize Biomedically Relevant Glycans. *ACS Chem Biol* 8:152–160. <https://doi.org/10.1021/cb300399s>
163. Lipovšek D, Lippow SM, Hackel BJ, et al (2007) Evolution of an Interloop Disulfide Bond in High-Affinity Antibody Mimics Based on Fibronectin Type III Domain and Selected by Yeast Surface Display: Molecular Convergence with Single-Domain Camelid and Shark Antibodies. *J Mol Biol* 368:1024–1041. <https://doi.org/10.1016/j.jmb.2007.02.029>
164. Lee C-H, Park K-J, Sung E-S, et al (2010) Engineering of a human kringle domain into agonistic and antagonistic binding proteins functioning in vitro and in vivo. *Proceedings of the National Academy of Sciences* 107:9567–9571. <https://doi.org/10.1073/pnas.1001541107>

165. Lee C-H, Park K-J, Kim SJ, et al (2011) Generation of Bivalent and Bispecific Kringle Single Domains by Loop Grafting as Potent Agonists against Death Receptors 4 and 5. *J Mol Biol* 411:201–219. <https://doi.org/10.1016/j.jmb.2011.05.040>
166. Schütz M, Batyuk A, Klenk C, et al (2016) Generation of Fluorogen-Activating Designed Ankyrin Repeat Proteins (FADAs) as Versatile Sensor Tools. *J Mol Biol* 428:1272–1289. <https://doi.org/10.1016/j.jmb.2016.01.017>
167. Lipovšek D, Antipov E, Armstrong KA, et al (2007) Selection of Horseradish Peroxidase Variants with Enhanced Enantioselectivity by Yeast Surface Display. *Chem Biol* 14:1176–1185. <https://doi.org/10.1016/j.chembiol.2007.09.008>
168. Ostafe R, Prodanovic R, Nazor J, Fischer R (2014) Ultra-High-Throughput Screening Method for the Directed Evolution of Glucose Oxidase. *Chem Biol* 21:414–421. <https://doi.org/10.1016/j.chembiol.2014.01.010>
169. Cohen-Khait R, Schreiber G (2016) Low-stringency selection of TEM1 for BLIP shows interface plasticity and selection for faster binders. *Proceedings of the National Academy of Sciences* 113:14982–14987. <https://doi.org/10.1073/pnas.1613122113>
170. Kim Y-S, Bhandari R, Cochran JR, et al (2005) Directed evolution of the epidermal growth factor receptor extracellular domain for expression in yeast. *Proteins: Structure, Function, and Bioinformatics* 62:1026–1035. <https://doi.org/10.1002/prot.20618>
171. Traxlmayr MW, Obinger C (2012) Directed evolution of proteins for increased stability and expression using yeast display. *Arch Biochem Biophys* 526:174–180. <https://doi.org/10.1016/j.abb.2012.04.022>
172. Boder ET, Raeeszadeh-Sarmazdeh M, Price JV (2012) Engineering antibodies by yeast display. *Arch Biochem Biophys* 526:99–106. <https://doi.org/10.1016/j.abb.2012.03.009>
173. Black CB, Duensing TD, Trinkle LS, Dunlay RT (2011) Cell-Based Screening Using High-Throughput Flow Cytometry. *Assay Drug Dev Technol* 9:13–20. <https://doi.org/10.1089/adt.2010.0308>
174. McKinnon KM (2018) Flow Cytometry: An Overview. *Curr Protoc Immunol* 120:. <https://doi.org/10.1002/cpim.40>
175. Tomlinson MJ, Tomlinson S, Yang XB, Kirkham J (2013) Cell separation: Terminology and practical considerations. *J Tissue Eng* 4:204173141247269. <https://doi.org/10.1177/2041731412472690>
176. Jin S, Sun Y, Liang X, et al (2022) Emerging new therapeutic antibody derivatives for cancer treatment. *Signal Transduct Target Ther* 7:39. <https://doi.org/10.1038/s41392-021-00868-x>
177. Kaplon H, Crescioli S, Chenoweth A, et al (2023) Antibodies to watch in 2023. *MAbs* 15:. <https://doi.org/10.1080/19420862.2022.2153410>
178. Anand SP, Finzi A (2019) Understudied Factors Influencing Fc-Mediated Immune Responses against Viral Infections. *Vaccines (Basel)* 7:103. <https://doi.org/10.3390/vaccines7030103>
179. Ståhl S, Gräslund T, Eriksson Karlström A, et al (2017) Affibody Molecules in Biotechnological and Medical Applications. *Trends Biotechnol* 35:691–712. <https://doi.org/10.1016/j.tibtech.2017.04.007>
180. Nelson AL (2010) Antibody fragments. *MAbs* 2:77–83. <https://doi.org/10.4161/mabs.2.1.10786>
181. Sennhauser G, Grütter MG (2008) Chaperone-Assisted Crystallography with DARPins. *Structure* 16:1443–1453. <https://doi.org/10.1016/j.str.2008.08.010>
182. Guzman KM, Khosla C (2022) Fragment antigen binding domains (Fabs) as tools to study assembly-line polyketide synthases. *Synth Syst Biotechnol* 7:506–512. <https://doi.org/10.1016/j.synbio.2021.12.003>
183. Eigenbrot C, Ultsch M, Dubnovitsky A, et al (2010) Structural basis for high-affinity HER2 receptor binding by an engineered protein. *Proceedings of the National Academy of Sciences* 107:15039–15044. <https://doi.org/10.1073/pnas.1005025107>

184. Ostermeier C, Iwata S, Ludwig B, Michel H (1995) Fv fragment-mediated crystallization of the membrane protein bacterial cytochrome c oxidase. *Nat Struct Biol* 2:842–846. <https://doi.org/10.1038/nsb1095-842>
185. Tereshko V, Uysal S, Koide A, et al (2008) Toward chaperone-assisted crystallography: Protein engineering enhancement of crystal packing and X-ray phasing capabilities of a camelid single-domain antibody scaffold. *Protein Science* 17:1175–1187. <https://doi.org/10.1110/ps.034892.108>
186. Kruse AC, Ring AM, Manglik A, et al (2013) Activation and allosteric modulation of a muscarinic acetylcholine receptor. *Nature* 504:101–106. <https://doi.org/10.1038/nature12735>
187. Koth CM, Murray JM, Mukund S, et al (2012) Molecular basis for negative regulation of the glucagon receptor. *Proceedings of the National Academy of Sciences* 109:14393–14398. <https://doi.org/10.1073/pnas.1206734109>
188. Davies CW, Oh AJ, Mroue R, et al (2022) Conformation-locking antibodies for the discovery and characterization of KRAS inhibitors. *Nat Biotechnol* 40:769–778. <https://doi.org/10.1038/s41587-021-01126-9>
189. Tolmachev V, Orlova A, Nilsson FY, et al (2007) Affibody molecules: potential for in vivo imaging of molecular targets for cancer therapy. *Expert Opin Biol Ther* 7:555–568. <https://doi.org/10.1517/14712598.7.4.555>
190. Kim H Il, Kim J, Kim H, et al (2021) Biomolecular imaging of colorectal tumor lesions using a FITC-labeled scFv-Ck fragment antibody. *Sci Rep* 11:17155. <https://doi.org/10.1038/s41598-021-96281-z>
191. Ni D, Xu P, Gallagher S (2016) Immunoblotting and Immunodetection. *Curr Protoc Mol Biol* 114. <https://doi.org/10.1002/0471142727.mb1008s114>
192. Kang TH, Seong BL (2020) Solubility, Stability, and Avidity of Recombinant Antibody Fragments Expressed in Microorganisms. *Front Microbiol* 11. <https://doi.org/10.3389/fmicb.2020.01927>
193. Bird RE, Hardman KD, Jacobson JW, et al (1988) Single-Chain Antigen-Binding Proteins. *Science* (1979) 242:423–426. <https://doi.org/10.1126/science.3140379>
194. Ahmad ZA, Yeap SK, Ali AM, et al (2012) scFv Antibody: Principles and Clinical Application. *Clin Dev Immunol* 2012:1–15. <https://doi.org/10.1155/2012/980250>
195. Choo ABH, Dunn RD, Broady KW, Raison RL (2002) Soluble Expression of a Functional Recombinant Cytolytic Immunotoxin in Insect Cells. *Protein Expr Purif* 24:338–347. <https://doi.org/10.1006/prep.2001.1589>
196. Galeffi P, Lombardi A, Pietraforte I, et al (2006) Functional expression of a single-chain antibody to ErbB-2 in plants and cell-free systems. *J Transl Med* 4:39. <https://doi.org/10.1186/1479-5876-4-39>
197. Ho M, Nagata S, Pastan I (2006) Isolation of anti-CD22 Fv with high affinity by Fv display on human cells. *Proceedings of the National Academy of Sciences* 103:9637–9642. <https://doi.org/10.1073/pnas.0603653103>
198. Yokota T, Milenic DE, Whitlow M, Schlom J (1992) Rapid tumor penetration of a single-chain Fv and comparison with other immunoglobulin forms. *Cancer Res* 52:3402–8
199. Colcher D, Pavlinkova G, Beresford G, et al (1998) Pharmacokinetics and biodistribution of genetically-engineered antibodies. *Q J Nucl Med* 42:225–41
200. Stipsanelli E, Valsamaki P (2005) Monoclonal antibodies: old and new trends in breast cancer imaging and therapeutic approach. *Hell J Nucl Med* 8:103–8
201. Dana Jones S, Marasco WA (1998) Antibodies for targeted gene therapy: extracellular gene targeting and intracellular expression. *Adv Drug Deliv Rev* 31:153–170. [https://doi.org/10.1016/S0169-409X\(97\)00099-9](https://doi.org/10.1016/S0169-409X(97)00099-9)
202. McKittrick TR, Eris D, Mondal N, et al (2020) Antibodies from Lampreys as Smart Anti-Glycan Reagents (SAGRs): Perspectives on Their Specificity, Structure, and Glyco-genomics. *Biochemistry* 59:3111–3122. <https://doi.org/10.1021/acs.biochem.9b01015>
203. Bogen JP, Elter A, Grzeschik J, et al (2022) Humanization of Chicken-Derived Antibodies by Yeast Surface Display. pp 335–360

204. Burger D, Ramus M-A, Schapira M (1985) Antibodies to human plasma kallikrein from egg yolks of an immunized hen: Preparation and characterization. *Thromb Res* 40:283–288. [https://doi.org/10.1016/0049-3848\(85\)90340-8](https://doi.org/10.1016/0049-3848(85)90340-8)
205. Gassmann M, Thömmes P, Weiser T, Hübscher U (1990) Efficient production of chicken egg yolk antibodies against a conserved mammalian protein. *The FASEB Journal* 4:2528–2532. <https://doi.org/10.1096/fasebj.4.8.1970792>
206. Spencer S, Bethea D, Raju TS, et al (2012) Solubility evaluation of murine hybridoma antibodies. *MAbs* 4:319–325. <https://doi.org/10.4161/mabs.19869>
207. Abdiche YN, Harriman R, Deng X, et al (2016) Assessing kinetic and epitopic diversity across orthogonal monoclonal antibody generation platforms. *MAbs* 8:264–277. <https://doi.org/10.1080/19420862.2015.1118596>
208. Hansson L, Flodin M, Nilsen T, et al (2007) Comparison between Chicken and Rabbit Antibody Based Particle Enhanced Cystatin C Reagents for Immunoturbidimetry. *J Immunoassay Immunochem* 29:1–9. <https://doi.org/10.1080/15321810701734644>
209. Carroll SB, Stollar BD (1983) Antibodies to calf thymus RNA polymerase II from egg yolks of immunized hens. *J Biol Chem* 258:24–6
210. Tizard I (1979) Avian Immune Responses: A Brief Review. *Avian Dis* 23:290. <https://doi.org/10.2307/1589558>
211. Kaiser P, Balic A (2015) The Avian Immune System. In: *Sturkie's Avian Physiology*. Elsevier, pp 403–418
212. Warr GW, Magor KE, Higgins DA (1995) IgY: clues to the origins of modern antibodies. *Immunol Today* 16:392–398. [https://doi.org/10.1016/0167-5699\(95\)80008-5](https://doi.org/10.1016/0167-5699(95)80008-5)
213. Bengtén E, Wilson M, Miller N, et al (2000) Immunoglobulin Isotypes: Structure, Function, and Genetics. pp 189–219
214. Parvari R, Avivi A, Lentner F, et al (1988) Chicken immunoglobulin gamma-heavy chains: limited VH gene repertoire, combinatorial diversification by D gene segments and evolution of the heavy chain locus. *EMBO J* 7:739–744. <https://doi.org/10.1002/j.1460-2075.1988.tb02870.x>
215. Baek D-S, Kim Y-S (2015) Humanization of a phosphothreonine peptide-specific chicken antibody by combinatorial library optimization of the phosphoepitope-binding motif. *Biochem Biophys Res Commun* 463:414–420. <https://doi.org/10.1016/j.bbrc.2015.05.086>
216. Tsurushita N, Park M, Pakabunto K, et al (2004) Humanization of a chicken anti-IL-12 monoclonal antibody. *J Immunol Methods* 295:9–19. <https://doi.org/10.1016/j.jim.2004.08.018>
217. Löfblom J, Feldwisch J, Tolmachev V, et al (2010) Affibody molecules: Engineered proteins for therapeutic, diagnostic and biotechnological applications. *FEBS Lett* 584:2670–2680. <https://doi.org/10.1016/j.febslet.2010.04.014>
218. Nygren P-Å, Skerra A (2004) Binding proteins from alternative scaffolds. *J Immunol Methods* 290:3–28. <https://doi.org/10.1016/j.jim.2004.04.006>
219. Nord K, Nilsson J, Nilsson B, et al (1995) A combinatorial library of an α -helical bacterial receptor domain. "Protein Engineering, Design and Selection" 8:601–608. <https://doi.org/10.1093/protein/8.6.601>
220. Löfblom J, Frejd FY, Ståhl S (2011) Non-immunoglobulin based protein scaffolds. *Curr Opin Biotechnol* 22:843–848. <https://doi.org/10.1016/j.copbio.2011.06.002>
221. Xue X, Wang B, Du W, et al (2016) Generation of affibody molecules specific for HPV16 E7 recognition. *Oncotarget* 7:73995–74005. <https://doi.org/10.18632/oncotarget.12174>
222. Zhao N, Liu S, Jiang Q, et al (2016) Small-Protein-Stabilized Semiconductor Nanoprobe for Targeted Imaging of Cancer Cells. *ChemBioChem* 17:1202–1206. <https://doi.org/10.1002/cbic.201600219>
223. Wällberg H, Ståhl S (2013) Design and evaluation of radiolabeled tracers for tumor imaging. *Biotechnol Appl Biochem* 60:365–383. <https://doi.org/10.1002/bab.1111>

-
224. Zielinski R, Lyakhov I, Jacobs A, et al (2009) Affitoxin—A Novel Recombinant, HER2-specific, Anticancer Agent for Targeted Therapy of HER2-positive Tumors. *Journal of Immunotherapy* 32:817–825. <https://doi.org/10.1097/CJI.0b013e3181ad4d5d>
225. Schardt JS, Oubaid JM, Williams SC, et al (2017) Engineered Multivalency Enhances Affibody-Based HER3 Inhibition and Downregulation in Cancer Cells. *Mol Pharm* 14:1047–1056. <https://doi.org/10.1021/acs.molpharmaceut.6b00919>
226. Malm M, Bass T, Gudmundsdottir L, et al (2014) Engineering of a bispecific affibody molecule towards HER2 and HER3 by addition of an albumin-binding domain allows for affinity purification and in vivo half-life extension. *Biotechnol J* 9:1215–1222. <https://doi.org/10.1002/biot.201400009>
227. Zhang Y, Jiang S, Zhang D, et al (2017) DNA–affibody nanoparticles for inhibiting breast cancer cells overexpressing HER2. *Chemical Communications* 53:573–576. <https://doi.org/10.1039/C6CC08495H>
228. Tong M, Jiang Y (2015) FK506-Binding Proteins and Their Diverse Functions. *Curr Mol Pharmacol* 9:48–65. <https://doi.org/10.2174/1874467208666150519113541>
229. Ghartey-Kwansah G, Li Z, Feng R, et al (2018) Comparative analysis of FKBP family protein: evaluation, structure, and function in mammals and *Drosophila melanogaster*. *BMC Dev Biol* 18:7. <https://doi.org/10.1186/s12861-018-0167-3>
230. Matsushita R, Hashimoto A, Tomita T, et al (2010) Enhanced expression of mRNA for FK506-binding protein 5 in bone marrow CD34 positive cells in patients with rheumatoid arthritis. *Clin Exp Rheumatol* 28:87–90
231. Koenen KC, Saxe G, Purcell S, et al (2005) Polymorphisms in FKBP5 are associated with peritraumatic dissociation in medically injured children. *Mol Psychiatry* 10:1058–1059. <https://doi.org/10.1038/sj.mp.4001727>
232. Ozer EJ, Best SR, Lipsey TL, Weiss DS (2003) Predictors of posttraumatic stress disorder and symptoms in adults: A meta-analysis. *Psychol Bull* 129:52–73. <https://doi.org/10.1037/0033-2909.129.1.52>
233. Storer CL, Dickey CA, Galigniana MD, et al (2011) FKBP51 and FKBP52 in signaling and disease. *Trends in Endocrinology & Metabolism* 22:481–490. <https://doi.org/10.1016/j.tem.2011.08.001>
234. Sinars CR, Cheung-Flynn J, Rimerman RA, et al (2003) Structure of the large FK506-binding protein FKBP51, an Hsp90-binding protein and a component of steroid receptor complexes. *Proc Natl Acad Sci U S A* 100:868–873. <https://doi.org/10.1073/pnas.0231020100>
235. Cioffi DL, Hubler TR, Scammell JG (2011) Organization and function of the FKBP52 and FKBP51 genes. *Curr Opin Pharmacol* 11:308–313. <https://doi.org/10.1016/j.coph.2011.03.013>
236. Pratt WB, Dittmar KD (1998) Studies with Purified Chaperones Advance the Understanding of the Mechanism of Glucocorticoid Receptor–hsp90 Heterocomplex Assembly. *Trends in Endocrinology & Metabolism* 9:244–252. [https://doi.org/10.1016/S1043-2760\(98\)00059-9](https://doi.org/10.1016/S1043-2760(98)00059-9)
237. Smith DF (1993) Dynamics of heat shock protein 90–progesterone receptor binding and the disactivation loop model for steroid receptor complexes. *Molecular Endocrinology* 7:1418–1429. <https://doi.org/10.1210/mend.7.11.7906860>
238. Barent RL, Nair SC, Carr DC, et al (1998) Analysis of FKBP51/FKBP52 Chimeras and Mutants for Hsp90 Binding and Association with Progesterone Receptor Complexes. *Molecular Endocrinology* 12:342–354. <https://doi.org/10.1210/mend.12.3.0075>
239. Renoir JM, Mercier-Bodard C, Hoffmann K, et al (1995) Cyclosporin A potentiates the dexamethasone-induced mouse mammary tumor virus-chloramphenicol acetyltransferase activity in LMCAT cells: a possible role for different heat shock protein-binding immunophilins in glucocorticosteroid receptor-mediated gene expression. *Proceedings of the National Academy of Sciences* 92:4977–4981. <https://doi.org/10.1073/pnas.92.11.4977>

-
240. Owens-Grillo JK, Hoffmann K, Hutchison KA, et al (1995) The Cyclosporin A-binding Immunophilin CyP-40 and the FK506-binding Immunophilin hsp56 Bind to a Common Site on hsp90 and Exist in Independent Cytosolic Heterocomplexes with the Untransformed Glucocorticoid Receptor. *Journal of Biological Chemistry* 270:20479–20484. <https://doi.org/10.1074/jbc.270.35.20479>
241. Wochnik GM, Rüegg J, Abel GA, et al (2005) FK506-binding Proteins 51 and 52 Differentially Regulate Dynein Interaction and Nuclear Translocation of the Glucocorticoid Receptor in Mammalian Cells. *Journal of Biological Chemistry* 280:4609–4616. <https://doi.org/10.1074/jbc.M407498200>
242. Karin M (1998) New Twists in Gene Regulation by Glucocorticoid Receptor: Is DNA Binding Dispensable? *Cell* 93:487–490. [https://doi.org/10.1016/S0092-8674\(00\)81177-0](https://doi.org/10.1016/S0092-8674(00)81177-0)
243. Denny WB, Valentine DL, Reynolds PD, et al (2000) Squirrel Monkey Immunophilin FKBP51 Is a Potent Inhibitor of Glucocorticoid Receptor Binding. *Endocrinology* 141:4107–4113. <https://doi.org/10.1210/endo.141.11.7785>
244. Davies TH, Ning Y-M, Sánchez ER (2002) A New First Step in Activation of Steroid Receptors. *Journal of Biological Chemistry* 277:4597–4600. <https://doi.org/10.1074/jbc.C100531200>
245. Riggs DL, Roberts PJ, Chirillo SC, et al (2003) The Hsp90-binding peptidylprolyl isomerase FKBP52 potentiates glucocorticoid signaling in vivo. *EMBO J* 22:1158–1167. <https://doi.org/10.1093/emboj/cdg108>
246. Pirkel F, Buchner J (2001) Functional analysis of the hsp90-associated human peptidyl prolyl Cis/Trans isomerases FKBP51, FKBP52 and cyp40 1 1 Edited by R. Huber. *J Mol Biol* 308:795–806. <https://doi.org/10.1006/jmbi.2001.4595>
247. Baughman G, Wiederrecht GJ, Chang F, et al (1997) Tissue Distribution and Abundance of Human FKBP51, an FK506-Binding Protein That Can Mediate Calcineurin Inhibition. *Biochem Biophys Res Commun* 232:437–443. <https://doi.org/10.1006/bbrc.1997.6307>
248. Vermeer H, Hendriks-Stegeman BI, van der Burg B, et al (2003) Glucocorticoid-Induced Increase in Lymphocytic FKBP51 Messenger Ribonucleic Acid Expression: A Potential Marker for Glucocorticoid Sensitivity, Potency, and Bioavailability. *J Clin Endocrinol Metab* 88:277–284. <https://doi.org/10.1210/jc.2002-020354>
249. Scammell JG, Denny WB, Valentine DL, Smith DF (2001) Overexpression of the FK506-Binding Immunophilin FKBP51 Is the Common Cause of Glucocorticoid Resistance in Three New World Primates. *Gen Comp Endocrinol* 124:152–165. <https://doi.org/10.1006/gcen.2001.7696>
250. Mukaide H, Adachi Y, Taketani S, et al (2008) FKBP51 Expressed by Both Normal Epithelial Cells and Adenocarcinoma of Colon Suppresses Proliferation of Colorectal Adenocarcinoma. *Cancer Invest* 26:385–390. <https://doi.org/10.1080/07357900701799228>
251. Nair SC, Rimerman RA, Toran EJ, et al (1997) Molecular Cloning of Human FKBP51 and Comparisons of Immunophilin Interactions with Hsp90 and Progesterone Receptor. *Mol Cell Biol* 17:594–603. <https://doi.org/10.1128/MCB.17.2.594>
252. Baughman G, Wiederrecht GJ, Campbell NF, et al (1995) Fkbp51, a Novel T-Cell-Specific Immunophilin Capable of Calcineurin Inhibition. *Mol Cell Biol* 15:4395–4402. <https://doi.org/10.1128/MCB.15.8.4395>
253. Van Duyne GD, Standaert RF, Karplus PA, et al (1991) Atomic Structure of FKBP-FK506, an Immunophilin-Immunosuppressant Complex. *Science* (1979) 252:839–842. <https://doi.org/10.1126/science.1709302>
254. Kozany C, März A, Kress C, Hausch F (2009) Fluorescent Probes to Characterise FK506-Binding Proteins. *ChemBioChem* 10:1402–1410. <https://doi.org/10.1002/cbic.200800806>
255. Riggs DL, Cox MB, Tardif HL, et al (2007) Noncatalytic Role of the FKBP52 Peptidyl-Prolyl Isomerase Domain in the Regulation of Steroid Hormone Signaling. *Mol Cell Biol* 27:8658–8669. <https://doi.org/10.1128/mcb.00985-07>

256. Nair SC, Rimerman RA, Toran EJ, et al (1997) Molecular Cloning of Human FKBP51 and Comparisons of Immunophilin Interactions with Hsp90 and Progesterone Receptor. *Mol Cell Biol* 17:594–603. <https://doi.org/10.1128/MCB.17.2.594>
257. Radanyi C, Chambraud B, Baulieu EE (1994) The ability of the immunophilin FKBP59-HBI to interact with the 90-kDa heat shock protein is encoded by its tetratricopeptide repeat domain. *Proceedings of the National Academy of Sciences* 91:11197–11201. <https://doi.org/10.1073/pnas.91.23.11197>
258. Scheufler C, Brinker A, Bourenkov G, et al (2000) Structure of TPR Domain–Peptide Complexes. *Cell* 101:199–210. [https://doi.org/10.1016/S0092-8674\(00\)80830-2](https://doi.org/10.1016/S0092-8674(00)80830-2)
259. Davies TH, Sánchez ER (2005) FKBP52. *Int J Biochem Cell Biol* 37:42–47. <https://doi.org/10.1016/j.biocel.2004.03.013>
260. D'Andrea L (2003) TPR proteins: the versatile helix. *Trends Biochem Sci* 28:655–662. <https://doi.org/10.1016/j.tibs.2003.10.007>
261. Li L, Lou Z, Wang L (2011) The role of FKBP5 in cancer aetiology and chemoresistance. *Br J Cancer* 104:19–23. <https://doi.org/10.1038/sj.bjc.6606014>
262. Tranguch S, Cheung-Flynn J, Daikoku T, et al (2005) Cochaperone immunophilin FKBP52 is critical to uterine receptivity for embryo implantation. *Proceedings of the National Academy of Sciences* 102:14326–14331. <https://doi.org/10.1073/pnas.0505775102>
263. Brandon DD, Markwick AJ, Chrousos GP, Loriaux DL (1989) Glucocorticoid resistance in humans and nonhuman primates. *Cancer Res* 49:2203s–2213s
264. Lamberts SW (2001) Hereditary glucocorticoid resistance. *Ann Endocrinol (Paris)* 62:164–7
265. Xin H-B, Rogers K, Qi Y, et al (1999) Three Amino Acid Residues Determine Selective Binding of FK506-binding Protein 12.6 to the Cardiac Ryanodine Receptor. *Journal of Biological Chemistry* 274:15315–15319. <https://doi.org/10.1074/jbc.274.22.15315>
266. Futer O, DeCenzo MT, Aldape RA, Livingston DJ (1995) FK506 Binding Protein Mutational Analysis. *Journal of Biological Chemistry* 270:18935–18940. <https://doi.org/10.1074/jbc.270.32.18935>
267. Chambraud B, Belabes H, Fontaine-Lenoir V, et al (2007) The immunophilin FKBP52 specifically binds to tubulin and prevents microtubule formation. *The FASEB Journal* 21:2787–2797. <https://doi.org/10.1096/fj.06-7667com>
268. Chambraud B, Sardin E, Giustiniani J, et al (2010) A role for FKBP52 in Tau protein function. *Proceedings of the National Academy of Sciences* 107:2658–2663. <https://doi.org/10.1073/pnas.0914957107>
269. Jinwal UK, Koren J, Borysov SI, et al (2010) The Hsp90 Cochaperone, FKBP51, Increases Tau Stability and Polymerizes Microtubules. *The Journal of Neuroscience* 30:591–599. <https://doi.org/10.1523/JNEUROSCI.4815-09.2010>
270. Makkonen H, Kauhanen M, Paakinaho V, et al (2009) Long-range activation of FKBP51 transcription by the androgen receptor via distal intronic enhancers. *Nucleic Acids Res* 37:4135–4148. <https://doi.org/10.1093/nar/gkp352>
271. Paakinaho V, Makkonen H, Jääskeläinen T, Palvimo JJ (2010) Glucocorticoid Receptor Activates Poised FKBP51 Locus through Long-Distance Interactions. *Molecular Endocrinology* 24:511–525. <https://doi.org/10.1210/me.2009-0443>
272. Periyasamy S, Warriar M, Tillekeratne MPM, et al (2007) The Immunophilin Ligands Cyclosporin A and FK506 Suppress Prostate Cancer Cell Growth by Androgen Receptor-Dependent and -Independent Mechanisms. *Endocrinology* 148:4716–4726. <https://doi.org/10.1210/en.2007-0145>

273. Ni L, Yang C-S, Gioeli D, et al (2010) FKBP51 Promotes Assembly of the Hsp90 Chaperone Complex and Regulates Androgen Receptor Signaling in Prostate Cancer Cells. *Mol Cell Biol* 30:1243–1253. <https://doi.org/10.1128/MCB.01891-08>
274. Pei H, Li L, Fridley BL, et al (2009) FKBP51 Affects Cancer Cell Response to Chemotherapy by Negatively Regulating Akt. *Cancer Cell* 16:259–266. <https://doi.org/10.1016/j.ccr.2009.07.016>
275. Breedlove SM, Rosenzweig M (2010) *Biological Psychology: An Introduction to Behavioral, Cognitive, and Clinical Neuroscience*. Sinauer Associates
276. Esch T, Stefano GB, Fricchione GL, Benson H (2002) The role of stress in neurodegenerative diseases and mental disorders. *Neuro Endocrinol Lett* 23:199–208
277. Dunlavey CJ (2018) Introduction to the Hypothalamic-Pituitary-Adrenal Axis: Healthy and Dysregulated Stress Responses, Developmental Stress and Neurodegeneration. *J Undergrad Neurosci Educ* 16:R59–R60
278. Ulrich-Lai YM, Ryan KK (2014) Neuroendocrine Circuits Governing Energy Balance and Stress Regulation: Functional Overlap and Therapeutic Implications. *Cell Metab* 19:910–925. <https://doi.org/10.1016/j.cmet.2014.01.020>
279. Westberry JM, Sadosky PW, Hubler TR, et al (2006) Glucocorticoid resistance in squirrel monkeys results from a combination of a transcriptionally incompetent glucocorticoid receptor and overexpression of the glucocorticoid receptor co-chaperone FKBP51. *J Steroid Biochem Mol Biol* 100:34–41. <https://doi.org/10.1016/j.jsbmb.2006.03.004>
280. Touma C, Gassen NC, Herrmann L, et al (2011) FK506 Binding Protein 5 Shapes Stress Responsiveness: Modulation of Neuroendocrine Reactivity and Coping Behavior. *Biol Psychiatry* 70:928–936. <https://doi.org/10.1016/j.biopsych.2011.07.023>
281. Binder EB (2008) Association of FKBP5 Polymorphisms and Childhood Abuse With Risk of Posttraumatic Stress Disorder Symptoms in Adults. *JAMA* 299:1291. <https://doi.org/10.1001/jama.299.11.1291>
282. Bancos I, Hatipoglu BA, Yuen KCJ, et al (2021) Evaluation of FKBP5 as a cortisol activity biomarker in patients with ACTH-dependent Cushing syndrome. *J Clin Transl Endocrinol* 24:100256. <https://doi.org/10.1016/j.jcte.2021.100256>
283. Wu B, Li P, Shu C, et al (2003) Crystallization and preliminary crystallographic studies of the C-terminal domain of human FKBP52. *Acta Crystallogr D Biol Crystallogr* 59:2269–2271. <https://doi.org/10.1107/S090744490301970X>
284. Gaali S, Feng X, Hähle A, et al (2016) Rapid, Structure-Based Exploration of Pipecolic Acid Amides as Novel Selective Antagonists of the FK506-Binding Protein 51. *J Med Chem* 59:2410–2422. <https://doi.org/10.1021/acs.jmedchem.5b01355>
285. Voll AM, Meyners C, Taubert MC, et al (2021) Macrocyclic FKBP51 Ligands Define a Transient Binding Mode with Enhanced Selectivity. *Angewandte Chemie - International Edition* 60:13257–13263. <https://doi.org/10.1002/anie.202017352>
286. Kolos JM, Voll AM, Bauder M, Hausch F (2018) FKBP Ligands—Where We Are and Where to Go? *Front Pharmacol* 9. <https://doi.org/10.3389/fphar.2018.01425>
287. Bauder M, Meyners C, Purder PL, et al (2021) Structure-Based Design of High-Affinity Macrocyclic FKBP51 Inhibitors. *J Med Chem* 64:3320–3349. <https://doi.org/10.1021/acs.jmedchem.0c02195>
288. Hartmann J, Wagner K V., Gaali S, et al (2015) Pharmacological inhibition of the psychiatric risk factor FKBP51 has anxiolytic properties. *Journal of Neuroscience* 35:9007–9016. <https://doi.org/10.1523/JNEUROSCI.4024-14.2015>

-
289. Feng X (2015) Rational Drug Design and Synthesis of Selective FKBP51 Ligands. Doctoral thesis, Ludwig-Maximilians-Universität München
290. Pajouhesh H, Lenz GR (2005) Medicinal chemical properties of successful central nervous system drugs. *NeuroRX* 2:541–553. <https://doi.org/10.1602/neurorx.2.4.541>
-

4 Cumulative Section

4.1 Binding pocket stabilization by high-throughput screening of yeast display libraries

Title:

Binding pocket stabilization by high-throughput screening of yeast display libraries

Authors:

Jorge A. Lerma Romero, Christian Meyners, Andreas Christmann, Lisa M. Reinbold, Anna Charalampidou, Felix Hausch, Harald Kolmar

Bibliographic Data:

Journal – *Frontiers in Molecular Biosciences*

Volume 9

Article published: 07 November 2022

DOI: 10.3389/fmolb.2022.1023131

PMID: 36419931

Copyright © 2022. Lerma Romero, Meyners, Christmann, Reinbold, Charalampidou, Hausch and Kolmar. This is an open-access article distributed under the terms of the Creative Commons Attribution License (CC BY).

Contributions by J.A. Lerma Romero:

- Generation and screening of YSD libraries
- Cloning, expression and purification of all FKBP51 variants
- Characterization of muteins together with Meyners C
- Writing of original manuscript draft
- Generation of figures



OPEN ACCESS

EDITED BY
Alessio Peracchi,
University of Parma, Italy

REVIEWED BY
Raghavan Varadarajan,
Indian Institute of Science (IISc), India
Marcus Fischer,
St. Jude Children's Research Hospital,
United States

*CORRESPONDENCE
Felix Hausch,
Felix.Hausch@TU-Darmstadt.de
Harald Kolmar,
Harald.Kolmar@TU-Darmstadt.de

SPECIALTY SECTION
This article was submitted to
Protein Biochemistry for Basic
and Applied Sciences,
a section of the journal
Frontiers in Molecular Biosciences

RECEIVED 19 August 2022
ACCEPTED 26 October 2022
PUBLISHED 07 November 2022

CITATION
Lerma Romero JA, Meyners C,
Christmann A, Reinbold LM,
Charalampidou A, Hausch F and
Kolmar H (2022), Binding pocket
stabilization by high-throughput
screening of yeast display libraries.
Front. Mol. Biosci. 9:1023131.
doi: 10.3389/fmolb.2022.1023131

COPYRIGHT
© 2022 Lerma Romero, Meyners,
Christmann, Reinbold, Charalampidou,
Hausch and Kolmar. This is an open-
access article distributed under the
terms of the [Creative Commons
Attribution License \(CC BY\)](#). The use,
distribution or reproduction in other
forums is permitted, provided the
original author(s) and the copyright
owner(s) are credited and that the
original publication in this journal is
cited, in accordance with accepted
academic practice. No use, distribution
or reproduction is permitted which does
not comply with these terms.

Binding pocket stabilization by high-throughput screening of yeast display libraries

Jorge A. Lerma Romero¹, Christian Meyners¹,
Andreas Christmann², Lisa M. Reinbold², Anna Charalampidou¹,
Felix Hausch^{1,2*} and Harald Kolmar^{1,2*}

¹Institute for Organic Chemistry and Biochemistry, Technical University of Darmstadt, Darmstadt, Germany, ²Centre for Synthetic Biology, Technical University of Darmstadt, Darmstadt, Germany

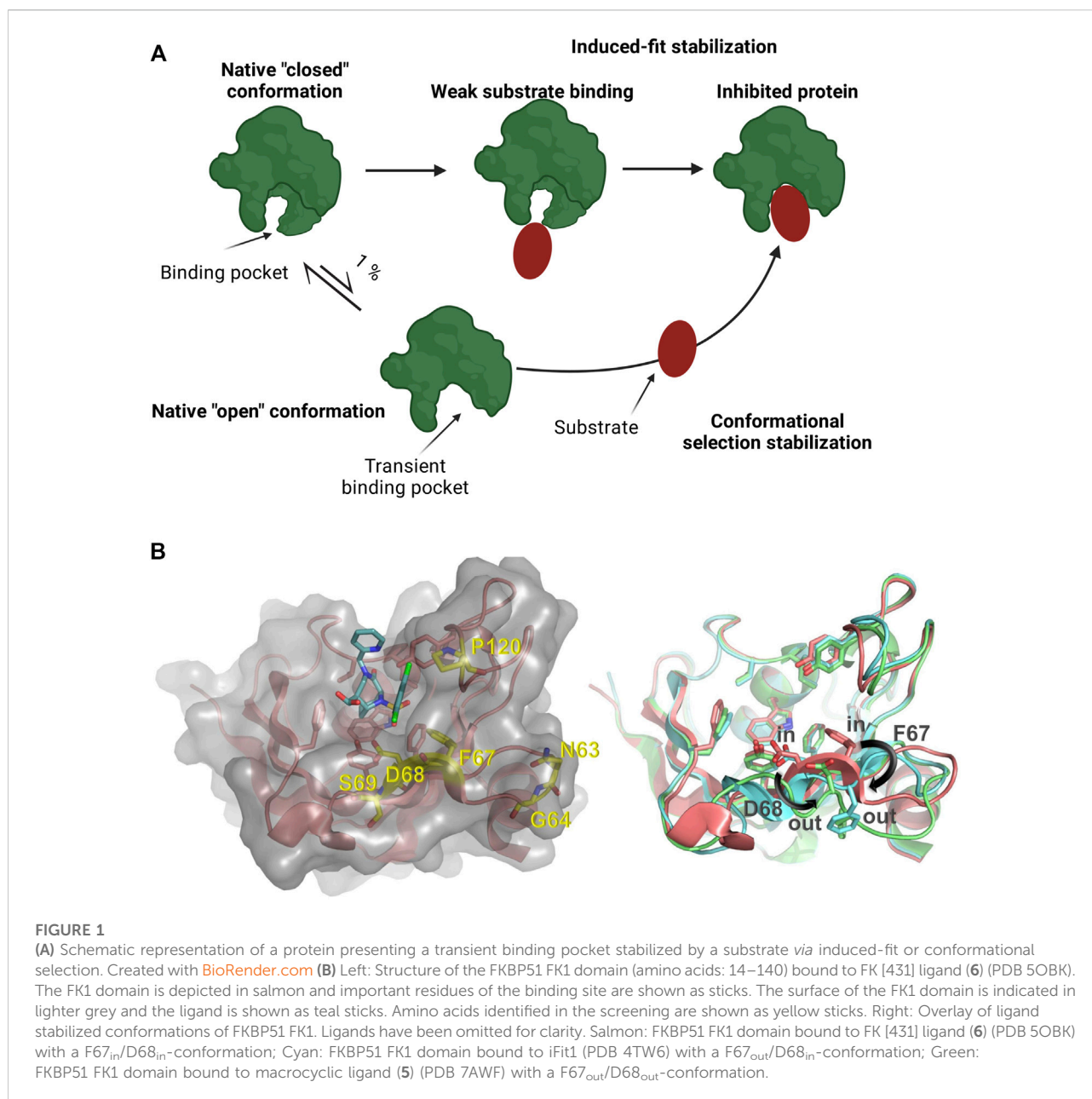
Protein dynamics have a great influence on the binding pockets of some therapeutic targets. Flexible protein binding sites can result in transient binding pocket formation which might have a negative impact on drug screening efforts. Here, we describe a protein engineering strategy with FK506-binding protein 51 (FKBP51) as a model protein, which is a promising target for stress-related disorders. High-throughput screening of yeast display libraries of FKBP51 resulted in the identification of variants exhibiting higher affinity binding of conformation-specific FKBP51 selective inhibitors. The gene libraries of a random mutagenesis and site saturation mutagenesis of the FK1 domain of FKBP51 encoding sequence were used to create a yeast surface display library. Fluorescence-activated cell sorting for FKBP51 variants that bind conformation-specific fluorescently labeled ligands with high affinity allowed for the identification of 15 different protein variants with improved binding to either, or both FKBP51-specific ligands used in the screening, with improved affinities up to 34-fold compared to the wild type. These variants will pave the way to a better understanding of the conformational flexibility of the FKBP51 binding pocket and may enable the isolation of new selective ligands that preferably and selectively bind the active site of the protein in its open conformation state.

KEYWORDS

protein engineering, transient binding pocket, yeast display, flow cytometry, FKBP, high-throughput screening

Introduction

Many proteins, including human drug targets, display large conformational flexibility (Carlson, 2002; Cozzini et al., 2008; Amaral et al., 2017). As a consequence, their binding pockets for small molecule ligands are frequently not well defined and ligand binding can result in conformational changes that eventually lead to the modification or even the appearance of a previously unidentified binding pocket (Monod et al., 1965; Garvey, 2010; Surade & Blundell, 2012; Stank et al., 2016). Upon ligand binding, the opening of a binding pocket displaying a closed conformation can also occur as a result of stabilizing



energy contributions of the bound ligand (Figure 1A) (Monod et al., 1965; Garvey, 2010; Voll et al., 2021). Such type of transient binding pockets are difficult to characterize and it is challenging to identify ligands that bind these drug targets with high affinity and selectivity, thereby modifying their function (Zheng et al., 2013; Umezawa & Kii, 2021).

The application of molecular biology methods such as random or focused target protein library generation and high throughput screening for target proteins with altered ligand binding properties can be useful for the identification and characterization of structural and functional consequences of ligand binding to such type of dynamic binding pockets.

A paradigmatic example for a drug target with a transient binding pocket is the FK506 binding protein 51 (FKBP51), encoded by the *FKBP5* gene. FKBP51 is an intracellular protein belonging to the immunophilin family (Sinars et al., 2003; Hähle et al., 2019). Like many other members of the FKBP family, it has a peptidyl-prolyl isomerase (PPIase) activity, can act as a co-chaperone of heat shock protein 90 (Hsp90) and it plays a role in the regulation of steroid hormone receptor activity (Cioffi et al., 2011; Kolos et al., 2018). In humans, FKBP51 is linked to several stress-related disorders (e.g., anxiety disorders or depression), obesity, type 2 diabetes, and chronic pain. Inhibition of FKBP51 may have beneficial effects on these

diseases (Cioffi et al., 2011; Pöhlmann et al., 2018; Häusel et al., 2019).

For a long time, all known FKBP51 ligands such as the immunosuppressive drugs FK506 and rapamycin were unselective, binding with similar affinity to most other members of the immunophilin family with a PPIase domain (Gali et al., 2015; Kolos et al., 2018). Selective inhibition of FKBP51, however, is thought to be crucial since inhibition of other FKBP members can cause diverse adverse effects. For instance, FKBP12 deficiency caused embryonic lethality due to cardiac defects (Kolos et al., 2018). Furthermore, FKBP52 deletion triggered female infertility and several defects in male sexual development in mice (C. Guy et al., 2015; Kolos et al., 2018; Sivils et al., 2011).

The iFit ligand class (including its analogs SAFit-FL and SAFit1) were the first molecules capable of selectively inhibiting FKBP51 (Gali et al., 2015). The selectivity of these compounds was enabled by differences in the dynamics in the FK1 domain of this protein family. The binding of these ligands stabilizes a conformational change in the FKBP51 FK1 domain. This conformational change is characterized by the displacement of the F67 side chain (Figure 1B) which creates a transient-binding pocket to accommodate the iFit ligands (Gali et al., 2015). The required conformational change is energetically highly unfavorable and has to be compensated by additional binding energy of the ligand, which can impose a substantial or even insurmountable barrier for the *de novo* identification of weak ligands, e.g., by fragment screening. For FKBP51, the relevant F67_{out}-conformation is populated to approximately 0.4% in the apo-state (Jagtap et al., 2019), and various screening approaches did not result in hits for the transient binding pocket. Similarly, the macrocyclic analogs of the iFit ligand class (e.g. Mcyc-TA) require a different rearrangement of the FKBP51 binding pocket (Bracher et al., 2011; Voll et al., 2021). While the displacement of F67 is mainly responsible for the strong selectivity of the iFit ligand against FKBP52, an additional displacement of the D68 residue to an outward conformation improves the macrocyclic ligands selectivity for FKBP51 over FKBP12, FKBP12.6 and FKBP52 (Voll et al., 2021).

Finding a ligand to a target like the transient binding pocket of FKBP51 is a challenging task. Drug design and optimization assisted by a better understanding of the target protein is a logical pathway to obtain a high-affinity ligand to this and many proteins of therapeutic interest. Numerous diseases are caused by the action of effector proteins or any of the subsequent reactions participating in the disease signaling pathway. Normally, the activity of the effector protein is regulated by a small molecule or another protein in the organism (Setiawan et al., 2018). Protein engineering has been an essential tool to elucidate protein structures and determine the protein-drug interactions. The obtained information facilitates the design or discovery of protein inhibitors which may disrupt the action of proteins participating in disease pathways. By optimizing the

protein-drug interactions we can improve the binding to the desired target protein and collect information to design an improved ligand in a rapid and iterative manner (Argiriadi et al., 2009; Liang et al., 2021).

It has been shown that by taking advantage of the flexibility or the presence of a transient binding pocket in a target protein, the specificity and selectivity of small molecules might be improved (Kokh et al., 2016; Umezawa & Kii, 2021). In recent years, there had been extensive research to detect transient pockets using *in silico* experiments to design new molecules that can efficiently bind to diverse protein targets (Eyrisch & Helms, 2007; Kokh et al., 2016). Even though the discovery of transient binding pockets is a challenging task and the open conformation state of a protein is an event that happens in less than 1% of the cases in some proteins, the information acquired through these experiments is of great value for the development of new potential therapeutic compounds (Eyrisch & Helms, 2007).

High throughput random mutagenesis and site saturation mutagenesis are powerful protein engineering tools that allow for the identification of amino acids that play an essential role in the structure and function of a protein. Here we describe a protein engineering strategy aimed at enhancing the binding affinity of conformation-specific selective FKBP51 ligands. With the help of fluorescence-activated cell sorting (FACS) of a yeast display library of FKBP51 mutants, a number of variants with improved binding of iFit class ligands were identified and protein crystallization indicated, at least for one variant, that this seems to be due to stabilization of the binding pocket. We expect that these variants will help to identify novel ligand scaffolds that selectively block FKBP51 over other members of the FKBP family. Furthermore, these variants may contribute to a better understanding of the protein-ligand interaction and the dynamics and plasticity of the FKBP51 transient-binding pocket.

Materials and methods

Random mutagenesis of FKBP51 (FK1 domain)

The coding sequence of the FK1 domain (1–140) of the FKBP51 (PDB: 3o5e) was used as a template for the generation of genetic diversity of the parent sequence. Sequence diversity was achieved through the introduction of random point mutations. A random mutagenesis reaction was prepared following the protocol of the GeneMorph II random mutagenesis kit (Agilent Technologies). Three different mutation rates were achieved by modifying the template amount (pCT-HsFKBP51 plasmid) in the random mutagenesis reaction. For a mutation frequency of 9–16 mutations/Kbp, 4.5–9 mutations/Kbp and 0–4.5 mutations/Kbp, the required template amount was 50 ng, 250 ng and 900 ng, respectively. The annealing

temperature for this reaction was established at 64°C and the pCT_FKBP51_fw and pCT_FKBP51_rv primers (Supplementary Table S1) were used. FKBP51 coding sequence length is 420 bp, therefore the amplification time was 1 min.

Site-saturation mutagenesis

For the site-saturation mutagenesis, a two-step PCR was performed. In the first PCR step, the degenerated primers (Supplementary Table S1) were paired with the pCT_FKBP51_fw or pCT_FKBP51_rv (e.g., pCT_FKBP51_fw and N63_deg_Rv). Two PCRs for each position were performed, generating two spliced DNA molecules of the FKBP51 gene.

The mutagenesis reactions were performed in a 50 µl volume containing 5X green Quick-Load reaction buffer, ~20 ng of pCT-HsFKBP51 plasmid as a template, 0.2 µm of each primer, 200 µm of dNTPs, and 1.25 units of OneTaq® Quick-Load® DNA Polymerase (New England Biolabs). Reactions were thermally cycled: 95°C for 2 min, followed by 30 cycles of 95°C for 20 s, 52–56°C for 50 s, and 68°C for 25 s, then a final incubation of 68°C for 5 min. At this step, the mutation was generated in both strands of the DNA sequence of the FKBP51 gene.

To fuse the two fragments, an overlap extension PCR was performed. The purified products of the first PCR step (1 µl each) were mixed with 5X green Quick-Load reaction buffer, 0.2 nM of each primer (pCT_FKBP51_fw and pCT_FKBP51_rv), 200 µm of dNTPs, 1.25 units of OneTaq® Quick-Load® DNA Polymerase (New England Biolabs) and filled up with ddH₂O to a final volume of 50 µl. Reactions were thermally cycled: 95°C for 2 min, followed by 30 cycles of 95°C for 20 s, 46°C for 50 s, and 68°C for 35 s, then a final incubation of 68°C for 5 min. Reactions were cooled on ice and digested with 5 units of DpnI for at least 1 h at 37°C to cleave methylated parental DNA, but not the newly synthesized mutant DNA molecules. The complete FKBP51 DNA sequence with one codon mutated was then purified and stored at -20°C.

DNA purification, concentration determination, and sequencing

PCR products and enzymatic restriction reactions were purified by Wizard® SV Gel and PCR Clean-up System Kit from Promega following the manufacturer's instruction. The purified DNA was recovered in nuclease-free water and the concentration was measured by spectrometry absorbance at 260 nm using the Biospec Nano™ from Shimadzu Europe GmbH. For sequencing, the cleaned-up DNA product was mixed with pCT_seq_up or pCT_seq_lo primer (Supplementary Table S1). The samples were sent for sequencing (SeqLab Göttingen GmbH).

Yeast library generation

The yeast library was generated *via* homologous recombination. Before the yeast transformation, the destination vector was linearized with the restriction enzymes BamHI (New England Biolabs) and NheI (New England Biolabs). The *Saccharomyces cerevisiae* strain EBY100 [MATa URA3-52 trp1 leu2Δ1 his3Δ200 pep4:HIS3 prb1Δ1.6R can1 GAL (pIU211:URA3)] (Thermo Fisher Scientific) was used for the generation of the FKBP51 mutant library. EBY100 yeast cells were cultivated in Yeast Extract–Peptone–Dextrose (YPD) medium composed of 20 g/L peptone-casein (Carl Roth GmbH & Co.KG), 20 g/L glucose (Carl Roth GmbH & Co.KG), and 10 g/L yeast extract (Sigma-Aldrich).

Electrocompetent yeast cells and libraries were generated following Benatuil *et al.* protocol (Benatuil *et al.*, 2010). Cell transformation was performed using 4 µg digested destination vector (pCT vector) and 12 µg purified PCR product within each transformation reaction. 20 electroporation reactions were performed for the generation of the FKBP51 mutant library in EBY100. The cells were electroporated at 2.5 kV and 25 mF in a 0.2 cm BioRad GenePulser cuvette. The cells were immediately resuspended in a 1:1 mix of 1 M sorbitol: YPD medium and incubated at 30°C for 1 h. Finally, the cells were collected and cultured in SD-Trp media which contained 20 g/L glucose, 6.7 g/L yeast nitrogen base without amino acids (Becton, Dickinson and Company), 5.4 g/L Na₂HPO₄ (Carl Roth GmbH & Co.KG), 8.6 g/L NaH₂PO₄·H₂O (Carl Roth GmbH & Co.KG), and 5 g/L casamino acids. Library sizes were calculated from serial dilution plating of transformed cells.

FACS screening and sorting

The library cells were grown overnight in SD medium at 30°C and 200 rpm. Afterward, cells were transferred to SG medium (20 g/L galactose, 6.7 g/L yeast nitrogen base without amino acids, 5.4 g/L Na₂HPO₄, 8.6 g/L NaH₂PO₄·H₂O, and 5 g/L casamino acids) at 10⁷ cells/ml followed by incubation at 30°C for approximately 24 h. Labeling of cells for FACS analysis or sorting was conducted by washing and resuspending the FKBP51 mutant library with PBS (6.4 mM Na₂HPO₄, 2 mM KH₂PO₄, 140 mM NaCl, 10 mM KCl) followed by incubation with biotin-conjugated c-Myc antibody (Miltenyi Biotec; diluted 1:75) on ice for approximately 30 min. Afterwards, the cells were washed and resuspended a second time in PBS, followed by staining with secondary labeling reagent Streptavidin conjugated to APC (eBioscience™; diluted 1:75) to differentiate between presenting and non-presenting yeast cells. Besides, 5 nM of SAFit-FL or 20 nM of Mcyc-TA was added to the library sample to sort the protein variants with a high affinity to either of those ligands. All the ligand tracers used for cell sorting had purities of more than 95%. Finally, cells were

washed one last time with PBS and resuspended in 1 ml of PBS for FACS analysis. FACS-sorting rounds were either performed on a Sony SH800 cell sorter (Sony) or a BD Influx™ cell sorter. Sorting gate was set to capture approximately 1% of the tracer binding population. For the Sony SH800 cell sorter mOrange fluorochrome configuration (561 nm excitation laser, 583/30 optical filter) was used to measure TAMRA labeled tracers; APC fluorochrome configuration (638 nm excitation laser, 665/30 optical filter) was used to measure APC stained myc-tag. For the BD Influx™ cell sorter a 488 nm excitation laser, 530/40 optical filter was used to measure FITC labeled tracers; 640 nm excitation laser, 670/30 optical filter was used to measure APC stained myc-tag.

The sorted cells were used subsequently for the next sorting round or single clone analysis.

Colony PCR

A single clone of the *S. cerevisiae* was picked and resuspended in 25 μ l of 20 nM NaOH and incubated for 20 min at 98°C. Afterward, a PCR was performed using 2 μ l of the yeast cell sample as a template and mixed with 5X green Quick-Load reaction buffer, 0.2 μ l of the pCT_seq_up and pCT_seq_lo primer, 200 μ l of dNTPs, 1.25 units of OneTaq® Quick-Load® DNA Polymerase (New England Biolabs), and filled up to 50 μ l with ddH₂O. Reactions were thermally cycled: 95°C for 1 min, followed by 30 cycles of 95°C for 20 s, 54°C for 50 s, and 68°C for 45 s, then a final incubation of 68°C for 5 min. The PCR products were analyzed by agarose gel electrophoresis, and if required, sent for sequencing.

Protein production, purification and characterization

E. coli BL21 (DE3) was transformed with each of the FKBP51 variants cloned in pET30b by electroporation at 2.5 kV and 25 mF in a 0.2 cm BioRad GenePulser cuvette. The transformed cells were spread on Double Yeast Tryptone (dYT)-agar plates with kanamycin (0.1% v/v) and were incubated at 37°C overnight. A single colony was picked to start a preculture in dYT medium composed of 16 g/L peptone-casein (Carl Roth GmbH & Co.KG), 10 g/L yeast extract (Sigma-Aldrich), and 5 g/L NaCl with kanamycin (0.1% v/v) and grown overnight at 37°C and 180 rpm. A shaking flask containing 1 L dYT-medium was inoculated to an OD₆₀₀: 0.1, using the overnight culture. The cell culture was incubated at 37°C and 180 rpm until an OD₆₀₀ of 0.6–0.8 was reached. Production was carried out overnight by adding 1 mM isopropyl 1-thio-D-galactopyranoside and incubated the cell culture at 30°C and 180 rpm.

Induced *E. coli* BL21 (DE3) cells containing FKBP51 were precipitated by centrifugation (6,000 rpm, 10 min, 4°C) and lysed

by sonication. Cellular debris were removed by centrifugation (13,500 rpm, 15 min, 4°C) and the supernatant was filtered through a 0.45 μ m syringe filter.

Utilization of an N-terminal His-tag allowed purification by Ni-NTA affinity chromatography (HisTrap HP - Cytiva). Finally, the recovered fractions were dialyzed against 20 mM HEPES, 150 mM NaCl, pH 8 or PBS pH 7.4. Protein purity was confirmed via 10% SDS-PAGE analysis under reducing conditions (Supplementary Figure S7).

In order to purify the FKBP51-G64S variant for crystallization trials, the G64S mutation was introduced into our His-SUMO-FKBP51 (16–140, A19T, C103A, C107I) construct and transformed into *E. coli* BL21 (DE3) cells. A single colony was used to inoculate 50 ml LB medium which was then incubated at 37°C overnight. For the main culture 1 L LB medium was inoculated to an OD₆₀₀ of 0.1 and incubated at 37°C and 180 rpm until an OD₆₀₀ of 0.6 was reached. The cell culture was cooled to 25°C, induced by addition of 0.5 mM isopropyl 1-thio-D-galactopyranoside and further incubated for additional 16 h.

The cells were harvested by centrifugation (13,000 \times g, 15 min, 4°C) and the cell pellet was solubilized in lysis buffer (20 mM HEPES, 300 mM NaCl, pH 8) supplemented with 1 mM PMSF, 2 mg/ml lysozyme, and 0.1 mg/ml DNase I. After incubation for 1 h, the cells were lysed using sonication and cellular debris were removed by centrifugation (20,000 \times g, 30 min, 4°C). The supernatant was loaded on a Nickel-NTA (Machery Nagel) column equilibrated with lysis buffer. The column was washed with 10 column volumes of washing buffer (20 mM HEPES, 300 mM NaCl, 10 mM imidazole pH 8) and the protein was eluted with elution buffer (20 mM HEPES, 300 mM NaCl, 300 mM imidazole pH 8). Target protein containing fractions were dialyzed against 20 mM HEPES, 150 mM NaCl, pH 8 and the His-SUMO tag was cleaved by addition of recombinant Ulp1. The cleaved His-SUMO tag was removed by passing the protein mixture through a Nickel-NTA column. The FKBP51-G64S containing flow-through was finally purified by size exclusion chromatography using a HiLoad® 16/600 Superdex® 75 pg column (Cytiva) equilibrated with 20 mM HEPES, 20 mM NaCl, pH 8. The pure protein was concentrated to 20 mg/ml using an Amicon® Ultra 2 ml centrifugal filter, flash frozen in liquid nitrogen, and stored at –80°C until used further.

Affinity measurement by fluorescence polarization

All ligands and tracers used for fluorescence polarization assays had purities of more than 95%. The following ligands and tracers were used for fluorescence polarization and FACS screening experiments:

- SAFit-FL tracer (1): Fluorescein conjugated analog of the iFit ligand class.
- McyC-TA tracer (2): TAMRA conjugated macrocyclic ligand (5).
- FK [431]-TA tracer (3): TAMRA conjugated FK [431] ligand (6).
- SAFit1 ligand (4): analog of the iFit ligand class.
- macrocylic ligand (5):macrocylic analog of the SAFit class ligands.
- FK [431] ligand (6):bicyclic analog of the immunosuppressive drug FK506

The binding of the generated FKBP51 variants to different conformation-sensitive FKBP ligands was investigated by fluorescence polarization assays. Therefore, a serial dilution of the respective FKBP51 variant in assay buffer (20 mM HEPES pH 8.0, 150 mM NaCl, 0.015% Triton X-100) was placed in a 384-well assay plate and a defined amount of the respective fluorescent tracer (0.5 nM of the SAFit based tracer SAFit-FL (1), 5 nM of the macrocyclic tracer McyC-TA 2) or 1 nM of the FK [431]-TA 3) in assay buffer was added to the protein buffer mixture. After incubation for 30 min at room temperature, the fluorescence polarization was measured with a plate reader. The obtained results for each 3 independent experiments were normalized with respect to the maximal binding signal and fitted to a one-site binding model as described by Wang et al., 1992 yielding the respective binding constants.

$$\text{tracer bound} = \frac{100}{L_t} \times 0.5 \times \left(R_t + L_t + K_D - \sqrt{(R_t + L_t + K_D)^2 - 4 \times L_t R_t} \right)$$

With L_t , total concentration of the tracer, R_t , total concentration of the receptor and K_D binding constant of the complex RL.

In order to rule out artifacts introduced by the fluorophore of the tracers, competitive fluorescence polarization assays were carried out. Therefore, a serial dilution of an FK [431] ligand (6), SAFit1 (4), or a macrocyclic ligand 5) (Supplementary Figure S8) in assay buffer was placed in a 384-well assay plate. To the compounds, a mixture of the respective protein (20 nM WT, 10–40 nM G64S or 80–100 nM D68Y) and 1 nM of the FK [431]-TA in assay buffer was added. After incubating for 30 min at room temperature, the fluorescence polarization was measured. The obtained results for each 3 independent experiments were normalized with respect to the maximal binding and fitted to a competitive binding model as described by Wang, 1995 yielding the respective binding constants.

$$\text{tracer bound} = 100 \times \frac{\{2 \times \sqrt{(a^2 - 3b)} \times \cos(\theta/3) - a\}}{3 \times K_D + \{2 \times \sqrt{(a^2 - 3b)} \times \cos(\theta/3) - a\}}$$

$$a = K_D + K_I + L_t + I_t - R_t$$

$$b = K_I(L_t - R_t) + K_D(I_t - R_t) + K_D K_I$$

$$c = -K_D K_I R_t$$

$$\theta = \arccos \frac{-2a^3 + 9ab - 27c}{2\sqrt{(a^2 - 3b)^3}}$$

With L_t , total concentration of the tracer, R_t , total concentration of the receptor, K_D , binding constant of the complex RL, I_t , total concentration of the titrated ligand and K_I , binding constant of the complex RI.

Protein crystallization

For the crystallization of the FKBP51-G64S complexes, each complex was prepared by mixing FKBP51FK1 A19T, G64S, C103A, C107I (14–140) at 15 mg/ml with a slight molar excess of SAFit1 (4), macrocyclic ligand 5) or FK [431] ligand (6), previously dissolved at 20 mM in DMSO. Crystallization was performed at room temperature using the hanging drop vapour-diffusion method by equilibrating mixtures of 1 μ L protein complex and 1 μ L reservoir against 500 μ L reservoir solution containing 12% (4), 30% 5) or 40% 6) PEG-3350, 0.2 M NH_4 -acetate, and 0.1 M HEPES-NaOH pH 7.5. The crystals were fished, cryoprotected with 30% PEG-3350, 20% glycerol, 0.2 M NH_4 -acetate, and 0.1 M HEPES-NaOH pH 7.5 and flash frozen in liquid nitrogen.

The crystallographic experiments were performed on the BL14.1 beamline at the Helmholtz-Zentrum BESSY II synchrotron, Berlin, Germany (Gerlach et al., 2016). Diffraction data were integrated with XDS implemented in XDSapp3 and further processed with the implemented programs of the CCP4i and CCP4i2 interface (Collaborative Computational Project, N. 4, 1994; Kabsch, 2010; E. Potterton et al., 2003; L. Potterton et al., 2018; Sparta et al., 2016; Winn et al., 2011). The data reduction was conducted with Aimless (Evans, 2011; Evans & Murshudov, 2013). The crystal structure was solved by molecular replacement using Phaser. Iterative model improvement and refinement were performed with Coot and Refmac5 (Murshudov et al., 1997, 2011; Vagin et al., 2004; McCoy et al., 2007; Emsley et al., 2010; Winn et al., 2011; Nicholls et al., 2012). The dictionaries for the compounds were generated with PRODRG implemented in CCP4i (van Aalten et al., 1996). Residues facing solvent channels without detectable side chain density were truncated.

Results

In order to identify FKBP51 variants with improved binding affinities to selective FKBP51 ligands we aimed to combine protein engineering strategies with conformation-specific ligands for the selection rounds. Therefore, we started by synthesizing a pool of randomly mutated FKBP51 DNA

sequences covering the whole FK1 domain and used them to generate a yeast display library with a size of approximately 3.5×10^6 clones. The library was screened for three rounds *via* FACS (Figure 2A) using the two known conformation-specific FKBP51 tracers SAFit-FL 1) and Mcyc-TA (2). For the characterization FK [431]-TA 3) was included as a third tracer (Figure 2B). SAFit-FL 1) is a fluorescent analog of the iFit ligand class, which binds preferentially to the F67^{out}/D68ⁱⁿ-conformation of FKBP51 (Gaali et al., 2015). Mcyc-TA (out/out) (2, compound 14 in (Voll et al., 2021)) is a macrocyclic analog of the SAFit class ligands that binds to an F67^{out}/D68^{out} conformation and, unlike the previous generations of iFit ligands, displays additional selectivity over FKBP12 and FKBP12.6 (Voll et al., 2021). The fluorescently labeled FK [431]-TA (in/in) 3) is a bicyclic analog of the FK506, which binds to the canonical F67ⁱⁿ/D68ⁱⁿ-conformation. In the following the preferred binding modes of these ligands are abbreviated with *out/in*, *out/out*, and *in/in*, respectively.

Two library screening campaigns with three sorting rounds each using 5 nM of SAFit-FL(out/in) 1 or 20 nM of Mcyc-TA (out/out) 2, respectively, revealed accumulation of FKBP51 variants with enhanced ligand binding compared to wildtype protein (Figure 3). From a gene sequencing of 20 individual clones from our third round FACS sorting of the FKBP51 random mutagenesis library (Supplementary Figure S1-S5), in total seven different protein variants were obtained: G64E, G64S, F67S, D68N, D68Y, S69Y, and P120R.

Interestingly, six out of the seven protein variants displayed an amino acid exchange in the region spanning G64 to S69 (Supplementary Figure S9). It has been shown that the higher conformational plasticity of the FKBP51 β_3 strand and the β_{4-5} interconnecting loop (Y113-T127) differs in a great manner to FKBP52 (Hähle et al., 2019). These differences in the conformational plasticity of FKBP51 allow F67 to be displaced to an out-conformation creating a transient binding pocket in the protein (Gaali et al., 2015; Hähle et al., 2019). Aimed at increasing the number of possible mutants and to find variants with further improved FKBP51 ligand interaction, we generated a variant subset by site saturation mutagenesis for positions 63 to 70. By mutating a single amino acid position at a time with degenerate primers (NNK) coding for all 20 amino acids for the 8 selected residues, we expect a combined library consisting of 160 variants of the FKBP51 FK1 domain.

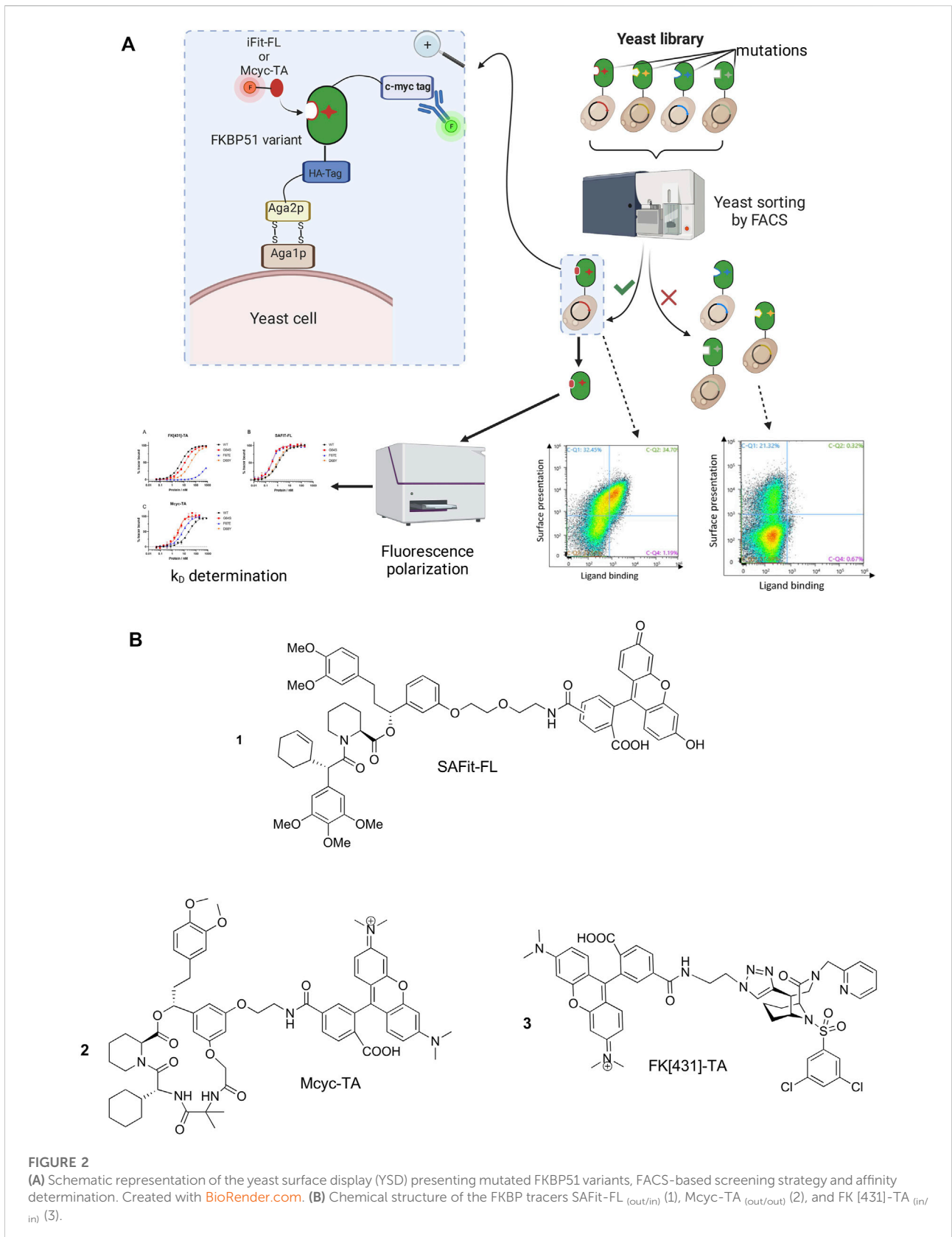
The combined Site Saturation Mutagenesis (SSM) PCR products were used to create a yeast library. After three sorting rounds *via* FACS (Figure 4), 13 different FKBP51 variants were identified containing amino acid exchanges in five of the chosen eight positions (Table 1 and Supplementary Figures S1-S5). The variants G64A, G64S, and F67W were found after sorting the SSM library with both ligands, independently. The variant D68Y, which also was found during the random mutagenesis library sorting was found in 16 of the

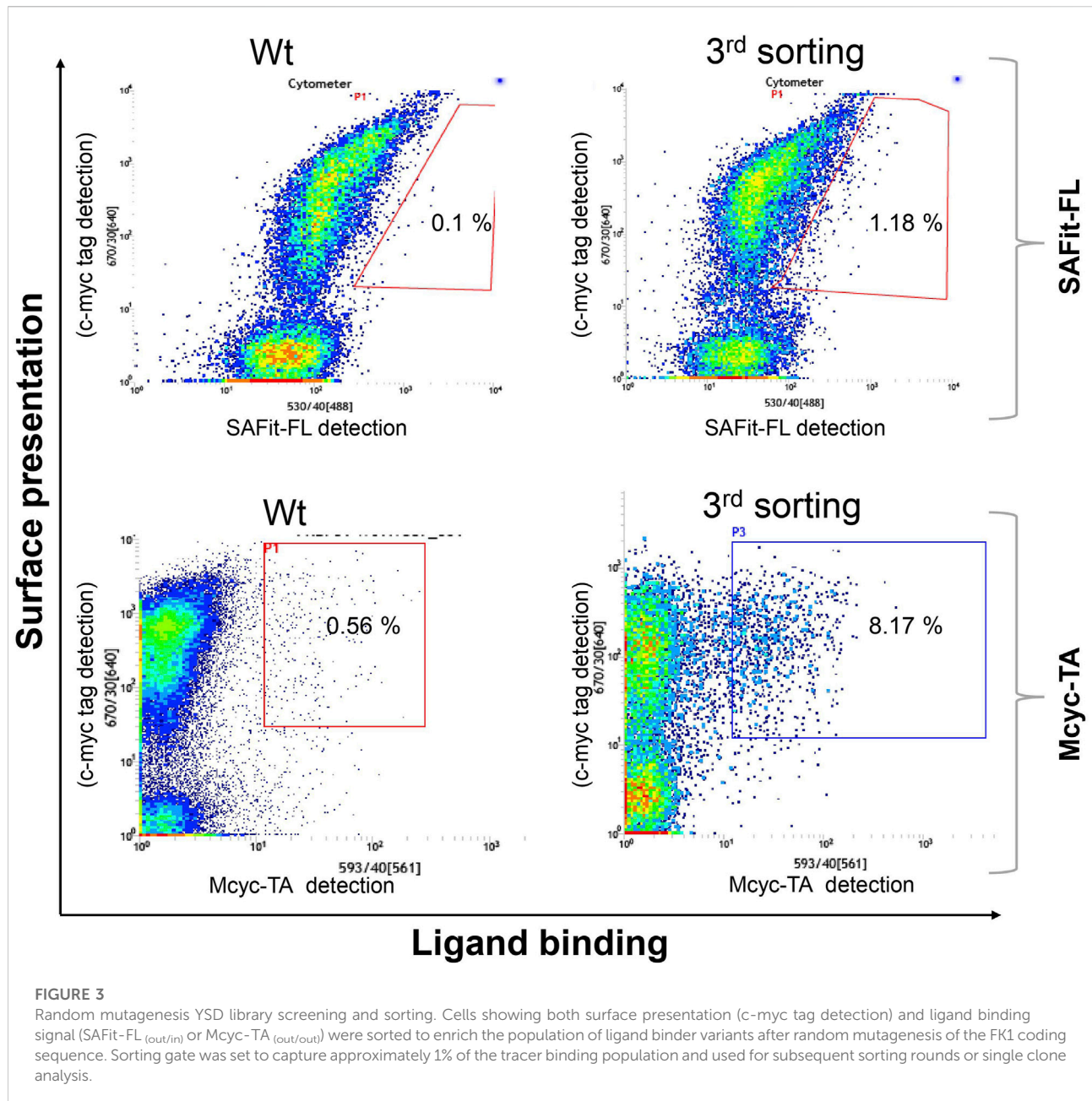
20 picked yeast colonies sorted with the Mcyc-TA ligand (out/out) 2, indicating a strong enrichment.

All identified variants were expressed in *E. coli* BL21(DE3) and purified by immobilized metal ion affinity chromatography (Supplementary Figure S7). To quantitatively assess the contribution of each residue replacement to ligand binding the affinities for binding ligands 1, 2 and 3 were determined *via* measurement of concentration-dependent change of fluorescence polarization (Table 2 and Figure 5). Additionally, competitive fluorescence polarization assays were carried out to validate that the binding results were not influenced by the fluorophore of each ligand (Supplementary Table S2, Supplementary Figure S6). An analysis of the obtained data revealed that most variants bound at least one of the ligands 1 or 2 with enhanced affinities compared to wild-type FKBP51.

While most variants exhibited only moderately improved affinities, three variants stood out with 8- to 34- fold increased binding affinities. The FKBP51 variant G64S had a remarkable improvement in the binding affinity of both FKBP51-selective ligands (Figure 5). With a K_d of 0.09 ± 0.01 nM for SAFit-FL (out/in) and 0.7 ± 0.2 nM for Mcyc-TA (out/out), the affinity of this variant showed a 10- and 34-fold increase, respectively, while no improvement of ligand binding was seen for the canonical inhibitor FK [431]-TA (in/in) 3. Likewise, the D68Y variant was another of the mutations that presented a remarkable improvement on the binding of Mcyc-TA (out/out) with a 34-fold increase compared to wildtype FKBP51, whereby no improvement for binding of 1 or 3 was observed. The third interesting variant is the F67E with an 8-fold tighter binding to SAFit-FL (out/in) compared to wildtype FKBP51 and a moderately improved binding for Mcyc-TA (out/out). Interestingly, none of the variants indicated improved binding for the FK [431]-TA (in/in) and in fact, for most variants, a decrease in the binding affinity could be observed. This effect was especially pronounced for all variants with a substitution at position F67, which displayed a dramatic decrease in the binding affinity (Figure 5A).

As the G64S variant showed the strongest improvements in the binding affinity of both FKBP51-selective ligands and its role in the formation of the transient binding pocket is not obvious, we decided to explore the molecular basis for the binding affinity enhancement in more detail. Therefore, we solved the crystal structures of FKBP51-G64S in complex with SAFit1 (out/in) (PDB: 7R0L), macrocyclic ligand 5) (out/out) (PDB: 8BA6) and FK [431] ligand 6) (in/in) (PDB: 8BA), data collection and refinement statistics in Supplementary Table S4). Overall, the complexes crystallized in very similar conformations as observed for wild-type FKBP51 in complex with the respective ligands (PDB: 4TW6, 7AWF, 5OBK Figure 6). A structural alignment of the respective structure pairs indicates RMSD values $> 1 \text{ \AA}$ only for FKBP51-G64S:SAFit1 (out/in) amino acids 62–65 and for FKBP51-G64S:FK [431] ligand 6) (in/in) G43

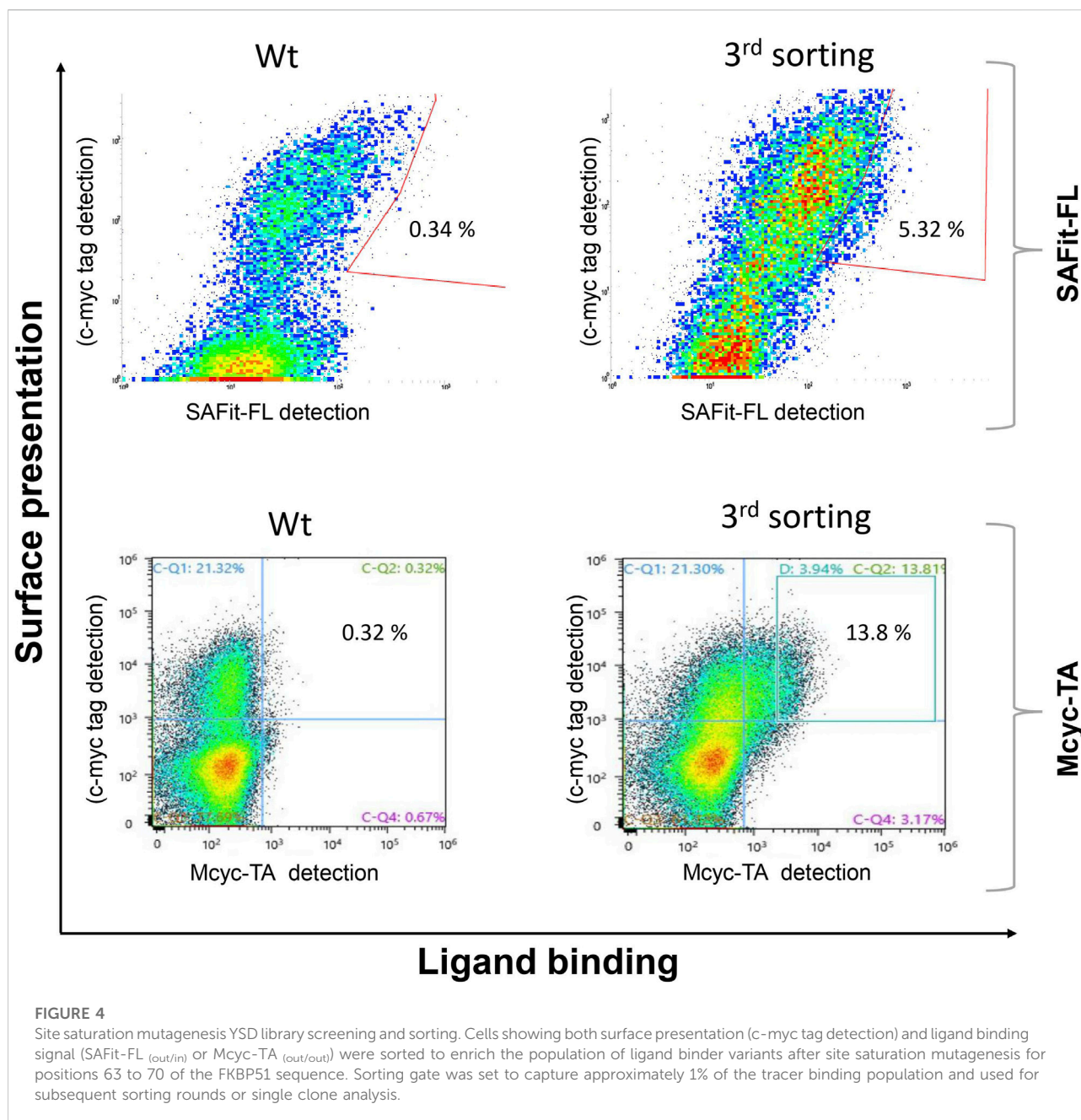




(Supplementary Figure S11). Interestingly, for none of the three ligands a direct interaction between the ligand and the newly introduced serine 64 can be observed. In the FKBP51-G64S:SAFit1_(out/in) complex the loop involving serine 64 is slightly shifted and S64 engages in a hydrogen bond with K60 (Figure 6A). In complex with the macrocyclic ligand 5_(out/out) S64 is not shifted in comparison to wild-type FKBP51 G64 and engages in a hydrogen bond network with water molecules (Figure 6B). In the FKBP51-G64S: FK [431] ligand 6_(in/in) complex only S64 is slightly shifted and comes in close contact to the carbonyl oxygen of N73 (Figure 6C).

Discussion

The FK506-binding protein 51 (FKBP51) has been identified as a key player in several diseases such as chronic pain, obesity, and like stress-related disorders (Cioffi et al., 2011; Pöhlmann et al., 2018; Häusl et al., 2019). A linear analog of FK506 called SAFit was shown to be highly selective for FKBP51 over its closest homologue FKBP52 (Gali et al., 2015). It has been shown that the displacement of phenylalanine 67 from the binding site to an outward position is the key observation during the binding of SAFit-like and also of Mcyc-TA-like ligands and is responsible



for the observed selectivity of these ligand classes. In this study, we performed random mutagenesis over the coding sequence for the FKBP51 FK1 domain and applied a high throughput yeast display screening strategy to identify variants with enhanced affinity to fluorescently labelled conformation-specific ligands. Not unexpectedly, the phenylalanine 67 amino acid position was also identified in our HTS screen as a key residue for selective SAFit_(out/in) and Mcyc-TA_(out/out) ligand binding. The substitution for glutamic acid resulted in a substantial improvement of SAFit-FL_(out/in) and Mcyc-TA_(out/out) binding. If a similar displacement for E67 is assumed as it is

observed for F67, E67 would locate between K58 and K60, whose positive charges may stabilize E67 in the outward conformation. To further corroborate the importance of the phenylalanine 67 to the specific ligand binding we observed in our results that all variants with a mutation at position F67, presented a drop in the binding affinity to FK [431]-TA_(in/in). These mutations hamper the binding to FK [431]-TA_(in/in), which binds to the F67ⁱⁿ/D68ⁱⁿ-conformation of the protein. Analogous binding experiments of the FK [431] ligand_(in/in) to F67V and F67Y variants revealed opposing results (Jagtap et al., 2019). While F67Y displayed a decrease in its binding affinity (similar to all our

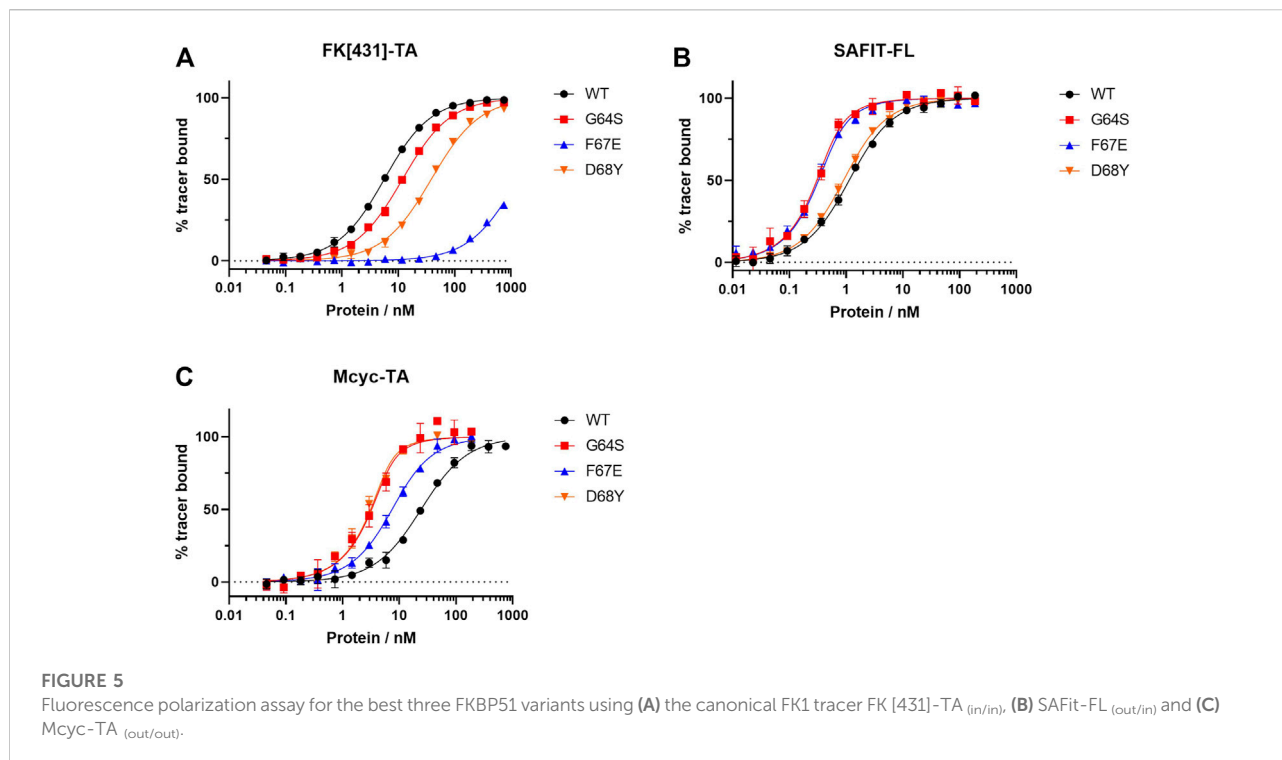
TABLE 1 Identified FKBP51 variants after FACS sorting of the random mutagenesis and SSM yeast library with SAFit-FL_(out/in) or Mcyc-TA tracers.

FKBP51 variant	Sorted with		Library source	
	SAFit-FL _(out/in)	Mcyc-TA _(out/out)	Random mutagenesis	SSM
N63A	✓			✓
N63G	✓			✓
G64A	✓	✓		✓ [3 SAFit-FL]
G64D	✓			✓
G64E	✓	✓	✓	✓
G64R	✓	✓	✓	✓
G64S	✓	✓		✓ [3 SAFit-FL]
G64K	✓			✓
G64T	✓			✓
F67E	✓			✓
F67R	✓			✓
F67S	✓		✓	
F67W	✓	✓		✓ [3 SAFit-FL]
D68N	✓		✓	
D68Y		✓	✓	✓ [16 Mcyc-TA]
S69Y	✓		✓	
P120R	✓		✓	

The number of times that a mutation was found out of 20 picked colonies is depicted in brackets.

TABLE 2 Ligand binding affinities measured by fluorescence polarization and fold change in K_d improvement with the canonical FK [431]-TA_(in/in) and the two FKBP51 specific tracers (SAFit-FL_(out/in) and Mcyc-TA_(out/out)).

FKBP51 variant	Tracer/K _d -value [nM]			Fold change in K _d improvement		
	FK [431]-TA _(in/in)	SAFit-FL _(out/in)	Mcyc-TA _(out/out)	FK [431]-TA _(in/in)	SAFit-FL _(out/in)	Mcyc-TA _(out/out)
WT	5.1 ± 0.1	0.92 ± 0.05	24 ± 2	1	1.00	1.00
N63A	6.0 ± 0.2	0.36 ± 0.02	4.3 ± 0.5	0.850	2.56	5.58
N63G	6.0 ± 0.2	0.33 ± 0.02	7.6 ± 0.9	0.850	2.79	3.16
G64A	61 ± 2	0.73 ± 0.05	4.2 ± 0.5	0.084	1.26	5.71
G64D	17 ± 1	0.50 ± 0.04	8.7 ± 1	0.300	1.84	2.76
G64E	19 ± 1	0.40 ± 0.03	3.3 ± 0.3	0.268	2.30	7.27
G64R	32 ± 2	1.1 ± 0.1	9.9 ± 1	0.159	0.84	2.42
G64S	11 ± 1	0.09 ± 0.01	0.7 ± 0.2	0.464	10.22	34.29
G64K	18 ± 1	0.93 ± 0.04	3.5 ± 0.5	0.283	0.99	6.86
G64T	61 ± 2	1.2 ± 0.1	17 ± 1	0.084	0.77	1.41
F67E	1331 ± 66	0.11 ± 0.01	5.0 ± 0.5	0.004	8.36	4.80
F67R	312 ± 14	2.3 ± 0.2	24 ± 3	0.016	0.40	1.00
F67S	1245 ± 60	0.68 ± 0.05	21 ± 2	0.004	1.35	1.14
F67W	1331 ± 66	1.6 ± 0.1	16 ± 1	0.004	0.58	1.50
D68N	146 ± 6	1.8 ± 0.1	6 ± 1	0.035	0.51	4.00
D68Y	38 ± 2	0.69 ± 0.03	0.7 ± 0.1	0.134	1.33	34.29
S69Y	66 ± 2	0.93 ± 0.05	17 ± 1	0.077	0.99	1.41



F67 variants), F67V had a slight improvement of the K_d value compared to the WT.

Similar to phenylalanine 67, the displacement of D68 from the binding pocket is a hallmark of the binding of Mcyc-TA-like ligands (but not of SAFit-like ligands). Upon binding of Mcyc-TA_(out/out) to wildtype FKBP51, D68 is displaced by the ligand, which takes its place as a hydrogen bond acceptor for the Y57 hydroxyl group (Voll et al., 2021). Lowering the energy needed for this conformational rearrangement would likely result in an increased binding affinity of Mcyc-TA_(out/out) and this might be indeed the case for the improved binding properties of the D68N variant. However, the improvement of the binding affinity of Mcyc-TA_(out/out) to the D68Y and the fact that no other amino acids substitutions were observed in this position suggests a more complex explanation for D68Y. A tyrosine in position 68 cannot easily exist in the canonical F67ⁱⁿ/Y68ⁱⁿ-conformation as observed for the apo state (F67ⁱⁿ/D68ⁱⁿ) of wildtype FKBP51 due to some steric clashes (Supplementary Figure S10) (Bracher et al., 2011). We postulate that in addition to destabilizing the F67ⁱⁿ conformation, the phenol side chain of Y68 is especially well suited to stabilize a F67^{out}/Y68^{out} conformation.

In contrast to F67 and D68, the contribution of glycine 64 to the stabilization of the binding pocket is less obvious. However, 7 out of 17 protein variants that were found in these experiments displayed a mutated G64 suggesting an important role of G64 for the binding of FKBP ligands. The role of glycine in proteins is unique as it lacks a sidechain which allows glycine to adopt unique backbone conformations. Indeed, G64 consistently adopts ϕ/ψ angles of approx. $91^\circ/-9^\circ$, respectively, in the available

FKBP51 apo structures or cocrystal structures with canonical ligands (e.g. 3O5Q, 3O5R, 5OBK, 7APT, 7APW) (Bischoff et al., 2014; Gopalakrishnan et al., 2012; Kolos et al., 2021; Pomplun et al., 2018; Y. Wang et al., 2013), thus populating a conformation allowed for glycine but disfavored for other amino acids. Moreover, G64 consistently adopts conformations of ϕ/ψ angles of approx. $68^\circ/25^\circ$ for SAFit-like cocrystal structures (F67_{out}/D68_{in}) (Feng et al., 2015, 2020; Gaali et al., 2015, 2016; Bauder et al., 2021) and of approx. $-74^\circ/149^\circ$ for Mcyc-TA-like cocrystal structures (F67_{out}/D68_{out}) (Supplementary Table S3) (Voll et al., 2021). The conformation of G64 thus seems to be coupled to the conformation of the β 3a strand, where the canonical F67_{in}/D68_{in} conformation favors a glycine-specific conformation at position 64, whereas F67_{out}/D68_{in} or F67_{out}/D68_{out} do not. A similar observation can be made for the FKBP51-G64S structures. Here, serine 64 adopts ϕ/ψ angles of $53.5^\circ/26^\circ$ in complex with SAFit1_(out/in) and $-77^\circ/149.8^\circ$ in complex with macrocyclic ligand 5_(out/out). Interestingly, in the complex with FK [431] ligand 6_(in/in) S64 adopts with observed ϕ/ψ angles of $89.4^\circ/-8.2^\circ$ a high energy conformation similar to G64 highlighting the importance of this conformation for the binding of canonical FK [431]_(in/in) ligands. In the case of serine 64 this conformation seems to be tolerated by establishing a hydrogen bond to the carbonyl oxygen of N73 upon binding of FK [431] ligand 6_(in/in) (Figure 6C). This seems not to be case for the other G64 variants as these show a more pronounced decrease in binding affinity for FK [431]-TA_(in/in) especially observable for G64A and G64T.

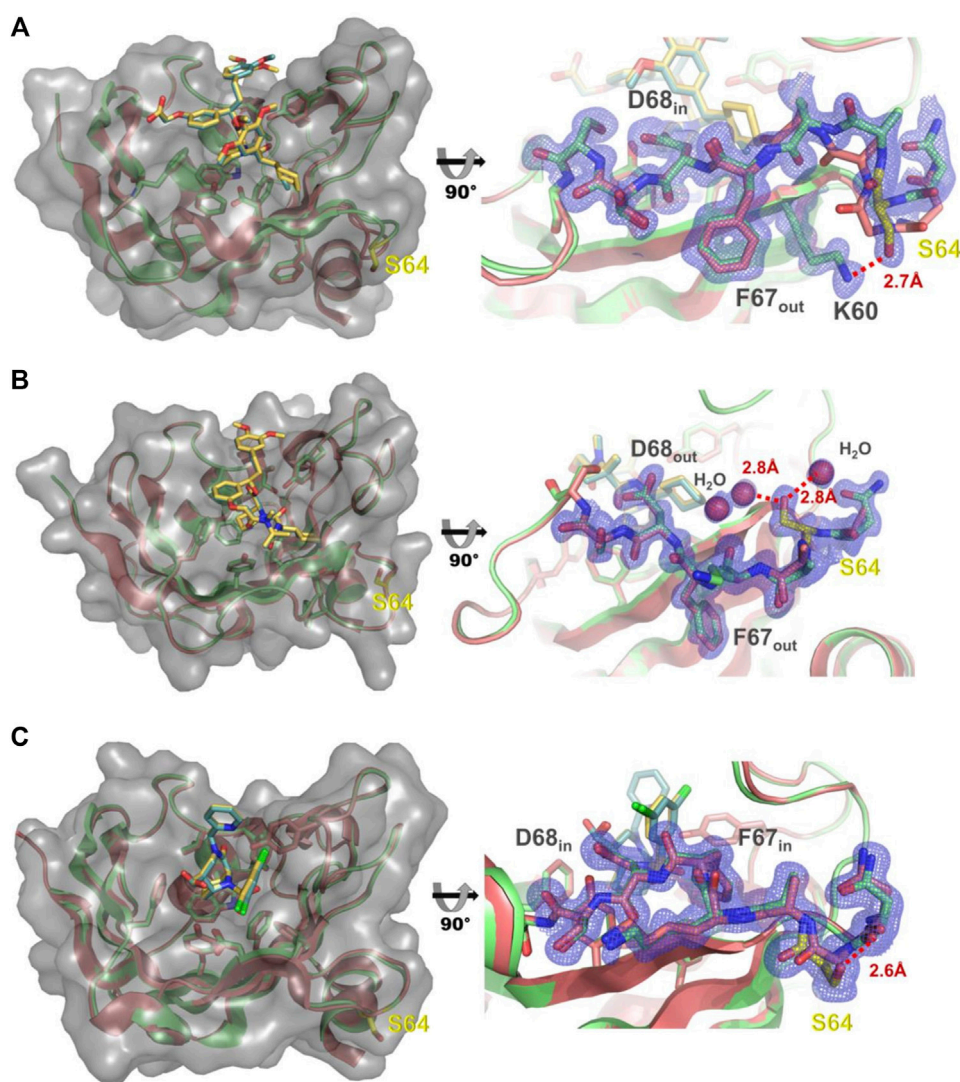


FIGURE 6

(A) Left: Structure of FKBP51-G64S (green cartoon, PDB: 7R0L) bound to SAFit1 (golden sticks) superposed with the FKBP51:iFit1 complex (cyan cartoon, teal sticks, PDB: 4TW6). The surface of FKBP-G64S is indicated in lighter grey. Right: Detailed view of the glycine to serine substitution. The observed electron density contoured at 1σ for residues 60 and 63–70 is shown as blue mesh. The hydrogen bond between lysine 60 and serine 64 is depicted as red line. (B) Left: Structure of FKBP51-G64S (green cartoon, PDB: 8BA6) bound to macrocyclic ligand (5) (golden sticks) superposed with the FKBP51 bound to the same ligand (cyan cartoon, teal sticks, PDB: 7AWF). The surface of FKBP-G64S is indicated in lighter grey. Right: Detailed view of the glycine to serine substitution. The observed electron density contoured at 1σ for residues 63–69 is shown as blue mesh. The hydrogen bonds between serine 64 and two water molecules are depicted as red lines. (C) Left: Structure of FKBP51-G64S (green cartoon, PDB: 8BAJ) bound to FK [431] ligand (6) (golden sticks) superposed with the FKBP51 bound to the same ligand (cyan cartoon, teal sticks, PDB: 5OBK). The surface of FKBP-G64S is indicated in lighter grey. Right: Detailed view of the glycine to serine substitution. The observed electron density contoured at 1σ for residues 63–69 is shown as blue mesh. The hydrogen bond between asparagine 63 and serine 64 is depicted as red line.

The allosteric destabilization of the F67 in-state by requiring a high energy backbone conformation on position 64 is certainly not sufficient to explain the unique improvement of binding affinities observed for the G64S variant. For the binding of SAFit-FL_(out/in) only a serine substitution on position 64 shows a strong improvement in binding affinity. Strikingly, in the SAFit1-bound state S64 forms a hydrogen bond with the side chain of lysine 60

(Figure 6A), which seems not to be possible for the other G64 variants. In contrast to SAFit-FL_(out/in) several G64 variants show improved binding constants for Mcyc-TA_(out/out) but again a serine substitution was strongly preferred. The structure of the FKBP51-G64S: macrocyclic ligand 5_(out/out) complex reveals that serine 64 participates in a water mediated hydrogen bond cluster stabilizing the conformation of the residues 62–66 (Figure 6B). From the

determined affinity data, it seems that besides G64S, only G64K and G64E are to some extent able to integrate reasonably well into this water cluster. Taken together, our results for the FKBP51-G64 variants strongly suggest that the improvement of the binding affinity of our conformation-specific ligands is due to a combination of destabilization of unproductive protein conformations, augmented for very favorable cases by specific stabilization of the productive conformation, and not due to novel contacts with the ligand.

The P120R is the only residue replacement outside the residue 63 to 69 amino acid stretch that we have identified in this work to enhance the binding of ligand **1** in FACS measurements. It has been reported that the carbonyl oxygen atom of P120 in FKBP51 is directed toward the binding pocket and its *cis* conformation differs from the *trans* conformation adopted in FKBP52. Moreover, it has been suggested that targeting the amino acids between positions 119 and 124 (L/P119 loop) might have an effect on steroid hormone receptors modulation (Schmidt et al., 2012). Additional structural and functional analysis of the influence of these residues on SAFit-FL_(out/in) and Mcyc-TA_(out/out) ligand binding will be required to understand, whether this region plays a role in the stabilization of the binding pocket of FKBP51.

In conclusion, we established a combined yeast display and FACS sorting strategy to identify variants of the FKBP51 FK1 domain with improved binding properties for conformation-specific tracers of FKBP51. Most of the 17 identified variants displayed an improved binding to either or both of the FKBP51 specific ligands (SAFit-FL_(out/in) and Mcyc-TA_(out/out)). Of all the found variants, G64S, D68Y, and F67E mutations presented the most significant K_d improvement. These three FKBP51 variants will be further investigated in the future to elucidate if they can be used for the identification of new ligand scaffolds targeting the transient binding pocket of FKBP51. Furthermore, we hope to obtain further insights how these mutations affect the protein dynamics and the molecular details of transient pocket formation and ligand recognition. Collectively, our results show how protein engineering using yeast display and conformation-specific tracers can be used to identify variants with improved binding affinities most likely by stabilizing the binding pocket of a protein. As soon as conformation-specific tracers are available, this approach may facilitate drug discovery by substituting target proteins with inaccessible binding pockets with the improved variants for ligand screening.

Data availability statement

The original contributions presented in the study are included in the article/Supplementary Material, further inquiries can be directed to the corresponding authors.

Author contributions

JL: Investigation, Methodology, Conceptualization, Visualization, Writing Original Draft. CM: Investigation, Analysis. AChristmann: Methodology. LR: Investigation. AC: Investigation. FH and CM: Conceptualization, Review and Editing, Project administration. HK: Supervision, Conceptualization, Review and Editing, Project administration.

Funding

Funding for this work was provided by the Ministry of Higher Education, Research and Arts of the State of Hesse under the LOEWE project “TRABITA”.

Acknowledgments

We thank HZB for the allocation of synchrotron radiation beamtime and we would particularly like to acknowledge the help and support of Manfred Weiss and the whole MX team during the experiment. We acknowledge support by the Deutsche Forschungsgemeinschaft (DFG–German Research Foundation) and the Open Access Publishing Fund of Technical University of Darmstadt.

Conflict of interest

The authors declare that the research was conducted in the absence of any commercial or financial relationships that could be construed as a potential conflict of interest.

Publisher's note

All claims expressed in this article are solely those of the authors and do not necessarily represent those of their affiliated organizations, or those of the publisher, the editors and the reviewers. Any product that may be evaluated in this article, or claim that may be made by its manufacturer, is not guaranteed or endorsed by the publisher.

Supplementary material

The Supplementary Material for this article can be found online at: <https://www.frontiersin.org/articles/10.3389/fmolb.2022.1023131/full#supplementary-material>

References

- Amaral, M., Kokh, D. B., Bomke, J., Wegener, A., Buchstaller, H. P., Eggenweiler, H. M., et al. (2017). Protein conformational flexibility modulates kinetics and thermodynamics of drug binding. *Nat. Commun.* 8 (1), 2276. doi:10.1038/s41467-017-02258-w
- Argiriadi, M. A., Sousa, S., Banach, D., Marcotte, D., Xiang, T., Tomlinson, M. J., et al. (2009). Rational mutagenesis to support structure-based drug design: MAPKAP kinase 2 as a case study. *BMC Struct. Biol.* 9 (1), 16. doi:10.1186/1472-6807-9-16
- Bauder, M., Meyners, C., Purder, P. L., Merz, S., Sugiarto, W. O., Voll, A. M., et al. (2021). Structure-based design of high-affinity macrocyclic FKBP51 inhibitors. *J. Med. Chem.* 64 (6), 3320–3349. doi:10.1021/acs.jmedchem.0c02195
- Benatouil, L., Perez, J. M., Belk, J., and Hsieh, C. M. (2010). An improved yeast transformation method for the generation of very large human antibody libraries. *Protein Eng. Des. Sel.* 23 (4), 155–159. doi:10.1093/protein/gzq002
- Bischoff, M., Sippel, C., Bracher, A., and Hausch, F. (2014). Stereoselective construction of the 5-hydroxy diazabicyclo[4.3.1]decane-2-one scaffold, a privileged motif for FK506-binding proteins. *Org. Lett.* 16 (20), 5254–5257. doi:10.1021/ol5023195
- Bracher, A., Kozany, C., Thost, A.-K., and Hausch, F. (2011). Structural characterization of the PPIase domain of FKBP51, a cochaperone of human Hsp90. *Acta Crystallogr. D. Biol. Crystallogr.* 67 (6), 549–559. doi:10.1107/S0907444911013862
- Carlson, H. A. (2002). Protein flexibility and drug design: How to hit a moving target. *Curr. Opin. Chem. Biol.* 6 (4), 447–452. doi:10.1016/S1367-5931(02)00341-1
- Cioffi, D. L., Hubler, T. R., and Scammell, J. G. (2011). Organization and function of the FKBP52 and FKBP51 genes. *Curr. Opin. Pharmacol.* 11 (4), 308–313. doi:10.1016/j.coph.2011.03.013
- Collaborative Computational Project, N. 4 (1994). The CCP4 suite: Programs for protein crystallography. *Acta Crystallogr. D. Biol. Crystallogr.* 50 (5), 760–763. doi:10.1107/S0907444994003112
- Cozzini, P., Kellogg, G. E., Spyrikis, F., Abraham, D. J., Costantino, G., Emerson, A., et al. (2008). Target flexibility: An emerging consideration in drug discovery and design. *J. Med. Chem.* 51 (20), 6237–6255. doi:10.1021/jm800562d
- Emsley, P., Lohkamp, B., Scott, W. G., and Cowtan, K. (2010). Features and development of Coot. *Acta Crystallogr. D. Biol. Crystallogr.* 66 (4), 486–501. doi:10.1107/S0907444910007493
- Evans, P. R. (2011). An introduction to data reduction: Space-group determination, scaling and intensity statistics. *Acta Crystallogr. D. Biol. Crystallogr.* 67 (4), 282–292. doi:10.1107/S090744491003982X
- Evans, P. R., and Murshudov, G. N. (2013). How good are my data and what is the resolution? *Acta Crystallogr. D. Biol. Crystallogr.* 69 (7), 1204–1214. doi:10.1107/S0907444913000061
- Eyrich, S., and Helms, V. (2007). Transient pockets on protein surfaces involved in protein-protein interaction. *J. Med. Chem.* 50 (15), 3457–3464. doi:10.1021/jm070095g
- Feng, X., Sippel, C., Bracher, A., and Hausch, F. (2015). Structure-affinity relationship analysis of selective FKBP51 ligands. *J. Med. Chem.* 58 (19), 7796–7806. doi:10.1021/acs.jmedchem.5b00785
- Feng, X., Sippel, C., Knaup, F. H., Bracher, A., Staibano, S., Romano, M. F., et al. (2020). A novel decalin-based bicyclic scaffold for FKBP51-selective ligands. *J. Med. Chem.* 63 (1), 231–240. doi:10.1021/acs.jmedchem.9b01157
- Gaali, S., Feng, X., Hähle, A., Sippel, C., Bracher, A., and Hausch, F. (2016). Rapid, structure-based exploration of pipercolic acid amides as novel selective antagonists of the FK506-binding protein 51. *J. Med. Chem.* 59 (6), 2410–2422. doi:10.1021/acs.jmedchem.5b01355
- Gaali, S., Kirschner, A., Cuboni, S., Hartmann, J., Kozany, C., Balsevich, G., et al. (2015). Selective inhibitors of the FK506-binding protein 51 by induced fit. *Nat. Chem. Biol.* 11 (1), 33–37. doi:10.1038/nchembio.1699
- Garvey, E. P. (2010). Structural mechanisms of slow-onset, two-step enzyme inhibition. *Curr. Chem. Biol.* 4 (1), 64–73. doi:10.2174/187231310790226215
- Gerlach, M., Mueller, U., and Weiss, M. S. (2016). The MX beamlines bl14.1-3 at BESSY II. *J. Large-Scale Res. Facil. JLSRF* 2, A47. doi:10.17815/jlsrf-2-64
- Gopalakrishnan, R., Kozany, C., Gaali, S., Kress, C., Hoogeland, B., Bracher, A., et al. (2012). Evaluation of synthetic FK506 analogues as ligands for the FK506-binding proteins 51 and 52. *J. Med. Chem.* 55 (9), 4114–4122. doi:10.1021/jm201746x
- Guy, C. N., Garcia, Y. A., and Cox, B. M. (2015). Therapeutic targeting of the FKBP52 Co-chaperone in steroid hormone receptor-regulated physiology and disease. *Curr. Mol. Pharmacol.* 9 (2), 109–125. doi:10.2174/1874467208666150519114115
- Hähle, A., Merz, S., Meyners, C., and Hausch, F. (2019). The many faces of FKBP51. *Biomolecules* 9 (1), E35. doi:10.3390/biom9010035
- Häusel, A. S., Balsevich, G., Gassen, N. C., and Schmidt, M. V. (2019). Focus on FKBP51: A molecular link between stress and metabolic disorders. *Mol. Metab.* 29, 170–181. doi:10.1016/j.molmet.2019.09.003
- Jagtap, P. K. A., Asami, S., Sippel, C., Kaila, V. R. I., Hausch, F., and Sattler, M. (2019). Selective inhibitors of FKBP51 employ conformational selection of dynamic invisible states. *Angew. Chem. Int. Ed. Engl.* 58 (28), 9429–9433. doi:10.1002/anie.201902994
- Kabsch, W. (2010). Xds. *Acta Crystallogr. D. Biol. Crystallogr.* 66 (2), 125–132. doi:10.1107/S0907444909047337
- Kokh, D. B., Czodrowski, P., Rippmann, F., and Wade, R. C. (2016). Perturbation approaches for exploring protein binding site flexibility to predict transient binding pockets. *J. Chem. Theory Comput.* 12 (8), 4100–4113. doi:10.1021/acs.jctc.6b00101
- Kolos, J. M., Pomplun, S., Jung, S., Rieß, B., Purder, P. L., Voll, A. M., et al. (2021). Picomolar FKBP inhibitors enabled by a single water-displacing methyl group in bicyclic [4.3.1] aza-amides. *Chem. Sci.* 12 (44), 14758–14765. doi:10.1039/D1SC04638A
- Kolos, J. M., Voll, A. M., Bauder, M., and Hausch, F. (2018). FKBP ligands—where we are and where to go? *Front. Pharmacol.* 9, 1425. doi:10.3389/fphar.2018.01425
- Liang, C. T., Roscow, O. M. A., and Zhang, W. (2021). Recent developments in engineering protein-protein interactions using phage display. *Protein Eng. Des. Sel.* 34, gzab014–13. doi:10.1093/protein/gzab014
- McCoy, A. J., Grosse-Kunstleve, R. W., Adams, P. D., Winn, M. D., Storoni, L. C., and Read, R. J. (2007). Phaser crystallographic software. *J. Appl. Crystallogr.* 40 (4), 658–674. doi:10.1107/S0021889807021206
- Monod, J., Wyman, J., and Changeux, J.-P. (1965). On the nature of allosteric transitions: A plausible model. *J. Mol. Biol.* 12 (1), 88–118. doi:10.1016/S0022-2836(65)80285-6
- Murshudov, G. N., Skubák, P., Lebedev, A. A., Pannu, N. S., Steiner, R. A., Nicholls, R. A., et al. (2011). REFMAC 5 for the refinement of macromolecular crystal structures. *Acta Crystallogr. D. Biol. Crystallogr.* 67 (4), 355–367. doi:10.1107/S0907444911001314
- Murshudov, G. N., Vagin, A. A., and Dodson, E. J. (1997). Refinement of macromolecular structures by the maximum-likelihood method. *Acta Crystallogr. D. Biol. Crystallogr.* 53 (3), 240–255. doi:10.1107/S0907444996012255
- Nicholls, R. A., Long, F., and Murshudov, G. N. (2012). Low-resolution refinement tools in REFMAC 5. *Acta Crystallogr. D. Biol. Crystallogr.* 68 (4), 404–417. doi:10.1107/S090744491105606X
- Pöhlmann, M. L., Häusel, A. S., Harbich, D., Balsevich, G., Engelhardt, C., Feng, X., et al. (2018). Pharmacological modulation of the psychiatric risk factor FKBP51 alters efficiency of common antidepressant drugs. *Front. Behav. Neurosci.* 12, 262–268. doi:10.3389/fnbeh.2018.00262
- Pomplun, S., Sippel, C., Hähle, A., Tay, D., Shima, K., Klages, A., et al. (2018). Chemogenomic profiling of human and microbial FK506-binding proteins. *J. Med. Chem.* 61 (8), 3660–3673. doi:10.1021/acs.jmedchem.8b00137
- Potterton, E., Briggs, P., Turkenburg, M., and Dodson, E. (2003). A graphical user interface to the CCP 4 program suite. *Acta Crystallogr. D. Biol. Crystallogr.* 59 (7), 1131–1137. doi:10.1107/S0907444903008126
- Potterton, L., Agirre, J., Ballard, C., Cowtan, K., Dodson, E., Evans, P. R., et al. (2018). CCP 4 i 2: The new graphical user interface to the CCP 4 program suite. *Acta Crystallogr. D. Struct. Biol.* 74 (2), 68–84. doi:10.1107/S2059798317016035
- Schmidt, M. V., Paez-Pereda, M., Holsboer, F., and Hausch, F. (2012). The prospect of FKBP51 as a drug target. *ChemMedChem* 7 (8), 1351–1359. doi:10.1002/cmdc.201200137
- Setiawan, D., Brender, J., and Zhang, Y. (2018). Recent advances in automated protein design and its future challenges. *Expert Opin. Drug Discov.* 13 (7), 587–604. doi:10.1080/17460441.2018.1465922
- Sinars, C. R., Cheung-Flynn, J., Rimerman, R. A., Scammell, J. G., Smith, D. F., and Clardy, J. (2003). Structure of the large FK506-binding protein FKBP51, an Hsp90-binding protein and a component of steroid receptor complexes. *Proc. Natl. Acad. Sci. U. S. A.* 100 (3), 868–873. doi:10.1073/pnas.0231020100
- Sivits, J. C., Storer, C. L., Galigniana, M. D., and Cox, M. B. (2011). Regulation of steroid hormone receptor function by the 52-kDa FK506-binding protein (FKBP52). *Curr. Opin. Pharmacol.* 11 (4), 314–319. doi:10.1016/j.coph.2011.03.010

- Sparta, K. M., Krug, M., Heinemann, U., Mueller, U., and Weiss, M. S. (2016). XDSAPP2.0. *J. Appl. Crystallogr.* 49 (3), 1085–1092. doi:10.1107/S1600576716004416
- Stank, A., Kokh, D. B., Fuller, J. C., and Wade, R. C. (2016). Protein binding pocket dynamics. *Acc. Chem. Res.* 49 (5), 809–815. doi:10.1021/acs.accounts.5b00516
- Surade, S., and Blundell, T. L. (2012). Structural biology and drug discovery of difficult targets: The limits of ligandability. *Chem. Biol.* 19 (1), 42–50. doi:10.1016/j.chembiol.2011.12.013
- Umezawa, K., and Kii, I. (2021). Druggable transient pockets in protein kinases. *Molecules* 26 (3), 651. doi:10.3390/molecules26030651
- Vagin, A. A., Steiner, R. A., Lebedev, A. A., Potterton, L., McNicholas, S., Long, F., et al. (2004). REFMAC 5 dictionary: Organization of prior chemical knowledge and guidelines for its use. *Acta Crystallogr. D. Biol. Crystallogr.* 60 (12), 2184–2195. doi:10.1107/S0907444904023510
- van Aalten, D. M. F., Bywater, R., Findlay, J. B. C., Hendlich, M., Hooft, R. W. W., and Vriend, G. (1996). PRODRG, a program for generating molecular topologies and unique molecular descriptors from coordinates of small molecules. *J. Comput. Aided. Mol. Des.* 10 (3), 255–262. doi:10.1007/BF00355047
- Voll, A. M., Meyners, C., Taubert, M. C., Bajaj, T., Heymann, T., Merz, S., et al. (2021). Macrocyclic FKBP51 ligands define a transient binding mode with enhanced selectivity. *Angew. Chem. Int. Ed. Engl.* 60 (24), 13257–13263. doi:10.1002/anie.202017352
- Wang, Y., Kirschner, A., Fabian, A.-K., Gopalakrishnan, R., Kress, C., Hoogeland, B., et al. (2013). Increasing the efficiency of ligands for FK506-binding protein 51 by conformational control. *J. Med. Chem.* 56 (10), 3922–3935. doi:10.1021/jm400087k
- Wang, Z.-X. (1995). An exact mathematical expression for describing competitive binding of two different ligands to a protein molecule. *FEBS Lett.* 360 (2), 111–114. doi:10.1016/0014-5793(95)00062-E
- Wang, Z.-X., Ravi Kumar, N., and Srivastava, D. K. (1992). A novel spectroscopic titration method for determining the dissociation constant and stoichiometry of protein-ligand complex. *Anal. Biochem.* 206 (2), 376–381. doi:10.1016/0003-2697(92)90381-G
- Winn, M. D., Ballard, C. C., Cowtan, K. D., Dodson, E. J., Emsley, P., Evans, P. R., et al. (2011). Overview of the CCP 4 suite and current developments. *Acta Crystallogr. D. Biol. Crystallogr.* 67 (4), 235–242. doi:10.1107/S0907444910045749
- Zheng, X., Gan, L., Wang, E., and Wang, J. (2013). Pocket-based drug design: Exploring pocket space. *AAPS J.* 15 (1), 228–241. doi:10.1208/s12248-012-9426-6

Supplementary Material

1 Primers

TABLE S1. Utilized primers for SSM, amplification and sequencing of the FKBP51 coding sequence in pCT vector

Primer	Forward (fw) primer 5'-3'
N63_deg_Fw	CATTACAAAGGAAAATTGTCANNKGGAAAGAAGTTTGATTCC
N63_deg_Rv	GACTGGAATCAAACCTTCTTCCMNNTGACAATTTTCC
G64_deg_Fw	CAAAGGAAAATTGTCAAATNNKAAGAAGTTTGATTCC
G64_deg_Rv	GACTGGAATCAAACCTTCTTMNNATTTGACAATTTTCC
K65_deg_Fw	GGAAAATTGTCAAATGGANNKAAGTTTGATTCCAG
K65_deg_Rv	CTATCATGACTGGAATCAAACCTTMNNTCCATTTGAC
K66_deg_Fw	GGAAAATTGTCAAATGGAAAGNNKTTTGATTCCAGTCATG
K66_deg_Rv	CTATCATGACTGGAATCAAAMNNCTTCCATTTGAC
F67_deg_Fw	GGAAAATTGTCAAATGGAAAGAAGNNKGATTCCAGTCATG
F67_deg_Rv	CATTTCTATCATGACTGGAATCMNNCTTCTTCCATTTGAC
D68_deg_Fw	CAAATGGAAAGAAGTTTNNKTCCAGTCATGATAGAAATG
D68_deg_Rv	GGTTCATTTCTATCATGACTGGAMNNAACCTTCTTTCC
S69_deg_Fw	GTCAAATGGAAAGAAGTTTGATNNKAGTCATGATAG
S69_deg_Rv	GGTTCATTTCTATCATGACTMNNATCAAACCTTCTTTCC
S70_deg_Fw	GGAAAGAAGTTTGATTCCNNKCATGATAGAAATG
S70_deg_Rv	GGTTCATTTCTATCATGMNNGGAATCAAACCTTCC
pCT_FKBP51_fw	AGTGGTGGTGGTGGTCTGGTGGTGGTGGTCTGGTGGTGGTGGTCTGCTAGCATGAC
pCT_FKBP51_rv	TGTTGTTATCAGATCTCGAGCTATTACAAGTCCTCTTCAGAAATAAGCTTTGCTCGGATCC
pCT_seq_up	TACCCATACGACGTTCCAGACTAC
pCT_seq_lo	CAGTGGGAACAAAGTCGATTTTGTTAC

NNK is a degenerated codon with N = any nucleotide and K = G or C. MNN is the complementary codon with M = A or T.

2 FACS analysis

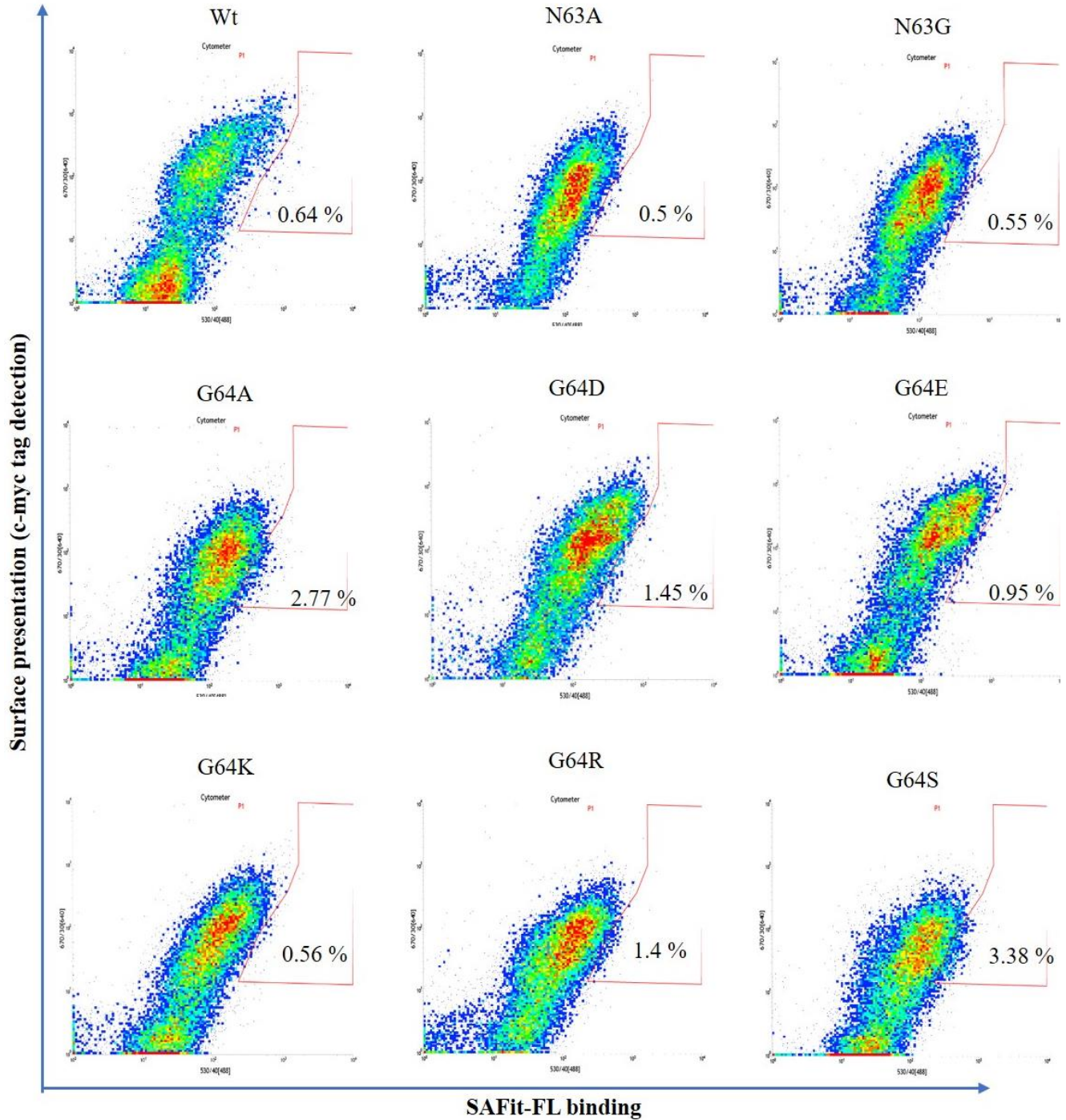


FIGURE S1. Individual dot-plots of the YSD presenting FKBP51 Wt and variants measured in a flow cytometer (part 1 of 3). Cells showing both surface presentation (c-myc tag detection) and SAFit-FL_(out/in) binding signal are presented in the polygonal gate. Clones were sorted due to the general population shift close to the established gate

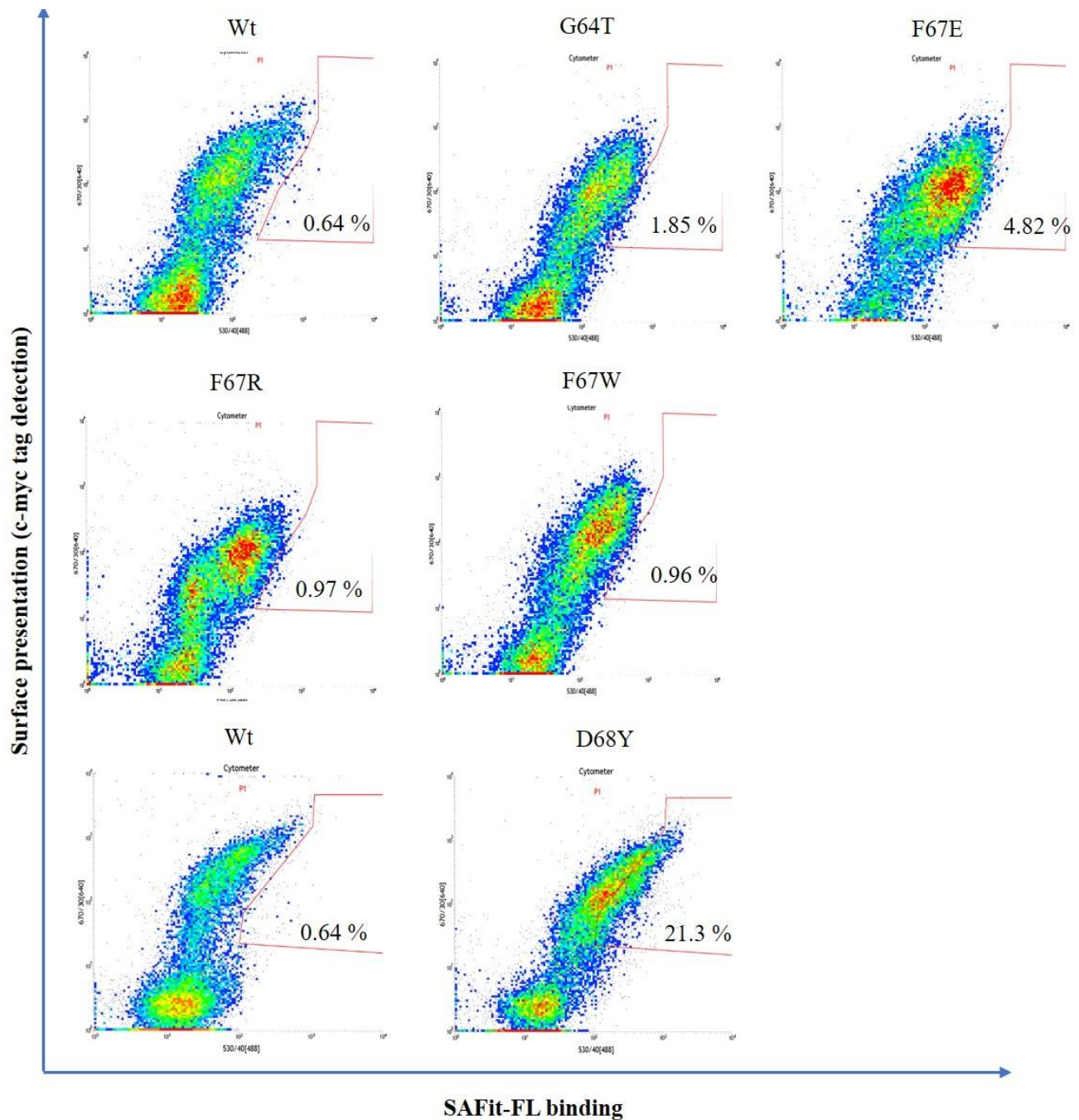


FIGURE S2. Individual dot-plots of the YSD presenting FKBP51 Wt and variants measured in a flow cytometer (part 2 of 3). Cells showing both surface presentation (c-myc tag detection) and SAFit-FL_(out/in) binding signal are presented in the polygonal gate. Clones were sorted due to the general population shift close to the established gate

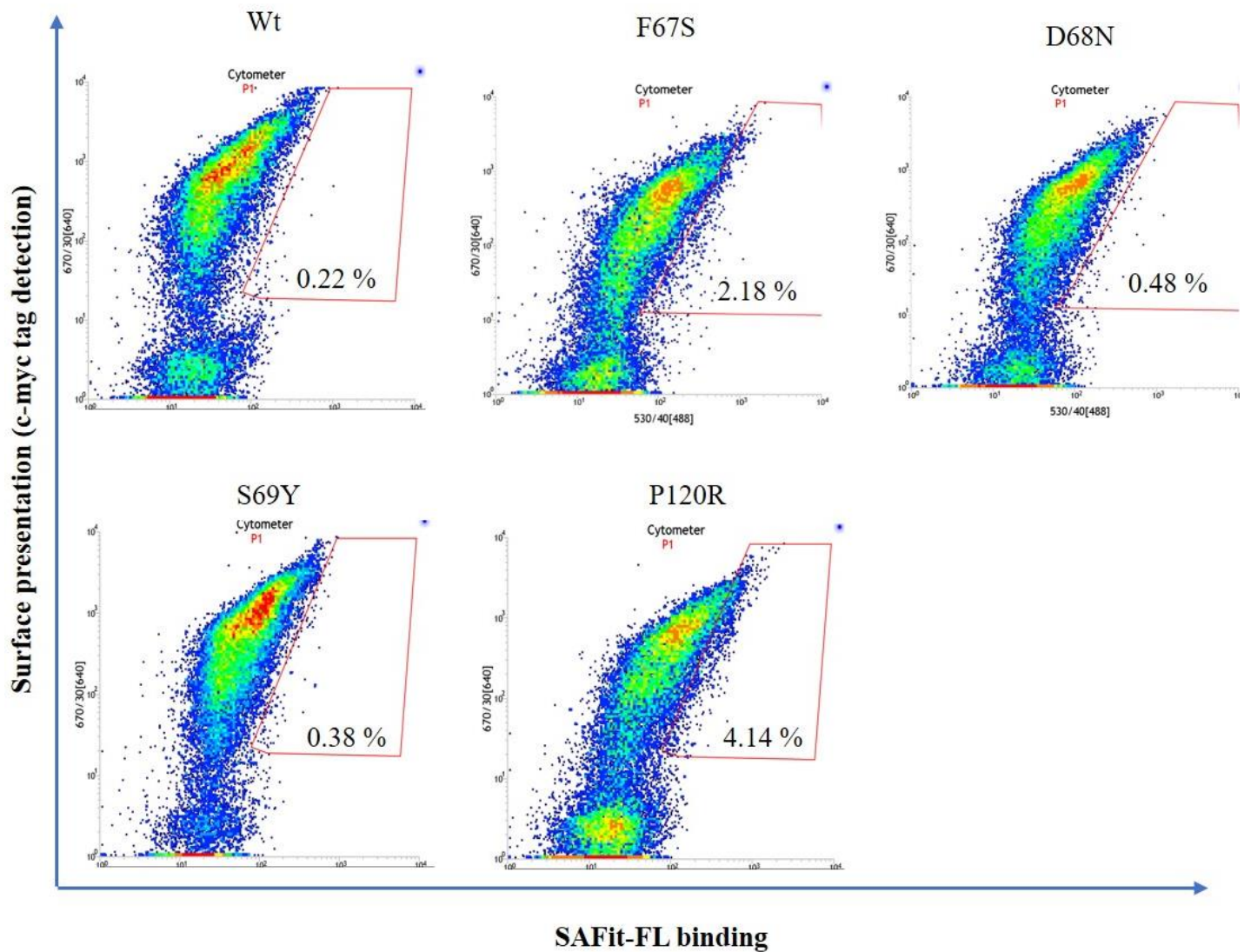


FIGURE S3. Individual dot-plots of the YSD presenting FKBP51 Wt and variants measured in a flow cytometer (part 3 of 3). Cells showing both surface presentation (c-myc tag detection) and SAFit-FL_(out/in) binding signal are presented in the polygonal gate. Clones were sorted due to the general population shift close to the established gate

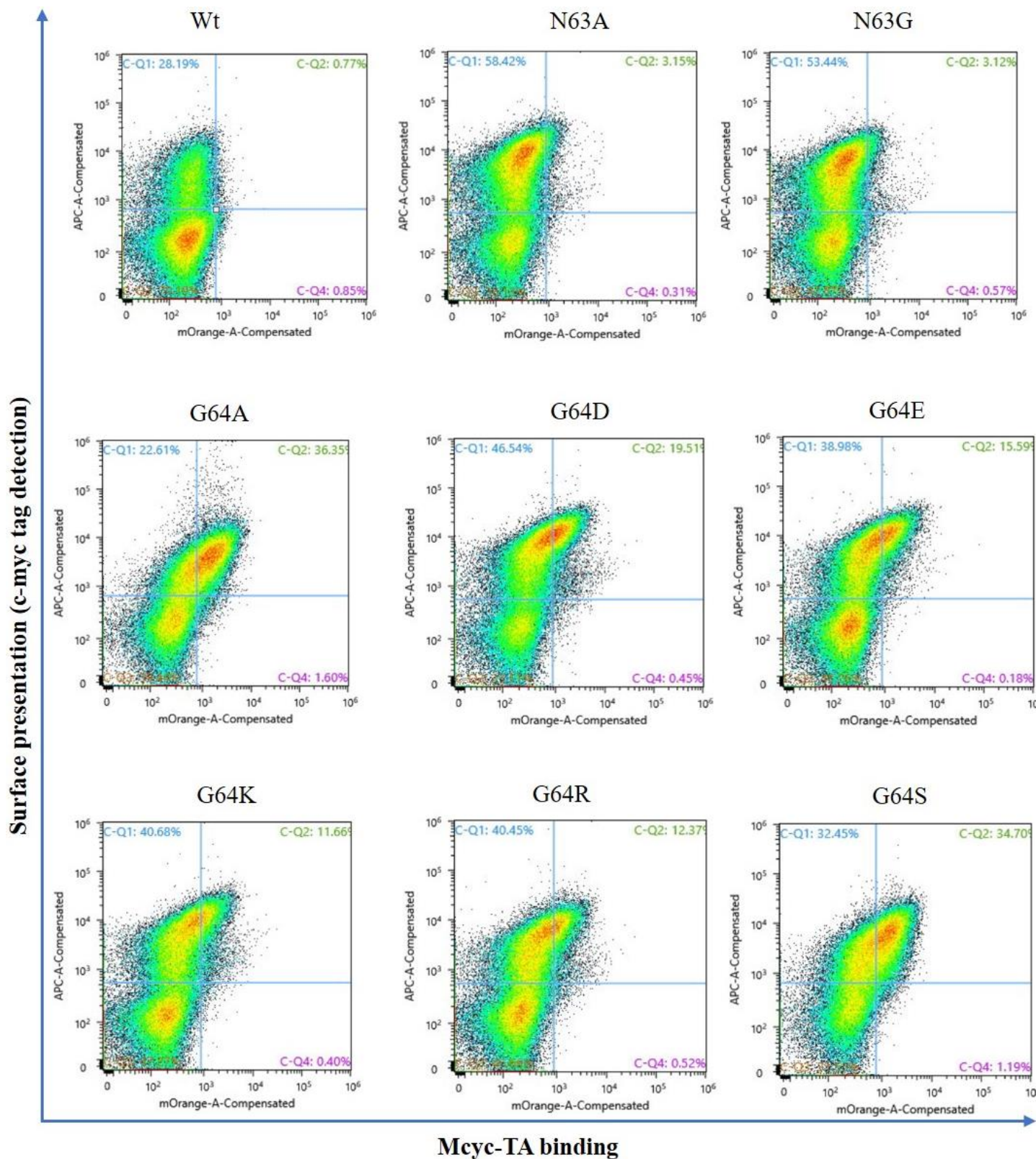


FIGURE S4. Individual dot-plots of the YSD presenting FKBP51 Wt and variants measured in a flow cytometer (part 1 of 2). Cells showing both surface presentation (c-myc tag detection) and Mycy-TA_(out/out) binding signal are presented in the second quadrant.

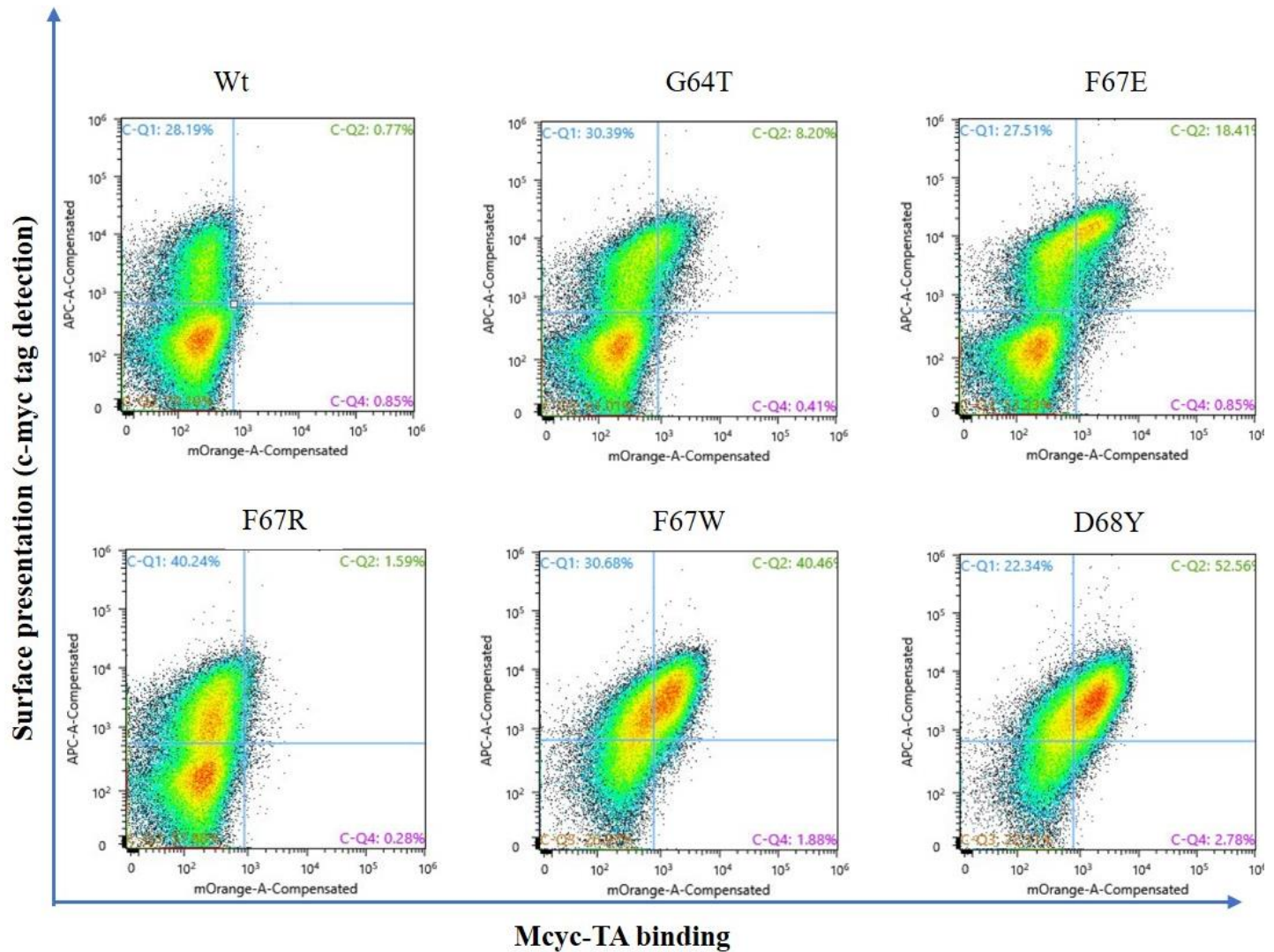


FIGURE S5. Individual dot-plots of the YSD presenting FKBP51 Wt and variants measured in a flow cytometer (part 2 of 2). Cells showing both surface presentation (c-myc tag detection) and Mcyc-TA_(out/out) binding signal are presented in the second quadrant.

3 Fluorescence polarization

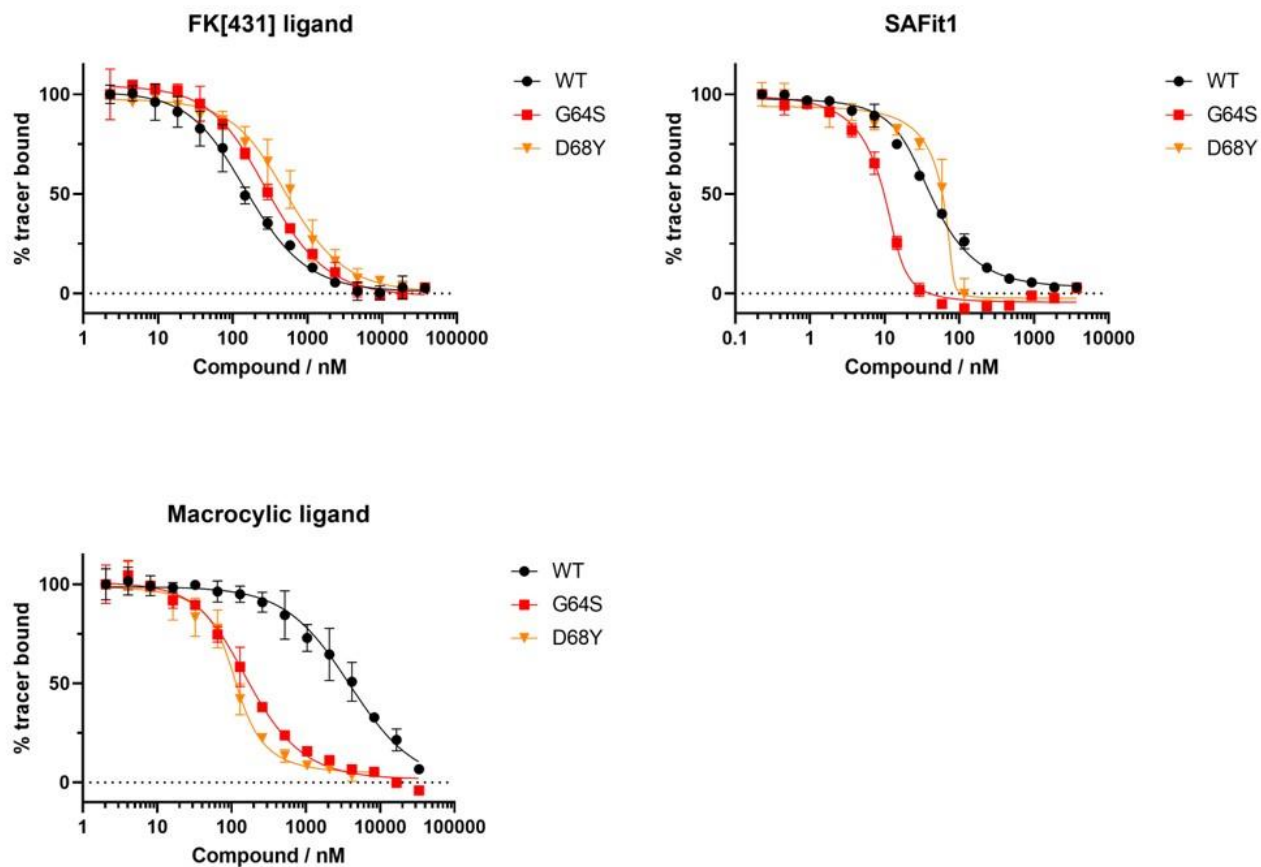


FIGURE S6. Competitive fluorescence polarization assays. FK[431] ligand (*in/in*), SAFit1 (*out/in*) or a macrocyclic ligand (*out/out*) with FKBP51 WT, 10-40 nM G64S or 80-100 nM D68Y (without fluorophores) and 1 nM of the FK[431]-based tracer (*in/in*) were used to rule out any effects of the fluorophores on the binding of the ligands to the FKBP51 variants.

TABLE S2. Ligand binding constants measured by competitive fluorescence polarization assays with the canonical FK[431] ligand _(in/in) and the two FKBP51 specific ligands (SAFit1 _(out/in) and Micyclic_(out/out))

FKBP51 variant	FK[431]-16h [Kd-value / nM]	SAFit1 [Kd-value / nM]	Macrocyclic ligand [Kd-value / nM]
WT	27±3	4.8±0.4	780±100
G64S	56±4	0.5±0.2	29±3
D68Y	126±14	0.2±0.5	10±1

4 Protein characterization

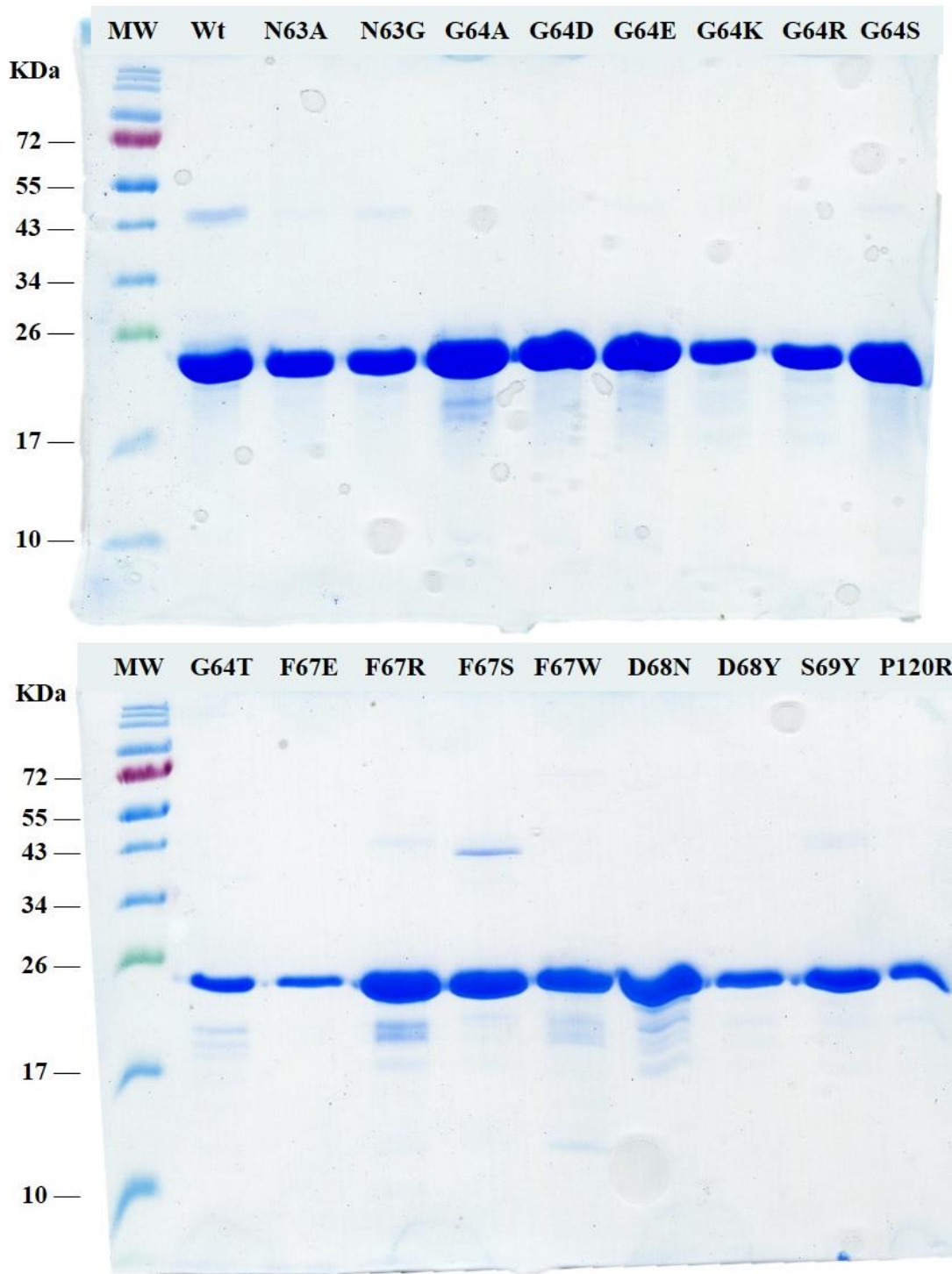


FIGURE S7. SDS-PAGE analysis of all FKBP51 variants after IMAC purification and dialysis in PBS. A molecular weight of ~19 KDa is expected for all the reduced samples.

5 Tracers and ligands

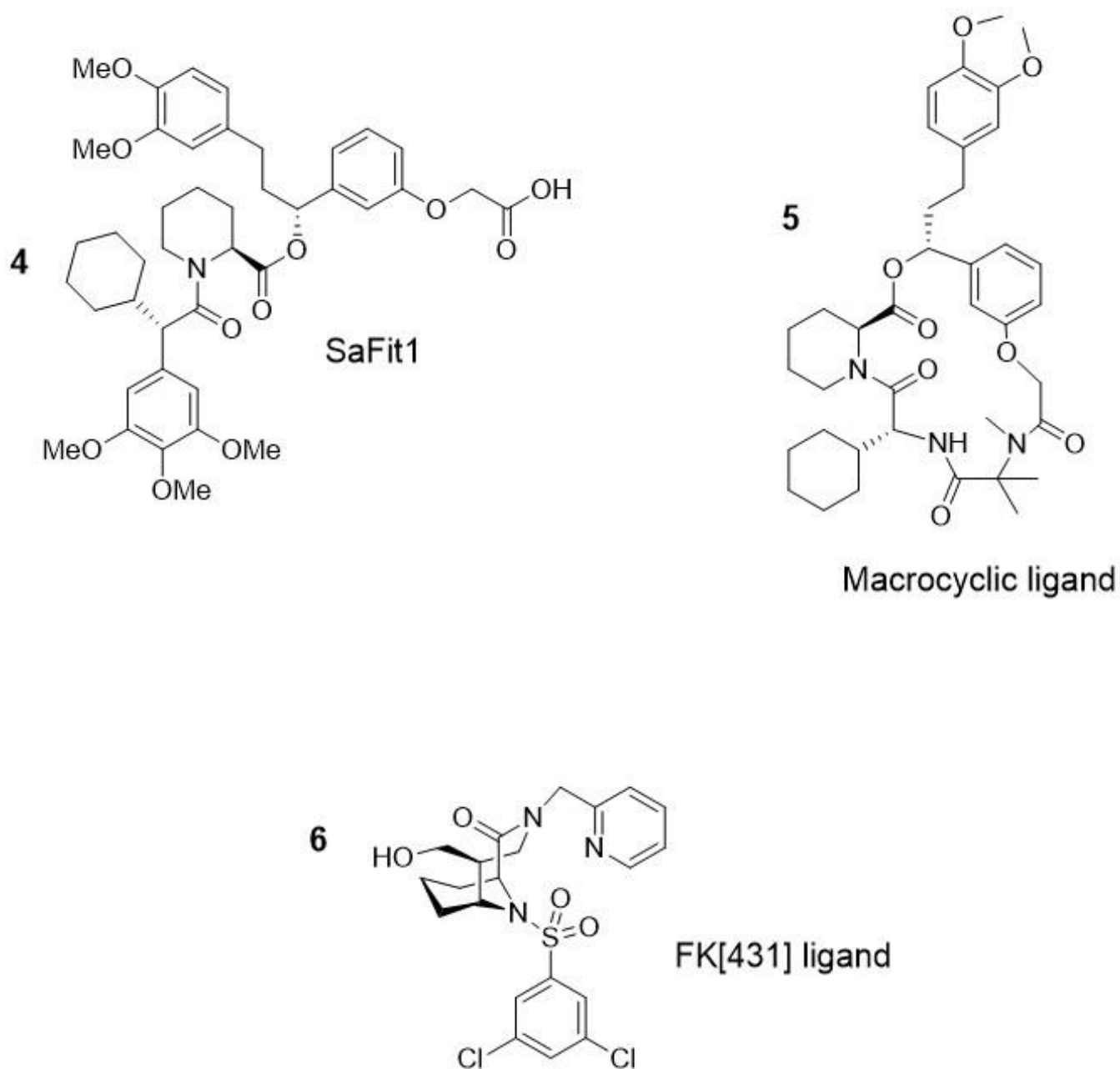


FIGURE S8. Chemical structure of the unlabeled FKBP51 ligands. The two FKBP51-spelective ligands SAFit1 (4) and macrocyclic ligand (5); these correspond to compounds SAFit1 from Gaali et al., *Nat. Chem. Biol.* 2015, 11 (1), 33–37 and compound 13 from Voll et al., *Angew. Chem. Int. Ed.* 2021, 60 (24), 13257–13263, respectively. canonical FKBP inhibitor FK[431]-16g correspond to compound 16g from Pomplun et al., *J. Med. Chem.* 2018, 61, 3660–3673

6 Protein structures

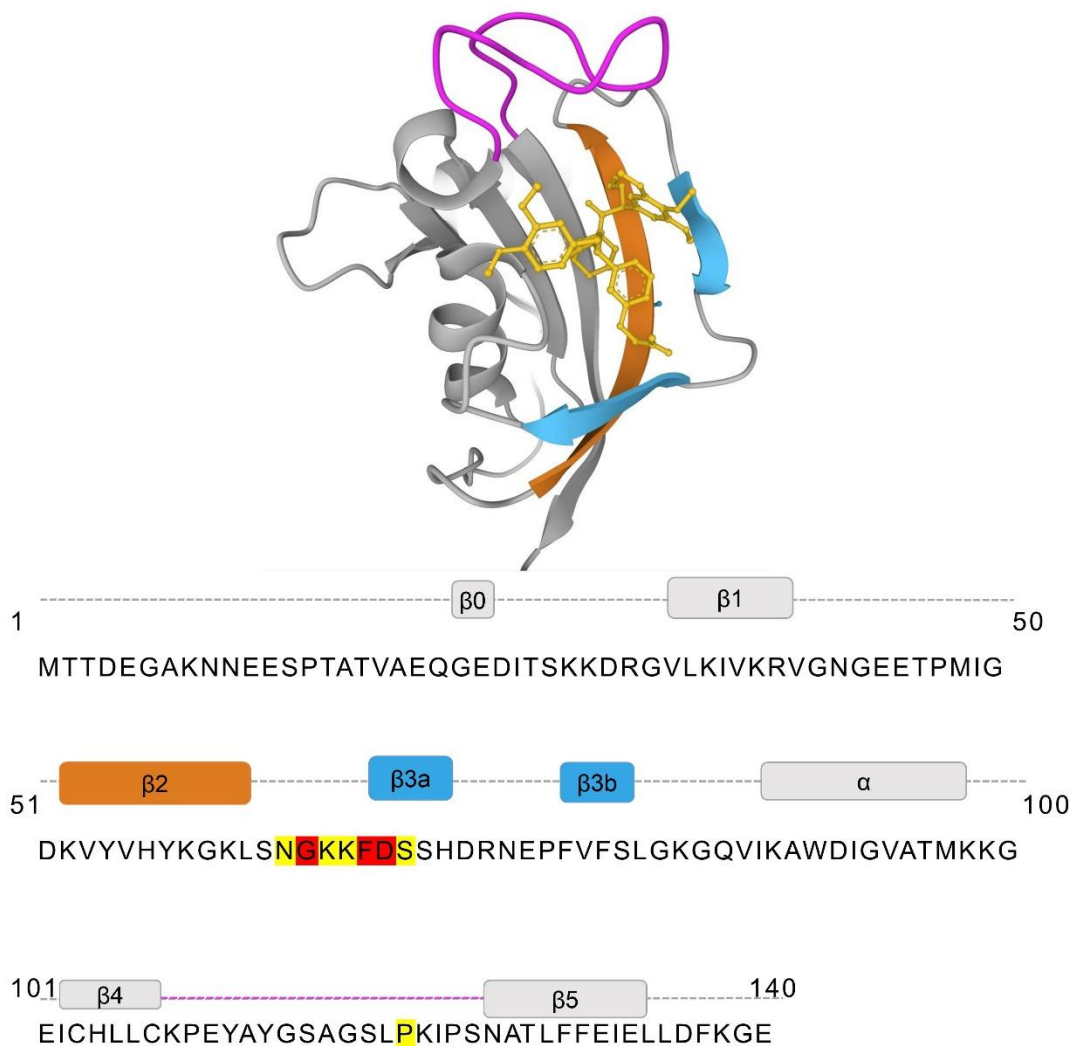


FIGURE S9. 3D structure of the FKBP51 FK1 domain (1-140) in complex with iFit1 (PDB: 4TW6).β2 and β3 strands are indicated in light blue, the β4-5 interconnecting loop is indicated in magenta and iFit1 is represented as golden sticks. The found variant positions of the protein-coding sequence are highlighted in yellow and the 3 best variants (G64, F67 and D68) positions identified by mutagenesis of the protein-coding sequence are highlighted in red.

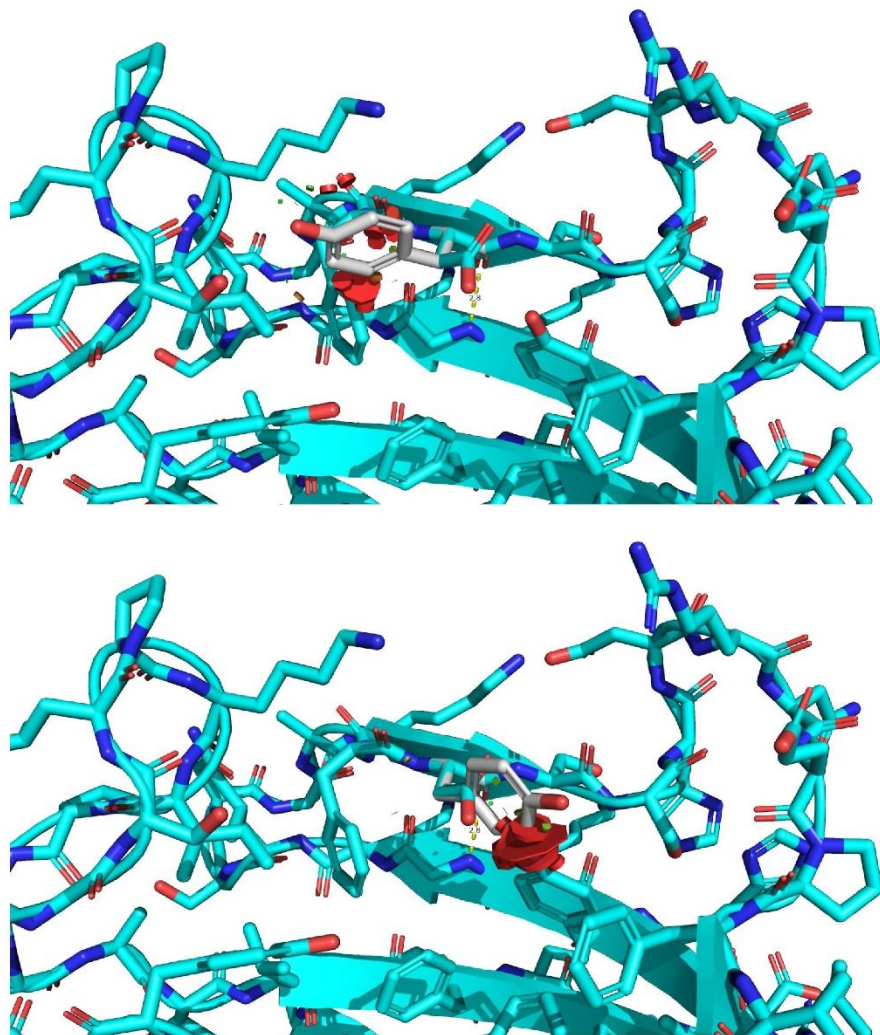


FIGURE S10. Modified structure of the FKBP51 FK1 domain in Apo state (amino acids: 14-140, PDB 3O5Q) with a D68Y amino acid exchange. The model demonstrates the steric clashes of the Y68 side chain in the canonical F67in/Y68in-conformation.

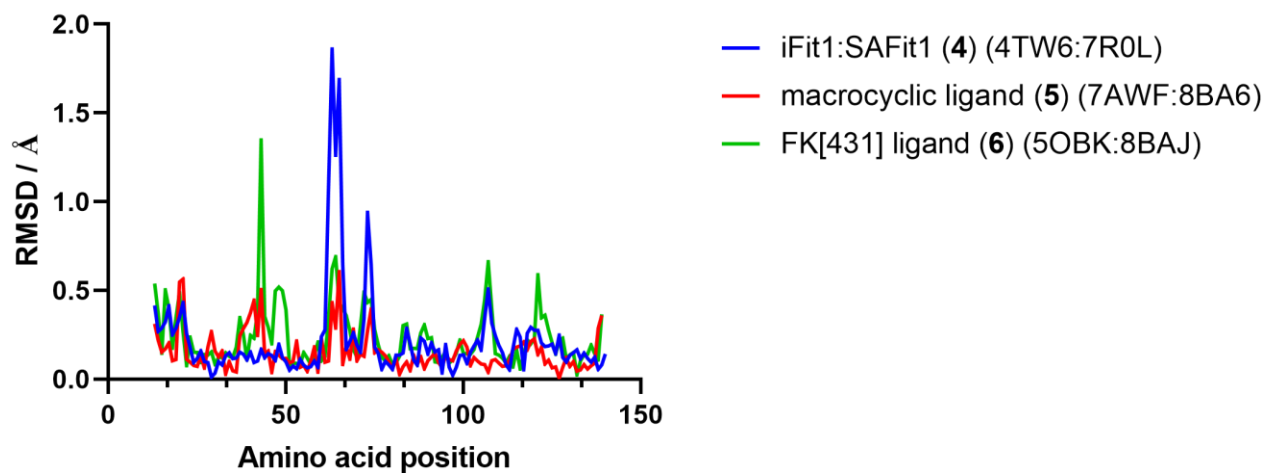


FIGURE S11. C_{α} RMSD values of a structural alignment of FKBP51-G64S in complex with SAFit1 (blue, PDB 7R0L), macrocyclic ligand (5) (red, PDB 8BA6) or FK[431] ligand (6) (green, PDB 8BAJ) aligned with structures of wild-type FKBP51 in complex with similar or the same ligands.

TABLE S3. ϕ/ψ angles of G64 of available FKBP51 apo structures or cocrystal structures with conformation-specific ligands.

State	PDB-ID	ϕ of G64	ψ of G64
	3O5E	91.5°	-12.6°
Apo (F67in/D68in)	3O5G	91.5°	-10.6°
	3O5Q	91.9°	-9.5°
	3O5R	92.9°	-11.4°
Canonical ligand bound (F67in/D68in)	5OBK	88.3°	-6.8°
	7APW	89.3°	-8.8°
	7A6X	69.2°	31.4°
SAFit-like ligand bound (F67out/D68in)	7B9Y	67.9°	25.2°
	7B9Z	68.5°	25.6°
	7AOT	-72.4°	149.8°
Mcyc-like ligand bound (F67out/D68out)	7AOU	-77.3°	152.8°
	7AWF	-72.1°	147.0°

TABLE S4. Data collection and refinement statistics for the FK1 domain of the FKBP51 G64S variant structure of in complex with SAFit1_(out/in).

PDB entry	7R0L	8BA6	8BAJ
Ligand	SAFit1	macrocyclic ligand (5)	FK[431] ligand (6)
Data collection			
Beamline	BESSY II (BL14.1)	BESSY II (BL14.1)	BESSY II (BL14.1)
Wavelength	$\lambda = 0.9184 \text{ \AA}$	$\lambda = 0.9184 \text{ \AA}$	$\lambda = 0.9184 \text{ \AA}$
Space group	P2 ₁ 2 ₁ 2 ₁	P2 ₁ 2 ₁ 2 ₁	P2 ₁ 2 ₁ 2 ₁
Cell dimensions			
<i>a, b, c</i> (Å)	45.11, 48.59, 57.19	43.58, 50.42, 59.07	40.86, 54.24, 56.86
<i>α, β, γ</i> (°)	90, 90, 90	90, 90, 90	90, 90, 90
Resolution (Å)	37.00-1.10 (1.12-1.10)	29.54-1.10 (1.12-1.10)	39.28-1.20 (1.22-1.20)
<i>R</i> _{merge}	0.067 (1.450)	0.052 (0.781)	0.115 (1.362)
<i>R</i> _{pim}	0.039 (0.869)	0.032 (0.348)	0.068 (0.824)
<i>I</i> / σ (<i>I</i>)	11.9 (1.3)	16.5 (2.2)	5.7 (1.2)
CC1/2	0.999 (0.633)	1.000 (0.745)	0.993 (0.559)
Completeness (%)	99.9 (99.4)	95.2 (89.7)	98.4 (95.7)
Redundancy	6.3 (6.1)	6.6 (6.7)	6.8 (6.8)
Refinement			
Resolution (Å)	37.00-1.10	29.55-1.10	39.28-1.-20
No. of reflections	51662	50756	39464
<i>R</i> _{work} / <i>R</i> _{free} (%)	14.2/17.1	14.1/16.2	17.6/21.0
No. of atoms			
Protein	1929	2060	1864
Ligand	106	100	53
Water	147	222	156
<i>B</i> -factors			
Protein	15.9	13.3	15.1
Ligand	13.8	9.7	15.5
Water	34.7	30.7	29.4
R.m.s. deviations			
Bond lengths (Å)	0.0192	0.0129	0.0108
Bond angles (°)	2.149	1.770	1.713
Ramachandran plot			
Favoured (%)	97.00	98.00	97.00
Allowed (%)	3.00	2.00	3.00
Outlier (%)	0.00	0.00	0.00

4.2 Accessing Transient Binding Pockets by Protein Engineering and Yeast Surface Display Screening

Title:

Accessing Transient Binding Pockets by Protein Engineering and Yeast Surface Display Screening

Authors:

Jorge A. Lerma Romero and Harald Kolmar

Bibliographic Data:

Journal – Genotype Phenotype Coupling - Methods in Molecular Biology

Volume 2681

Article published: 06 July 2023

DOI: 10.1007/978-1-0716-3279-6_14

PMID: 37405652

Copyright © 2023 Lerma Romero and Kolmar, under exclusive license to Springer Science+Business Media, LLC, part of Springer Nature

Contributions by J.A. Lerma Romero:

- Experimental design
- Performing experiments and reproducibility experiments
- Writing of original manuscript draft
- Generation of figures



Accessing Transient Binding Pockets by Protein Engineering and Yeast Surface Display Screening

Jorge A. Lerma Romero and Harald Kolmar

Abstract

The binding pocket of some therapeutic targets can acquire multiple conformations that, to some extent, depend on the protein dynamics and the interaction with other molecules. The inability to reach the binding pocket can impose a substantial or even insurmountable barrier for the de novo identification or optimization of small-molecule ligands. Herein, we describe a protocol for the engineering of a target protein and a yeast display FACS sorting strategy to identify protein variants with a stable transient binding pocket with improved binding for a cryptic site-specific ligand. This strategy may facilitate drug discovery using the resulting protein variants with accessible binding pockets for ligand screening.

Key words Transient binding pockets, Protein engineering, Yeast surface display, Cell cytometry

1 Introduction

In the early stages of drug research and development, it is crucial to have knowledge about the active site of a disease-related protein. Particularly important is to have an NMR, X-ray crystal structure, or a comparative homology model of the protein and information of the ligand binding site localization [1, 2]. The binding site or also called binding pocket is a cavity usually located on the surface or inside the protein, which in most cases binds a natural ligand [3, 4].

While most protein binding pockets are accessible in their ligand-free state and easily visualized by NMR or X-ray crystallography, some proteins present no apparent binding pocket [5–8]. However, in the presence of a ligand, a cryptic binding site of these proteins can be exposed [5, 7, 9]. Mostly, the discovery of cryptic sites is unforeseen and is only found after the crystal structures of ligand-bound proteins show that the ligand binds in a new transient binding pocket or in a previously known pocket that underwent a conformational change [4, 9]. Small-molecule drug

discovery for targets belonging to a large protein family is being hindered due to low selectivity and adverse off-target effects [4, 10, 11]. Proteins with transient binding pockets, which for a long time had been considered undruggable, are now attractive drug targets and give an alternative to redesigning drugs with low selectivity [11].

Unfortunately, finding and characterizing new cryptic sites are not easy tasks. There are several *in silico* methods, which attempt to find allosteric sites by molecular dynamics simulations [1]. The first hurdle when using computational simulations was to overcome the initial lock-and-key theory of protein–ligand interaction, which set a protein as a rigid molecule that was able to bind a ligand without any kind of conformational changes [6, 12]. Actually, there are many available structure prediction algorithms that take into consideration the protein and ligand flexibility that facilitate the search for potential druggable transient binding pockets for therapeutic targets like β -lactamase, interleukin-2, diverse kinases, FKBP, and heat shock protein 90 [11, 13–20].

Some exemplary methods for new allosteric site identification are virtual high-throughput screening, which involves the screening of thousands of compounds against a therapeutic target and *de novo* drug design, a structure-based approach that demands a protein structure [21]. Likewise, peptide phage display [22] and tethering (site-directed ligand discovery) [23, 24] are some practical approaches to identifying cryptic sites and low-affinity binders.

Once a transient binding pocket was identified, high-affinity ligands development is the next logic step. Even when the localization of a cryptic site in a protein is known, the screening of high-affinity binders is a challenging task. Therefore, a general strategy to identify new or analogs of low-affinity ligands for cryptic sites is required (Fig. 1). To facilitate the access of a new small-molecule library to the transient binding pocket, a protein variant with a stabilized and accessible transient binding pocket (in the absence of a ligand) is advantageous. Herein, we describe a method combining protein engineering and fluorescence-activated cell sorting (FACS) of a yeast display library of the target protein of interest. This method is designed to find variants of a selected protein with a stabilized transient binding pocket with the goal to ease the discovery of ligands that selectively interact with them. Additionally, the variants can be further studied and characterized to gain a better understanding of the protein–ligand interaction, and the dynamics and plasticity of the transient binding pocket of the protein of interest.

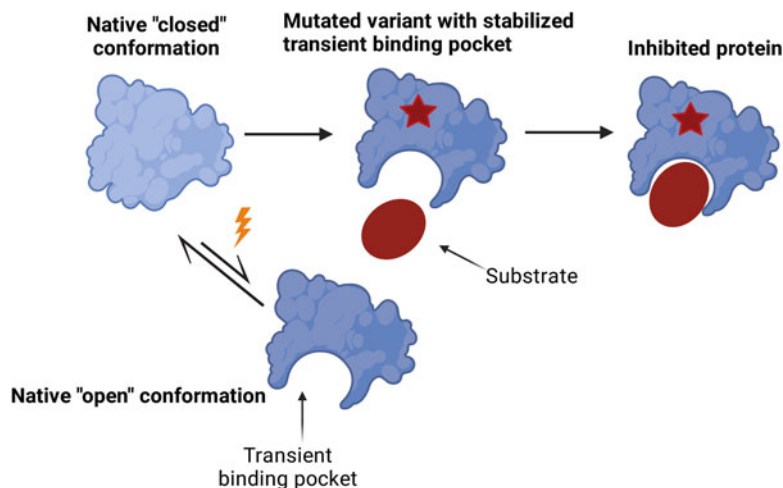


Fig. 1 Schematic representation of a protein with a confirmed transient binding pocket. To study the cryptic site of a protein, it is necessary to overcome high energy barriers or to stabilize the transient binding pocket by modifying key amino acids in the protein. A protein variant with a stabilized open conformation is helpful to facilitate ligand discovery. Created with BioRender.com

2 Materials

2.1 Protein Engineering

2.1.1 Random Mutagenesis

1. GeneMorph II Random Mutagenesis Kit (Agilent Technologies).
2. dNTPs.
3. Nuclease-free water.
4. Thermocycler.
5. DpnI (New England BioLabs).
6. Wizard SV Gel and PCR Clean-Up System (Promega) or similar.
7. 1% agarose gel and device for gel electrophoresis.
8. OneTaq® DNA Polymerase (New England BioLabs).

2.1.2 Site Saturation Mutagenesis

1. OneTaq® DNA Polymerase (New England BioLabs).
2. dNTPs.
3. Nuclease-free water.
4. Thermocycler.
5. DpnI (New England BioLabs).
6. Wizard SV Gel and PCR Clean-Up System (Promega) or similar.
7. 1% agarose gel and device for gel electrophoresis.

Table 1

Utilized primers for random mutagenesis, SSM, amplification, and sequencing of the FKBP51 coding sequence in pCT vector

Name	5'-3' sequence
F67_deg_Fw	GGAAAATTGTCAAATGGAAAGAAGNNKGATTCCAGTCATG
F67_deg_Rv	CATTTCTATCATGACTGGAATCMNNCTTCTTTCCATTTGAC
pCT_FKBP51_fw	AGTGGTGGTGGTGGTTCTGGTGGTGGTGGTTCTGGTGGTGGTGGTTC TGCTAGCATGAC
pCT_FKBP51_rv	TGTTGTTATCAGATCTCGAGCTATTACAAGTCTCTTCAGAAATAAGC TTTTGCTCGGATCC
pCT_seq_up	TACCCATACGACGTTCCAGACTAC
pCT_seq_lo	CAGTGGGAACAAAGTCGATTTTGTAC

Degenerate positions for oligonucleotides follow the subsequent code: N = G + T + A + C; K = G + T
NNK is a degenerated codon with N = any nucleotide and K = G or C. MNN is the complementary codon with M = A or T

2.1.3 *Primers for Protein Randomization* See Table 1.

2.2 **Yeast Surface Display (YSD) Library Generation and Sorting**

2.2.1 *Testing Correct Protein Cell Surface Display and Optimal Ligand Concentration for Library Screening*

SD-Trp: 8.6 g/L NaH₂PO₄ × H₂O, 5.4 g/L Na₂HPO₄, 1.7 g/L yeast nitrogen base without amino acids, 5 g/L ammonium sulfate, 5 g/L Bacto Casamino Acids, 20 g/L glucose, and 75 µg/mL kanamycin (+14 g/L agar agar for agar plates).

1. SG-Trp: 8.6 g/L NaH₂PO₄ × H₂O, 5.4 g/L Na₂HPO₄, 1.7 g/L yeast nitrogen base without amino acids, 5 g/L ammonium sulfate, 5 g/L Bacto Casamino Acids, 20 g/L galactose, and 75 µg/mL kanamycin.
2. Spectrophotometer.
3. Centrifuge.
4. PBS: phosphate-buffered saline, pH 7.4.
5. Anti-c-Myc–Biotin antibody (Miltenyi Biotec).
6. Streptavidin-APC (eBioscience).
7. SAFit-FL [25] (*see Note 1*).
8. BD Influx™ cell sorter or similar device.
9. CytoFLEX Flow Cytometer (Beckman Coulter) or similar device.
10. Thermocycler.
11. Wizard SV Gel and PCR Clean-Up System (Promega) or similar.

12. 1% agarose gel and device for gel electrophoresis.
13. Yeast cells: *S. cerevisiae* EBY100 [MATa URA3-52 trp1 leu2Δ1 his3Δ200 pep4::HIS3 prb1Δ1.6R can1 GAL (pIU211:URA3)] (Thermo Fisher Scientific).

2.2.2 YSD Library Generation

1. BamHI-HF (New England BioLabs).
2. NheI-HF (New England BioLabs).
3. Wizard SV Gel and PCR Clean-Up System (Promega) or similar.
4. Yeast peptone dextrose (YPD): 20 g/L peptone-casein, 20 g/L glucose, and 10 g/L yeast extract.
5. Platform flask shaker.
6. Spectrophotometer.
7. Deionized water.
8. Electroporation buffer: 1 M sorbitol and 1 mM CaCl₂.
9. Conditioning buffer: 0.1 M LiAc and 10 mM DTT.
10. 2 mm Bio-Rad Gene Pulser Cuvette.
11. Bio-Rad Gene Pulser Xcell.
12. Yeast pCT_entry vector (*see* **Note 2** and Fig. 5).
13. 1 M sorbitol.
14. SD-Trp: 8.6 g/L NaH₂PO₄ × H₂O, 5.4 g/L Na₂HPO₄, 1.7 g/L yeast nitrogen base without amino acids, 5 g/L ammonium sulfate, 5 g/L Bacto Casamino Acids, 20 g/L glucose, and 75 μg/mL kanamycin (+14 g/L agar agar for agar plates).
15. Yeast cells: *S. cerevisiae* EBY100 [MATa URA3-52 trp1 leu2Δ1 his3Δ200 pep4::HIS3 prb1Δ1.6R can1 GAL (pIU211:URA3)] (Thermo Fisher Scientific).

2.2.3 Library Sorting by FACS

1. SD-Trp: 8.6 g/L NaH₂PO₄ × H₂O, 5.4 g/L Na₂HPO₄, 1.7 g/L yeast nitrogen base without amino acids, 5 g/L ammonium sulfate, 5 g/L Bacto Casamino Acids, 20 g/L glucose, and 75 μg/mL kanamycin (+14 g/L agar agar for agar plates).
2. SG-Trp: 8.6 g/L NaH₂PO₄ × H₂O, 5.4 g/L Na₂HPO₄, 1.7 g/L yeast nitrogen base without amino acids, 5 g/L ammonium sulfate, 5 g/L Bacto Casamino Acids, 20 g/L galactose, and 75 μg/mL kanamycin.
3. Spectrophotometer.
4. Platform flask shaker.
5. Centrifuge.
6. PBS: phosphate-buffered saline, pH 7.4.
7. Anti-c-Myc–Biotin antibody (Miltenyi Biotec).

8. Streptavidin-APC (eBioscience).
9. SAFit-FL [25].
10. BD Influx™ cell sorter or similar device.
11. Yeast cells: *S. cerevisiae* EBY100 (generated library).

2.2.4 Single Clone Analysis

1. SD-Trp: 8.6 g/L NaH₂PO₄ × H₂O, 5.4 g/L Na₂HPO₄, 1.7 g/L yeast nitrogen base without amino acids, 5 g/L ammonium sulfate, 5 g/L Bacto Casamino Acids, 20 g/L glucose, and 75 µg/mL kanamycin (+14 g/L agar agar for agar plates).
2. SG-Trp: 8.6 g/L NaH₂PO₄ × H₂O, 5.4 g/L Na₂HPO₄, 1.7 g/L yeast nitrogen base without amino acids, 5 g/L ammonium sulfate, 5 g/L Bacto Casamino Acids, 20 g/L galactose, and 75 µg/mL kanamycin.
3. Platform flask shaker.
4. BD Influx™ cell sorter or similar device.
5. CytoFLEX Flow Cytometer (Beckman Coulter) or similar device.
6. 20 nM NaOH aqueous solution.
7. Thermoblock.
8. OneTaq® DNA Polymerase (New England BioLabs).
9. dNTPs.
10. Nuclease-free water.
11. Thermocycler.
12. Wizard SV Gel and PCR Clean-Up System (Promega) or similar.
13. 1% agarose gel and device for gel electrophoresis.

2.3 Production of Identified Protein Variants

1. Q5® High-Fidelity DNA Polymerase (NEB).
2. dNTPs.
3. Nuclease-free water.
4. Thermocycler.
5. Wizard SV Gel and PCR Clean-Up System (Promega) or similar.
6. DpnI (New England BioLabs).
7. 2 mm Bio-Rad Gene Pulser Cuvette.
8. Bio-Rad Gene Pulser Xcell.
9. dYT: 5 g/L NaCl, 16 g/L tryptone, 10 g/L yeast extract (+14 g/L agar agar for agar plates).
10. 75 mg/mL kanamycin.
11. 100 mg/mL ampicillin.

12. Bacterial cells: electrocompetent *Escherichia coli* top 10.
13. Bacterial cells: electrocompetent *Escherichia coli* BL21 (DE3).
14. Incubator at 37 °C.
15. 1 M isopropyl β -D-1-thiogalactopyranoside (IPTG) stock solution.
16. Centrifuge.
17. IMAC A buffer: 50 mM Tris-HCl, 600 mM NaCl, 20 mM imidazol.
18. IMAC B buffer: 50 mM Tris-HCl, 600 mM NaCl, 500 mM imidazol.
19. Ultrasonic cell disruptor (Bandelin Sonopuls) or another cell disruption device.
20. Cell culture shaker.
21. ÄKTA Pure 25 M (Cytiva) or similar chromatography system.
22. HisTrap HP column (Cytiva) or comparable Ni-NTA column.
23. PBS, pH 7.4.
24. Dialysis membrane.
25. 15% SDS-PAGE gel and electrophoretic chamber.

3 Methods

This chapter describes a workflow for the generation of protein variants through random mutagenesis and site-directed mutagenesis (see Fig. 2 for general process guidance). The randomized coding sequences of the target protein are used to generate a yeast surface display library, which is screened with a fluorescent conformation-specific ligand to obtain protein variants with a stabilized transient binding pocket. The positive variants can then be expressed and analyzed to determine the binding affinity improvement compared to the wild-type protein. In this exemplary study, the FK506-binding protein 51 (FKBP51) was mutated and screened with a published conformation-specific tracer. The protein engineering and screening strategy resulted in over a dozen of FKBP51 variants with improved affinities up to 34-fold compared to the wild type [26].

3.1 Protein Engineering

3.1.1 Random Mutagenesis

The target gene is randomized following the protocol of the GenMorph II random mutagenesis kit.

1. Prepare a 50 μ L reaction with the forward and reverse primer of the target DNA (pCT_FKBP51_fw and pCT_FKBP51_rv) and adjust the initial amount of target DNA depending on the desired mutation rate as shown in Table 2.

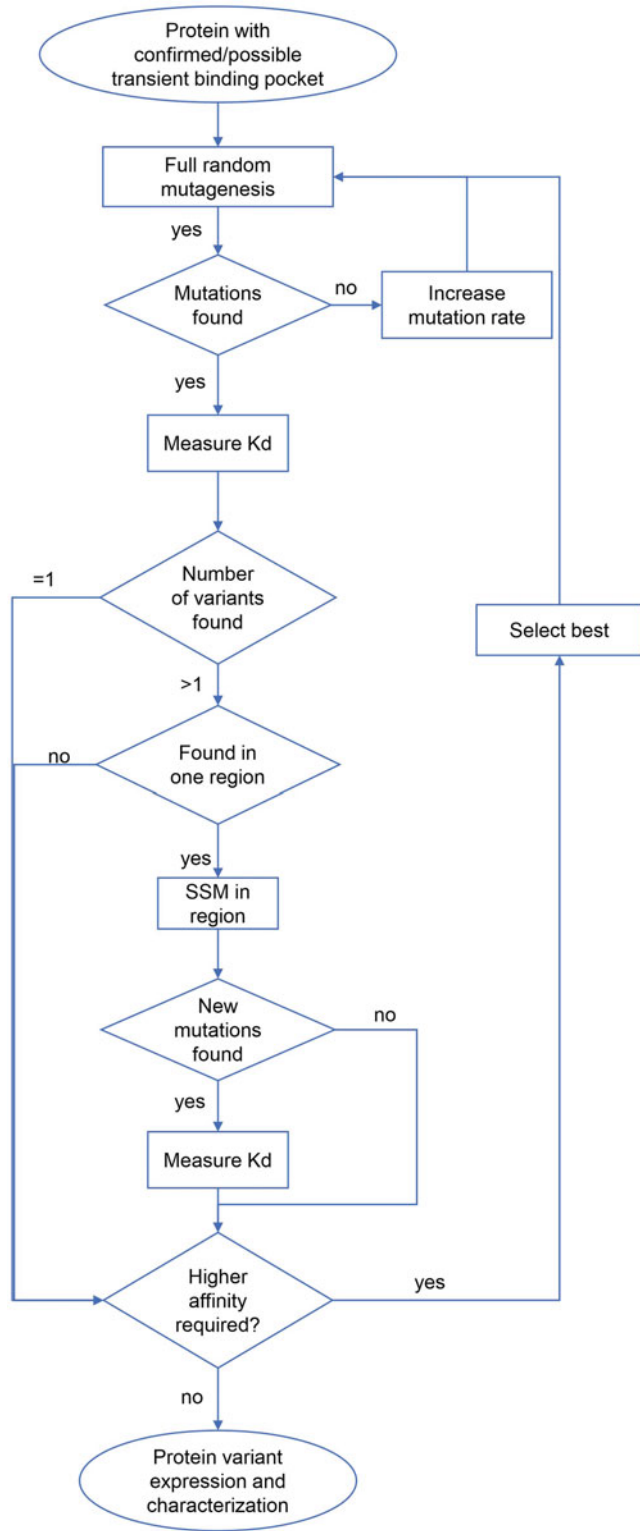


Fig. 2 Flowchart for generation of protein variants with stabilized transient binding pockets

Table 2

Random mutagenesis reaction setup dependent on the required mutation rate. For more information, refer to the manufacturer's protocol

	Low rate	Medium rate	High rate
10× Mutazyme II Reaction Buffer	5 µL	5 µL	5 µL
40 mM dNTP mix	1 µL	1 µL	1 µL
pCT FKBP51 primers (10 mM each)	1 µL	1 µL	1 µL
Mutazyme II DNA polymerase	1 µL	1 µL	1 µL
Template	900 ng	250 ng	50 ng
Nuclease-free water	Fill up to 50 µL	Fill up to 50 µL	Fill up to 50 µL

Table 3

Thermocycling conditions for random mutagenesis PCR

	Temperature	Duration [mm:ss]	Cycles
Initial denaturation	95 °C	2:00	X1
Denaturation	95 °C	00:30	X30
Annealing	64 °C	00:30	
Extension	72 °C	1:00	
Final extension	72 °C	10:00	X1

The PCR cycling conditions are described in Table 3. Adjust annealing temperature and extension time depending on the target DNA primers and template length.

- Cleave methylated parental DNA with five units of the restriction endonuclease DpnI for at least 3 h at 37 °C.
- Verify successful amplification by 1% (w/v) agarose gel electrophoresis and purify the amplicons using Wizard SV Gel and PCR Clean-Up System (Promega) or similar.
- Use 1 µL of the amplicon as a template for amplification with OneTaq polymerase. In this step, primers (pCT_FKBP51_fw and pCT_FKBP51_rv) are added that introduce overhangs that are also present in the enzymatically cleaved recipient vector to allow for gap repair cloning in yeast. Perform 25 × 100 µL PCRs in parallel as follows:
 - 20 µL 5× OneTaq reaction buffer.
 - 2 µL 10 mM dNPT mix.
 - 2 µL each primer (10 mM each).

Table 4
Thermocycling conditions for mutagenized insert amplification using OneTaq polymerase

	Temperature	Duration [mm:ss]	Cycles
Initial denaturation	94 °C	2:00	X1
Denaturation	94 °C	00:20	X30
Annealing	64 °C	00:50	
Extension	68 °C	00:35	
Final extension	68 °C	5:00	X1

- 0.5 µL OneTaq DNA polymerase.
- 1 µL template.
- Fill up to 50 µL with nuclease-free water.

The PCR cycling conditions are described in Table 4.

5. Purify amplified DNA using Wizard SV Gel and PCR Clean-Up System (Promega) or similar. At least 240 µg of the insert is required for 20 electroporation reactions for the library generation. If a larger library is required, 12 µg of additional insert DNA is required for each electroporation step.
6. Store DNA insert at -20 °C until further use.

3.1.2 Site Saturation Mutagenesis

For the site saturation mutagenesis, a two-step PCR is performed. Two separate PCR reactions are performed to generate two spliced DNA molecules of the FKBP51 gene with a single mutation and an overlap extension PCR to fuse the two fragments together.

1. First PCR step: Prepare a 50 µL reaction where the forward degenerated primer (Table 1) is paired with the reverse primer of the target DNA and vice versa (e.g., pCT_FKBP51_fw + F67_deg_Rv and pCT_FKBP51_rv + F67_deg_fw).

The PCR samples were prepared for a volume of 50 µL each as follows:

- 10 µL 5× OneTaq reaction buffer.
- 1 µL 10 mM dNPT mix.
- 1 µL each primer (10 mM each).
- 0.25 µL OneTaq DNA polymerase.
- ~ 20 ng template.
- Fill up to 50 µL with nuclease-free water.

The PCR cycling conditions are described in Table 5.

2. Purify both amplified fragments using Wizard SV Gel and PCR Clean-Up System (Promega) or similar.

Table 5
Thermocycling conditions for SSM using OneTaq polymerase

	Temperature	Duration [mm:ss]	Cycles
Initial denaturation	95 °C	02:00	X1
Denaturation	95 °C	00:20	X30
Annealing	52–56 °C	00:50	
Extension	68 °C	00:25	
Extension	68 °C	05:00	X1

Table 6
Thermocycling conditions for overlap extension PCR using OneTaq polymerase

	Temperature	Duration [mm:ss]	Cycles
Initial denaturation	95 °C	02:00	X1
Denaturation	95 °C	00:20	X30
Annealing	64 °C	00:50	
Extension	68 °C	00:35	
Extension	68 °C	05:00	X1

3. Second PCR step: Use 1 μ L of each purified product of the first PCR step for an overlap extension PCR. The reaction is made with the target DNA primers (pCT_FKBP51_fw + pCT_FKBP51_rv).
 - 10 μ L 5 \times OneTaq reaction buffer.
 - 1 μ L 10 mM dNPT mix.
 - 1 μ L primers (10 mM each).
 - 0.25 μ L OneTaq DNA polymerase.
 - 1 μ L of each fragment as template.
 - 35.75 μ L nuclease-free water.

The PCR cycling conditions are described in Table 6.

4. Cleave methylated parental DNA with five units of the restriction endonuclease DpnI overnight at room temperature.
5. Purify both amplified fragments using Wizard SV Gel and PCR Clean-Up System (Promega) or similar.
6. Use 1 μ L of the purified DNA as a template for amplification with OneTaq polymerase. Perform 25 \times 100 μ L PCRs in parallel shown in Subheading 3.1.1. Divide the reaction by the number of modified amino acid positions of the protein

(e.g., eight positions modified, $3 \times 100 \mu\text{L}$ PRCs of each modified residue).

7. Verify successful amplification by 1% (w/v) agarose gel electrophoresis and purify amplified DNA using Wizard SV Gel and PCR Clean-Up System (Promega) or similar. At least $240 \mu\text{g}$ of the insert is required for 20 electroporation reactions for the library generation. If a larger library is required, $12 \mu\text{g}$ of additional insert DNA is required for each electroporation step.
8. Store DNA insert at -20°C until further use.

3.2 Yeast Surface Display (YSD)

3.2.1 Testing Correct Protein Cell Surface Display and Optimal Ligand Concentration for Library Screening

Before generating a yeast library with modified amino acid sequences, it should be confirmed that the wild-type protein can be successfully displayed over the yeast surface of *S. cerevisiae* *EBY100*.

1. Transform yeast cells with a pCT vector containing the target gene fused to yeast surface anchored protein Aga2p following the protocol by Benatuil et al. [27–29]. Only one electroporation reaction is necessary.
2. Grow the transformed cells in 50 mL SD-Trp medium overnight at 30°C and 180 rpm.
3. Induce the transformed yeast cells by inoculating 50 mL SG-Trp at an OD_{600} of 1.0 with the grown cells in SD-Trp medium overnight at 30°C , 180 rpm.
4. The following day, measure the OD_{600} of the cell culture and aliquot in $5 \times 1.5 \text{ mL}$ reaction tubes 2×10^7 induced yeast cells per tube ($1\text{OD} = 2 \times 10^7$ cells/mL).
5. Harvest the cells by centrifugation, discard the supernatant, and wash the yeast cells with 1 mL of PBS.
6. Incubate the washed yeast cells with a biotin-conjugated c-Myc antibody (diluted 1:75) on ice for 30 min (see **Note 3**).
7. Wash the yeast cells with 1 mL of PBS.
8. Stain with the secondary labeling reagent Streptavidin-APC (eBioscience) diluted 1:75. Incubate on ice for 30 min. Additionally, add different concentrations of the fluorescently labeled protein-specific ligand (SAFit-FL in the specific case of FKBP51) to four of the five reaction tubes. The fifth reaction tube without tracer serves as a negative control.
9. Wash the yeast cells with 1 mL of PBS and resuspend the cell pellet in $600 \mu\text{L}$ PBS.
10. Analyze cells using a cell sorter such as a BD Influx™ cell sorter, CytoFLEX Flow Cytometer (Beckman Coulter), or similar devices. If a cell population presents APC fluorescence, the yeast display system has successfully expressed and displayed the protein of interest on the cell surface.

11. Sorting gates should be set appropriately, with a low ($<1\%$) number of events in the negative control of cells positive to the protein-specific tracer, fluorescein (FITC) in this exemplary case.
12. Analyze the yeast cells labeled with different concentrations of the tracer and determine at which concentration a rather low population shift ($\sim 1\text{--}2\%$) is visible. This is the initial concentration for the screening of the mutant library. An exemplary FACS histogram is shown in Fig. 3.

3.2.2 Yeast Surface Display (YSD) Library Generation

YSD library is generated using a modified version of the previously published protocol by Benatuil et al. (2010) [30]. Only the modifications of the protocol are listed in this section, and the remaining steps were not modified from the original protocol.

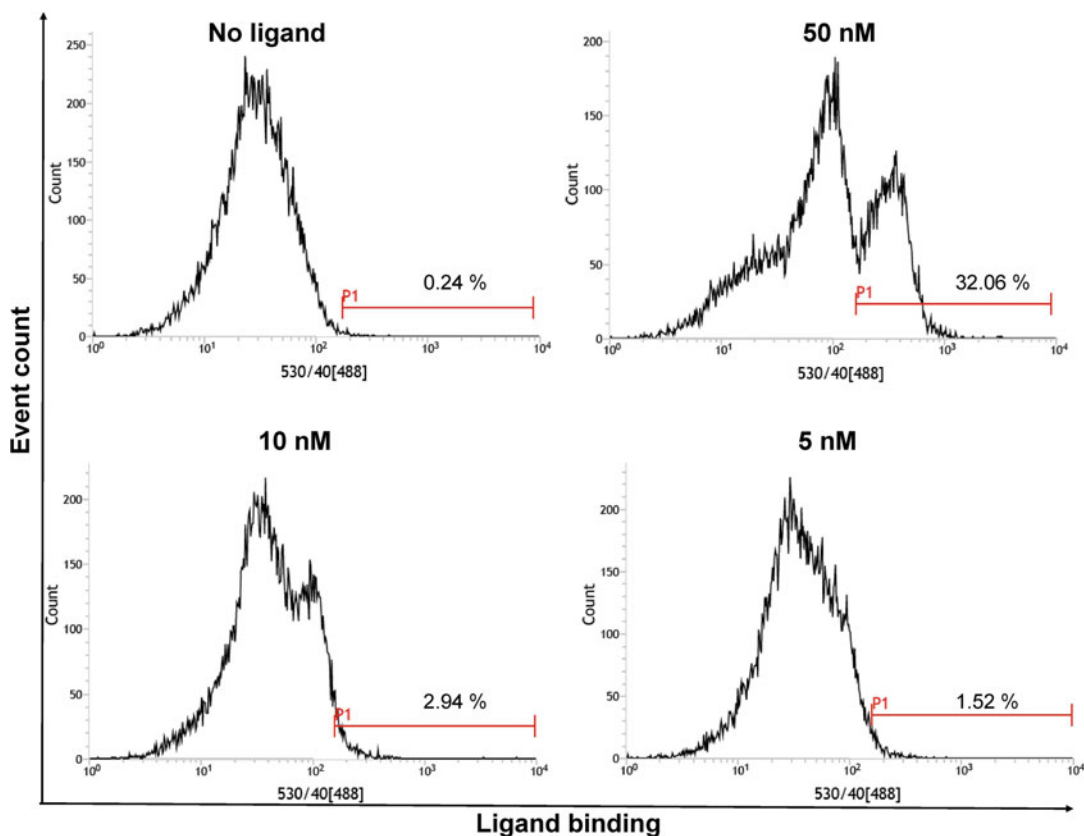


Fig. 3 FACS-generated histograms displaying the cell count (y -axis) and ligand binding (x -axis) of EBYP100 cells presenting the Wt FK1 domain of FKBP51 with different tracer concentrations to determine the proper starting point for a screening of a mutant library of the same protein. In this particular case, a concentration of 5 nM was chosen

1. Digest >100 µg of empty pCT with 50 units of BamHI-HF and 50 units of NheI-HF and incubate for 3 h at 37 °C and subsequently at room temperature overnight.
2. Purify the digested pCT plasmid using Wizard SV Gel and PCR Clean-Up System (Promega) or similar. At least 80 µg of digested vector backbone is required for 20 electroporation reactions.
3. Preparation of electrocompetent *S. cerevisiae* cells (EBY100) starts by inoculating a shaking flask with 1 L YPD medium with the overnight culture at a 0.3 OD₆₀₀.
4. Cells are washed three times with ice-cold deionized water and twice with ice-cold electroporation buffer.
5. Cells are reconditioned in 200 mL of 0.1 M LiAc/10 mM DTT.
6. Collect the conditioned cells by centrifugation in 6 × 50 mL-centrifuge tubes, wash three times with 50 mL ice-cold electroporation buffer, and resuspended the cell pellet with electroporation buffer to reach a final volume of 10 mL.
7. For 20 electroporation reactions, create a master mix with 80 µg of digested vector backbone and 240 µg of the DNA insert (4 µg of digested vector backbone and 12 µg of the DNA insert per electroporation reaction). 1/20 of the total volume of the master mix is to be used for one electroporation reaction.
8. Transfer the cells into 80 mL of 1:1 mix of 1 M sorbitol: YPD media. Incubate on a platform shaker at 225 rpm and 30 °C for 1 h.
9. Collect cells by centrifugation and resuspend in 1 L of SD-Trp media and grow cells at 30 °C overnight.

3.2.3 Library Sorting by FACS

1. Induce the yeast library and the yeast cells transformed with the Wt protein in 50 mL of SG-Trp media overnight at 30 °C, 180 rpm at an OD₆₀₀ of 1.0.
2. The following day measure the OD₆₀₀ of the cell cultures and aliquot in 1.5 mL reaction tubes 2×10^9 induced yeast cells (library) per tube. $1\text{OD} = 2 \times 10^7$ cells/mL The screening should be of at least 10× of the yeast library size determined by plating the transformed yeast cells after the library generation.
3. Harvest 2×10^7 induced yeast cells (Wt) per tube. This will follow the same incubation and staining procedure like the yeast library and will serve as a negative control for FACS sorting.
4. Wash the cells with 1 mL PBS.
5. Incubate the washed yeast cells with a biotin-conjugated c-Myc antibody (diluted 1:75) on ice for 30 min.
6. Wash the yeast cells with 1 mL of PBS.

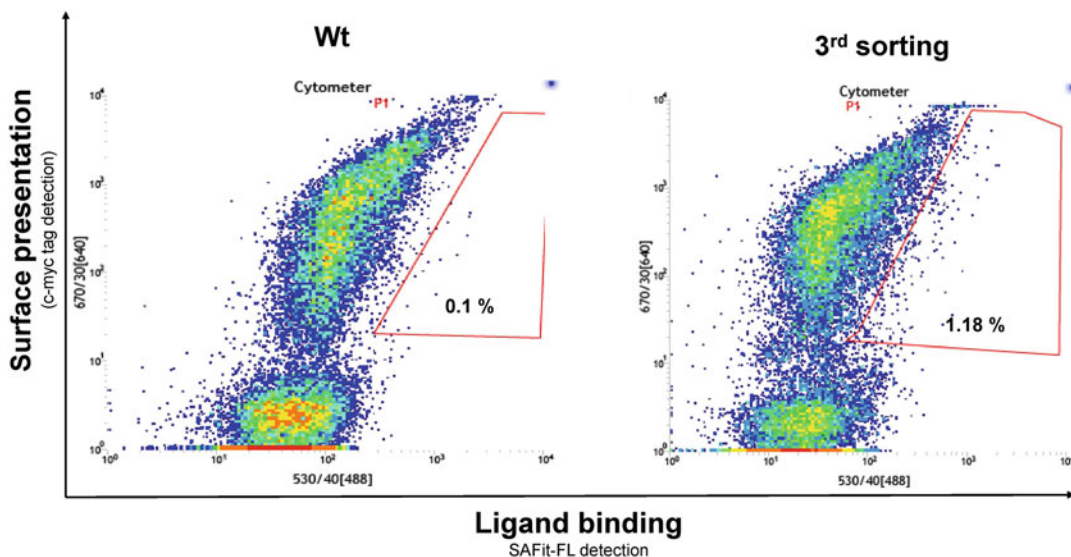


Fig. 4 FACS plots from library screening against FKBP51. As shown exemplarily for this, FKBP51 library cells show surface presentation (c-Myc-tag detection) on the y-axis and ligand binding signal (SAFit-FL) on the x-axis. The sorting gate was set to capture approximately 1% of the tracer binding population

7. Stain with the secondary labeling reagent Streptavidin-APC (eBioscience) diluted 1:75. Incubate on ice for 30 min. Additionally, the amount of the fluorescently labeled protein-specific ligand (SAFit-FL in the specific case of FKBP51) is determined in Subheading 3.2.1.
 8. Wash the yeast cells with 1 mL of PBS and resuspend the cell pellet of three to four reaction tubes in 1 mL PBS.
 9. Sort cells using a cell sorter such as a BD Influx™ cell sorter or similar devices. Set a sorting gate to capture approximately 1% of the tracer binding population. An exemplary FACS plot is shown in Fig. 4.
 10. Plate the sorted yeast cells on SD-Trp agar plates and then incubate at 30 °C for 48 h.
 11. Transfer cells to SD-Trp media and incubate further overnight at 30 °C.
 12. Inoculate 50 mL SG-Trp media at an initial OD₆₀₀ of 1.0 and induce the cells overnight at 30 °C.
 13. Repeat the screening procedure as required (*see Note 4*).
- 3.2.4 Single Clone Analysis**
1. After the last sorting round plate the sorted yeast cells were on SD-Trp agar plates (50 μL per plate) and incubate at 30 °C for 48 h.

2. Pick single colonies from the agar plate and inoculate 5 mL SG-Trp media and induce the cells overnight at 30 °C and 180 rpm.
3. Follow the steps of Subheading 3.2.3 to stain the selected clones and the induced yeast cells displaying the Wt protein.
4. Set the proper sorting gates and confirm positive clones by a strong shift of the yeast population to the tracer-positive quadrant of a dot plot.
5. From the liquid culture of the positive clones, harvest 20–30 μL by centrifugation and resuspend in 25 μL of 20 nM NaOH aqueous solution. Alternatively, pick the same colony of the positive clone and resuspend in 25 μL of 20 nM NaOH aqueous solution.
6. Incubate for 20 min at 98 °C.
7. Perform a 25 μL PCR for each positive clone using the pCT_seq_up and pCT_seq_lo primers as follows:
 - 5 μL 5 \times OneTaq reaction buffer.
 - 0.5 μL 10 mM dNPT mix.
 - 0.5 μL each primer (10 mM each).
 - 0.12 μL OneTaq DNA polymerase.
 - 1 μL template.
 - Fill up to 25 μL with nuclease-free water.

The PCR cycling conditions are described in Table 7.
8. Verify successful amplification by 1% (w/v) agarose gel electrophoresis and purify amplified DNA using Wizard SV Gel and PCR Clean-Up System (Promega) or similar.
9. Sequence the purified PCR products with the pCT_seq_up or pCT_seq_lo primers to evaluate which mutation(s) in the protein is responsible for the enhanced ligand binding.

Table 7
Thermocycling conditions for single clone check PCR using OneTaq polymerase

	Temperature	Duration [mm:ss]	Cycles
Initial denaturation	94 °C	2:00	X1
Denaturation	94 °C	00:20	X30
Annealing	54 °C	00:50	
Extension	68 °C	00:45	
Final extension	68 °C	5:00	X1

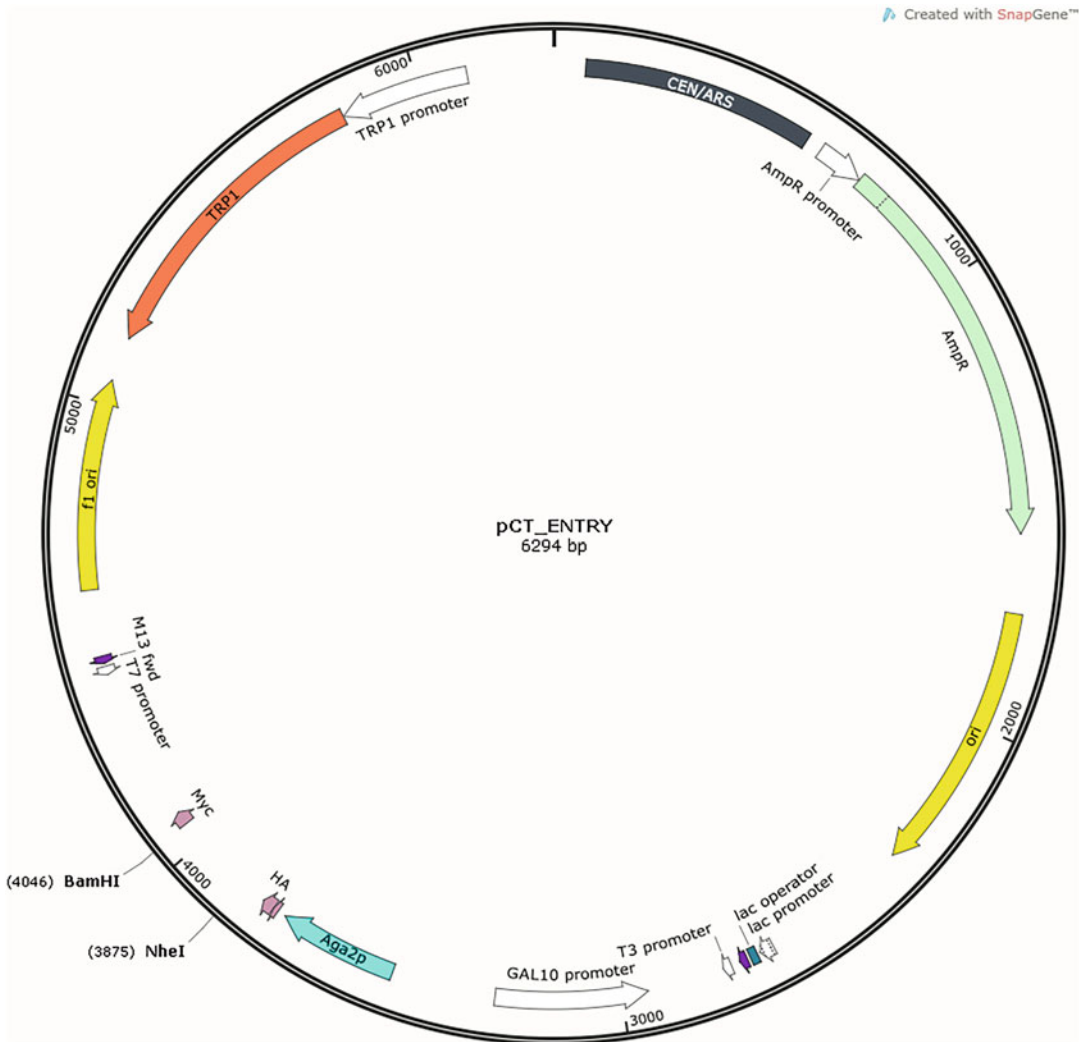


Fig. 5 Plasmid map of the yeast pCT_entry vector. The plasmid contains an ampicillin resistance gene for bacterial selection, tryptophan auxotroph gene for yeast selection, BamHI and NheI restriction sites for gap repair cloning of the gene of interest, an Aga2p gene for the surface presentation of the protein of interest, and a Myc tag to verify the correct protein expression

3.3 Production of Identified Protein Variants

1. Sub-clone the mutated target DNA to a proper destination vector depending on the expression organism of choice (pET30 was used for FKBP51 variants). Alternatively, insert a point mutation in an existent plasmid containing the Wt protein (pET30_FKBP51_FK1 Wt. *See Note 2* and Fig. 6) by full plasmid amplification with Q5 High-Fidelity DNA Polymerase and no-overlapping primers (e.g., F67E_FKBP51_Fw and F67E_FKBP51_Rv; Table 8) as follows:

- 10 μ L 5 \times Q5 Reaction Buffer.
- 2 μ L 10 mM dNPT mix.

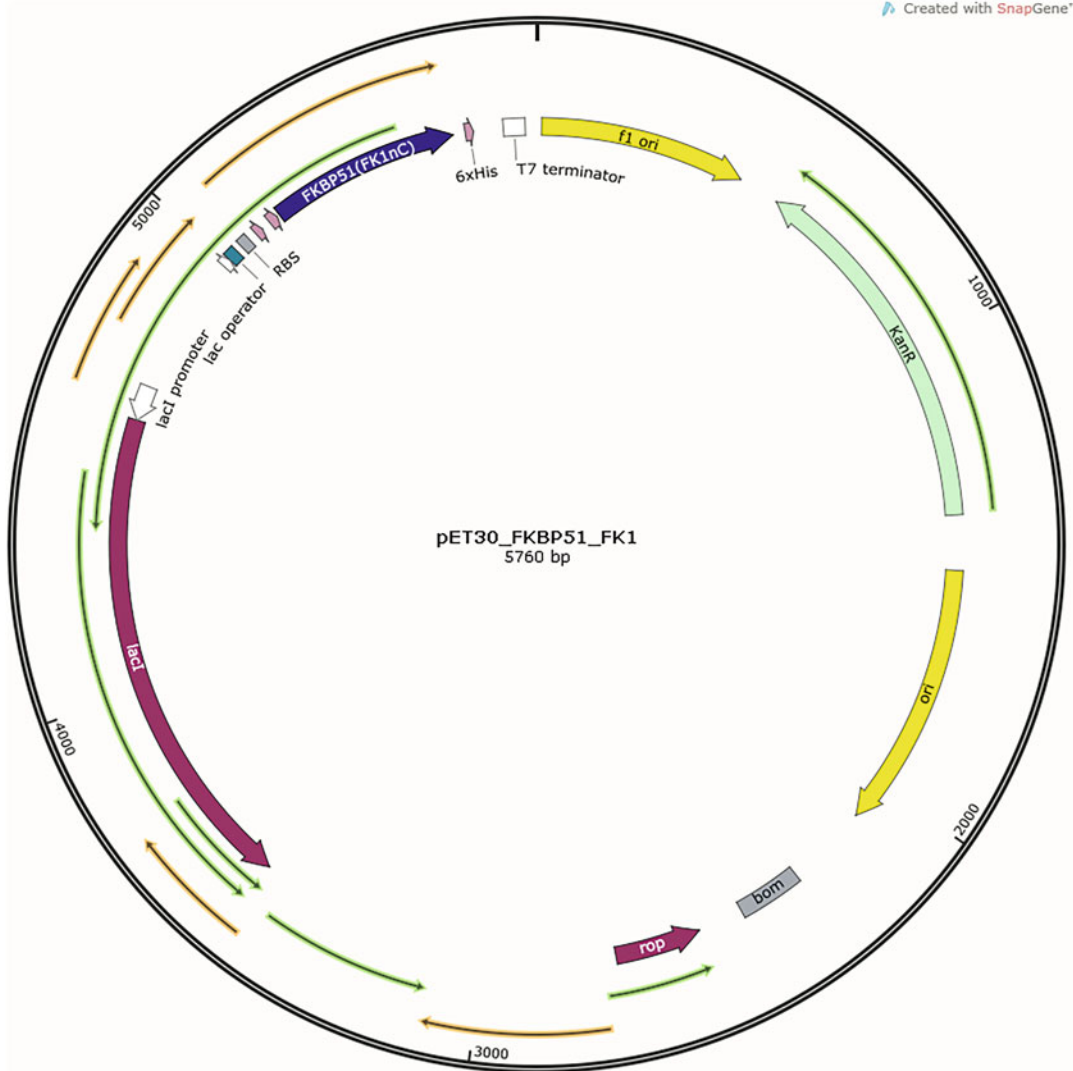


Fig. 6 Plasmid map of the pET30_FKBP51_FK1 Wt. The plasmid contains a kanamycin resistance gene for bacterial selection, T7 promoter, and lac repressor gene lacI for IPTG induction of the protein of interest (FK1 domain of FKBP51)

- 2.5 μL each primer (10 mM each).
- 0.5 μL Q5 High-Fidelity DNA Polymerase.
- 20 ng pET30_FKBP51_FK1 Wt.
- Fill up to 50 μL with nuclease-free water.

The PCR cycling conditions are described in Table 9.

2. Purify the mutated plasmid using Wizard SV Gel and PCR Clean-Up System (Promega) or similar.
3. Cleave methylated parental DNA with five units of the restriction endonuclease DpnI for at least 3 h at 37 °C and overnight at room temperature.

Table 8
Utilized primers for full plasmid amplification (no overlapping) for single amino acid exchange of FKBP51 coding sequence in pET30

Name	5'-3' sequence
F67E_FKBP51_Fw	CGGCAAAAAA GAA GATAGCAGCCATGATCGTAATG
F67E_FKBP51_Rv	TTGCTCAGTTTGCCTTTATAGTGCACATACACTTTATCACC

Table 9
Thermocycling conditions for full plasmid site-directed mutagenesis using Q5 polymerase

	Temperature	Duration [mm:ss]	Cycles
Initial denaturation	98 °C	1:00	X1
Denaturation	98 °C	00:10	X25
Annealing	70 °C	00:30	
Extension	72 °C	3:15	
Final extension	72 °C	5:00	X1

4. Purify the plasmid variant using Wizard SV Gel and PCR Clean-Up System (Promega) or similar.
5. Use 1 μ L of the purified plasmid to transform electrocompetent *Escherichia coli* top 10 cells by electroporation in a 2 mm Bio-Rad Gene Pulser Cuvette with a Gene Pulser Xcell from Bio-Rad at 2500 V and 25 μ F.
6. Resuspend electroporated cells in 1 mL of dYT media and incubate at 37 °C for 1 h.
7. Plate cells on a dYT agar plate with 75 μ g/mL kanamycin (or appropriate antibiotic for the used plasmid) and incubate at 37 °C overnight.
8. On the next day, pick a couple of colonies, generate a 5 mL dYT pre-culture inoculated with a positive colony, and incubate overnight at 37 °C and 170 rpm.
9. On the next morning, isolate the plasmid from the *E. coli* overnight culture with the Wizard® Plus Miniprep DNA Purification System Kit from Promega following the manufacturer's instruction.
10. Use 1 μ L of the purified plasmid to transform electrocompetent *E. Coli* BL21(DE3) cells by electroporation in a 2 mm Bio-Rad Gene Pulser Cuvette with a Gene Pulser Xcell from Bio-Rad at 2500 V and 25 μ F.
11. Resuspend electroporated cells in 1 mL of dYT media and incubate at 37 °C for 1 h.

12. Plate cells on a dYT agar plate with 75 $\mu\text{g}/\text{mL}$ kanamycin (or appropriate antibiotic for the used plasmid) and incubate at 37 °C overnight.
13. On the next day pick a colony and inoculate a shaking flask with 50 mL dYT + 75 $\mu\text{g}/\text{mL}$ kanamycin. Incubate overnight at 37 °C and 170 rpm.
14. Inoculate a shaking flask with 1 L dYT + 75 $\mu\text{g}/\text{mL}$ kanamycin to a 0.1 OD_{600} and incubate at 37 °C and 190 rpm until a 0.6–0.8 OD_{600} was reached.
15. Induce gene expression by the addition of 1 mM isopropyl β -D-1-thiogalactopyranoside (IPTG) and incubate at 30 °C and 190 rpm overnight.
16. Harvest the cells by centrifugation (6000 rpm, 10 min) and resuspend the pellet in 25 mL IMAC A buffer.
17. Transfer the suspension into 50 mL centrifuge tube and disrupt the cells by sonication using an ultrasonic cell disruptor (Bandelin Sonopuls) or similar device.
18. Centrifuge at 13500 rpm for 15 min to remove cell debris, filter the supernatant through a 0.45 μm syringe filter, and purify the expressed protein by Ni-NTA affinity chromatography.
19. Dialyze collected protein fractions in PBS pH 7.4.
20. Perform a 15% SDS–PAGE analysis to evaluate the presence and purity of the protein.

3.4 Evaluation of Identified Protein Variants

1. Purified variants can be characterized by determining thermal stability and comparing it to the Wt protein.
2. The affinity increase in the protein can be determined by fluorescence polarization or similar techniques. Conditions are dependent on the protein and ligand of choice.
3. Protein co-crystallization with the ligand can give a better understanding of the molecular basis for the allosteric stabilization /destabilization, which leads to the binding affinity enhancement.

4 Notes

1. If a crystal structure of the protein is available, virtual screening can be used as a first step to identify potential ligands for in vitro screening [13].
2. Vector sequences.

> Yeast pCT_entry vector

GACGAAAGGGCCTCGTGATACGCCTATTTTTATAGGTTAATGTCATGATAATAATGGTTTCTTAGGACGGATC
 GCTTGCCTGTAACTTACACGCGCCTCGTATCTTTAATGATGGAATAATTTGGGAATTTACTCTGTGTTTATTT
 ATTTTTATGTTTTGTATTGGATTTAGAAAAGTAAATAAAGAAGGTAGAAGAGTTACGGAATGAAGAAAAAA
 AAATAAACAAAGGTTTAAAAAATTTCAACAAAAAGCGTACTTTACATATATATTTATTAGACAAGAAAAGCA
 GATTAATAGATATACATTCGATTAACGATAAGTAAAATGTAAAATCACAGGATTTTCGTGTGTGGTCTTCTA
 CACAGACAAGATGAAACAATTCGGCATTAACTCTGAGAGCAGGAAGAGCAAGATAAAAGGTTAGTATTTGT
 TGGCGATCCCCCTAGAGTCTTTACATCTTCGGAACAAAAACTATTTTTCTTTAATTTCTTTTTTACTTTC
 TATTTTTAATTTATATATTTATATTAAAAAATTTAAATTATAATTATTTTTATAGCACGTGATGAAAAGGACCC
 AGGTGGCACTTTTCGGGGAAATGTGCGCGGAACCCCTATTTGTTTATTTTTCTAAATACATTCAAATATGTAT
 CCGCTCATGAGACAATAACCCTGATAAATGCTTCAATAATATTGAAAAAGGAAGAGTATGAGTATTCACACAT
 TTCCGIGTCGCCCTTATCCCTTTTTGCGGCATTTGCTTCTGTTTTGCTCACCCAGAAACGCTGGTGAA
 AGTAAAAGATGCTGAAGATCAGTTGGGTGCACGAGTGGGTACATCGAACTGGATCTCAACAGCGGTAAGAT
 CCTTGAGAGTTTTCGCCCCGAAGAACGTTTTCCAATGATGAGCACTTTTAAAGTTCTGCTATGTGGCGCGGTA
 TTATCCCGTATTGACGCCGGCAAGAGCAACTCGGTGCGCCATACACTATTCTCAGAATGACTTGGTTGAGT
 ACTCACCGATCACAGAAAAGCATCTTACGGATGGCATGACAGTAAGAGAATTATGCAGTGTGCCATAACCA
 TGAGTGATAACACTGCGGCAACTTACTTCTGACAACGATCGGAGGACCGAAGGAGCTAACCGCTTTTTTTC
 ACAACATGGGGGATCATGTAACCTCGCCTTGATCGTTGGGAACCGGAGCTGAATGAAGCCATACCAAACGACG
 AGCGTGACACCAGATGCTGTAGCAATGGCAACAACGTTGCGCAAACTATTAAGTGGCGAACTACTTACTC
 TAGCTTCCCGCAACAATTAAGACTGGATGGAGGCGGATAAAGTTCAGGACCACTTCTGCGCTCGGCC
 TTCCGGCTGGCTGGTTTATTGCTGATAAATCTGGAGCCGGTGAGCGTGGGTCTCGCGGTATCATTGCGAGCACT
 GGGGCCAGATGGTAAGCCCTCCCGTATCGTAGTTATCTACACGACGGGCAGTCAGGCAACTATGGATGAACG
 AAATAGACAGATCGTGAGATAGGTGCCTCACTGATTAAGCATTGGTAACGTGCAGACCAAGTTTACTCATA
 TATACTTTAGATTGATTTAAAACCTCATTTTAATTTAAAAGGATCTAGGTGAAGATCCTTTTTGATAATCTCA
 TGACAAAATCCCTTAACGTGAGTTTTCGTTCCTGAGCGTCAGACCCCGTAGAAAAGATCAAAGGATCTTC
 TTGAGATCCTTTTTTCTGCGCGTAATCTGCTGCTTGCAAAACAAAAAACCACCGCTACCAGCGGTGGTTTGT
 TTGCCGGATCAAGAGCTACCAACTCTTTTTCCGAAGGTAAGTGGCTTCAGCAGAGCGCAGATACCAAATACT
 GTCCTTCTAGTGTAGCCGTAGTTAGGCCACCACTTCAAGAACTCTGTAGCACCGCCTACATACCTCGCTCTGC
 TAATCCTGTTACCAGTGGCTGTGCCAGTGGCGATAAGTCGTGTCTTACCGGGTTGGACTCAAGACGATAGTT
 ACCGGATAAGGCGCAGCGGTGCGGCTGAACGGGGGGTTCGTGCACACAGCCAGCTTGGAGCGAACGACCT
 ACACCGAACTGAGATACCTACAGCGTGAGCATTGAGAAAAGCGCCACGCTTCCCGAAGGGAGAAAAGCGGGAC
 AGGTATCCGGTAAGCGCAGGGTTCGGAACAGGAGAGCGCACGAGGGAGCTTCCAGGGGGAAACGCCTGGTA
 TCTTTATAGTCTGTGCGGTTTTCGCCACCTCTGACTTGAGCGTCGATTTTTGTGATGCTCGTCAGGGGGCCGA
 GCCTATGGA AAAACGCCAGCAACGCGGCCCTTTTTACGGTTCTGGCCTTTTGCTGGCCTTTTGCTCACATGTT
 TTTCTGCGTTATCCCTGATTCTGTGGATAACCGTATTACCGCCTTTGAGTGAGCTGATACCGCTCGCCGAG
 CCGAACGACCGAGCGCAGCGAGTCAAGTGTGAGCGAGGAAGCGGAAGAGCGCCCAATACGCAAAACCGCCTCC
 CCGCGCGTTGGCCGATTCAATTAATGCAGCTGGCAGCAGAGTTTCCCGACTGGAAAAGCGGGCAGTGAGCGCA
 ACGCAATTAATGTGAGTTACCTCACTCATTAGGCACCCAGGCTTTACACTTTATGCTTCCGGCTCCTATGTTG
 TGTGGAATTGTGAGCGGATAACAATTTACACAGGAAACAGCTATGACCATGATTACGCCAAGCTCGGAATT
 AACCTCACTAAAGGGAACAAAAGCTGGGTACCCGACAGGTTATCAGCAACAACACAGTCATATCCATTCTC
 AATTAGCTCTACCACAGTGTGTGAACCAATGTATCCAGCACCACCTGTAACCAAAAACAATTTAGAAAGTACTT
 TCACTTTGTAAGTGTGAGCTGTCAATTTATATGAATTTTCAAAAATTTCTACTTTTTTTTTGGATGGACGCAAAGA
 AGTTAATAATCATATTACATGGCATTACCACCATATACATATCCATATACATATCCATATCTAATCTTACTTA
 TATGTTGTGGAAATGTAAAGAGCCCCATTATCTTAGCCTAAAAAAACCTTCTCTTTGGAACTTTTCAGTAATAC
 GCTTAAGTCTCATTGCTATATTGAAGTACGGATTAGAAGCCGCCGAGCGGGTGACAGCCCTCCGAAGGAAG

ACTCTCCTCCGTGCGTCCTCGTCTTCACCGGTCGCGTTCCTGAAACGCAGATGTGCCTCGCGCCGCACTGCTC
CGAACAAATAAAGATTCTACAATACTAGCTTTTTATGGTTATGAAGAGGAAAAATTGGCAGTAACCTGGCCCCA
CAAACCTTCAAATGAACGAATCAAATTAACAACCATAGGATGATAATGCGATTAGTTTTTTAGCCTTATTCT
GGGTAATTAATCAGCGAAGCGATGATTTTTGATCTATTAACAGATATATAAATGAATTCTACTTCATACATT
TTCAATTAAGATGACAGTTACTTCGCTGTTTTCAATATTTCTGTTATTGCTTCAGTTTTAGCACAGGAAGTGA
CAACTATATGCGAGCAAATCCCCTCACCAACTTTAGAATCGACGCCGACTCTTTGTCAACGACTACTATTTT
GGCCAACGGGAAGGCAATGCAAGGAGTTTTTGAATATTACAAATCAGTAACGTTTGTGTAACGTAATTGCGGTT
TCACCCCTCAACAAGGCAAGGCAAGGCAAGGCAAGGCAAGGCAAGGCAAGGCAAGGCAAGGCAAGGCAAGGCA
TGAAGGTAGATACCCATACGACGTTCCAGACTACGCTCTGCAGGCTAGTGGTGGTGGTGGTCTGGTGGTGG
TGGTTCTGGTGGTGGTGGTCTGCTAGCGTCATCAAGGCATGGGACATTGGGGTGGCTACCATGAAGAAAGG
AGAGATATGCCATTTACTGTGCAAACCAGAATATGCATATGGCTCGGCTGGCAGTCTCCCTAAAAATCCCTCG
AATGCAACTCTCTTTTTGAGATTGAGCTCCTTGATTTCAAAGGAGAGGGATCCGAGCAAAAAGCTTATTCTG
AAGAGGACTGTAATAGCTCGAGATCTGATAACAACAGTGTAGATGTAACAAAATCGACTTTGTTCCCACTG
TACTTTTAGCTCGTACAAAATACAATATACTTTTCATTTCTCCGTAACAACATGTTTTCCCATGTAATATCCT
TTTCTATTTTTCGTTCGTTACCAACTTTACACATACTTTATATAGCTATTCACTTCTATACACTAAAAAACTA
AGACAATTTTAATTTTGCTGCCTGCCATATTTCAATTTGTTATAAATTCCTATAATTTATCCTATTAGTAGCTA
AAAAAAGATGAATGTGAATCGAATCCTAAGAGAATTGAGCTCCAATTCGCCCTATAGTGAGTCGTATTACAA
TTCACTGGCCGTCGTTTTACAACGTCGTGACTGGGAAAACCCCTGGCGTTACCCAACCTTAATCGCCTTGCAGCA
CATCCCCCTTCGCCAGCTGGCGTAATAGCGAAGAGGCCCGCACCGATCGCCCTTCCAACAGTTGCGCAGC
CTGAATGGCGAATGGCGCGACGCGCCCTGTAGCGGCGCATTAAAGCGGGCGGGTGTGGTGGTTACGCGCAGC
GTGACCGCTACACTTGCCAGCGCCCTAGCGCCCGTCTTTTCGTTTCTCCCTTCTTCTCGCCACGTTTCGC
CGGCTTTCCCGTCAAGCTCTAAATCGGGGGCTCCCTTTAGGGTTCGATTTAGTGCTTTACGGCACCTCGAC
CCCAAAAACTTGATTAGGGTGATGGTTCACGTAGTGGCCATCGCCCTGATAGACGGTTTTTCGCCCTTTGA
CGTTGGAGTCCACGTTCTTTAATAGTGGACTCTGTTCCAACTGGAACAACACTCAACCTATCTCGGTCTA
TTCTTTGATTTATAAGGGATTTTGGCGATTTGGCCCTATTGGTTAAAAATGAGCTGATTTAACAATAATTTA
ACGCGAATTTTAACAATAATTAACGTTTACAATTTCTGATGCGGTATTTTCTCCTTACGCATCTGTGCGGTA
TTTACACCCGAGGCAAGTGCACAAACAATACTTAAATAAATACTACTCAGTAATAACCTATTTCTTAGCATT
TTTGACGAAATTTGCTATTTTGTAGAGTCTTTTACACCAATTTGTCTCCACACCTCCGCTTACATCAACACCA
TAACGCCATTTAATCTAAGCGCATCACCAACATTTTCTGGCGTCAGTCCACCAGCTAACATAAAAATGTAAGCT
TTCGGGGCTCTCTTGCCTTCCAACCCAGTCAGAAAATCGAGTTCCAATCCAAAAGTTCACCTGTCCCACCTGCT
TCTGAATCAAACAAGGGAATAAACGAATGAGGTTTCTGTGAAGCTGCACTGAGTAGTATGTTGCAGTCTTTT
GGAAATACGAGTCTTTAATAAAGTGGCAAACCGAGGAACCTCTGGTATTCTTGCACGACTCATCTCCATGCA
GTTGGACGATATCAATGCCGTAATCATTGACCAGAGCCAAAACATCCTCCTTAGGTTGATTACGAAACACGC
CAACCAAGTATTTTCGGAGTGCCTGAACATTTTTATATGCTTTTACAAGACTTGAAATTTTCTTGAATAACC
GGGTCAATTTGTTCTTTCTATTGGGCACACATATAATACCCAGCAAGTCAGCATCGGAATCTAGAGCACATT
CTGCGGCCTCTGTGCTCTGCAAGCCGCAAACCTTACCAATGGACCAGAACTACCTGTGAAATTAATAACAG
ACATACTCCAAGTGCCTTTGTGTGCTTAATCACGTATACTACGTGCTCAATAGTCACCAATGCCCTCCCTCT
TGCCCTCTCCTTTTCTTTTTTCGACCGAATTAATCTTAATCGGCAAAAAAAGAAAAGCTCCGGATCAAGAT
TGTACGTAAGGTGACAAGCTATTTTTCAATAAAGAATATCTTCCACTACTGCCATCTGGCGTCATAACTGCAA
AGTACACATATATTACGATGCTGTCTATTAATGCTTCTATATTATATATATAGTAATGTCGTTTATGGTGA
CTCTCAGTACAATCTGCTCTGATGCCGCATAGTTAAGCCAGCCCCGACACCCGCCAACACCCGCTGACGCGCC
CTGACGGGCTTGCTGCTCCCGCATCCGCTTACAGACAAGCTGTGACCGTCTCCGGGAGCTGCATGTGTCAG
AGGTTTTACCCGTCATCACGAAACGCGCGA

AmpR Aga2p Myc-Tag Gall-Promoter TrpI BamHI-HF NheI-HF

See the plasmid map in Fig. 5.

> Bacterial pET30_FKBP51_FK1 Wt

```
TGGCGAATGGGACGCGCCCTGTAGCGGGCGCATTAAGCGCGGGTGTGGTGGTTACGCGCAGCGTGACCGC
TACACTTGCCAGCGCCCTAGCGCCCGCTCCTTTCGCTTTCCTCCCTTCCTTTCGCCACGTTCCGCCGGCTTTC
CCGTCAAGCTCTAAATCGGGGGCTCCCTTAGGGTTCCGATTTAGTGCTTTACGGCACCTCGACCCCAAAAAA
CTTGATTAGGGTGATGGTTCACGTAGTGGGCCATCGCCCTGATAGA CGGTTTTTCGCCCTTTGACGTTGGAGT
CCACGTTCTTAATAGTGGACTCTTGTTCCAACTGGAACAACACTCAACCCTATCTCGGTCTATCTTTTGTAT
TTATAAGGGATTTTGCCGATTTCCGGCCTATTGGTTAAAAAATGAGCTGATTTAACAAAAATTTAACCGGAATT
TTAACAAAAATATTAACGTTTACAATTTACAGGTGGCACTTTTCGGGGAAATGTGCGCGGAACCCCTATTTGTTT
ATTTTTCTAAATACATTCAAATATGTATCCGCTCATGAATTAATTC TTAGAAAACTCATCGAGCATCAAATG
AAACTGCAATTTATTTCATATCAGGATTATCAATACCATATTTTTTGAAAAAGCCGTTTCTGTAATGAAGGAGAA
AACTCACCGAGGCAGTTCATAGGATGGCAAGATCCTGGTATCGGTCTGCGATTCCGACTCGTCCAACATCA
ATACAACCTATTAATTTCCCTCGTCAAAAAATAAGGTTATCAAGTGAGAAATCACCATGAGTGACGACTGAA
TCCGGTGAGAA TGGCAAAAGTTTATGCATTTCTTCCAGACTTGTTCAACAGGCCAGCCATTACGCTCGTCAT
CAAAATCACTCGCATCAACCAACCGTTATTTCATTCGTGATTGCGCCTGAGCGAGACGAAATACGCGATCGC
TGTTAAAAGGACAATTACAAACAGGAATCGAATGCAACCGGCGCAGGAACACTGCCAGCGCATCAACAATA
TTTTACCTGAATCAGGATATTCTTCTAATACCTGGAATGCTGTTTTCCCGGGATCGCAGTGGTGAGTAACC
ATGCATCATCAGGAGTACGGATAAAATGCTTGATGGTCGGAAGAGGCATAAATCCGTCAGCCAGTTTAGTC
TGACCATCTCATCTGTAACATCATTGGCAACGCTACCTTTGCCATGTTTCAGAAACAACCTTGCGCATCGGG
CTTCCATACAATCGATAGATTGTCGCACCTGATTGCCGACATTATCGCGAGCCCATTTATACCCATATAAA
TCAGCATCCATGTTGGAATTAATCGCGGCCTAGAGCAAGACGTTTCCCGTTGAATATGGCTCATAACACCCC
TTGTATTACTGTTTATGTAAGCAGACAGTTTTATTGTTTCATGACCAAAATCCCTTAACGTGAGTTTTCGTTCCA
CTGAGCGTCAGACCCCGTAGAAAAGATCAAAGGATCTTCTTGAGATCCTTTTTTCTGCGGTAATCTGCTGC
TTGCAAAACAAAAAACCACCGCTACCAGCGGTGGTTTGTGTTGCCGGATCAAGAGCTACCAACTCTTTTTCCGA
AGGTAACCTGGCTTCAGCAGAGCGCAGATACCAATACTGCTCTTCTAGTGTAGCCGTAGTTAGGCCACCACTT
CAAGAACTCTGTAGCACCGCCTACATACCTCGCTCTGCTAATCCTGTTACCAGTGGCTGCTGCCAGTGGCGAT
AAGTCGTGTCTTACCGGGTTGACTCAAGACGATAGTTACCAGGATAAGGCGCAGCGGTCCGGGCTGAACGGGG
GGTTCGTGCACACAGCCAGCTTGAGCGAACGACCTACACCGAACTGAGATACCTACAGCGTGAGCTATGA
GAAAAGGCCACGCTTCCGAAGGGGAGAAAGGCGGACAGGTATCCGGTAAGCGGCAGGGTCCGAACAGGAG
AGCGCACGAGGGAGCTTCCAGGGGAAACGCCTGGTATCTTTATAGTCCTGTGCGGGTTTCGCCACCTCTGACT
TGAGCGTCGATTTTTGTGATGCTCGTCAGGGGGCGGAGCCTATGAAAAACGCCAGCAACCGGCCTTTTT
ACGGTTCCTGGCCTTTTGCTGGCCTTTTGCTCACATGTTCTTCTGCGTTATCCCCTGATTCTGTGGATAACC
GTATTACCGCCTTTGAGTGAGCTGATACCGCTCGCCGAGCCGAACGACCGAGCGCAGCGAGTCAGTGAGCG
AGGAAGCGGAAGAGCGCCTGATGCGGTATTTCTCCTACGCATCTGTGCGGTATTTACACCCGCATATATGG
TGC ACTCTCAGTACAATCTGCTCTGATGCCGCATAGTTAAGCCAGTATACTCCGCTATCGCTACGTGACTG
GGTCATGGCTGCGCCCCGACACCCGCCAACACCCGCTGACGCGCCCTGACGGGCTTGCTGCTCCCGCATCC
GCTTACAGACAAGCTGTGACCGTCTCCGGGAGCTGCATGTGTGAGAGTTTTACCGTCATCACCGAAACGC
GCGAGGCAGCTGCGGTAAGCTCATCAGCGTGGTCGTGAAGCGATTACAGATGCTGCTGCTGCTGCTGCTGCTG
TCCAGCTCGTTGAGTTTCTCCAGAAGCGTTAATGTCTGGCTTCTGATAAAGCGGGCCATGTTAAGGGCGGTTT
TTTCTGTTTGGTCACTGATGCCTCCGTGTAAGGGGGATTCTGTTTCATGGGGTAATGATACCGATGAAACG
AGAGAGGATGCTCACGATACGGGTTACTGATGATGAACATGCCCGTTACTGGAACGTTGTGAGGGTAAACA
ACTGGCGGTATGGATGCGGCGGGACCAGAGAAAAATCACTCAGGGTCAATGCCAGCGCTTCGTTAATACAGA
TG TAGGTGTTCCACAGGGTAGCCAGCAGCATCCTGCGATGCAGATCCGGAACATAATGGTGCAGGGCGCTGA
```

CTTCCGCGTTTCCAGACTTTACGAAACACGGAAACCGAAGACCATTTCATGTTGTTGCTCAGGTTCGACAGCGTT
 TTGCAGCAGCAGTCGCTTACGTTTCGCTCGCGTATCGGTGATTCATTCTGCTAACAGTAAGGCAACCCCGCC
 AGCCTAGCCGGTCTCAACGACAGGAGCAGATCATGCGCACCCGTGGGGCCGCCATGCCGGCGATAATGC
 CCTGCTTCTCGCCGAAACGTTTGGTGGCGGGACCAGTGACGAAGGCTTGAGCGAGGGCGTGAAGATTCCGA
 ATACCGCAAGCGACAGGCCGATCATCGTCGCGCTCCAGCGAAAGCGGTCTCGCCGAAAAATGACCCAGAGC
 GCTGCCGGCACCTGTCTACGAGTTGCATGATAAAGAAGACAGTCATAAGTGGCGCGACGATAGTCATGCC
 CGCGCCACCGGAAGGAGCTGACTGGGTGAAAGGCTCTCAAGGGCATCGGTTCGAGATCCCGGTGCCTAATGA
 GTGAGCTAACTTACATTAATTGCGTTGCGCTCACTGCCCGCTTCCAGTCGGGAAACCTGTCGTGCCAGCTGC
 ATTAATGAATCGGCCAACGCGCGGGGAGAGGCGTGGTTCGATTTGGGCGCCAGGGTGGTTTTTCTTTTACCA
 GTGAGACGGGCAACAGCTGATTGCCCTTACCGCCTGGCCCTGAGAGAGTTGCAGCAAGCGGTCCACGCTGG
 TTTGCCCCAGCAGGCGAAAAATCTGTTTGTATGGTGGTTAACGGCGGGATATAACATGAGCTGTCTTCGGTATC
 GTCGTATCCACTACCGAGATGTCCGCACCAACGCGCAGCCCGACTCGGTAATGGCGCGCATTGCGCCAG
 CGCCATCTGATCGTTGGCAACCAGCATCGCAGTGGGAACGATGCCCTCATTACGATTTGCATGGTTTGTGA
 AAACCGGACATGGCACTCCAGTCGCCTTCCCGTTCGCTATCGGCTGAATTTGATTGCGAGTGAGATATTTAT
 GCCAGCCAGCCAGACGCAGACGCGCCGAGACAGAATTAATGGGCCCGTAACAGCGCGATTGCTGGTGA
 CCAATGCGACCAGATGCTCCACGCCAGTCGCGTACCGTCTTCATGGGAGAAAAATAATACTGTTGATGGGT
 GTCTGGTCAGAGACATCAAGAAATAACGCCGGAACATTAGTGCAGGCAGCTTCCACAGCAATGGCATCTCG
 TCATCCAGCGGATAGTTAATGATCAGCCACTGACGCGTTGCGCGAGAAGATTGTGCACCGCCGCTTTACAG
 GCTTCGACGCCGCTTCGTTTACCATCGACACCACCACGCTGGCACCCAGTTGATCGGCGCGAGATTTAATCG
 CCGCGACAATTTGCGACGGCGCGTGCAGGGCCAGACTGGAGGTGGCAACGCCAATCAGCAACGACTGTTTGC
 CCGCCAGTTGTTGTGCCACGCGGTTGGGAATGTAATTCAGCTCCGCCATCGCCGCTTCCACTTTTTCCCGCGTT
 TTCGAGAAACGTGGCTGGCCTGGTTACCACGCGGGAAACGGTCTGATAAGAGACACCGGCATACTCTGCG
 ACATCGTATAACGTTACTGGTTTACATTCACCACCCTGAATTGACTCTCTCCGGGCGCTATCATGCCATACC
 GCGAAAGGTTTTGCGCCATTGATGGTGTCCGGGATCTCGACGCTCTCCCTTATGCGACTCCTGCATTAGGAA
 GCAGCCCAGTAGTAGGTTGAGGCGGTTGAGCACCGCCCGCAAGGAATGGTGCATGCAAGGAGATGGCGC
 CCAACAGTCCCCCGGCCACGGGGCTGCCACCATAACCCACGCCGAAACAAGCGCTCATGAGCCCCAAGTGGC
 GAGCCCAGATCTCCCCATCGGTGATGTGCGGATATAGGCGCCAGCAACCGCACCTGTGGCGCCGGTGTATGC
 CGGCCACGATGCGTCCGGCGTAGAGGATCGAGATCGATCTCGATCCCGCGAAATTAATACGACTCACTATAG
 CGGAATTGTGAGCGGATAACAATTCCCTCTAGAAATAATTTGTTAACTTTAAGAAGGAGATATACATATG
 AGCTATTATCATCATCACCATCACCACGATTATGATATTCCGACCACCAGAAAACCTGTATTTTCAAGCGCCC
 CTATGACCACCGATGAAGGTGCAAAAAACAATGAAGAAAGCCCGACCGCAACCGTTGCAGAACAGGGTGAA
 GATATTACCAGCAAAAAAGATCGTGGCGTGCTGAAAAATTGTTAAACGTGTTGGTAATGGTGAAGAAACGCCG
 ATGATTGGTGATAAAGTGTATGTGCACTATAAAGGCAAACCTGAGCAACGGCAAAAAATTCGATAGCAGCCAT
 GATCGTAATGAACCGTTTGTGTTTAGCCTGGGTAAAGGCCAGGTTATTAAGCATGGGATATTGGTGTGCCA
 CCATGAAAAAAGGTGAAATTGCACATCTGCTGATCAAACCGGAATATGCCTATGGTAGCGCAGGTAGCCTGC
 CGAAAAATCCGAGCAATGCAACCCTGTTTTTTGAAATTGAACTGCTGGATTTCAAAGCGAATAAGTCGACA
 AGCTTGGCGCCGCACTCGAGCACCACCACCACCACCTGAGATCCGGCTGCTAACAAAGCCCCGAAAGGAA
 GCTGAGTTGGCTGCTGCCACCGCTGAGCAATAACTAGCATAACCCCTTGGGGCCTCTAACGGGTCTTGAGG
 GTTTTTTGTGCTGAAAGGAGGAACTATATCCGGAT

FKBP51-FK1 KanR T7 Promoter LacI F1Or Position F67

See the plasmid map in Fig. 6.

3. The gene of interest contains a Myc tag at the C-terminus to verify the correct expression of the protein on the surface of the yeast cells.
4. In the exemplified study, only three screening rounds were performed as a sufficient number of positive clones was obtained. Nonetheless, more screening rounds with decreasing tracer concentration may be performed if necessary/desired.

References

1. Laurie ATR, Jackson RM (2006) Methods for the prediction of protein-ligand binding sites for structure-based drug design and virtual ligand screening. *Curr Protein Pept Sci* 7: 395–406
2. Gao M, Skolnick J (2013) A comprehensive survey of small-molecule binding pockets in proteins. *PLoS Comput Biol* 9:e1003302
3. Kokh DB, Czodrowski P, Rippmann F, Wade RC (2016) Perturbation approaches for exploring protein binding site flexibility to predict transient binding pockets. *J Chem Theory Comput* 12:4100–4113
4. Stank A, Kokh DB, Fuller JC, Wade RC (2016) Protein binding pocket dynamics. *Acc Chem Res* 49:809–815
5. Beglov D, Hall DR, Wakefield AE, Luo L, Allen KN, Kozakov D, Whitty A, Vajda S (2018) Exploring the structural origins of cryptic sites on proteins. *Proc Natl Acad Sci* 115:E3416–E3425
6. Durrant JD, McCammon JA (2011) Molecular dynamics simulations and drug discovery. *BMC Biol* 9:71
7. Shan Y, Mysore VP, Leffler AE, Kim ET, Sagawa S, Shaw DE (2022) How does a small molecule bind at a cryptic binding site? *PLoS Comput Biol* 18:e1009817
8. Arkin MR, Randal M, DeLano WL et al (2003) Binding of small molecules to an adaptive protein–protein interface. *Proc Natl Acad Sci* 100:1603–1608
9. Bowman GR, Geissler PL (2012) Equilibrium fluctuations of a single folded protein reveal a multitude of potential cryptic allosteric sites. *PNAS*. <https://doi.org/10.1073/pnas.1209309109/-/DCSupplemental>
10. Huggins DJ, Sherman W, Tidor B (2012) Rational approaches to improving selectivity in drug design. *J Med Chem* 55:1424–1444
11. Umezawa K, Kii I (2021) Druggable Transient Pockets in Protein Kinases. *Molecules* 26:651
12. Nussinov R, Ma B (2012) Protein dynamics and conformational selection in bidirectional signal transduction. *BMC Biol* 10:2
13. Eyrich S, Helms V (2007) Transient pockets on protein surfaces involved in protein–protein interaction. *J Med Chem* 50:3457–3464
14. Kokh DB, Richter S, Henrich S, Czodrowski P, Rippmann F, Wade RC (2013) TRAPP: a tool for analysis of *Transient binding Pockets in Proteins*. *J Chem Inf Model* 53:1235–1252
15. Meiler J, Baker D (2006) ROSETTALIGAND: protein-small molecule docking with full side-chain flexibility. *Proteins: Structure Function Bioinformatics* 65:538–548
16. Zacharias M (2004) Rapid protein-ligand docking using soft modes from molecular dynamics simulations to account for protein deformability: binding of FK506 to FKBP. *Proteins: Structure, Function Bioinformatics* 54:759–767
17. Oleinikovas V, Saladino G, Cossins BP, Gervasio FL (2016) Understanding cryptic pocket formation in protein targets by enhanced sampling simulations. *J Am Chem Soc* 138:14257–14263
18. Kumar S, Ma B, Tsai C-J, Wolfson H, Nussinov R (1999) Folding funnels and conformational transitions via hinge-bending motions. *Cell Biochem Biophys* 31:141–164
19. Ma B, Kumar S, Tsai C-J, Nussinov R (1999) Folding funnels and binding mechanisms. *Protein Eng Des Sel* 12:713–720
20. Teague SJ (2003) Implications of protein flexibility for drug discovery. *Nat Rev Drug Discov* 2:527–541
21. Rath VL, Ammirati M, Danley DE et al (2000) Human liver glycogen phosphorylase inhibitors bind at a new allosteric site. *Chem Biol* 7: 677–682
22. Maun HR, Eigenbrot C, Lazarus RA (2003) Engineering exosite peptides for complete inhibition of factor VIIa using a protease switch with substrate phage. *J Biol Chem* 278:21823–21830
23. Hardy JA, Lam J, Nguyen JT, O'Brien T, Wells JA (2004) Discovery of an allosteric site in the caspases. *Proc Natl Acad Sci* 101:12461–12466

24. Braisted AC, Oslob JD, Delano WL, Hyde J, McDowell RS, Waal N, Yu C, Arkin MR, Raimundo BC (2003) Discovery of a potent small molecule IL-2 inhibitor through fragment assembly. *J Am Chem Soc* 125:3714–3715
25. Gaali S, Kirschner A, Cuboni S et al (2015) Selective inhibitors of the FK506-binding protein 51 by induced fit. *Nat Chem Biol* 11:33–37
26. Lerma Romero JA, Meyners C, Christmann A, Reinbold LM, Charalampidou A, Hausch F, Kolmar H (2022) Binding pocket stabilization by high-throughput screening of yeast display libraries. *Front Mol Biosci*. <https://doi.org/10.3389/fmolb.2022.1023131>
27. Benatuil L, Perez JM, Belk J, Hsieh CM (2010) An improved yeast transformation method for the generation of very large human antibody libraries. *Protein Eng Des Sel* 23:155–159
28. Bogen JP, Grzeschik J, Krah S, Zielonka S, Kolmar H (2020) Rapid generation of chicken immune libraries for yeast surface display. *Methods Mol Biol* 2070:289–302
29. Becker S, Schmoldt HU, Adams TM, Wilhelm S, Kolmar H (2004) Ultra-high-throughput screening based on cell-surface display and fluorescence-activated cell sorting for the identification of novel biocatalysts. *Curr Opin Biotechnol* 15:323–329
30. Benatuil L, Perez JM, Belk J, Hsieh C-M (2010) An improved yeast transformation method for the generation of very large human antibody libraries. *Protein Eng Des Sel* 23:155–159

4.3 A protein engineering approach towards understanding FKBP51 conformational dynamics and mechanisms of ligand binding

Title:

A protein engineering approach towards understanding FKBP51 conformational dynamics and mechanisms of ligand binding

Authors:

Jorge A. Lerma Romero, Christian Meyners, Nicole Rupp, Felix Hausch, and Harald Kolmar

Bibliographic Data:

Journal – Protein Engineering Design and Selection

Volume gzad014

Article published: 30 October 2023

DOI: 10.1093/protein/gzad014

PMID: 37903068

Copyright © 2023 Lerma Romero, Meyners, Rupp, Hausch, and Kolmar. Published by Oxford University Press.

All rights reserved.

Contributions by J.A. Lerma Romero:

- Generation and screening of YSD libraries
- Cloning, expression and purification of all FKBP51 variants
- Characterization of muteins together with Meyners C.
- Writing of original manuscript draft
- Generation of figures

A protein engineering approach toward understanding FKBP51 conformational dynamics and mechanisms of ligand binding

Jorge A. Lerma Romero¹, Christian Meyners¹, Nicole Rupp^{1,2}, Felix Hausch^{1,2} and Harald Kolmar^{1,2,*}

¹Institute for Organic Chemistry and Biochemistry, Technical University of Darmstadt, Darmstadt 64287, Germany

²Centre for Synthetic Biology, Technical University of Darmstadt, Darmstadt 64287, Germany

*To whom correspondence should be addressed. Email: Harald.Kolmar@TU-Darmstadt.de

Abstract

Most proteins are flexible molecules that coexist in an ensemble of several conformations. Point mutations in the amino acid sequence of a protein can trigger structural changes that drive the protein population to a conformation distinct from the native state. Here, we report a protein engineering approach to better understand protein dynamics and ligand binding of the FK506-binding protein 51 (FKBP51), a prospective target for stress-related diseases, metabolic disorders, some types of cancers and chronic pain. By randomizing selected regions of its ligand-binding domain and sorting yeast display libraries expressing these variants, mutants with high affinity to conformation-specific FKBP51 selective ligands were identified. These improved mutants are valuable tools for the discovery of novel selective ligands that preferentially and specifically bind the FKBP51 active site in its open conformation state. Moreover, they will help us understand the conformational dynamics and ligand binding mechanics of the FKBP51 binding pocket.

Keywords: conformational dynamics, FKBP, protein engineering, transient binding pocket, yeast display

Introduction

The FK506 binding protein 51 (FKBP51) is a member of the immunophilin family with peptidyl-prolyl cis-trans isomerase (PPIase) activity, and it is linked to many diseases like obesity, some types of cancer, stress-related and metabolic disorders (Storer *et al.*, 2011; Touma *et al.*, 2011; Gaali *et al.*, 2015; Hartmann *et al.*, 2015; Schmidt *et al.*, 2015; Häusl *et al.*, 2019). High structural and sequence homology exists between FKBP51 and its close counterpart with opposite function, FKBP52. Moreover, other members of this family have a similar FK1 domains too, such as FKBP12 (Guy *et al.*, 2015; Kolos *et al.*, 2018; Häusl *et al.*, 2019). The FK1 domain of these proteins is responsible for binding to immunosuppressive drugs such as FK506 and rapamycin that inhibit their PPIase activity (Kang *et al.*, 2008; Gaali *et al.*, 2015; Häusl *et al.*, 2019).

Despite the high similarity between FKBP51 and FKBP52, the FK1 domains of these proteins have distinct conformational dynamics (Mustafi *et al.*, 2014; LeMaster *et al.*, 2015; Anderson *et al.*, 2023). This property can be exploited for the development of selective drugs (Gaali *et al.*, 2015; Voll *et al.*, 2021; Knaup *et al.*, 2023). It has been reported that the so-called iFit-type inhibitors induce conformational changes, particularly to the β_2 strand, β_{3a} - β_{3b} loop, β_3 strand and β_{4-5} loop of FKBP51. On the other hand, after binding to the canonical inhibitor FK[431]-16 h, FKBP51 behaves exactly like FKBP52. The protein structure rigidifies upon binding of this ligand and increases its stability, as expected for most proteins (Pomplun *et al.*, 2018; Jagtap *et al.*, 2019).

Many proteins, including FKBP51, are flexible molecules that may exist in an ensemble of several related conformations (Oroz *et al.*, 2018; Zgajnar *et al.*, 2019). Any kind of allosteric interaction with a protein or small molecule ligand does not necessarily generate new conformations, but it changes the distribution and interconversion rates of the already-existing conformational ensembles of the protein (Kumar *et al.*, 2000; Goodey and Benkovic, 2008; Nussinov and Ma, 2012). It is already well known that the FKBP51 FK1 domain structure with a displaced F67 side chain, which results in an ‘open’ ligand-accessible conformation, is a low populated conformer of the protein (Gaali *et al.*, 2016; Hähle *et al.*, 2019; Jagtap *et al.*, 2019). Despite the low abundance of this F67^{out} conformer, the protein ensemble population shifts to this open conformation after binding to a ligand of the SAFit family, whereas different ligands cause different conformational changes (Fig. 1) (Feng *et al.*, 2015; Kolos *et al.*, 2018; Bauder *et al.*, 2021; Voll *et al.*, 2021).

Comprehension of the molecular mechanisms behind protein-ligand interactions offers opportunities to control biological activities (de Wolf and Brett, 2000; Seo *et al.*, 2014). In some of these interactions, ligand binding is frequently followed by structural changes in the protein (Evenäs *et al.*, 2001; Sooriyaarachchi *et al.*, 2010; Jagtap *et al.*, 2019). But in some other cases, even in the apo-state, a protein can momentarily switch to a structure that resembles the ligand-bound form (Eyrisch and Helms, 2007; Jagtap *et al.*, 2019; Lerma Romero *et al.*, 2022). Protein engineering provides a tool to generate variants of a target protein,

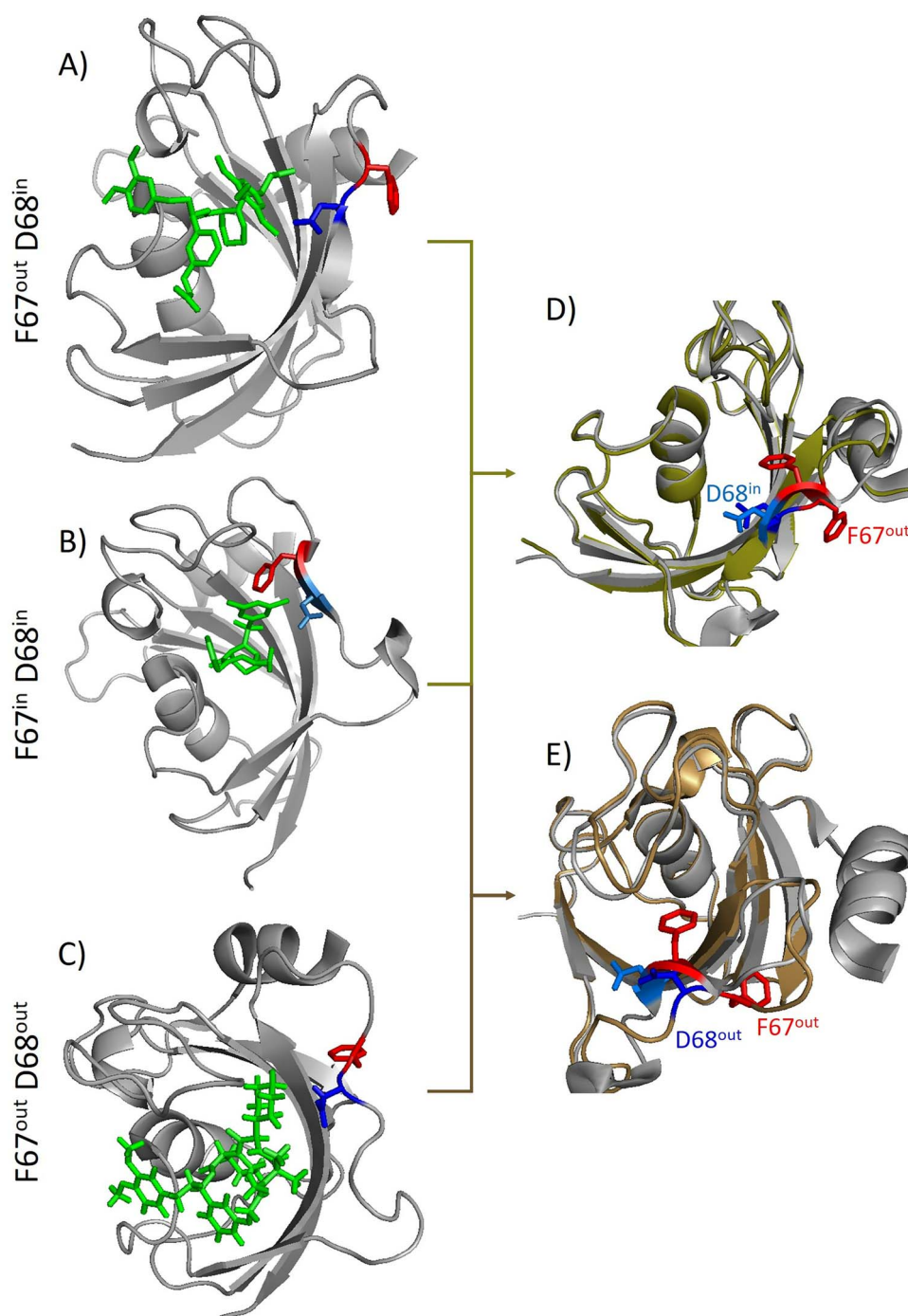


Fig. 1. Crystal structure of the FKBP51 FK1 domain (16–140) in complex with **(A)** iFit1 (4) (PDB: 4TW6) with a F67^{out}/D68ⁱⁿ-conformation; **(B)** FK [431] (6) (PDB: 5OBK) with a F67ⁱⁿ/D68ⁱⁿ-conformation and **(C)** macrocyclic ligand (5) (PDB: 7AWF) with a F67^{out}/D68^{out}-conformation. In **(A, B and C)**, the FK1 domain is depicted in gray, the respective ligand in green sticks, F67 in red sticks and D68 in blue sticks. **(D)** Overlay of **(A)** depicted in olive and **(B)** depicted in gray. **(E)** Overlay of **(B)** depicted in gray and **(C)** depicted in brown. For both overlays, the ligands have been omitted for clarity

where particular states are highly populated compared to the wildtype. In general, by mutating selected residues in a protein, changes in conformation, dynamics, biochemistry, and packing interactions can be triggered (Riggs *et al.*, 2007; Hartmann *et al.*, 2015; LeMaster *et al.*, 2015; Naganathan, 2019; Lerma Romero *et al.*, 2022). However, successful engineering to achieve the desired activity may need multiple modifications to the protein sequence (Risso *et al.*, 2013; Kaltenbach *et al.*, 2018; Naganathan, 2019).

Protein engineering techniques like site saturation mutagenesis, combinatorial mutagenesis and iterative mutagenesis, together with high throughput screening, are invaluable tools that not only enable the discovery of amino acids that are crucial for the structure and function of a protein, but also provide crucial information that allows the analysis of the molecular dynamics during protein-ligand interactions (Fig. 2). In this study, we outline a variety of protein engineering methods for further improving the binding affinity

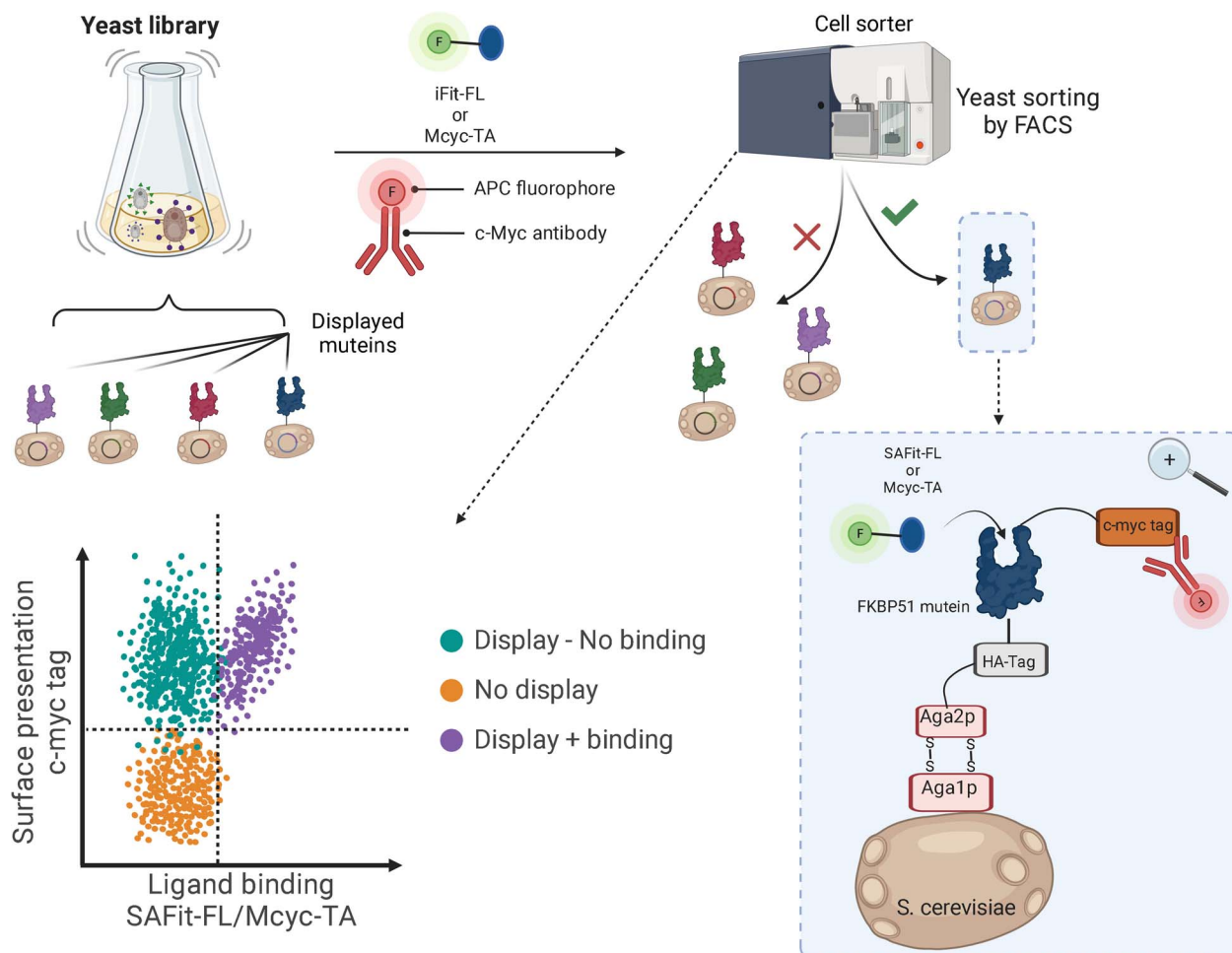


Fig. 2. Schematic representation of the strategy to screen a yeast surface display library of FKBP51 mutants *via* FACS. This approach allows to sort for correctly folded FKBP51 variants with high affinity to the open-conformation ligands SAFit-FL_(out/in) or Mcyc-TA_(out/out). Created with BioRender.com

of conformation-specific selective FKBP51 ligands to either the FKBP51 wt or three reported enhanced mutants (G64S, F67E and D68Y) (Lerma Romero *et al.*, 2022). Numerous variants with improved ligand binding due to conformational selection of a ligand accessible open state were discovered using fluorescence-activated cell sorting (FACS) of two independent yeast display libraries of FKBP51 mutants. These new variants may be used as a tool for fragment-based drug discovery screenings to ultimately aid in the identification of new ligand scaffolds that specifically inhibit FKBP51 without cross-reactivity to other FKBP family members.

Materials and methods

Site-saturation mutagenesis and yeast display library generation

To create the site saturation mutagenesis 1 library (SSM1), the coding sequence of the FK1 domain (1–140) of the FKBP51 (PDB: 3O5E) was employed as a template. For the site saturation mutagenesis 2 library (SSM2), three previously described variants of the same template were used: G64S, F67E and D68Y. All methods for the mutation and cloning of the DNA material, and yeast library generation are extensively described by Lerma Romero *et al.*, (2023) (Lerma Romero and Kolmar, 2023). For the first PCR, the primers

pCT_FKBP51_fw or pCT_FKBP51_rv were coupled with the degenerated primers from Table SI available at PEDS online (e.g. pCT_FKBP51_fw and H56 Rv).

FACS screening and sorting

The library cells were grown in SD medium at 30°C and 200 rpm overnight. Subsequently, cells were induced by starting a culture with 10⁷ cells/ml in SG medium (20 g/l galactose, 6.7 g/l yeast nitrogen base without amino acids, 5.4 g/l Na₂HPO₄, 8.6 g/l NaH₂PO₄·H₂O, and 5 g/l casamino acids) and incubating at 30°C for approximately 24 h. For FACS analysis or sorting, the labeling of cells started by washing and resuspending the SSM1 or SSM2 library with PBS (6.4 mM Na₂HPO₄, 2 mM KH₂PO₄, 140 mM NaCl, 10 mM KCl) followed by incubation with biotin-conjugated c-Myc antibody (Miltenyi Biotec; diluted 1:75) on ice for approximately 30 min. Afterwards, the yeast library was washed with PBS and stained by resuspending in PBS with the secondary labeling reagent Streptavidin conjugated to APC (eBioscience™; diluted 1:75) to identify yeast cells with correct protein display. Additionally, 5 nM of SAFit-FL or 20 nM of Mcyc-TA was added to the SSM1 library sample, while 1 nM of SAFit-FL or 4 nM of Mcyc-TA was added to the SSM2 library sample to sort the protein variants with a high affinity to either of those ligands. All the ligand tracers used for cell

sorting had purities of more than 95%. Finally, the labeled cells were washed with PBS and resuspended in 1 ml of PBS for FACS analysis. Either a Sony SH800 cell sorter (Sony) or a BD Influx™ cell sorter was used for sorting. The sorting gates were set to capture approximately 1% of the tracer binding population. For the Sony SH800 cell sorter mOrange fluorochrome configuration (561 nm excitation laser, 583/30 optical filter) was used to measure TAMRA labeled tracers; APC fluorochrome configuration (638 nm excitation laser, 665/30 optical filter) was used to measure APC stained myc-tag. For the BD Influx™ cell sorter a 488 nm excitation laser, 530/40 optical filter was used to measure FITC labeled tracers; 640 nm excitation laser, 670/30 optical filter was used to measure APC stained myc-tag. The resulting sorted cells were used for the subsequent sorting rounds or single clone analysis.

Colony PCR

After the last sorting round, a single clone of the *Saccharomyces cerevisiae* was picked and resuspended in 25 μ l of 20 nM NaOH and incubated for 20 min at 98°C. Afterward, 2 μ l of the yeast cell sample was used as a template for a PCR reaction with 5X green Quick-Load reaction buffer, 0.2 μ M of the pCT_seq_up and pCT_seq_lo primer, 200 μ M of dNTPs, 1.25 units of OneTaq® Quick-Load® DNA Polymerase (New England Biolabs), and filled up to 50 μ l with ddH₂O. Reactions were amplified with the following program: 95°C for 1 min, followed by 30 cycles of 95°C for 20 s, 54°C for 50 s, and 68°C for 45 s, and a final incubation of 68°C for 5 min. The PCR products were analyzed by agarose gel electrophoresis, and sent for sequencing.

Protein production, purification and characterization

To express each of the FKBP51 mutants, *Escherichia coli* BL21 (DE3) was transformed with each identified FKBP51 variant cloned in pET30b by electroporation at 2.5 kV and 25 mF in a 0.2 cm BioRad GenePulser cuvette. The transformed cells were spread on Double Yeast Tryptone (dYT)-agar plates with kanamycin (0.1% v/v) and were incubated at 37°C overnight. A single colony was picked to inoculate a preculture in dYT medium which contains 16 g/l peptone-casein (Carl Roth GmbH & Co.KG), 10 g/l yeast extract (Sigma-Aldrich), and 5 g/l NaCl with kanamycin (0.1% v/v) and grown overnight at 37°C and 180 rpm. On the next day, the overnight culture was used to inoculate 1 l of dYT-medium to an OD₆₀₀: 0.1, and incubated at 37°C and 180 rpm until an OD₆₀₀ of 0.6–0.8 was reached. Subsequently, the cells were induced by adding 1 mM isopropyl 1-thio-d-galactopyranoside and incubated the cell culture overnight at 30°C and 180 rpm.

The bacterial cells containing the FKBP51 variants were precipitated by centrifugation (6000 rpm, 10 min, 4°C) and lysed by sonication. Cellular debris were removed by centrifugation (13 500 rpm, 15 min, 4°C) and the supernatant was filtered through a 0.45 μ m syringe filter.

Our constructs contain a N-terminal His-tag which allow purification by Ni-NTA affinity chromatography (HisTrap HP—Cytiva). Finally, the recovered fractions were dialyzed against PBS pH 7.4 or 20 mM HEPES, 150 mM NaCl, pH 8. The dialyzed protein was analyzed with a 10% SDS-PAGE under reducing conditions to determine protein purity.

Thermal protein unfolding of the best variants was monitored by Nano differential scanning fluorimetry (nanoDSF) using the Prometheus NT.48 instrument (NanoTemper Technologies). The IMAC purified FKBP51 variants were suspended in PBS, pH 7.4 at a concentration of \sim 0.5 mg/ml. Approximately 10 μ l of each sample were filled into nanoDSF Grade Standard Capillaries (NanoTemper Technologies), and loaded into the instrument. The thermal unfolding of the proteins was monitored in a 1°C/min thermal ramp from 20°C to 90°C. The T_m values were determined automatically by the control software.

Affinity measurement by fluorescence polarization

All ligands and tracers used for fluorescence polarization assays had purities of more than 95%. The following ligands and tracers were used for fluorescence polarization and FACS screening experiments:

- SAFit-FL tracer (1): analog of the iFit ligand class.
- Mcyc-TA tracer (2): TAMRA conjugated macrocyclic ligand.
- ACh277 tracer (3): Fluorescein conjugated analog of the iFit ligand class.
- SAFit1 ligand (4): analog of the iFit ligand class.
- macrocyclic ligand (5): macrocyclic analog of the SAFit class ligands.
- FK [431] ligand (6): bicyclic analog of the immunosuppressive drug FK506.

The structures of all ligands and tracers can be found in Fig. S1 available at PEDS online.

Results

In a recent study, we performed a random mutagenesis of the entire FK1 domain of FKBP51. The experiments resulted in the identification of three mutants (G64S, F67E and D68Y) that stabilize the open conformation of FKBP51 without directly interacting with ligand binding. These variants significantly enhanced binding to FKBP51-open-conformation specific ligands such as SAFit-FL_(out/in) and Mcyc-TA_(out/out) (Fig. 1) (Lerma Romero *et al.*, 2022). These three variants were used as a starting point to find additional mutations that enhance the binding of substrates of the SAFit family. SAFit-FL_(out/in) is a fluorescent tracer derived from SAFit1, an analog of the iFit ligand class that binds selectively to FKBP51 after the displacement of the F67 side chain (F67^{out}) (Fig. 1A) (Gaal *et al.*, 2015). Likewise, Mcyc-TA_(out/out) is a fluorescently labeled macrocyclic analog of the iFit ligand class that requires an additional displacement of D68 and binds to a F67^{out}D68^{out} conformation of FKBP51 (Fig. 1C). This macrocyclic ligand is not only selective against FKBP52, but also against FKBP12 and FKBP12.6 (Bracher *et al.*, 2011; Voll *et al.*, 2021).

Aimed at identifying variants with further enhanced population of the FKBP51 open conformation, two different libraries containing mutants of the FK1 domain of FKBP51 were generated and screened. In the first library (SSM1), randomization on a wildtype background *via* site saturation mutagenesis with degenerate primers (NNK) was performed at positions H56, K58, K60, L61, S62, which are located in the β 2 strand of the protein; and at positions L119, P120, K121,

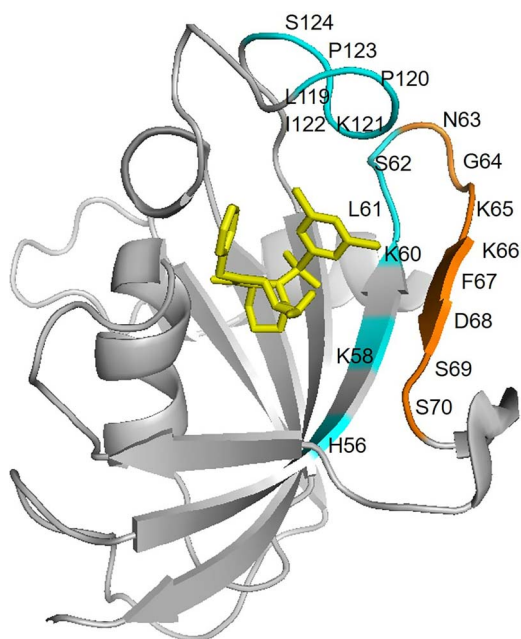


Fig. 3. Crystal structure of the FKBP51 FK1 domain (16–140) (PDB: 5OBK) showing in cyan the residues randomized for the SSM1 library and in orange the residues randomized for the SSM2 library. In yellow sticks the FK [431] (6) ligand is shown to facilitate the visualization of the binding pocket

I122, P123 and S124, located in the β_4 - β_5 interconnecting loop of the FKBP51 FK1 domain. Both regions are located in close proximity to a ligand in the orthosteric site of FKBP51. For the second library (SSM2), the aforementioned three FKBP51 mutants (G64S, F67E and D68Y) with an already improved binding to SAFit-FL_(out/in) and Mcyc-TA_(out/out) (Lerma Romero *et al.*, 2022) were used as a template. For this second library, additional mutations at individual positions in the region spanning from N63 to S70 were introduced, as this region has proven to be of great importance for FKBP51 ligand binding (Fig. 3).

The different sequences derived from the SSM1 randomizations were used to create a yeast display library vastly exceeding 106 clones indicating full coverage of the theoretical diversity. The SSM1 yeast surface display library was examined and sorted *via* fluorescence-activated cell sorting (FACS), using FKBP51 wt as a control. FKBP51 variants displaying a higher affinity for the selective ligands SAFit-FL_(out/in) and Mcyc-TA_(out/out), were enriched after three selection rounds for each ligand using 5 nM of SAFit-FL_(out/in) or 20 nM of Mcyc-TA_(out/out), respectively (Fig. 4). After the fourth sorting round, 20 single clones from each screening campaign were selected and finally six protein variants were identified by gene sequencing. From the SAFit-FL_(out/in) screening, K60N and P120R were identified (Fig. S2 available at PEDS online); while sorting for Mcyc-TA_(out/out) binders, L61V, L61V + L119Y, L61V + P120F, and V55A + S62A were found (Fig. S3 available at PEDS online). Even though no double mutants were expected in this library, it is assumed that spontaneous mutations or polymerase error lead to these mutants.

In a similar manner, the SSM2 randomized sequences with G64S, F67E or D68Y as a starting mutant were used to create a yeast display library exceeding 107 clones. The SSM2

yeast surface display library was examined and sorted *via* FACS. Because the already ligand-binding improved mutants G64S, F67E, or D68Y were used as a starting point to create the SSM2 library, the G64S variant was used as a control when sorting for SAFit-FL_(out/in) high affinity mutants, while D68Y was the control variant used to sort for Mcyc-TA_(out/out) binding to account for the contribution of these mutants to ligand binding (Fig. 5). FKBP51 mutants displaying a higher affinity for the previously mentioned ligands were enriched after four selection rounds for each ligand using 1 nM of SAFit-FL_(out/in) or 4 nM of Mcyc-TA_(out/out). After the three sorting rounds, 20 single clones from each screening campaign were characterized by gene sequencing and finally 12 protein variants were identified from the SAFit-FL_(out/in) screening (Fig. S4 available at PEDS online), while 9 variants were identified as high affinity Mcyc-TA_(out/out) binders (Fig. S5 available at PEDS online) (Table I).

Additionally, a cross test was performed to determine the binding of the newly identified FKBP51 mutants that were screened with SAFit-FL_(out/in) for Mcyc-TA_(out/out) binding and *vice versa*. From these experiments, we concluded that all variants are able to bind SAFit-FL_(out/in) with higher affinity compared to G64S. On the other hand, not all variants found for Mcyc-TA_(out/out) are able to bind SAFit-FL_(out/in) (data not shown).

To facilitate the analysis of the found mutants, the variants from the SSM1 were expressed as single mutants, and mutations found out of the defined randomized positions from the SSM2 library (spontaneous mutations at Table I), were not further analyzed. Even when mutations at position K121 were not planned for during the SSM2, we continued to work with them as this mutation is known to be relevant for ligand binding (Hähle *et al.*, 2019). Moreover, the double mutant F67E + G64S was added to the next analysis steps as we hypothesized that if both independent mutations enhance the affinity to the selected ligands, the combination might show an additive effect to the binding of the ligands.

The selected FKBP51 mutants were expressed in *E. coli* BL21(DE3) and purified by immobilized metal ion affinity chromatography. In order to compare the affinity improvement of the newly identified mutants compared to the wildtype and previously reported variants G64S and D68Y, concentration-dependent change of fluorescence polarization measurements was carried out. For this measurements, two different tracers were used: ACh277_(out/in) is a low-affinity fluorescein-conjugated analog of the iFit ligand class that binds to the F67^{out}D68ⁱⁿ conformation (Charalampidou, 2023), while Mcyc-TA_(out/out) binds to the F67^{out}D68^{out} conformation of FKBP51 (compound 14 in (Voll *et al.*, 2021)).

For the SSM1 library, some of the found variants had a slight affinity enhancement to either one or both of the tested tracers compared to the FKBP51 wt (Table II). However, none of them were better than the known G64S or D68Y constructs. For this reason, these variants were not considered for further analysis.

The SSM2 library led to mutants with an improved affinity to one or both ligands compared to the FKBP51 wt (Table III and IV). For the SAFit-FL_(out/in) screening, most of the variants with an improved affinity had a G64S base mutation. The difference on the affinity of most variants with the G64S mutation alone is not significant. In the case of the Mcyc-TA_(out/out) screening, no multiple mutants were better than the D68Y, with two exceptions being

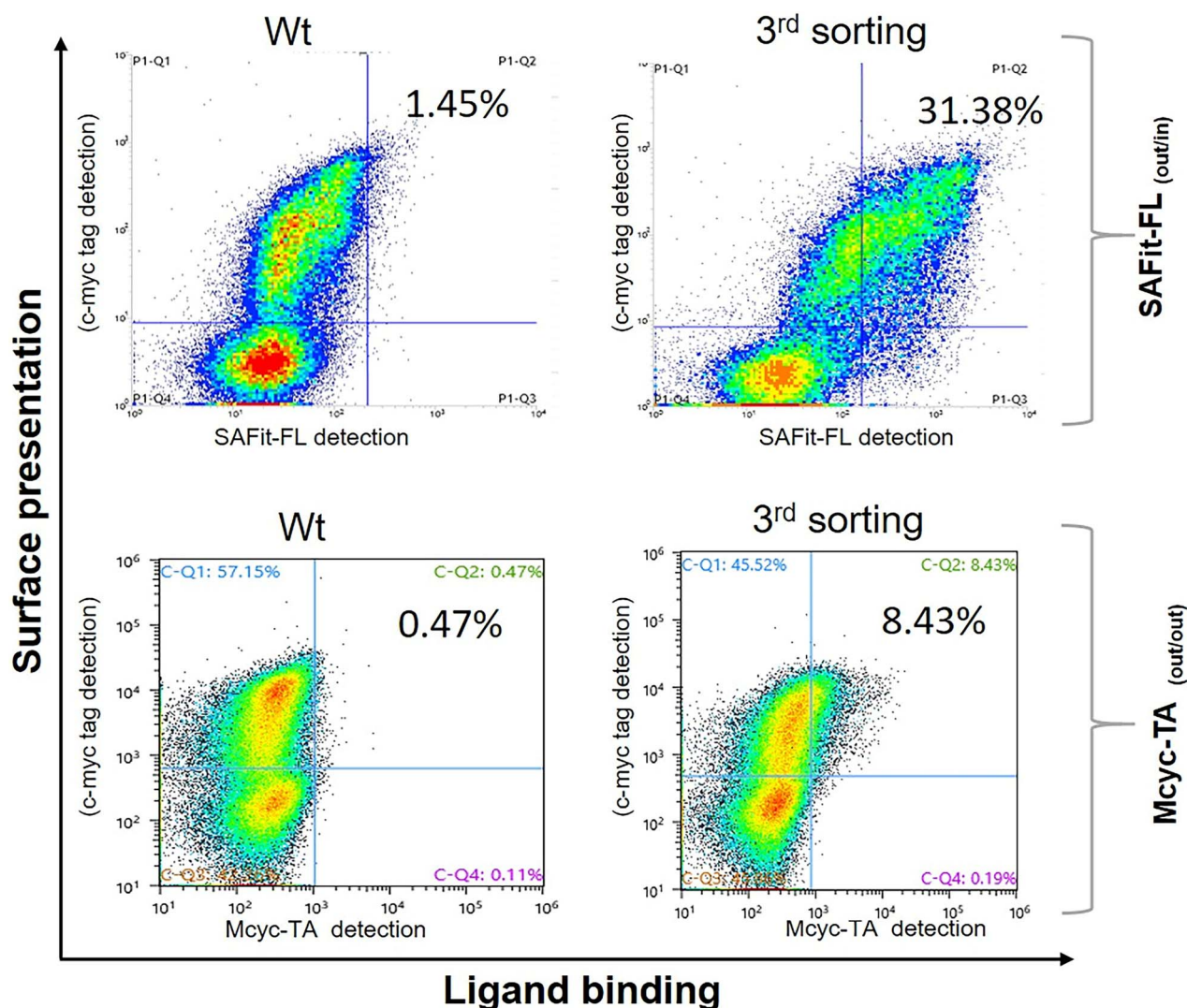


Fig. 4. SSM1 library screening and sorting. Cells with positive surface presentation (c-myc tag detection) and ligand binding signal (SAFit-FL_(out/in) or Mcyc-TA_(out/out)) were selected to enhance the population of ligand binder variants. All three sorting rounds were performed with a sorting gate calibrated to collect ~1% of the tracer binding population. Yeast cells displaying FKBP51 wt were used as a negative control

Combination 18 (G64S + D68Y + K121I) and Combination 20 (D68Y + K121I) (Table IV).

Combination 18 and Combination 20 were the only two mutants that improved the binding of both tracers compared to the starting variants, G64S and D68Y (Table III and IV). These two combinations stood out with up to 147-fold increase of binding affinity compared to the original wildtype FKBP51. Combination 18 (G64S + D68Y + K121I) increased binding 89-fold the binding to ACh277_(out/in) and 88-fold Mcyc-TA_(out/out) compared to FKBP51 wt, surpassing the affinity of all single mutants to the same tracers. Furthermore, combination 20 (D68Y + K121I) increased binding 47-fold the binding to ACh277_(out/in) and 147-fold Mcyc-TA_(out/out) compared to FKBP51 wt, values that are again superior to those of all single mutants (Table III and IV).

These double and triple mutants have a D68Y (+G64S in case of Combination 18) base mutation with a newly detected amino acid exchange of the lysine at position 121 to isoleucine. To compare the influence of the mutation found at position 121 on the binding of the ligands, the mutant with K121I as a single mutation was created and the affinity was

measured. In the same way, G64S + K121I, which was not found during the library sorting, was expressed and analyzed aimed at investigating whether D68Y is required for the high affinity ligand binding of the triple mutant Combination 18 (G64S + D68Y + K121I) or the double mutant Combination 20 (D68Y + K121I). We also addressed the question, whether K121I can be combined with another improved mutant like G64S to create an additive effect on ligand binding affinity. According to the fluorescence polarization measurements, when K121I is combined with the base mutation D68Y, it shows better affinity to both ligands than when combined with G64S. In the same experiment the single mutant K121I was measured, showing a slightly improved binding to the SAFit-FL_(out/in) and Mcyc-TA_(out/out) when compared to the FKBP51 wt.

Finally, the selected reported mutants were characterized by Nano differential scanning fluorimetry (Table SII available at PEDS online, Fig. S6 available at PEDS online) with respect to temperature stability. All base mutations, mutant K121I and Combination 1 (G64S + D68Y), Combination 18 (G64S + D68Y + K121I), and Combination 20

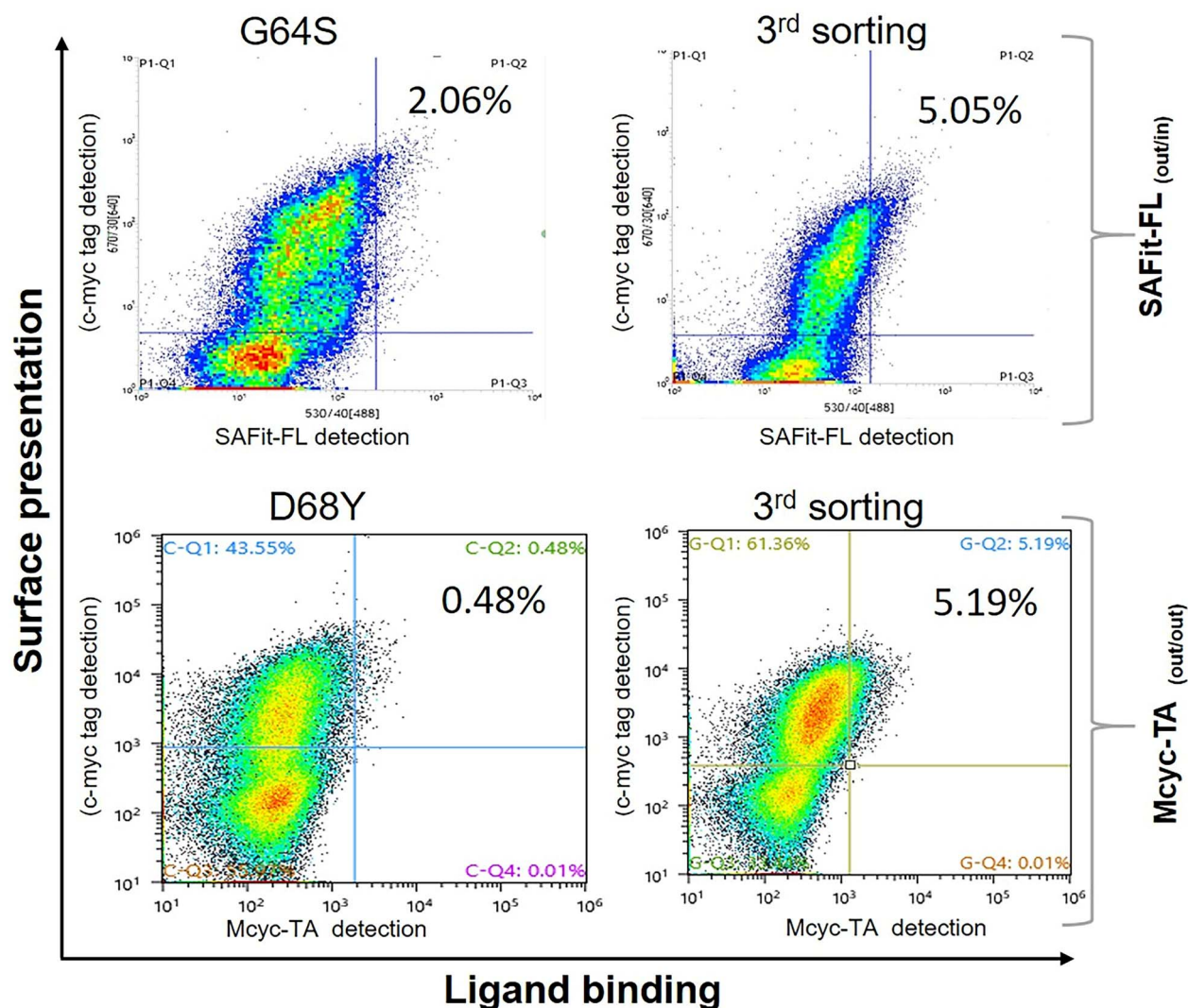


Fig. 5. SSM2 library screening and sorting. Cells with positive surface presentation (c-myc tag detection) and ligand binding signal (SAFit-FL_(out/in) or Mcyc-TA_(out/out)) were selected to enhance the population of ligand binder variants. All three sorting rounds were performed with a sorting gate calibrated to collect ~1% of the tracer binding population. Yeast cells displaying G64S or D68Y were used as a negative control for the sorting campaigns with SAFit-FL_(out/in) or Mcyc-TA_(out/out), respectively

(D68Y + K121I) decreased the unfolding temperature. With 55.8°C set as the benchmark for FKBP51 wt, mutant K121I ($T_m = 53.9^\circ\text{C}$) has the lowest effect on the T_m , while F67E has the highest drop with a T_m of 44.9°C.

The mutation G64S causes a ~10°C drop of the T_m compared to the wt, but the stability of the protein improved with the addition of a second or third mutation. After K121I, D68Y is the most stable mutant with a T_m of 53.1°C, which increases to 53.9°C after the addition of K121I mutation. Mostly, the combination of mutations in the FKBP51 amino acid sequence causes an averaging effect of the single mutants.

Discussion

Several studies supported an important role of the FK506-binding protein 51 (FKBP51) in psychiatric disorders and many other stress-related diseases (Binder *et al.*, 2004; Cioffi *et al.*, 2011; Storer *et al.*, 2011; Pöhlmann *et al.*, 2018; van Doeselaar *et al.*, 2023). Highly selective ligands had been proved to be useful to specifically inhibit FKBP51, but finding

such ligands is a challenging task (Gaali *et al.*, 2015; Bauder *et al.*, 2021; Voll *et al.*, 2021). The use of tools such as protein engineering and high throughput screening of mutant libraries to facilitate the development of selective ligands for the FKBP51 and other therapeutic targets with a flexible orthosteric site is a valuable method that delivers new variants of the target protein with enhanced binding properties that can be used to design and screen new and more potent ligands (Kokh *et al.*, 2016; Lerma Romero *et al.*, 2022; Lerma Romero and Kolmar, 2023).

Previous research revealed that after randomization of the FK1 domain of FKBP51, mutants with amino acid exchanges in the β_3 strand enhanced the binding of selected ligands (Lerma Romero *et al.*, 2022). Based on this results, special focus was given to the region between position 63 to 70 of the protein. The mutants G64S, F67E, and D68Y improved the affinity of two FKBP51 selective ligands, and these variants were used as a reference for this work (Fig. 3).

The binding of these selective inhibitors is attributed to specific conformations involving two residues F67 and D68. Due

Table I. Identified FKBP51 mutants after FACS sorting of the SSM2 library with SAFit-FL_(out/in) or Mcyc-TA tracers_(out/out)

Sorted with	Starting mutant	Observed exchanges at randomization sites	Spontaneous mutations
SAFit-FL _(out/in)	G64S	S69H	
SAFit-FL _(out/in)	G64S	S69V	
SAFit-FL _(out/in)	G64S	D68Y, S69R	K121R
SAFit-FL _(out/in)	D68Y	G64R	H71Y
SAFit-FL _(out/in) Mcyc-TA _(out/out)	G64S	D68Y	
SAFit-FL _(out/in)	G64S	D68V	
SAFit-FL _(out/in)	G64S	D68T	
SAFit-FL _(out/in)	G64S	D68Y, K65S	N42S/K121I
SAFit-FL _(out/in) Mcyc-TA _(out/out)	D68Y	K65G	
Mcyc-TA _(out/out)	D68Y	K65G	K52R
SAFit-FL _(out/in)	F67E	K65N	
SAFit-FL _(out/in) Mcyc-TA _(out/out)	D68Y	F67E	
Mcyc-TA _(out/out)	D68Y	F67E	I49V
Mcyc-TA _(out/out)	D68Y		K121E
Mcyc-TA _(out/out)	D68Y		K121I
Mcyc-TA _(out/out)	D68Y	K58R	K121E
Mcyc-TA _(out/out)	D68Y	G64S	K121E
SAFit-FL _(out/in)	G64S	S70I	

Table II. Ligand binding affinities measured by fluorescence polarization and fold change in K_d improvement with ACh277_(out/in) or Mcyc-TA_(out/out) tracers of the identified mutants from the SSM1 library

Variant	ACh277 _(out/in) K _d [nM]	factor WT	factor G64S	Mcyc-TA _(out/out) K _d [nM]	factor WT	factor G64S	factor D68Y
WT	2800 ± 300	1	0.03	44 ± 15	1	0.05	0.02
G64S	91 ± 7	31	1	2.3 ± 0.8	19	1	0.3
D68Y	315 ± 12	8.8	0.28	0.7 ± 0.1	63	3	1
K58A	6600 ± 1700	0.4	0.01	300 ± 100	0.2	0.01	0.002
K60N	5700 ± 800	0.5	0.02	250 ± 20	0.2	0.01	0.003
L61V	300 ± 15	10	0.3	9.8 ± 0.6	5	0.2	0.07
S62A	1310 ± 80	2	0.07	35 ± 2	1	0.07	0.02
L119Y	3600 ± 300	0.8	0.03	150 ± 11	0.3	0.02	0.005
P120F	1240 ± 80	2	0.07	18 ± 1	3	0.1	0.04
S124A	2600 ± 300	1	0.04	110 ± 10	0.4	0.02	0.01

to its higher conformational flexibility compared to FKBP52, the binding pocket of FKBP51 can adopt a conformation where the side chain of the phenylalanine at position 67 is displaced from the binding pocket, allowing to accept the cyclohexyl group of SAFit1 (Feng *et al.*, 2015; Gaali *et al.*, 2015; Kolos *et al.*, 2018). The displaced F67 is maintained in an F67^{out} conformation by interaction with K58, K60, and F129 of FKBP51. Because the residues T58, W60, and V129 in FKBP52 are bulkier and do not permit similar rearrangements, these interactions are not feasible for this protein. Likewise, this conformation is not favored in the apo- or the FK506-bound state of FKBP51 (Kolos *et al.*, 2018). The D68^{out} conformation is a result of the displacement of D68 by the macrocyclic ligand, which substitutes D68 as a hydrogen bond acceptor for the hydroxy group of Y57. Additionally, an inward flip of H71 replaces S70 as a hydrogen bond donor for Y57, stabilizing the conformer (Voll *et al.*, 2021).

Similar to the preceding work, the SSM1 library generated a variant pool by site saturation mutagenesis for positions in the β_2 strand and the β_{4-5} interconnecting loop regions. The β_2 strand is physically localized below the β_3 strand, and even when the amino acids from the β_2 strand are not

in direct contact with the ligands in the pocket, a change in these amino acids may provide a structural rearrangement which allows the formation and stabilization of the F67^{out} and/or D68^{out} conformation to accommodate the FKBP51 selective ligands. It is known that the residues K58, K60 and F129 stabilize the F67^{out} conformation which allows the transient binding pocket formation to accommodate SAFit ligands (Jagtap *et al.*, 2019). Moreover, if these residues are changed to the corresponding amino acids in FKBP52 (T58, W60, and V129), the binding affinity to SAFit ligands is lost (Jagtap *et al.*, 2019). We inferred that, if an amino acid change at these positions may hinder the F67^{out} conformation of FKBP51, the randomization of such positions and others in the vicinity, may lead to an improved stabilization of the flipped-out phenylalanine 67 leading to a stable ‘open’ pocket which can be then used as a tool for new fragment-based screenings.

The SSM1 screening yielded four variants with an improved open conformation ligand binding compared to the wt protein: L61V, S62A, P120F and S124A. Notably, these residues do not participate in substrate binding as they are located away from the FKBP51 binding site. L61 at the β_2 strand

Table III. Ligand binding affinities measured by fluorescence polarization and fold change in K_d improvement with ACh277_(out/in) of the identified mutants from the SSM2 library

Variant	Mutations	ACh277 _(out/in) K _d [nM]	factor WT	factor G64S
WT	–	2800 ± 300	1	0.03
G64S	–	91 ± 7	31	1
Comb 1	G64S + D68Y	200 ± 6	14	0.5
Comb 2	G64S + D68V	87 ± 3	33	1
Comb 3	G64S + D68T	85 ± 4	33	1
Comb 4	G64S + S69H	99 ± 4	28	1
Comb 5	G64S + S69V	82 ± 3	35	1
Comb 6	D68Y + K65G	220 ± 10	13	0.4
Comb 7	D68Y + G64R	208 ± 9	14	0.4
Comb 8	F67E + D68Y	175 ± 5	16	0.5
Comb 9	G64S + D68Y + S69R	378 ± 14	8	0.2
Comb 10	G64S + D68Y + K65G	223 ± 8	13	0.4
Comb 11	G64S + D68Y + K65S	206 ± 7	14	0.4
Comb 12	G64S + F67E	107 ± 4	27	0.9
Comb 13	F67E + K121E	233 ± 20	12	0.4
Comb 14	D68Y + K121E	1680 ± 100	2	0.05
Comb 15	L61V + L119Y	125 ± 4	23	0.7
Comb 16	L61V + P120F	1210 ± 70	2	0.08
Comb 17	G64S + D68Y + K121R	173 ± 6	16	0.5
Comb 18	G64S + D68Y + K121I	32 ± 2	89	3
Comb 19	V55A + S62A	282 ± 12	10	0.3
Comb 20	D68Y + K121I	60 ± 2	47	2
Comb 21	D68Y + K58R + K121I	1600 ± 100	2	0.06
Comb 22	D68Y + G64S + K121E	940 ± 50	3	0.1
Comb 23	G64S + S70I	134 ± 11	21	0.7
	K121I	535 ± 40	5	0.2
	G64S + K121I	101 ± 7	28	1

Table IV. Ligand binding affinities measured by fluorescence polarization and fold change in K_d improvement with Mcyc-TA_(out/out) of the identified mutants from the SSM2 library

Variant	Mutations	Mcyc-TA _(out/out) K _d [nM]	factor WT	factor G64S	factor D68Y
WT	–	44 ± 15	1	0.05	0.02
D68Y	–	0.7 ± 0.1	63	3	1
G64S	–	2.3 ± 0.8	19	1	0.3
Comb 1	G64S + D68Y	3.3 ± 0.4	13	0.7	0.2
Comb 2	G64S + D68V	3.3 ± 0.4	13	0.7	0.2
Comb 3	G64S + D68T	1.8 ± 0.4	25	1	0.4
Comb 4	G64S + S69H	2.4 ± 0.3	18	1	0.3
Comb 5	G64S + S69V	1.4 ± 0.2	32	2	0.5
Comb 6	D68Y + K65G	1.7 ± 0.3	26	1	0.4
Comb 7	D68Y + G64R	0.7 ± 0.2	63	3	1
Comb 8	F67E + D68Y	0.8 ± 0.3	55	3	0.9
Comb 9	G64S + D68Y + S69R	6 ± 1	7	0.4	0.1
Comb 10	G64S + D68Y + K65G	2.2 ± 0.3	20	1	0.3
Comb 11	G64S + D68Y + K65S	2.1 ± 0.3	21	1	0.3
Comb 12	G64S + F67E	8 ± 1	6	0.3	0.09
Comb 13	F67E + K121E	4 ± 1	11	0.6	0.2
Comb 14	D68Y + K121E	5.2 ± 0.3	9	0.4	0.1
Comb 15	L61V + L119Y	13 ± 1	3	0.2	0.05
Comb 16	L61V + P120F	14 ± 1	3	0.2	0.05
Comb 17	G64S + D68Y + K121R	1.2 ± 0.1	37	2	0.6
Comb 18	G64S + D68Y + K121I	0.5 ± 0.1	88	5	1
Comb 19	V55A + S62A	9 ± 1	5	0.3	0.08
Comb 20	D68Y + K121I	0.3 ± 0.1	147	8	2
Comb 21	D68Y + K58R + K121I	0.8 ± 0.1	55	3	0.9
Comb 22	D68Y + G64S + K121E	0.8 ± 0.1	55	3	0.9
Comb 23	G64S + S70I	2.0 ± 0.3	22	1	0.4
	K121I	30 ± 3	2	0.08	0.02
	G64S + K121I	1.7 ± 0.2	26	1	0.4

PEDS Board Member responsible for editing: Dr Roberto Chica (Editor in Chief, PEDS).

is a residue that together with I122 and P123 is very well conserved among FKBP51, FKBP52, and FKBP12 and participates in the packing of F67 in the normal F67ⁱⁿ conformation (Galat, 2008; LeMaster *et al.*, 2015). Given that the mutation was found three times as a single mutant and another three times in double mutations, valine at position 61 or probably rather the absence of leucine at this position favorably influences binding affinity to SAFit-FL_(out/in) and Mcyc-TA_(out/out). This mutation emerged from two independent directed evolution events, as two different codons leading to valine were identified when sequencing the picked single clones (data not shown). Leucine and valine are quite similar, both are hydrophobic branched amino acids with valine being slightly smaller. Hence, it might not seem as a major change to the protein sequence, but it is sufficient to destabilize the inward conformation of F67 and in turn facilitate the binding of open-conformation ligands.

At the end of the β_2 strand of the FKBP51 wt, S62 and N63 form a hydrogen bond. The mutant S62A is unable to create hydrogen bonds with N63, which might disturb the overall stability and configuration of the protein (Gali *et al.*, 2015).

High flexibility at the β_{4-5} interconnecting loop seems to assist a conformational shift in the β_{3a} strand (LeMaster *et al.*, 2015). Since proline is the most rigid amino acid, its presence in flexible regions of proteins may rigidify the region and increase their thermostability (Yu *et al.*, 2015). Replacing the proline at position 120 might increase the flexibility of the β_{4-5} interconnecting loop, therefore, facilitating a conformational shift in the binding pocket.

S124 and L119 are other two residues that had been extensively investigated in FKBP51, as these are the only two amino acids that are distinct when compared to the FKBP52 β_{4-5} loop (Mustafi *et al.*, 2014). Reports on N-NMR relaxation measurements of the FK1 domains of FKBP51 and FKBP52 as well as variants of positions 119 and 124, show that FKBP51 and FKBP52's conformational sampling varied significantly (Mustafi *et al.*, 2014). Upon interchanging the amino acids at these positions, the conformational transitions are either suppressed or promoted, which in consequence influences the binding of some ligands. The variant S124A might positively influence the conformational transitions that favors SAFit-FL_(out/in) binding compared to the wt protein.

From the SSM2 library screening, 23 different combinations were analyzed. The majority of them showed no improvement when compared to the base mutations G64S or D68Y. The only two mutants with an improved binding for the selective ligands SAFit-FL_(out/in) to Mcyc-TA_(out/out) were Combination 18 and 20. The improvement of these combinations was mostly attributed to the mutation at position 121.

The lysine side chain at position 121 forms a series of hydrophobic contacts with the side chains of I122 and P123, which are in close contact with the phenyl ring of F67 in the β_{3a} strand and the side chain of L61 at β_2 strand (LeMaster *et al.*, 2015). These interactions are conserved among FKBP51, FKBP52, FKBP12, and FKBP12.6 family members (Bracher *et al.*, 2011). The FKBP51 β_{4-5} loop plays a crucial role in the cryptic pocket formation (F67^{out}). It has been observed that the iFit1 inhibitor binding is followed by the β_{4-5} loop migrating approximately 2.5 Å away from the β_{3a} strand, which demonstrated that the tip of the loop stabilizes the F67ⁱⁿ conformation (Bracher *et al.*, 2011; LeMaster *et al.*, 2015). A change in the loop sequence can result in not only a change on the overall conformation and flexibility of the loop,

but the β_2 and β_{3a} strands undergo a transient conformational modification that allows the F67 to get out from the heavily packed interface where it was buried (Bracher *et al.*, 2011; Mustafi *et al.*, 2014; Gali *et al.*, 2015; LeMaster *et al.*, 2015).

Rapamycin interacts in a similar manner with FKBP51, FKBP52 and FKBP12. This molecule binds in a hydrophobic pocket situated between an α -helix and a β -sheet, and only 5 or 6 direct hydrogen bonds are formed between the protein and rapamycin (FKBP12: D37, Q53, E54, I56, Y82; FKBP51: D68, G84, Q85, I87, R73, Y113; FKBP52: D68, G84, Q85, I87, Y113, K121). Moreover, residues Y57, F67, D68, R73, G84, E/Q85, V86, I87 participate in the binding of rapamycin to FKBP51 and FKBP52 (März, 2011). The highly conserved pocket and regions interacting with rapamycin differ in only one single residue. The position lysine at position 121 is present in both, FKBP51 and FKBP52. Nevertheless, in FKBP51, K121 is oriented away from the binding pocket and it does not interact with rapamycin as it does in FKBP52 (März, 2011). On the other hand, for the FKBP51-SAFit1 complex, hydrophobic interactions are formed at F77, V86, I87, W90, and Y113, and hydrogen bonds at Q85 and K121. Besides, cation- π interaction are formed with K121, and V78 and Y113 form hydrogen bonds for the FKBP51-SAFit2 complex (Barge *et al.*, 2022).

Taken together, lysine at position 121 gives every indication of being an important residue for ligand binding, especially when open conformation ligands like SAFit1 and SAFit2 are bound to FKBP51. Interestingly, the mutation K121I found during our sorting, resembles more the β_{4-5} loop of FKBP12 which has an isoleucine at that position (residue 90 for FKBP12). I90 is oriented in the direction of the ligand binding site, but its interaction (if any) to the iFit class ligands has not been described (LeMaster *et al.*, 2015). It has been demonstrated that the β_{4-5} loop region in some of the FKBP5s is of great importance for ligand affinity, and by mutating multiple key residues of FKBP51 to resemble the β_{4-5} loop of FKBP52 or FKBP12, a change in the affinity to FK506 can be observed (Bracher *et al.*, 2013). However, comparable mutagenesis experiments were reported with FKBP12, where the I90K variant, which is the inverse mutation of our K121I mutant, did not alter the affinity of FKBP12-I90K to FK506 or rapamycin, demonstrating no direct interaction between FK506 and K/I at position 90 of FKBP12 (Futer *et al.*, 1995).

While it is unclear what the exact influence on ligand binding of the isoleucine at position 121 is in our Combination 18 and 20 mutants with the SAFit-FL_(out/in) or Mcyc-TA_(out/out) ligand, K121I alone does not improve significantly the binding to ACh277_(out/in) or Mcyc-TA_(out/out) ligands. The K121I exchange provides an additive affinity improvement of both selective ligands only when it is mutated together with D68Y (and G64S).

The inverse correlation that exists between protein flexibility and thermal stability is well known and generally accepted (Vihinen, 1987; Karshikoff *et al.*, 2015; Quezada *et al.*, 2017). The nanoDSF thermal stability measurements demonstrated that G64S, F67E and D68Y present a lower thermal stability when compared to the FKBP51 wt (Fig. S6 available at PEDS online, Table SII available at PEDS online). The decreased thermostability of the base mutations (G64S, F67E and D68Y) implies that the overall flexibility of the protein is increased. This information suggests that the single amino acid change of these variants improved their flexibility, which at the same time indicates a destabilization of the protein conformation.

However, the addition of multiple mutations to those three previously reported variants, averaged the stability measured by nanoDSF. For both of the affinity improved combinations (Combination 18 and 20), the stability of the protein increased compared to their base mutations G64S and/or D68Y, while the affinity to the open-conformation ligands increased too.

In conclusion, we demonstrate a protein engineering approach to obtain mutants to be used as tools for research and development of FKBP51-specific drug candidates. A focused site saturation mutagenesis and combinatorial or iterative mutagenesis together with high throughput screening of two yeast surface display libraries helped for the identification of new FKBP51 variants with up to a 147-fold improved affinity to FKBP51-specific ligands. Some of the randomized regions (β_2) are not in close proximity to the orthosteric site of the protein, and no interactions from the residues in these regions are reported. Nevertheless, allosteric effects on the protein are sufficient to destabilize the closed conformation of the protein and allow for open conformation ligands to enter the formed transient binding pocket. Moreover, a double and triple FKBP51 mutant with a novel modified residue (K121I) are the current benchmarks for FKBP51 mutants that can be used as a tool for research and identification of FKBP51 specific ligands.

Acknowledgments

We would like to thank Dr. Andreas Christmann for his assistance in this project and Prof. Dr. Fessner for permitting the use of the Prometheus NT.48 instrument in his laboratory.

Supplementary data

Supplementary data are available at PEDS online.

Authors contribution

Jorge Lerma Romero (Conceptualization [equal], Formal analysis [equal], Investigation [lead], Methodology [lead], Writing—original draft [lead]), Harald Kolmar (CRediT contribution not specified), Christian Meyners (Data curation [equal], Formal analysis [equal], Investigation [equal], Writing—review & editing [equal]), Nicole Rupp (Formal analysis [supporting], Investigation [supporting]), Felix Hausch (Conceptualization [equal], Project administration [equal], Supervision [equal], Writing—review & editing [equal]), and Harald Kolmar (Conceptualization [equal], Funding acquisition [equal], Project administration [equal], Supervision [equal], Writing—review & editing [equal]).

Conflict of interest

None.

Funding

Funding for this work was provided by the Ministry of Higher Education, Research and Arts of the State of Hesse under the LOEWE project 'TRABITA'.

Data availability statement

The data that supports the findings of this study are available in the supplementary material of this article.

References

- Anderson, J.S., LeMaster, D.M. and Hernández, G. (2023) *J. Biol. Chem.*, **299**, 105159. <https://doi.org/10.1016/j.jbc.2023.105159>.
- Barge, S., Jade, D., Ayyamperumal, S. *et al.* (2022) *J. Biomol. Struct. Dyn.*, **40**, 13799–13811. <https://doi.org/10.1080/07391102.2021.1994877>.
- Bauder, M., Meyners, C., Purder, P.L. *et al.* (2021) *J. Med. Chem.*, **64**, 3320–3349. <https://doi.org/10.1021/acs.jmedchem.0c02195>.
- Binder, E.B., Salyakina, D., Lichtner, P. *et al.* (2004) *Nat. Genet.*, **36**, 1319–1325. <https://doi.org/10.1038/ng1479>.
- Bracher, A., Kozany, C., Thost, A.K. *et al.* (2011) *Acta Crystallogr. D. Biol. Crystallogr.*, **67**, 549–559. <https://doi.org/10.1107/S0907444911013862>.
- Bracher, A., Kozany, C., Hähle, A. *et al.* (2013) *J. Mol. Biol.*, **425**, 4134–4144. <https://doi.org/10.1016/j.jmb.2013.07.041>.
- Guy, N.C., Garcia, Y.A. and Cox, M.B. (2015) *Curr. Mol. Pharmacol.*, **9**, 109–125. <https://doi.org/10.2174/1874467208666150519114115>.
- Charalampidou, A. (2023) Automated flow peptide synthesis enables engineering of proteins with stabilized transient binding pockets. [Unpublished manuscript] [Preprint].
- Cioffi, D.L., Hubler, T.R. and Scammell, J.G. (2011) *Curr. Opin. Pharmacol.*, **11**, 308–313. <https://doi.org/10.1016/j.coph.2011.03.013>.
- van Doeselaar, L., Stark, T., Mitra, S. *et al.* (2023) *Proc. Natl. Acad. Sci. U.S.A.*, **120**, e2300722120.
- Evenäs, J., Tugarinov, V., Skrynnikov, N.R. *et al.* (2001) *J. Mol. Biol.*, **309**, 961–974. <https://doi.org/10.1006/jmbi.2001.4695>.
- Eyrisch, S. and Helms, V. (2007) *J. Med. Chem.*, **50**, 3457–3464. <https://doi.org/10.1021/jm070095g>.
- Feng, X., Sippel, C., Bracher, A. *et al.* (2015) *J. Med. Chem.*, **58**, 7796–7806. <https://doi.org/10.1021/acs.jmedchem.5b00785>.
- Futer, O., DeCenzo, M.T., Aldape, R.A. *et al.* (1995) *J. Biol. Chem.*, **270**, 18935–18940. <https://doi.org/10.1074/jbc.270.32.18935>.
- Gaali, S., Kirschner, A., Cuboni, S. *et al.* (2015) *Nat. Chem. Biol.*, **11**, 33–37. <https://doi.org/10.1038/nchembio.1699>.
- Gaali, S., Feng, X., Hähle, A. *et al.* (2016) *J. Med. Chem.*, **59**, 2410–2422. <https://doi.org/10.1021/acs.jmedchem.5b01355>.
- Galat, A. (2008) *J. Chem. Inf. Model.*, **48**, 1118–1130. <https://doi.org/10.1021/ci700429n>.
- Goodey, N.M. and Benkovic, S.J. (2008) *Nat. Chem. Biol.*, **4**, 474–482. <https://doi.org/10.1038/nchembio.98>.
- Hähle, A., Merz, S., Meyners, C. *et al.* (2019) *Biomolecules*, **9**, 35. <https://doi.org/10.3390/biom9010035>.
- Hartmann, J., Wagner, K.V., Gaali, S. *et al.* (2015) *J. Neurosci.*, **35**, 9007–9016. <https://doi.org/10.1523/JNEUROSCI.4024-14.2015>.
- Häusl, A.S., Balsevich, G., Gassen, N.C. *et al.* (2019) *Mol. Metab.*, **29**, 170–181. <https://doi.org/10.1016/j.molmet.2019.09.003>.
- Jagtap, P.K.A., Asami, S., Sippel, C. *et al.* (2019) *Angew. Chem. Int. Ed.*, **58**, 9429–9433. <https://doi.org/10.1002/anie.201902994>.
- Kaltenbach, M., Burke, J.R., Dindo, M. *et al.* (2018) *Nat. Chem. Biol.*, **14**, 548–555. <https://doi.org/10.1038/s41589-018-0042-3>.
- Kang, C.B., Hong, Y., Dhe-Paganon, S. *et al.* (2008) *Neurosignals*, **16**, 318–325. <https://doi.org/10.1159/000123041>.
- Karshikoff, A., Nilsson, L. and Ladenstein, R. (2015) *FEBS J.*, **282**, 3899–3917. <https://doi.org/10.1111/febs.13343>.
- Knaup, F.H., Meyners, C., Sugiarto, W.O. *et al.* (2023) *J. Med. Chem.*, **66**, 5965–5980. <https://doi.org/10.1021/acs.jmedchem.3c00249>.
- Kokh, D.B., Czodrowski, P., Rippmann, F. *et al.* (2016) *J. Chem. Theory Comput.*, **12**, 4100–4113. <https://doi.org/10.1021/acs.jctc.6b00101>.
- Kolos, J.M., Voll, A.M., Bauder, M. *et al.* (2018) *Front. Pharmacol.*, **9**, 1425. <https://doi.org/10.3389/fphar.2018.01425>.
- Kumar, S., Tsai, C.J. and Nussinov, R. (2000) *Protein Eng.*, **13**, 179–191.
- LeMaster, D.M., Mustafi, S.M., Brecher, M. *et al.* (2015) *J. Biol. Chem.*, **290**, 15746–15757. <https://doi.org/10.1074/jbc.M115.650655>.
- Lerma, Romero, J.A., Meyners, C., Christmann, A. *et al.* (2022) *Front. Mol. Biosci.*, **9**. <https://doi.org/10.3389/fmolb.2022.1023131>.

- Lerma Romero, J.A. and Kolmar, H. (2023), in S. Zielonka and S. Krah (eds) *Methods in Molecular Biology*. New York, NY: Humana, pp. 249–274. https://doi.org/10.1007/978-1-0716-3279-6_14.
- März, A.M. (2011) *A New Player in mTOR Regulation: Introducing FKBP51* Doctoral thesis. Munich: Max Planck Institute of Psychiatry.
- Mustafi, S.M., LeMaster, D.M. and Hernández, G. (2014) *Biochem. J.*, **461**, 115–123. <https://doi.org/10.1042/BJ20140232>.
- Naganathan, A.N. (2019) *Curr. Opin. Struct. Biol.*, **54**, 1–9. <https://doi.org/10.1016/j.sbi.2018.09.004>.
- Nussinov, R. and Ma, B. (2012) *BMC Biol.*, **10**, 2. <https://doi.org/10.1186/1741-7007-10-2>.
- Oroz, J., Chang, B.J., Wysoczanski, P. *et al.* (2018) *Nat. Commun.*, **9**, 4532. <https://doi.org/10.1038/s41467-018-06880-0>.
- Pöhlmann, M.L., Häusl, A.S., Harbich, D. *et al.* (2018) *Front. Behav. Neurosci.*, **12**, 1–8. <https://doi.org/10.3389/fnbeh.2018.00262>.
- Pomplun, S., Sippel, C., Hähle, A. *et al.* (2018) *J. Med. Chem.*, **61**, 3660–3673. <https://doi.org/10.1021/acs.jmedchem.8b00137>.
- Quezada, A.G., Díaz-Salazar, A.J., Cabrera, N. *et al.* (2017) *Structure*, **25**, 167–179. <https://doi.org/10.1016/j.str.2016.11.018>.
- Riggs, D.L., Cox, M.B., Tardif, H.L. *et al.* (2007) *Mol. Cell. Biol.*, **27**, 8658–8669. <https://doi.org/10.1128/mcb.00985-07>.
- Risso, V.A., Gavira, J.A., Mejia-Carmona, D.F. *et al.* (2013) *J. Am. Chem. Soc.*, **135**, 2899–2902. <https://doi.org/10.1021/ja311630a>.
- Schmidt, U., Buell, D.R., Ionescu, I.A. *et al.* (2015) *Psychoneuroendocrinology*, **52**, 43–58. <https://doi.org/10.1016/j.psyneuen.2014.11.005>.
- Seo, M.-H., Park, J., Kim, E. *et al.* (2014) *Nat. Commun.*, **5**, 3724. <https://doi.org/10.1038/ncomms4724>.
- Sooriyaarachchi, S., Ubhayasekera, W., Park, C. *et al.* (2010) *J. Mol. Biol.*, **402**, 657–668. <https://doi.org/10.1016/j.jmb.2010.07.038>.
- Storer, C.L., Dickey, C.A., Galigniana, M.D. *et al.* (2011) *Trends Endocrinol. Metab.*, **22**, 481–490. <https://doi.org/10.1016/j.tem.2011.08.001>.
- Touma, C., Gassen, N.C., Herrmann, L. *et al.* (2011) *Biol. Psychiatry*, **70**, 928–936. <https://doi.org/10.1016/j.biopsych.2011.07.023>.
- Vihinen, M. (1987) *Protein Eng. Des. Sel.*, **1**, 477–480. <https://doi.org/10.1093/protein/1.6.477>.
- Voll, A.M., Meyners, C., Taubert, M.C. *et al.* (2021) *Angew. Chem. Int. Ed. Engl.*, **60**, 13257–13263. <https://doi.org/10.1002/anie.202017352>.
- de Wolf, F.A. and Brett, G.M. (2000) *Pharmacol. Rev.*, **52**, 207–236.
- Yu, H., Zhao, Y., Guo, C. *et al.* (2015) *Biochim. Biophys. Acta.*, **1854**, 65–72. <https://doi.org/10.1016/j.bbapap.2014.10.017>.
- Zgajnar, N., de Leo, S., Lotufo, C. *et al.* (2019) *Biomolecules*, **9**, 52. <https://doi.org/10.3390/biom9020052>.

Supplementary Material

Primers

Table S1. Utilized degenerated primers for SSM1 and SSM2, and primers for amplification and sequencing of the FKBP51 coding sequence in pCT vector.

Primer	Sequence 5'-3'
H56 Fw	GGAGACAAAGTTTATGTCNNKTACAAAGGAAAATTG
H56 Rv	GACAATTTTCCTTTGTAMNNGACATAAACTTTGTG
K58 Fw	CAAAGTTTATGTCCATTACNNKGGAAAATTGTC
K58 Rv	CCATTTGACAATTTTCCMNNGTAAATGGACATAAAC
K60 Fw	CCATTACAAAGGANNKTTGTCAAATGGAAAGAAG
K60 Rv	CTTTCCATTTGACAAMNNTCCTTTGTAATGGAC
L61 Fw	GTCCATTACAAAGGAAAANNKTCAAATGGAAAG
L61 Rv	CAAACCTTTCCATTTGAMNNTTTTCCTTTGTAATG
S62 Fw	CCATTACAAAGGAAAATTGNNKAATGGAAAGAAG
S62 Rv	CAAACCTTTCCATTMNCAATTTTCCTTTGTAATG
L119 Fw	CATATGGCTCGGCTGGCAGTNNKCCTAAAATTCCC
L119 Rv	GCATTGAGGGGAATTTAGGMNNACTGCCAGCCGAGC
P120 Fw	GGCTCGGCTGGCAGTCTCNNKAAAATTCCTCGAATGC
P120 Rv	GCATTGAGGGGAATTTMNNAGACTGCCAGCCGAGCC
K121 Fw	CGGCTGGCAGTCTCCCTNNKATTCCCTCGAATGC
K121 Rv	GTTGCATTGAGGGGAATMNNAGGGAGACTGCCAGC
I122 Fw	GCTGGCAGTCTCCCTAAANNKCCCTCGAATGCAAC
I122 Rv	GAGAGTTGCATTGAGGGMNNNTTLAGGGAGACTGC
P123 Fw	GGCAGTCTCCCTAAAATTNNKTGAATGCAACTC
P123 Rv	GAGAGTTGCATTGAMNNAATTTTLAGGGAGACTGC
S124 Fw	GCAGTCTCCCTAAAATTCNNKAATGCAACTCTC
S124 Rv	CAAAAAGAGAGTTGCATTMNNGGAATTTTAGGG
N63 Fw (+F67E)	CATTACAAAGGAAAATTGTCANNKGGAAAGAAGGAAGATTC C
N63 Rv (+F67E)	GACTGGAATCTTCCTTCTTTCCMNNTGACAATTTTCC
G64 Fw (+F67E)	CAAAGGAAAATTGTCAAATNNKAAGAAGGAAGATTCC
G64 Rv (+F67E)	GACTGGAATCTTCCTTCTTMNNTTTGACAATTTTCC
K65 Fw (+F67E)	GGAAAATTGTCAAATGGANNKAAGGAAGATTCCAG
K65 Rv (+F67E)	CTATCATGACTGGAATCTTCCTTMNNTCCATTTGAC
K66 Fw (+F67E)	GGAAAATTGTCAAATGGAAAGNNKGAAGATTCCAGTCATG
K66 Rv (+F67E)	CTATCATGACTGGAATCTTCMNNCTTTCCATTTGAC
D68 Fw (+F67E)	CAAATGGAAAGAAGGAANNKTCCAGTCATGATAGAAATG
D68 Rv (+F67E)	GGTTCATTTCTATCATGACTGGAMNNTTCTTCTTTCC
S69 Fw (+F67E)	GTCAAATGGAAAGAAGGAAGATNNKAGTCATGATAG
S69 Rv (+F67E)	GGTTCATTTCTATCATGACTMNNATCTTCTTCTTTCC
S70 Fw (+F67E)	GGAAAGAAGGAAGATTCCNNKCATGATAGAAATG
S70 Rv (+F67E)	GGTTCATTTCTATCATGMNNGGAATCTTCTTCC
N63 Fw (+G64S/D68Y)	TACAAAGGAAAATTGTCANNKRGMAAGAAGTTTKATTCCAG TC
N63 Rv (+G64S/D68Y)	GACTGGAATMAAATCTTKCYMNNTGACAATTTTCC
G64 Fw (+G64S/D68Y)	CAAAGGAAAATTGTCAAATNNKAAGAAGTTTKATTCCAGTC
G64 Rv (+G64S/D68Y)	GACTGGAATMAAATCTTMNNTTTGACAATTTTCC
K65 Fw (+G64S/D68Y)	GGAAAATTGTCAAATRGMNNAAGTTTKATTCCAG

K65 Rv (+G64S/D68Y)	CTATCATGACTGGAATMAAACTTMNNKCYATTTGAC
K66 Fw (+G64S/D68Y)	GGAAAATTGTCAAATRGMAAGNNKTTTKATTCCAGTCATG
K66 Rv (+G64S/D68Y)	CTATCATGACTGGAATMAAAMNNCTTKCYATTTGAC
F67 Fw (+G64S/D68Y)	GGAAAATTGTCAAATRGMAAGAAGNNKKATTCCAGTCATG
F67 Rv (+G64S/D68Y)	CATTTCTATCATGACTGGAATMMNNCTTCTTKCYATTTGAC
D68 Fw (+G64S/D68Y)	CAAATRGMAAGAAGTTTNNKTCCAGTCATGATAGAAATG
D68 Rv (+G64S/D68Y)	AAATGGTTCATTTCTATCATGACTGGAMNNAAACTTCTT
S69 Fw (+G64S/D68Y)	GTCAAATRGMAAGAAGTTTKATNNKAGTCATGATAG
S69 Rv (+G64S/D68Y)	AAATGGTTCATTTCTATCATGACTMNNATMAAACTTCTT
S70 Fw (+G64S/D68Y)	AAGAAGTTTKATTCCNNKCATGATAGAAATGAAC
S70 Rv (+G64S/D68Y)	GGTTCATTTCTATCATGMNNGGAATMAAACTTC
pCT_FKBP51_fw	AGTGGTGGTGGTGGTTCTGGTGGTGGTGGTTCTGGTGGTG GTGGTTCTGCTAGCATGAC
pCT_FKBP51_rv	TGTTGTTATCAGATCTCGAGCTATTACAAGTCCTCTTCAGAA ATAAGCTTTTGCTCGGATCC
pCT_seq_up	TACCCATACGACGTTCCAGACTAC
pCT-seq_lo	CAGTGGGAACAAAGTCGATTTTGTTAC

NNK is a degenerated codon with N = any nucleotide and K = G or C. MNN is the complementary codon with M = A or T.

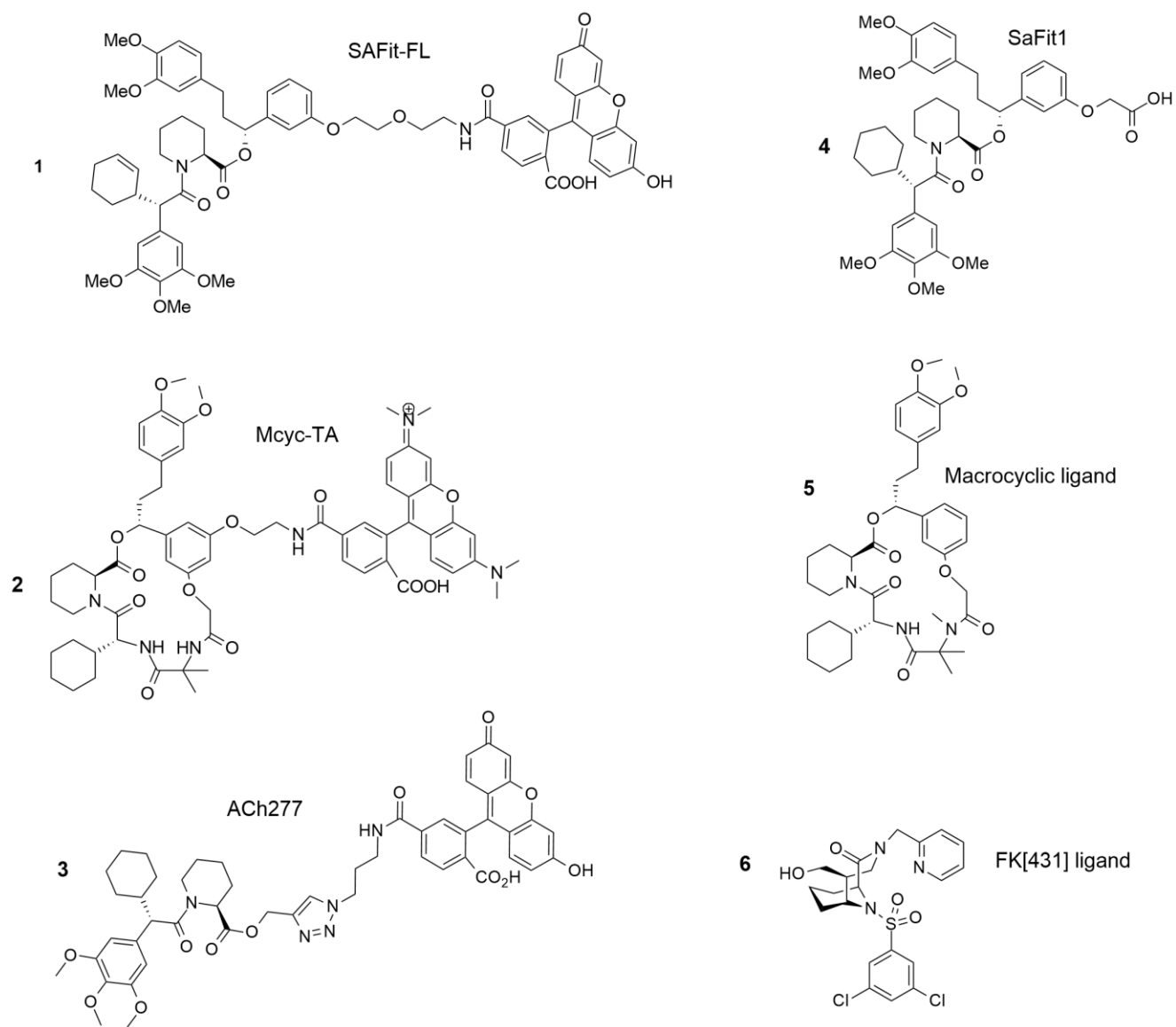


Figure S1. Chemical structure of the FKBP51 tracers and ligands. (1) SAFit-FL (out/in) is the fluorescein conjugated version of compound (4). (2) Mcyc-TA (out/out) is the TAMRA conjugated compound (5). (3) ACh277 is a fluorescein conjugated analogue of the iFit ligand class. The FKBP51-spelective ligands SAFit1 (4) and macrocylic ligand (5) correspond to compounds SAFit1 published by Gaali et al., *Nat. Chem. Biol.* 2015, 11 (1), 33–37 and compound 13 published by Voll et al., *Angew. Chem. Int. Ed.* 2021, 60 (24), 13257–13263, respectively. The canonical FKBP ligand (6) FK[431]-16g correspond to compound 16g published by Pomplun et al., *J. Med. Chem.* 2018, 61, 3660–3673.

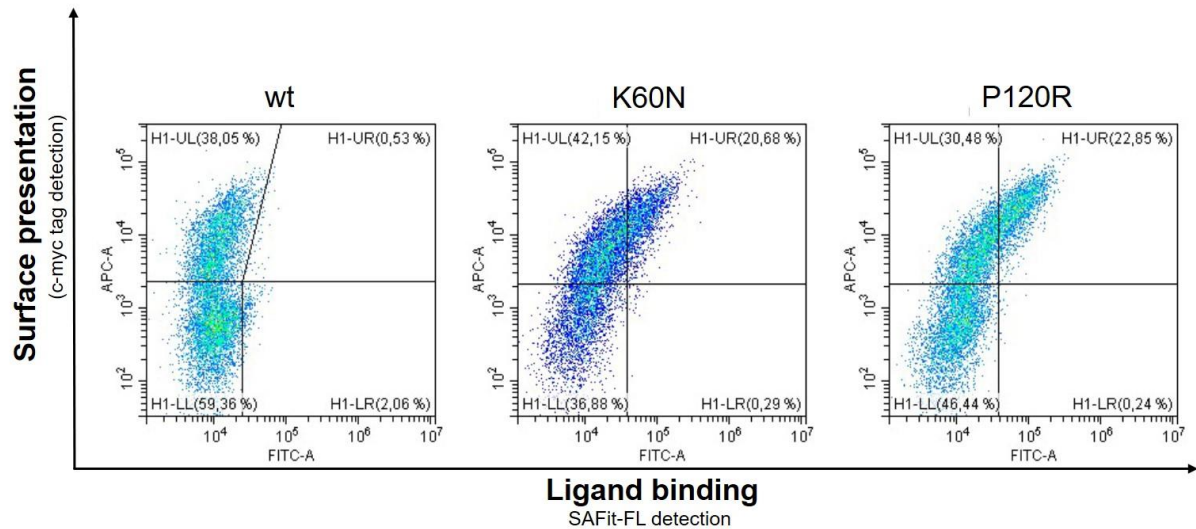


Figure S2. Single clone YSD dot-plots displaying FKBP51 Wt and the mutants found from the SSM1 library when sorting for SAFit FL (*out/in*). The data was recorded in a flow cytometer, and the single clones were selected due to the overall population shift into the established gate where cells exhibit both surface presentation (c-myc tag detection) and SAFit FL (*out/in*) binding signal.

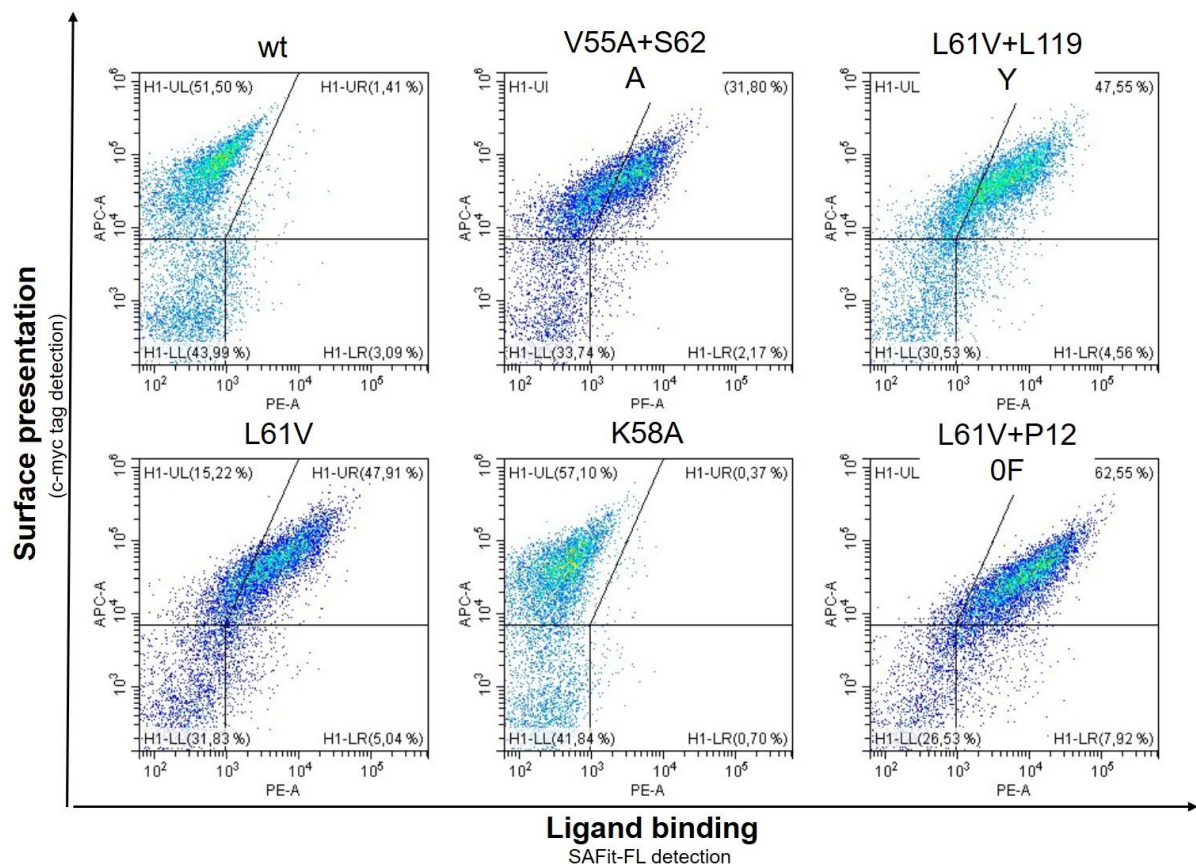


Figure S3. Single clone YSD dot-plots displaying FKBP51 Wt and the mutants found from the SSM1 library when sorting for Mcyc-TA (*out/out*). The data was recorded in a flow cytometer, and the single clones were selected due to the overall population shift into the established gate where cells exhibit both surface presentation (c-myc tag detection) and Mcyc-TA (*out/out*) binding signal.

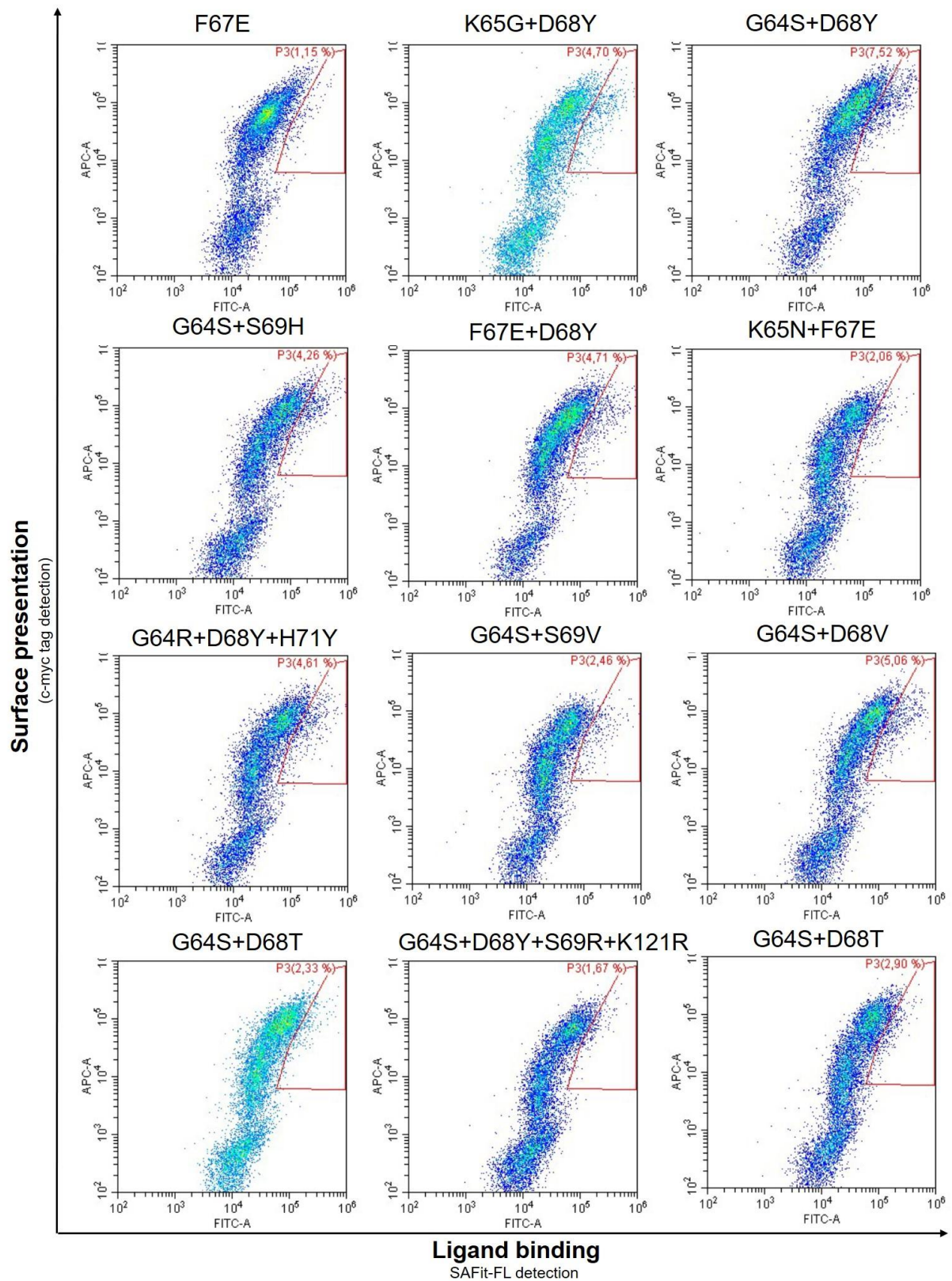


Figure S4. Single clone YSD dot-plots displaying FKBP51 Wt and the mutants found from the SSM2 library when sorting for SAFit FL (*out/in*). The data was recorded in a flow cytometer, and the single clones were selected due to the overall population shift into the established gate where cells exhibit both surface presentation (c-myc tag detection) and SAFit FL (*out/in*) binding signal.

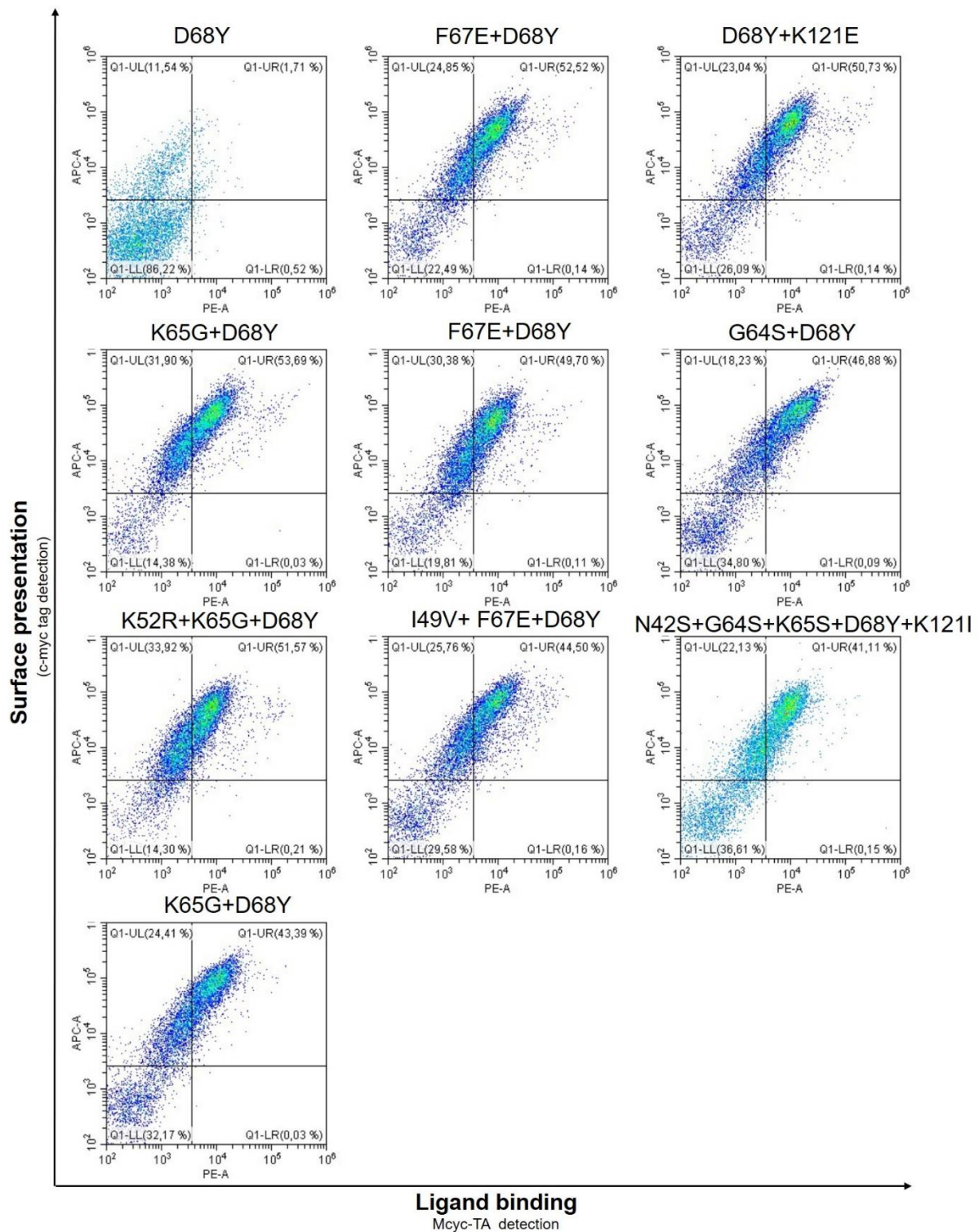


Figure S5. Single clone YSD dot-plots displaying FKBP51 Wt and the mutants found from the SSM2 library when sorting for Mcyc-TA (*out/out*). The data was recorded in a flow cytometer, and the single clones were selected due to the overall population shift into the established gate where cells exhibit both surface presentation (c-myc tag detection) and Mcyc-TA (*out/out*) binding signal.

Table S2. Melting temperatures of selected FKBP51 muteins determined by NanoDSF.

Sample	Melting temperature (T_m)
Wt	55.8°C
G64S	45.9°C
F67E	44.9°C
D68Y	53.1°C
K60N	53.8°C
L61V	53.5°C
S64A	57.1°C
L119Y	57.8°C
P120F	50.7°C
K121I	53.9°C
S124A	58.4°C
G64S+K121I	46.7°C
Comb1	51.0°C
Comb4	44.0°C
Comb5	48.3°C
Comb6	51.5°C
Comb7	40.8°C
Comb8	47.9°C
Comb9	47.5°C
Comb11	49.2°C
Comb12	40.8°C
Comb13	42.5°C
Comb15	50.8°C
Comb16	47.9°C
Comb17	45.3°C
Comb18	48.7°C
Comb19	43.8°C
Comb20	53.6°C

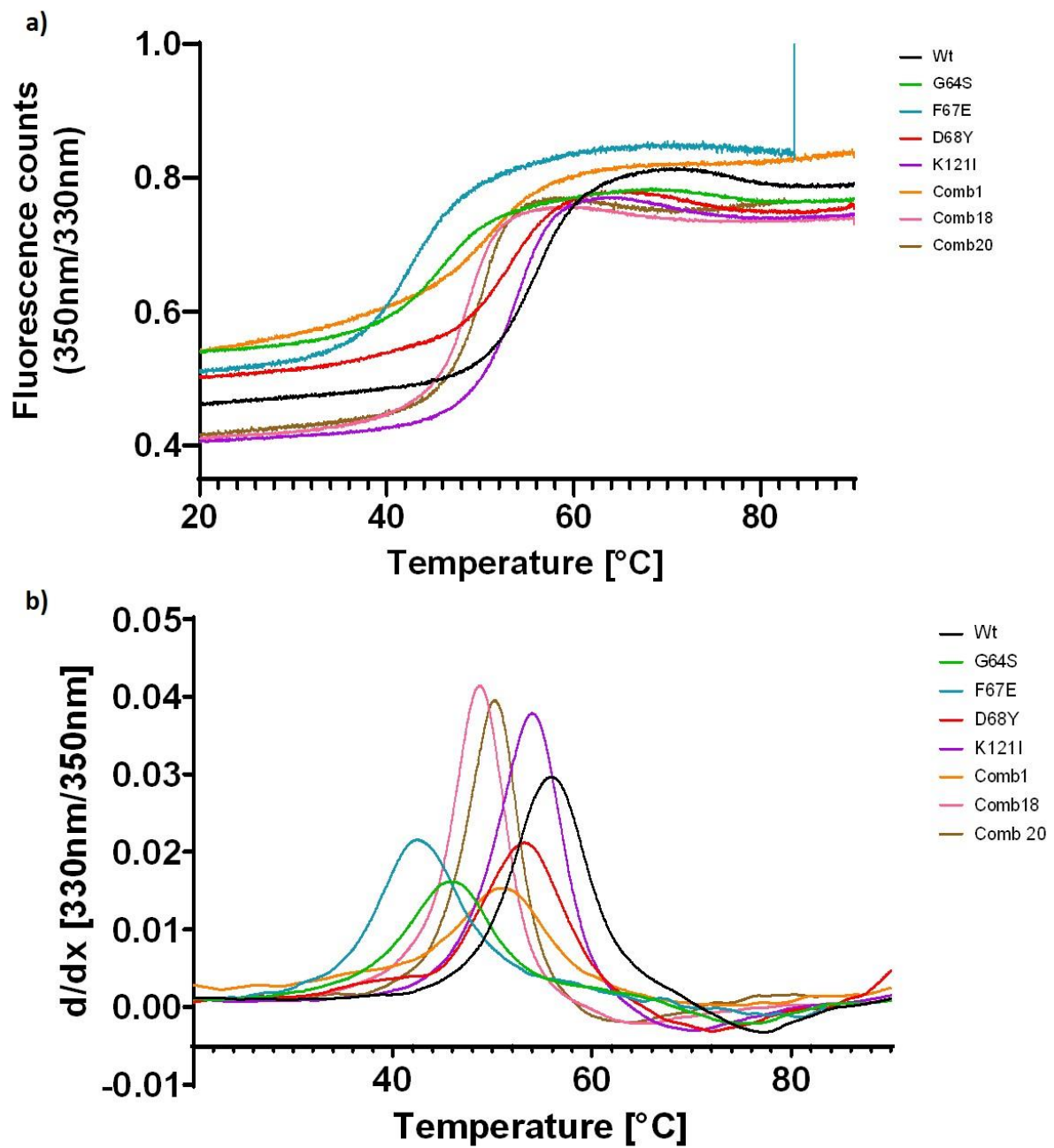


Figure S6. NanoDSF measured melting temperatures of the previously reported FKBP51 variants (G64S, F67E and D68Y), K121I and their combinations. a) intrinsic fluorescence intensity ratio (350 nm/330 nm). b) First derivative of the intrinsic fluorescence intensity ratio (350 nm/330 nm).

4.4 Conformation locking scFvs and affibodies for the research of FKBP51 transient binding pocket

The data presented in the following section was generated in the scope of this doctoral study. This unpublished research represents important contributions to the topic of allosteric modulators of FKBP51 for the characterization of the FKBP51 transient binding pocket, and facilitate the screening of new compounds able to bind selectively to FKBP51. The following section may be totally or partially submitted to a scientific journal in the future.

Conformation-locking scFvs and affibodies for the research of FKBP51 transient binding pocket

Jorge A. Lerma Romero¹, Christian Meyners¹, Thomas Nehls¹, Dominic Happel¹, Stefania Carrara¹, Frederik Lermyte¹, Felix Hausch^{1,2}, Torbjörn Gräslund³, and Harald Kolmar^{1,2*}

¹Institute for Organic Chemistry and Biochemistry, Technical University of Darmstadt, 64287 Darmstadt, Germany

²Centre for Synthetic Biology, Technical University of Darmstadt, 64287 Darmstadt, Germany

³Division of Protein Technology, KTH Royal Institute of Technology, SE-10691 Stockholm, Sweden

* Correspondence:

Harald Kolmar

Harald.Kolmar@TU-Darmstadt.de

Keywords: conformational dynamics, FKBP, scFv, affibody, display of biologics

Abstract

The FK506 binding protein 51 (FKBP51) has received increasing attention because of its involvement in several psychiatric, metabolic, and stress-related disorders as well as many other known diseases. Like many other members of the FKBP family, FKBP51 has an FK1 domain with a highly conserved binding pocket. Despite the similarity between the proteins of this family, small differences in the FKBP51 sequence endow this protein with a higher conformational flexibility. This property allows it to form a low-populated “open conformation” that binds a set of FKBP51-selective so-called iFit ligands family.

ScFvs are small antibody fragments that have been reported to assist in conformation-locking of specific conformations of diverse proteins. In this work, a yeast surface display library expressing chicken-derived scFvs was screened via fluorescence-activated cell sorting (FACS) to identify molecules able to lock FKBP51 conformers. From multiple screening campaigns, a clone able to modify the ligand uptake behavior of FKBP51 was isolated and characterized. Besides, blocking and high-affinity binders were sorted and tested. Similarly, an af-fibody *E. coli* display library was screened in a similar way to obtain conformation-locking, blocking, or high-affinity binding molecules.

FKBP51 conformation-locking molecules have the potential to be invaluable research tools able to shift the FKBP51 ensemble population to an open conformation and facilitate the screening of new compounds with the ability to selectively bind to FKBP51. Moreover, blocking and high-affinity binders are of great value for the biochemical characterization and *in vitro* experiments involving this protein.

Introduction

All proteins have a certain degree of flexibility that depends on many factors such as their amino acid sequence, domains arrangement, and environmental conditions [1]. The conformation of a protein may affect its biological activity. This can be exemplified by proteins that participate in processes like enzyme catalysis, signal transduction, protein transport, or antigen recognition where conformational changes must occur in the presence of other molecules or changes in the environment to effectuate such tasks [2, 3]. Because of their dynamic nature, proteins can be found in an ensemble of several related conformations, rather than as one single conformer [4, 5]. All these conformations are populated at varied rates, exchanging on distinct timescales that can range from nanoseconds to hours [4, 6].

Over the years, it has been studied how a protein structure and function may be affected by another molecule without binding in the protein orthosteric site (active site). This phenomenon called allostery, can be defined as the regulation of a protein (activity and/or structure) by the interaction of an effector molecule with a distant site of the protein, also called allosteric site [7–10]. Instead of generating new conformations, an allosteric effector interaction with a protein changes the distribution and interconversion rates of the protein's already existing conformational ensembles [11]. Either by computational or experimental methods, the search for

allosteric sites is an attractive way to regulate the activity of a protein while avoiding highly conserved orthosteric sites, for example, while trying to target a specific member of a protein family [12–17].

One invaluable use for allosteric protein regulation is to target proteins within a family with highly conserved orthosteric sites [18–20]. The homology between proteins in a family may be relatively high, but even with similar structural characteristics, they may differ in terms of functional traits such as substrate selectivity, reaction chemistry, domain recruitment, subunit assembly, or regulatory principles [19, 21]. Numerous studies have suggested that variations in the conformational dynamics among different proteins in a family may have an impact on the subtype selectivity of orthosteric ligands, especially if the formation of a transient binding pocket (also known as cryptic pocket) is involved [22–25].

The FK506 binding protein 51 (FKBP51) is a 51-kDa protein member of the immunophilin family [26]. It has been identified as a potential therapeutic target for a number of diseases such as cancer, neurodegenerative diseases, chronic pain, obesity, and other stress- and metabolic-related disorders [26–33].

FKBP51, as well as its close homolog FKBP52, are co-chaperones of the 90-kDa heat shock protein (Hsp90) and are part of the steroid receptor complex responsible for hormone level regulation [26, 34–36]. These two proteins have 70% sequence homology and high structural similarity [26, 37]. The FK1 domain of these proteins is responsible for the peptidyl-prolyl isomerase activity, which can also bind the immunosuppressive drugs FK506 and rapamycin [38–40]. Despite the high similarity between these two proteins, they have opposing activity. While FKBP51 inhibits steroid receptor activity by reducing the hormone binding affinity to the glucocorticoid receptor (GR)-Hsp90 complex, FKBP52 binds GR with high affinity, allowing nuclear translocation and activating FKBP51 transcription. Expression of FKBP51 causes a short negative feedback loop to stop steroid receptor nuclear localization and signaling [41–43]. Due to small differences in the sequence of FKBP51, the conformational plasticity of the β_3 strand and the β_{4-5} loop vary significantly from FKBP52 [36, 44].

The high conformational flexibility of FKBP51 was exploited to develop the iFit-ligand series [45]. These ligands are able to selectively bind FKBP51 thanks to their ability to adapt a conformation where the side chain of the phenylalanine at position 67 is displaced from the binding pocket, which allows to accommodate the trimethoxyphenyl-cyclohexyl group of SAFit1 [45–47]. This conformational change is not seen in either the apo-form or the FK506-bound FKBP51. A similar restructuring of the FKBP52 conformation to accommodate SAFit1 is not possible because of the FKBP52 bulky residues T58, W60, and V129 [46].

The study of this ligand-induced transient binding pocket is necessary to develop better FKBP51 selective ligands with improved pharmacological properties than the SAFit ligands [48]. Different approaches have been used to study the cryptic pocket of FKBP51, from muteins to stabilize the open-state of the protein to molecular dynamics simulations, NMR, and crystallographic structure determination [14, 49–51].

An alternative to study the binding pocket of FKBP51 and facilitate the screening of compounds that bind with high affinity and selectivity FKBP51 over other members of the FKBP family is the use of allosteric modulators to stabilize the open conformation of the protein without amino acid exchanges or a ligand already occupying the binding pocket. Higher selectivity, especially subtype selectivity within protein families, is one of the main benefits of utilizing allosteric modulators over direct molecule interaction at the orthosteric site [7, 52, 53].

Recently, monoclonal antibodies and antibody fragments have been used as allosteric modulators together with *in vitro* selections for the discovery of conformation-specific ligands for some proteins [54–58]. Single-chain fragment variable (scFv) is an antibody format consisting of the variable regions of the heavy chain (V_H) and light (V_L) chain of an antibody connected by a linker [59]. This antibody format has some advantages over regular IgGs, like the possibility of a cost-effective and fast expression in bacterial strains, and they can be widely used in medical applications and diagnostics as delivery vehicles for radionuclides, for radioimmunoimaging, and for delivery of cytotoxic drugs [60–62]. Thanks to its reduced size (~25 kDa), scFvs have better and more uniform tumor and tissue penetration compared to full length antibodies. Besides, these molecules have a fast blood clearance, which is an advantage if they are used as vehicles for toxic drugs and radionuclides [63–67].

Affibody molecules are small molecular weight protein scaffolds (~58 amino acids) engineered to mimic antibodies and bind with high affinity a target protein [68, 69]. These 6.5 kDa engineered proteins are derived from the Z domain of *Staphylococcus aureus* Protein A and consist of a 3-helix structure where some residues on two out of the three helices are randomized to create an affibody library [69, 70]. Similar to scFvs, affibodies can be easily expressed in bacterial cells, and due to their small size, exhibit fast blood clearance and effective tissue penetration. They can be used as diagnostic imaging tools, targeted delivery of payloads, and cancer therapeutics [68, 71–73].

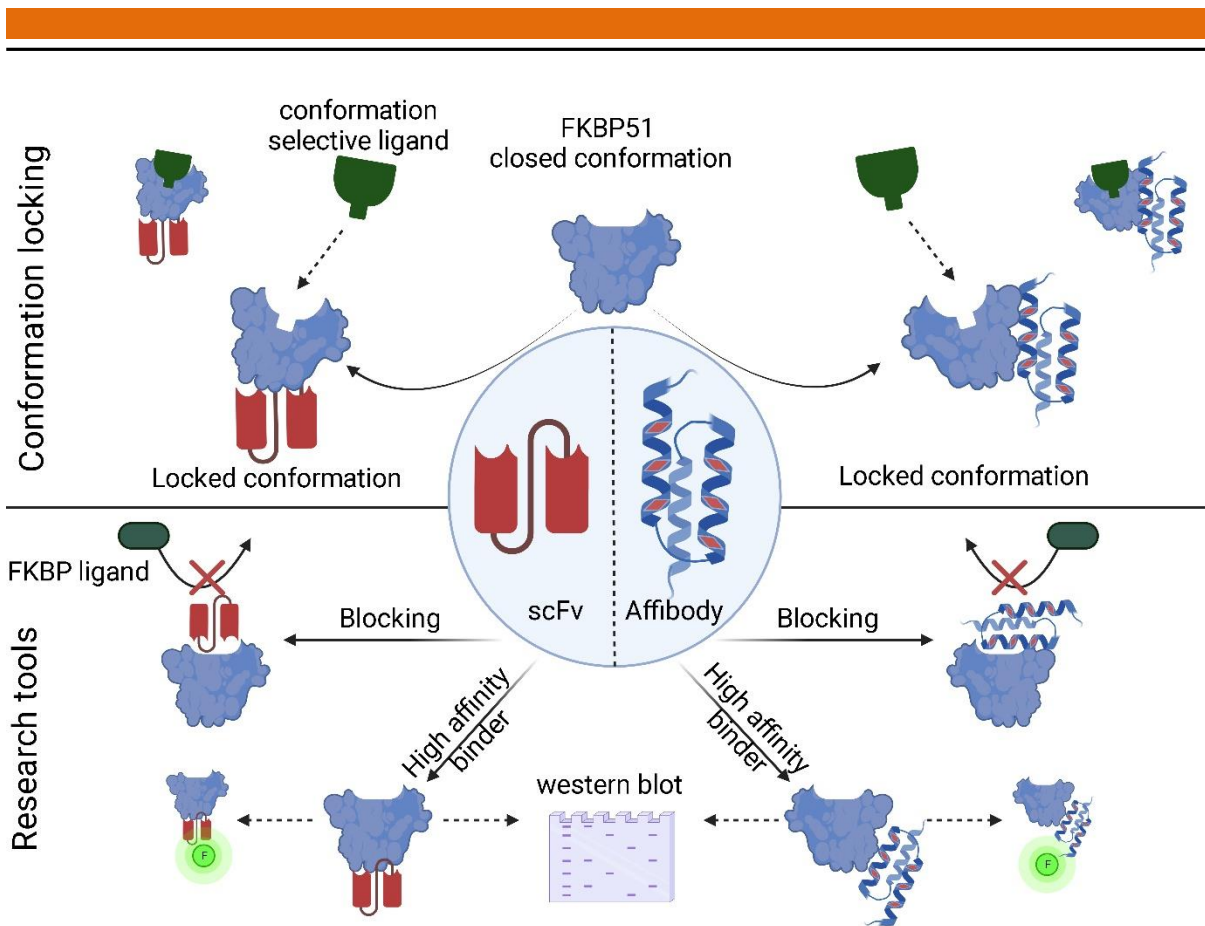


Figure 1. Schematic representation of the different effects that molecules such as scFvs and affibodies may have on a target protein. The influence of these molecules on conformation-locking, blocking or high-affinity binders for biochemical characterization are the evaluated in this work. Created with BioRender.com

ScFvs and affibodies are two molecules that can be effectively used as high-affinity labeling molecules or conformation-locking molecules to promote a population shift of FKBP51 to an open conformation which allows binding of ligands that can selectively bind to the transient binding pocket of FKBP51 (Figure 1). By combining conformation-locking molecules that can shift the FKBP51 population to an open-state with fragment screening methods, this may facilitate the discovery and characterization of new inhibitory ligands that selectively bind to FKBP51 over other members of the FKBP family. In this work, we isolated scFvs and affibodies able to regulate the conformation of FKBP51 and influence ligand binding. Besides, a set of high-affinity scFvs and affibodies were identified and characterized. All these biomolecules are promising candidates to facilitate the screening of new FKBP51 selective inhibitors or as research tools for the biochemical analysis, labeling and, characterization of FKBP51.

Materials and methods

Chicken immunization and RNA isolation

To obtain the genetic material of human FKBP51-binding antibodies, a healthy adult laying hen (*Gallus gallus domesticus*) was immunized at Davids Biotechnologie GmbH, Germany. The hen was intramuscularly injected with 150 µg of a mix of the FK1 domain of FKBP51 and FKBP51-G64S (mutain with a G64S mutation) using AddaVax (InvivoGen) as vaccine adjuvant. Boosters were given 14, 28, 32, and 42 days after the first immunization. After 56 days, the immunized animal was sacrificed and the splenic RNA was isolated using TriFast reagent (VWR). To confirm a strong immune response against the antigen, an ELISA titer with the chicken blood was performed.

Experimental procedures and animal care were in accordance with EU animal welfare protection laws and regulations.

cDNA synthesis and chicken scFv amplification

A pool of scFv inserts was obtained from the immunized chicken splenic RNA following the protocol by Bogen et al., 2020 [74]. cDNA synthesis was carried out using the SuperScript™ III First-Strand Synthesis System Kit (Invitrogen) following the manufacturer's instructions. The chicken-derived scFvs were constructed in two steps. Firstly, the V_H and V_L genes were amplified from the synthesized cDNA with the primer pairs VH_gr_up + VH_SOE_lo for V_H genes amplification, and VL_SOE_up + VL_gr_lo for V_L genes amplification (Table S1).

The amplification reactions contained 3 µL of cDNA, 2 µL of each primer (10 µM stock), 2 µL dNTPs (10 mM each), 10 µL 10X Standard OneTaq Buffer, 0.5 µL OneTaq polymerase, and the reaction was filled-up to a final volume of 100 µL with nuclease-free water. For each chain, at least six 100 µL-reactions were prepared. The reactions were thermally cycled with the following program: 95 °C for 2 min, followed by 30 cycles of 95 °C for 20 s, 55 °C for 30 s, and 68 °C for 30 s, and a final incubation of 68 °C for 5 min. The PCR products were analyzed on a 1% (w/v) agarose gel to confirm the correct amplification of V_H and V_L genes with an approximate size of 450 bp and 380 bp, respectively. The PCR products were purified utilizing the Promega Wizard® SV Gel and PCR Clean-up System.

The primers for these first PCRs created an overhang that encodes the (Gly₄Ser)₃ linker for the subsequent fusion PCR to create scFv-encoding fragments. Using an overlap extension PCR, the two fragments were combined. 200 ng of each purified PCR product (V_H and V_L), 0.2 nM of each primer (VH_gr_up and VL_gr_lo), 5X green Quick-Load reaction buffer, 200 µM of dNTPs, 1.25 units of OneTaq® Quick-Load® DNA Polymerase (New England Biolabs) were combined and filled up with ddH₂O to a final volume of 100 µL. To allow the annealing and elongation of both fragments, the first 15 cycles were run without primers in the reaction. Afterward, 2 µL of each primer (VH_gr_up and VL_gr_lo) were added to the reaction, and 15 further amplification cycles were carried out. The resulting PCR product encodes for the scFv with overhangs on both sides for homologous recombination in yeast. Around 40 parallel reactions were prepared and thermally cycled: 95 °C for 2 min, followed by 30 cycles of 95 °C for 20 s, 55 °C for 50 s, and 68 °C for 50 s, then a final incubation of 68 °C for 5 min.

Yeast library generation

An scFv yeast library was generated via homologous recombination. Firstly, the destination vector (pCT vector, Figure S1) was linearized with the restriction enzymes BamHI (New England Biolabs) and NheI (New England Biolabs). The *Saccharomyces cerevisiae* strain EBY100 [MATa URA3-52 trp1 leu2Δ1 his3Δ200 pep4:HIS3 prb1Δ1.6R can1 GAL (pIU211:URA3)] (Thermo Fisher Scientific) was used for the generation of the chicken derived scFv library. EBY100 yeast cells were cultivated in Yeast Extract–Peptone–Dextrose (YPD) medium which contained 20 g/L peptone-casein (Carl Roth GmbH &Co.KG), 20 g/L glucose (Carl Roth GmbH &Co.KG), and 10 g/L yeast extract (Sigma-Aldrich).

Electrocompetent EBY100 cells and the scFv library were generated following the Benatuil *et al.* protocol [75]. To transform electrocompetent yeast cells, 4 μg digested pCT vector and 12 μg purified scFv PCR product were added to each transformation reaction. 20 electroporation reactions were performed; each in a 0.2 cm BioRad GenePulser cuvette and electroporated at 2.5 kV and 25 mF. The cells were immediately resuspended in a 1:1 mix of 1 M sorbitol: YPD medium and incubated at 30 °C for 1 h. The cells were collected and cultured in SD-Trp media composed of 20 g/L glucose, 6.7 g/L yeast nitrogen base without amino acids (Becton, Dickinson and Company), 5.4 g/L Na₂HPO₄ (Carl Roth GmbH &Co.KG), 8.6 g/L NaH₂PO₄·H₂O (Carl Roth GmbH &Co.KG), and 5 g/L casamino acids. Library sizes were calculated from plating serial dilutions of transformed cells.

ScFv YSD library screening and sorting via FACS

The scFv YSD library was grown in SD medium at 30 °C and 200 rpm overnight. Next, cells were induced in SG medium (20 g/L galactose, 6.7 g/L yeast nitrogen base without amino acids, 5.4 g/L Na₂HPO₄, 8.6 g/L NaH₂PO₄·H₂O, and 5 g/L casamino acids) at a cell density of 10⁷ cells/ml and incubated at 30 °C for approximately 24 h. To prepare the cells for FACS analysis or sorting, the yeast cells were washed and resuspended with PBS (6.4 mM Na₂HPO₄, 2 mM KH₂PO₄, 140 mM NaCl, 10 mM KCl) followed by incubation with 1000 nM, 750 nM, or 400 nM of biotinylated FKBP51 on ice for 30 min. Afterward, the cells were washed and resuspended a second time in PBS, followed by staining with Streptavidin conjugated to APC (eBioscience™; diluted 1:75) to identify FKBP51 binders and c-Myc-FITC antibody (Miltenyi Biotec; diluted 1:75) to differentiate between presenting and non-presenting yeast cells. For the sorting rounds aiming to find either blocking or conformation-locking scFvs, no c-Myc-FITC antibody was used, but instead, SAFit-FL was added to a final concentration of 1000 nM or 500 nM, respectively. Subsequently, cells were washed one last time with PBS and resuspended in 1 ml of PBS for FACS analysis. FACS-sorting rounds were either performed on a Sony SH800 cell sorter (Sony) or a BD Influx™ cell sorter. A sorting gate was set to capture approximately 1% of the FKBP51 binding population (and SAFit-FL binding/non-binding population) (Figure 2). For the Sony SH800 cell sorter APC fluorochrome configuration (638 nm excitation laser, 665/30 optical filter) was used to measure APC stained FKBP51; and FITC fluorochrome configuration (488 nm excitation laser, 530/40 optical filter) was used to measure SAFit-FL or FITC stained myc-tag. For the BD Influx™ cell sorter a 488 nm excitation

laser, 530/40 optical filter was used to measure SAFit-FL or FITC stained myc-tag; a 640 nm excitation laser, 670/30 optical filter was used to measure APC stained FKBP51. The FACS output was used for subsequent sorting rounds or single clone analysis.

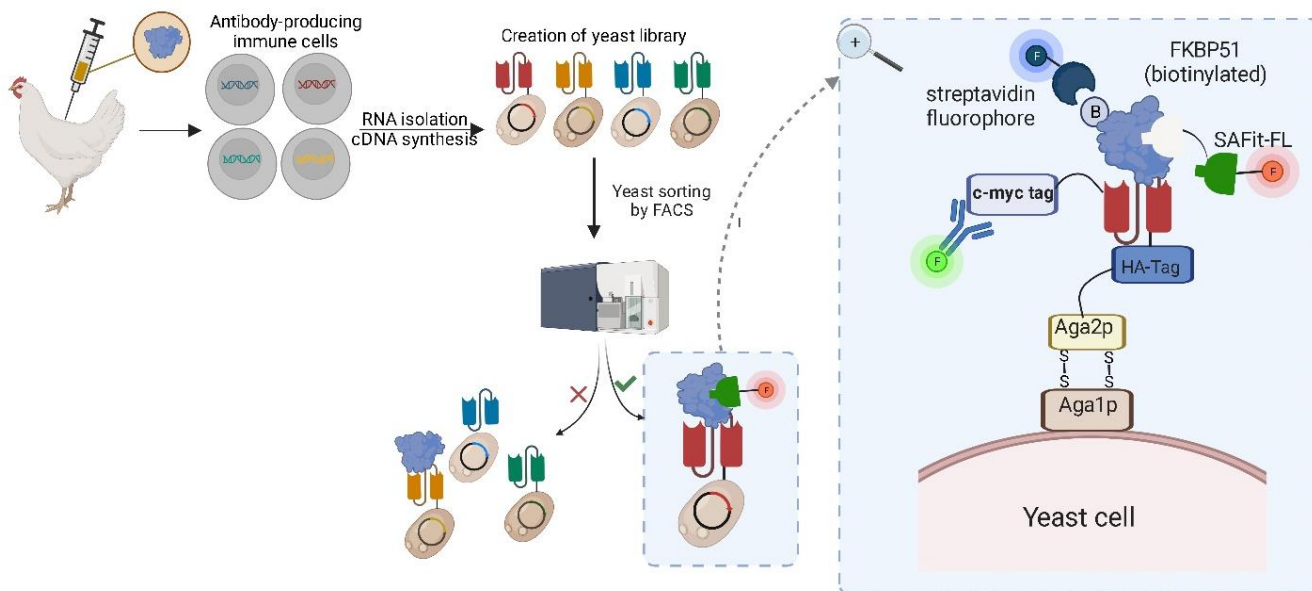


Figure 2. Schematic representation of the general process for generation and FACS screening of a YSD library presenting scFvs to identify FKBP51 conformation stabilizing scFvs. Created with BioRender.com.

For single clone analysis of conformation-locking scFvs, each yeast culture was incubated with 800 nM of FKBP51 and 50 nM of SAFit-FL. For single clone analysis of blocking scFvs, each yeast culture was incubated with 800 nM of FKBP51 and 1000 nM of SAFit-FL.

Affibody library sorting via MACS

FKBP51 binders MACS

An aliquot of the recombinant *E. coli* BL21 (DE3) (pAraBAD-Z-EC) displaying a synthetic affibody library (Figure S3) was thawed and resuspended in Luria-Bertani (LB) medium (Thermo Fisher Scientific) with carboxymycin (Carb) (100 µg/mL) to an $OD_{600} = 0.17$. The culture was incubated at 37 °C and 150 rpm overnight.

From the overnight culture, 1×10^{11} cells were incubated in 1.25 L LB with Carb (100 µg/mL) at 37 °C and 150 rpm until an $OD_{600} = 0.5$. The cells were then induced by adding Arabinose to a final concentration of 0.6 %. The induced culture was incubated at 25 °C and 150 rpm overnight. From the induced culture 1×10^{11} cells were washed three times with PBSP (PBS with 0.1% Pluronic F108 NF surfactant (BASF Corporation)).

For every MACS round, there should be a ratio of 1:50 beads to cells (e.g. 2×10^9 beads for 1×10^{11} cells). To sort 1×10^{11} cells $2 \times 200 \mu\text{l}$ of Dynabeads™ MyOne™ Streptavidin were washed with 20 ml PBSP with magnetic separation. One aliquot of the washed beads was resuspended in 20 ml of 500 nM biotinylated FKBP51 and incubated for 1h. The FKBP51-coated beads were washed twice and resuspended in 20 ml PBSP.

The second non-coated aliquot of magnetic beads was used to resuspend the washed cells and the mix was incubated for 1 h on a rotamixer at room temperature to sort out the affibodies that bind the uncoated beads. The mix was set for 10 min on a magnetic rack, and the supernatant was collected for sorting. The *E. coli* library was resuspended with 20 ml of the FKBP51-coated beads and incubated for 2 h on a rotamixer. The captured cells were washed three times with PBSP with a 3 min incubation on ice after starting the next was. This in order to avoid affibodies with a fast K_{off} . The sorted cells were resuspended in 50 ml LB with Carb and incubated at 37 °C and 150 rpm overnight. Dilution plates with the output of the library were plated to determine the number of sorted cells. The enrichment was determined after each sorting round by flow cytometry. For subsequent MACS rounds, all amounts were scaled down based on 10X the number of cells determined by the previous sort, and taking no less than 1 μl of magnetic beads for the last rounds (Figure 3A).

Ligand dependent MACS selection

For this sorting method, the same induced preculture was used. To sort 1×10^{11} cells $3 \times 200 \mu\text{l}$ of Dynabeads™ MyOne™ Streptavidin were washed with 20 ml PBSP with magnetic separation. Two aliquots of the washed beads were resuspended in 20 ml of PBSP and SAFit-biotin was added to a final concentration of 200 nM and incubated for 1h. The SAFit-coated beads were washed twice and resuspended in 20 ml PBSP.

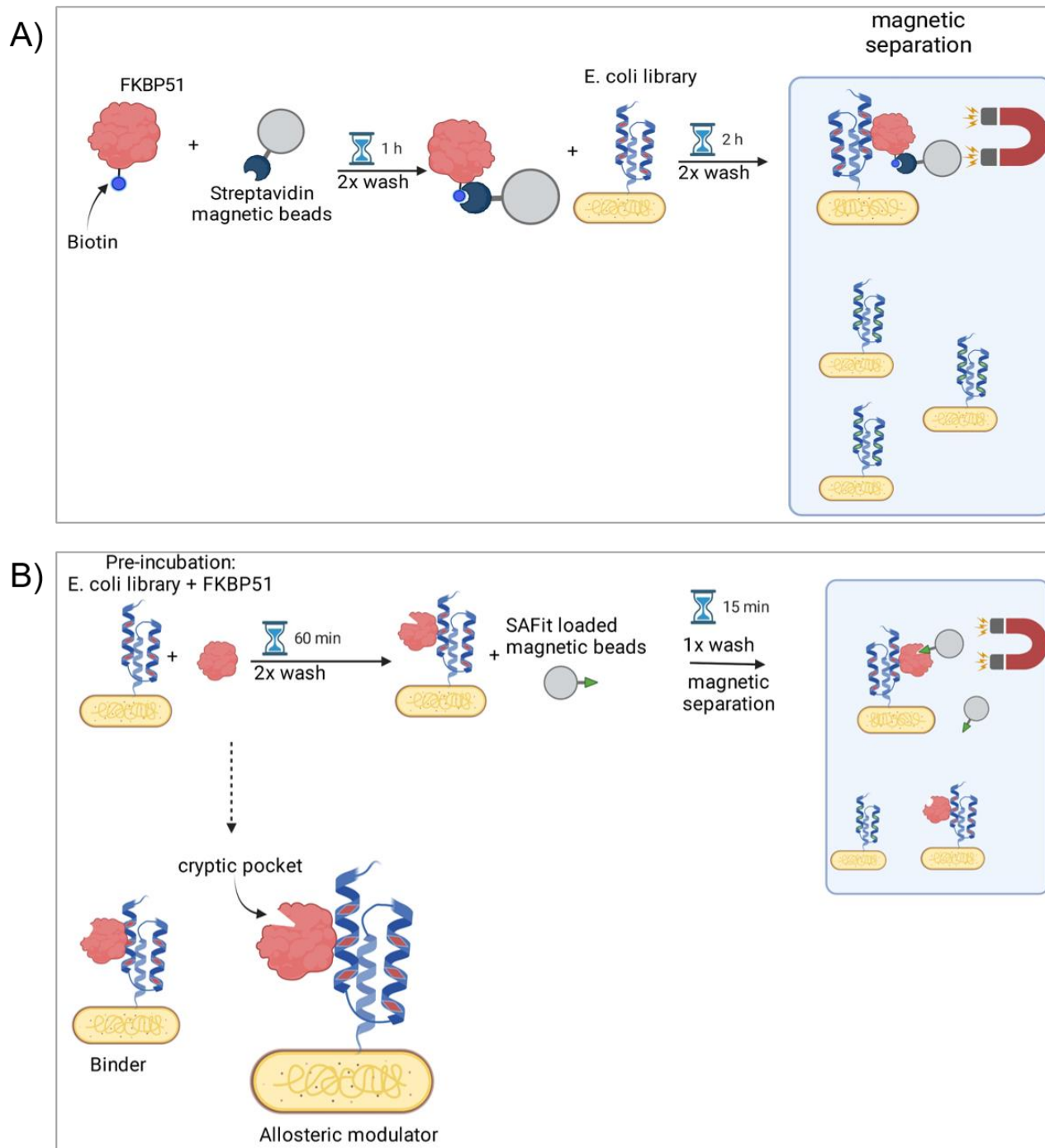


Figure 3. Schematic representation of the *E. coli* display presenting affibodies, MACS-based screening strategy for A) high-affinity FKBP51 binders and B) ligand dependent sorting to identify conformation stabilizing affibodies. Created with BioRender.com.

The non-coated aliquot of magnetic beads was used to resuspend the washed cells and the mix was incubated for 1 h on a rotamixer at room temperature. The mix was set for 10 min on a magnetic rack, and the same process was repeated with one of the SAFit-coated beads aliquot to sort out the affibodies which bind SAFit. The mix was set for 10 min on a magnetic rack, and the supernatant was collected for sorting. The *E. coli* library was resuspended with 20 ml of 400 nM FKBP51 (not biotinylated) and incubated for 2 h on rotamixer. The library with FKBP51 was used to resuspend the remaining aliquot of SAFit-coated beads and incubated for 1 h. After 15 min, 5 ml were taken out and captured in a magnetic rack to sort fast binders. The rest of the sorting process was made as described above for the FKBP51 binders only (Figure 3B).

Affibody *E. coli* display library screening and sorting via FACS

The affibody library was grown in LB medium with Carb (100 $\mu\text{g}/\text{mL}$) at 37 °C and 150 rpm overnight. On the next day, LB medium with Carb (100 $\mu\text{g}/\text{mL}$) was inoculated with the overnight culture to an $\text{OD}_{600}=0.1$ and incubated at 37 °C and 150 rpm until an $\text{OD}_{600} 0.5$ is reached. Cells were then induced by adding arabinose to a final concentration of 0.6% and incubated at 25 °C and 150 rpm overnight. To prepare the cells for FACS analysis or sorting, 5×10^8 induced *E. coli* cells were washed and resuspended with PBS followed by incubation with 200 nM of biotinylated FKBP51 on ice for 30 min. Afterward, the cells were washed and resuspended a second time in PBS, followed by staining the Albumin-binding domains (ABD) with 150 nM Alexa Fluor 647-Human Serum Albumin (HSA) conjugate to differentiate between presenting and non-presenting cells and 2 $\mu\text{g}/\text{mL}$ streptavidin conjugated with R-Phycoerythrin (SAPE) (Invitrogen) to identify FKBP51 binders. For the sorting rounds aiming to find either conformation-locking scFvs, SAFit-FL was added to a final concentration of 500 nM. Subsequently, cells were washed twice with PBS and resuspended in 1 ml of PBS for FACS analysis. FACS-sorting rounds were either performed on a MoFlo Astrios flow cytometer (Beckman Coulter). A sorting gate was set to capture approximately 1% of the FKBP51 binding population (and SAFit-FL binding population). The FACS output was used for subsequent sorting rounds or single clone analysis (Figure 4).

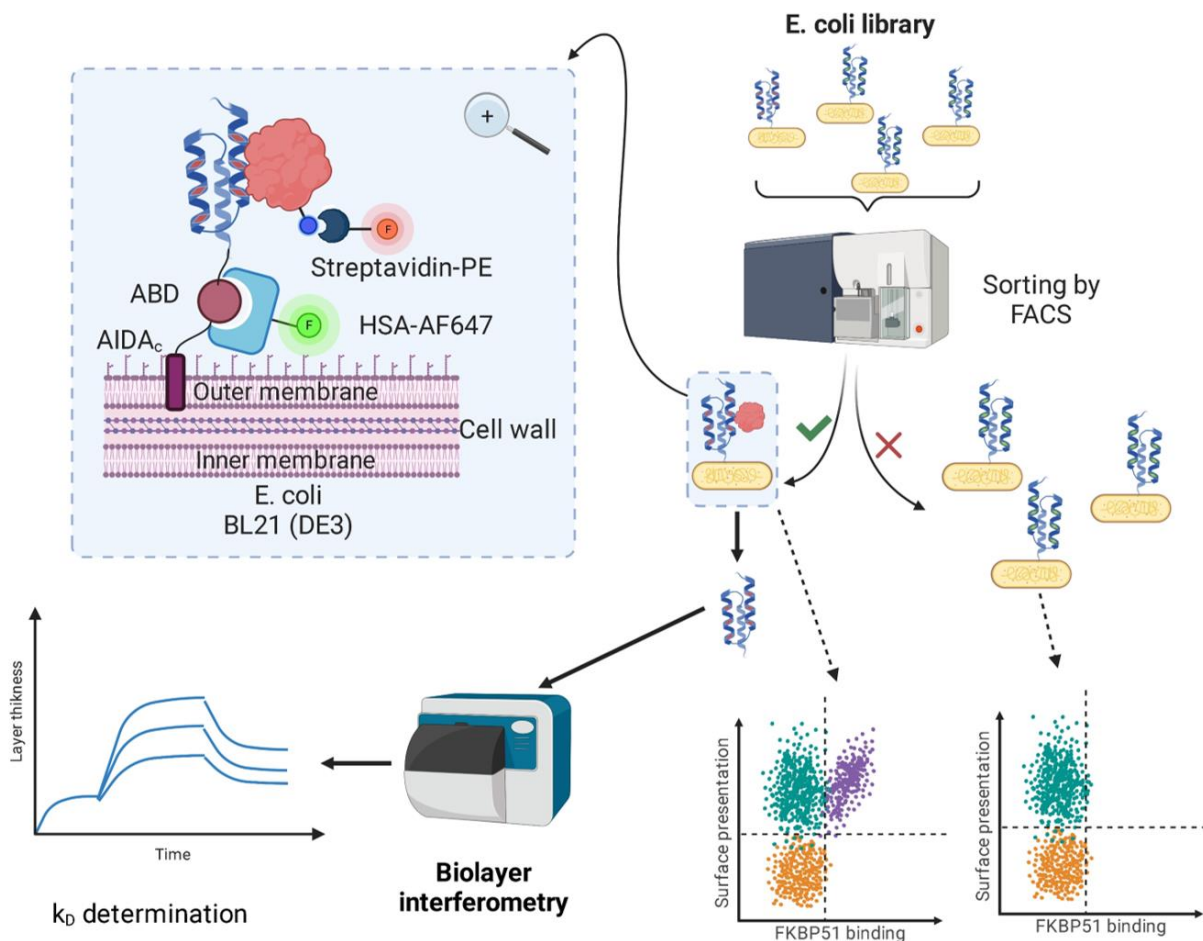


Figure 4. Schematic representation of the *E. coli* display library presenting affibodies, FACS-based screening strategy and affinity determination via BLI. Created with BioRender.com.

DNA purification, concentration determination, and sequencing

Products of PCR reactions and enzymatic restriction reactions were purified by Wizard® SV Gel and PCR Clean-up System Kit from Promega following the manufacturer's instructions. The purified DNA was eluted with nuclease-free water and the concentration was determined by spectrometry absorbance at 260 nm using the Biospec Nano™ from Shimadzu Europe GmbH. For sequencing, the cleaned-up DNA product was mixed with pCT_seq_up or pCT_seq_lo primer for the scFv yeast library, and pBAD_Fw for the affibody *E. coli* library (Table S1). The samples were sent for sequencing (SeqLab Göttingen GmbH or Eurofins Genomics GmbH).

Cloning, expression and purification of scFvs

After flow cytometric analysis of the isolated single clones, FKBP51-binding or conformation-locking scFvs expressing yeast cells were resuspended in 30 µL of 20 mM NaOH and incubated at 98 °C for 20 min. Afterward, a PCR reaction was prepared by mixing, 2 µL of the lysate as template, 10 µL of 5X green Quick-Load reaction buffer, 1 µL of the 10mM dNTPs, 1 µL of the pCT_seq_up and pCT_seq_lo primers (Table S1), 0.25 µL of OneTaq® Quick-load® DNA polymerase and filled up to 50 µL with ddH₂O. The reactions were thermally cycled with the following program: 95 °C for 2 min, followed by 30 cycles of 95 °C for 20 s, 54 °C for 30 s, and 68 °C for 1 min, then a final incubation of 68 °C for 5 min. The inserts were sequenced, and after grouping repeated results, the single clone yeast cells were lysed and the plasmid was isolated utilizing the Zymoprep kit according to the manufacturer's instructions. The isolated plasmids were transformed into *E. coli* Top10 to amplify and purify the pCT plasmid coding for the sorted scFvs.

To clone the scFvs into a pET30 plasmid for protein expression (Figure S2), a PCR of the pCT plasmids coding for the scFvs was prepared with 1 µL of the pCT plasmid, 10 µL of 5X Q5 Reaction Buffer, 1 µL of the 10 mM dNTPs, 2 µL of the scFv_chick_his_TEV_NdeI_up and scFv_chick_SII_TEV_NotI_lo primers (Table S1), 0.5 µL of Q5 High-Fidelity DNA Polymerase (NEB) and filled up to 50 µL with ddH₂O. Reactions were thermally cycled with the following program: 98 °C for 1 min, followed by 30 cycles of 98 °C for 20 s, 72 °C for 20 s, and 72 °C for 30 sec, then a final incubation of 72 °C for 5 min. The inserts were cleaved using the restriction enzymes NdeI and NotI (NEB), cleaned up, and ligated with a linearized pET30 vector using T4 ligase (NEB). The ligation product was used to transform *E. coli* Top10 cells by electroporation at 2.5 kV and 25 mF in a 0.2 cm BioRad GenePulser cuvette. The transformed cells were spread on Double Yeast Tryptone (dYT)-agar plates composed of composed of 16 g/L peptone-casein (Carl Roth GmbH &Co.KG), 10 g/L yeast extract (Sigma-Aldrich), 5 g/L NaCl and 15 g/L Agar-Agar with kanamycin (30 µg/ml) and incubated at 37 °C overnight. One colony was picked to inoculate dYT media composed of 16 g/L peptone-casein (Carl Roth GmbH &Co.KG), 10 g/L yeast extract (Sigma-Aldrich), and 5 g/L NaCl with kanamycin (30 µg/ml). On the next day, the plasmid was isolated from the cells.

Finally, *E. coli* T7 SHuffle® cell line expressing sulfhydryl oxidase (T7-SOX) was transformed with each of the scFvs cloned in pET30 by electroporation. The transformed cells were spread on dYT-agar plates with

kanamycin (30 µg/ml) and chloramphenicol (33 µg/ml) and were incubated at 37 °C overnight. A single colony was picked to start a preculture in dYT medium with kanamycin (30 µg/ml) and chloramphenicol (33 µg/ml) and grown overnight at 37 °C and 180 rpm. A shaking flask containing 250 mL SB medium composed of 32 g/L peptone-casein (Carl Roth GmbH & Co. KG), 20 g/L yeast extract (Sigma-Aldrich), and 5 g/L NaCl with kanamycin (30 µg/ml) and chloramphenicol (33 µg/ml) was inoculated to an OD₆₀₀ = 0.1, using the overnight culture. The cell culture was incubated at 37 °C and 180 rpm until an OD₆₀₀ of 0.6–0.8 was reached. Production was carried out overnight by adding 1 mM isopropyl 1-thio- β -D-galactopyranoside (IPTG) and 5 g/L Arabinose and incubated at 25 °C and 180 rpm overnight.

Induced T7-SOX cells containing the scFvs were precipitated by centrifugation (6,000 rpm, 10 min, 4 °C) and lysed by sonication. Cellular debris were removed by centrifugation (13,500 rpm, 15 min, 4 °C) and the supernatant was filtered through a 0.45 µm syringe filter.

The N-terminal His-tag allowed purification by Ni-NTA affinity chromatography (HisTrap HP - Cytiva), while a C-terminal Strep-II tag allowed purification by Strep-Tactin® Superflow® high capacity FPLC column (IBA Lifesciences GmbH). Finally, the recovered fractions were dialyzed against PBS pH 7.4. If required, purification tags were removed by TEV-protease cleavage.

Cloning, expression and purification of affibodies

After isolation and confirmation of *E. coli* presenting affibodies binding FKBP51, the cells were resuspended in 20 µL of water and incubated at 95 °C for 5 min. Afterward, a PCR reaction was prepared by mixing, 2 µL of the lysate supernatant as template, 10 µL of 5x HF Buffer, 1 µL of the 10mM dNTPs, 2.5 µL of the PALU 103F and PALU 104R primers (Table S1), 0.5 µL of Phusion Polymerase and filled up to 50 µL with ddH₂O. The reactions were thermally cycled with the following program: 98°C for 1 min, followed by 10 cycles of 98 °C for 10 s, 46 °C for 30 s, and 72 °C for 30 sec, followed by 25 cycles of 98 °C for 10 s, 64 °C for 30 s, and 72 °C for 30 sec, then a final incubation of 72°C for 10 min. The PCR products were mixed with 5 µL of 10X Cutsmart buffer and 1 µL of DpnI and incubated at 37 °C for 30 min and 80 °C for 10 min. The inserts were cleaned up and cloned into a pET45b plasmid (Figure S4) by mixing 5.47 ng of the insert with 25 ng of pET45b+ InFusion vector, 1 µL 5X InFusion HD Enzyme Premix and filled up to a total volume of 5 µL to then be incubated for 20 min at 50 °C. 1 µL of the cloning product was used to transform *E. coli* BL21(DE3) by heat shock, and the transformed cells were used to start a preculture in LB medium with Carb (100 µg/mL), and grown overnight at 37 °C and 150 rpm. A shaking flask containing 100 mL TSB+Y medium composed of 30 g/L tryptic soy broth (Merck), and 5 g/L yeast extract (Merck) with Carb (100 µg/mL) was inoculated to an OD₆₀₀ = 0.05, using the overnight culture. The cell culture was incubated at 37 °C and 150 rpm until an OD₆₀₀ of 0.5 was reached. Production was carried out overnight by adding 1 mM IPTG and incubated at 25 °C and 150 rpm overnight.

Induced *E. coli* cells containing the affibodies were precipitated by centrifugation (2,700 rpm, 10 min, 4 °C) and lysed by sonication. Cellular debris were removed by centrifugation (10,000 rpm, 20 min, 4 °C) and the

supernatant was filtered through a 0.45 μm syringe filter. The affibodies were purified on Talon Cobalt resin (Cytiva) and the eluted affibodies were dialyzed against PBS pH 7.4.

Affinity measurement by fluorescence polarization

The following ligands and tracers were used for fluorescence polarization and FACS screening experiments (Figure S5):

- SAFit-FL tracer (1): Fluorescein conjugated analog of the iFit ligand class.
- FK[431] tracer (3): TAMRA conjugated FK[431] ligand (4).
- SAFit1 ligand(2): analog of the iFit ligand class.
- FK[431] ligand (4): bicyclic analog of the immunosuppressive drug FK506

The binding of the scFvs to FKBP51 was investigated by fluorescence polarization assays. Therefore, a serial dilution of the respective scFv in assay buffer (20 mM HEPES pH 8.0, 150 mM NaCl, 0.015% Triton X-100) was placed in a 384-well assay plate and 20 nM of the fluorescently labeled FKBP51 (FKBP51-FSM) was added. After incubation for 30 min at room temperature, the fluorescence polarization was measured with a plate reader. The obtained results for each 3 independent experiments were normalized with respect to the maximal binding signal and fitted to a one-site binding model as described by Wang *et al.*, 1992 [76] yielding the respective binding constants.

$$\text{tracer bound} = \frac{100}{L_t} \times 0.5 \times \left(R_t + L_t + K_D - \sqrt{(R_t + L_t + K_D)^2 - 4 \times L_t R_t} \right)$$

L_t = total concentration of the tracer; R_t = total concentration of the receptor; K_D = binding constant of the complex RL

Bio-layer interferometry

ScFv dependent FKBP51-ligand binding determined via biolayer interferometry

To determine the scFvs effect on the ligand binding by FKBP51, high-precision streptavidin (SAX) biosensors were loaded with 300 nM of SAFit-biotin until a layer thickness of 0.8 nm was reached. Association was measured for 300 s using different concentrations of the FK1 domain of FKBP51 followed by a second association step of 300 s with the different scFvs, and a final dissociation step for 300 s. Alternatively, a 300 s association step using different concentrations of the FK1 domain of FKBP51 together with the scFvs was measured, followed by a dissociation step for 300 s. The biolayer thickness was then compared to assess the effects of the different scFvs on the FKBP51-ligand interaction.

All measurements were performed using the Octet RED96 system (FortéBio, Molecular Devices) at 30 °C and 1000 rpm.

Conformation-locking by ligand binding assay

To investigate the influence of scFvs or affibodies on ligand binding, a ligand assay was performed with biolayer interferometry (BLI). SAX biosensors were loaded with SAFit-biotin to then be associated with 250 nM FKBP51 and subsequently to 250 nM scFvs. Due to the binding of each scFv or affibody to FKBP51, the complex exhibits a larger molecular size compared to FKBP51 alone. Each binding step results in an increase in layer thickness, which in this case is dependent to the binding affinity to the molecule tested to FKBP51 and the size of the molecule.

Similarly, the SAFit-biotin loaded SAX biosensor was associated to a pre-incubated mix of FKBP51 and a 5-fold excess of each scFv or affibody to ensure saturation of FKBP51 with the molecules. The layer thickness was then compared to the first 2-step binding experiment to determine any influence of the scFvs or affibodies on ligand binding.

Conformation-locking by competitive binding assay

To investigate the influence of scFvs on ligand binding, a competitive assay was performed via biolayer interferometry. To determine, whether the effects of the scFv differ depending on the initial state of the protein, two different conformation-specific ligands were tested: SAFit1 (**2**) which binds to an F67^{out} conformation, or FK[431] (**4**) tracer which binds to a F67ⁱⁿ conformation.

For analysis of ligand competition after binding to a conformation-locking molecule, 500 nM FKBP51 were first incubated with a 10X excess of either FK[431] tracer or SAFit1 for 30 min and then, the scFvs were added to a final concentration of 500 nM. SAX biosensors were loaded with SAFit-biotin to then be associated to each of the ligand-FKBP51-scFv complexes. The difference in the layer thickness is dependent on the ability of the SAFit-loaded tip to compete for the FKBP51 binding pocket, which can be potentially regulated by the binding of an scFv.

Affibody aided competitive binding assay

To investigate the influence of affibodies on ligand binding, a competitive assay was performed via biolayer interferometry. 200 nM of FKBP51 were first incubated with 500 nM of either FK[431] tracer or SAFit1 for 30 min and then, the affibodies were added to a final concentration of 500 nM. SAX biosensors were loaded with SAFit-biotin to then be associated to each of the ligand-FKBP51-scFv complexes. The difference in the layer thickness is dependent on the ability of the SAFit-loaded tip to compete for the FKBP51 binding pocket.

Epitope mapping by HDX-MS

A stock FKBP51 solution of 278 μM and a stock scFv T32 solution of 211 μM were diluted with 20 mM sodium chloride and 20 mM Tris-HCl at pH 7.5 to 30 μM for FKBP51 and 75 μM for scFv T32. A solution of only 30 μM FKBP51 was prepared in the same manner. Both sample solutions were shaken at 25 °C for 1.5 h.

For back exchange, a myoglobin solution of 20 μM in water and a myoglobin solution of 20 μM in D_2O were prepared. For complete deuteration, the myoglobin in D_2O was shaken at 35 °C for 1.5 h, and 170 mg sodium chloride was added to reduce the freezing point.

Labeling and measurements were performed by using an HDX setup from Waters. This includes a PAL RTC Autosampler from LEAP Technologies, a UHPLC with μBinary Pump and Auxiliary Pump from Waters, the HDX Manager of separate column ovens for the pepsin column and analytical column from Waters, and a Synapt XS from Waters. Protein solutions were stored in the quench tray at 1 °C under nitrogen. 3 μL of protein solution was injected into the label vial. Then, 57 μL of label buffer (pD 7.5, 5 mM K_2HPO_4 and 5 mM KH_2PO_4 in D_2O) or equilibration buffer (pH 7.5, 5 mM K_2HPO_4 , and 5 mM KH_2PO_4 in H_2O) was added and allowed to react for the set time at 20 °C. A 50 μL portion of the reaction solution was transferred to the quench vial in the quench tray. In this process, 50 μL of the quench buffer (pH 2.3, 50 mM K_2HPO_4 , 50 mM KH_2PO_4 , and 6 M urea in H_2O) was pre-cooled at 1 °C. 50 μL of quenched sample was injected and flowed for 1 min with a flow of 75 $\mu\text{L}/\text{min}$, followed by 3 min with a flow of 170 $\mu\text{L}/\text{min}$ with 0.2% formic acid in H_2O over the BEH pepsin column, 5 μm , 30 \times 2.1 mm, 300 Å from Waters at 20 °C to the trap column ACQUITY UPLC BEH C18 VanGuard Precolumn, 1.7 μm , 5 \times 2.1 mm, 130 Å from Waters at 1 °C. Thereafter, a gradient with the eluent A (H_2O , adjusted with formic acid at pH 2.5) and eluent B (acetonitrile with 0.3% formic acid) was started over the trap column to the analytical column ACQUITY UPLC BEH C18, 1.7 μm , 150 \times 1 mm, 130 Å from Waters at 1 °C. The flow rate was 45 $\mu\text{L}/\text{min}$. The gradient is a developed version of Thomas Nehls (AK Lermyte – TU Darmstadt) which is based and upscaled on the publication by Walters *et al.*[77]. ESI was used as ionization source with the following settings: capillary voltage of 3.0 kV, source temperature of 90 °C, sampling cone of 50.0 V, source offset of 20.0 V, desolvation temperature of 150 °C, cone gas flow of 100 L/h, desolvation gas flow of 550 L/h, and nebulizer gas flow of 6 bar. The MS method was a UDMSe with argon as the collision gas and nitrogen as drift gas. The UDMSe method was developed by Thomas Nehls (AK Lermyte – TU Darmstadt) based on the publication by Neta *et al.* 2009 [78] for the individual collision energy for the charge states and mass to charge ratios. The wave velocity was ramped linearly from 1500 m/s to 450 m/s with a constant wave height of 40 V, a constant helium gas flow of 180 mL/min for cooling, and a constant drift gas flow of 90 mL/min. As Lock Spray for recalibration, a solution of 2 ng/ μL leucine enkephalin inside 50:50 acetonitrile/water with 0.1% formic acid was infused. The labeled protein samples were measured $n = 5$ times for each time point at 0.25, 2.5, 25, and 250 min, and the protein samples with equilibration buffer with time point 0 min were measured with $n = 4$ for each protein conformation.

All measurements with a time point of 0 min were combined as reference. For back exchange, the myoglobin sample in water was measured at $n = 5$ and $t = 0$ seconds, and the deuterated sample was measured at $n = 5$ and $t = 60$ seconds. The evaluation was performed using ProteinLynx Global Server and DynamX, both software from Waters. Based on the peptide fragmentation pattern, a score threshold of 7.00 was chosen for the identified peptides, an intensity threshold of 1500, mass error of maximum 10 ppm, minimum 2 fragment products and 0.11 fragments per amino acid, a sum product intensity of 470, and one conducted product (based on Sørensen *et al.* 2018)[79]. The cluster data from DynamX was further analyzed using an Excel sheet to generate the Uptake Plots and Butterfly Plots. This resulted in a sequence coverage of 100% with 60 peptides with an average back exchange of 37%.

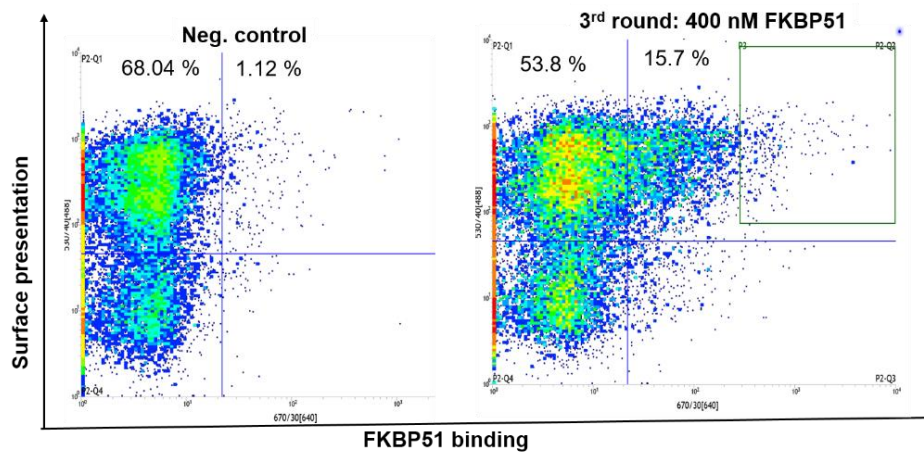
Results

In order to identify chicken-derived scFvs with high affinity binding to FKBP51 and conformation-locking qualities, an adult chicken was immunized with a mix of the FK1 domain of FKBP51 wt and FKBP51 G64S mutant. FKBP51 with a G64S mutation has previously been reported to shift the FKBP51 population to an open transient binding pocket conformation, favoring the binding of two conformation-specific ligands [14]. The chicken splenic RNA was isolated and cDNA was synthesized by reverse transcription. To generate a library of scFvs, the cDNA was used as a template to amplify the V_H and V_L domains independently, and fused by overlap extension PCR. This genetic material was used to generate a yeast display library with a size of approximately 8*10⁶ clones.

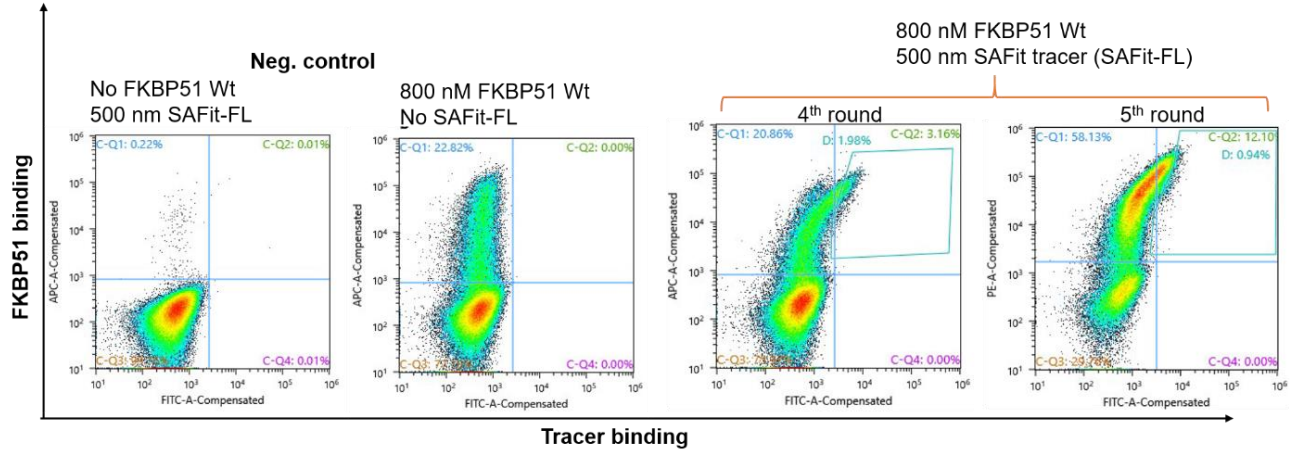
The scFv library was screened for three rounds via FACS (Figure 5) using decreasing concentrations of FKBP51 (1000 nM, 750 nM, and 400 nM) revealing an enrichment of high-affinity binders to the protein. Two subsequent sorting rounds using FKBP51 together with SAFit-FL (1), a conformation-specific tracer that binds preferentially to the F67^{out}-conformation of FKBP51, were used to select scFvs with high affinity to both FKBP51 and SAFit-FL (1) (Figure 5B) [45]. At the end of the fifth round, 40 individual clones were picked and sequenced. In total, five different scFvs were obtained: T4, T29, T32, T40, and T42 (Figure S8). From these five scFvs, T4, T29, T32, and T40 shared the same V_H, while T42 was the only unique clone. In a similar way, a parallel sorting campaign of two sorting rounds using FKBP51 together with SAFit-FL (1) was performed, where clones with affinity to FKBP51 but low ligand signal were isolated by FACS to identify blocking scFvs with an epitope close to the FK1 binding pocket which could impede ligand binding (Figure 5C). At the end of the fifth round, 20 individual clones were picked and sequenced. In total, two different scFvs were obtained: B1 and B4. Finally, one last screening campaign yielded three FKBP51-binding scFvs with no effect on ligand binding: G1, G4, and G7.

The FKBP51 binding affinity of each scFv was determined via fluorescence polarization (Figure S6): T4= 358 nM, T29= 6325 nM, T32= 29 nM, T40= 144 nM, T42=17700 nM, G1=>20 μM, G4=740 nM, and G7=980 nM. Due to the low binding affinity to FKBP51, T29 and T42 were not investigated further. The affinity for B1 and B4 could not be determined by FP because no binding was detected even though the single clone analysis by flow cytometry confirmed B1 and B4 as FKBP51 binders (Figure S9). Additionally, the scFv with the highest affinity to FKBP51 (T32) was tested for FKBP52 and FKBP12 binding, resulting in no binding to FKBP12 and a K_D= 3,000 nM to FKBP52 (Figure S15).

A) FKBP51 binder enrichment



B) Conformation stabilizing ScFvs



C) Blocking ScFvs

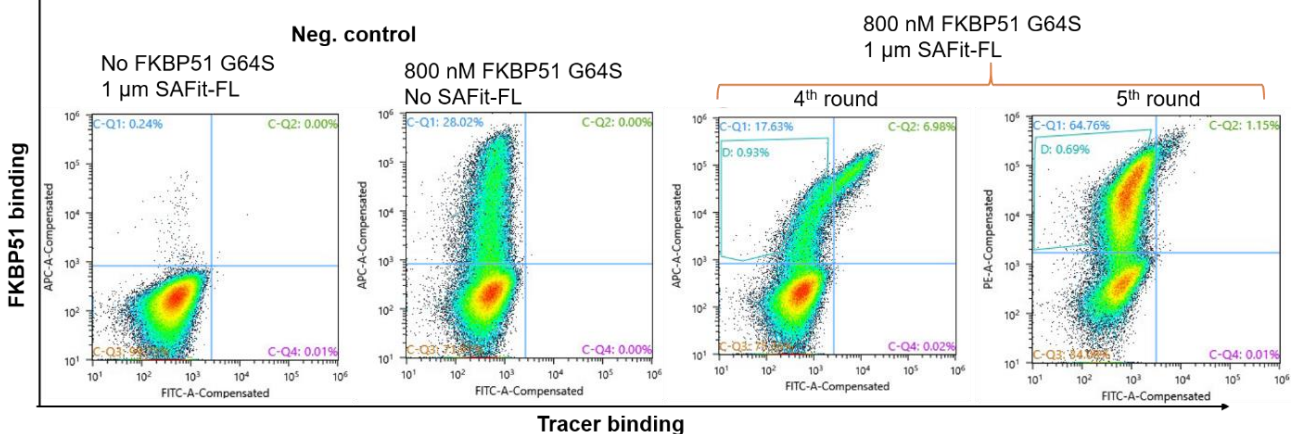


Figure 5. Chicken derived scFv YSD library screening and sorting. A) Cells showing both surface presentation (c-myc tag detection) and FKBP51 binding signal (APC/PE-streptavidin) were sorted for 3 rounds to enrich the population of protein binder scFvs. Sorting gate was set to capture approximately 1% of the FKBP51-binding population and used for subsequent sorting rounds. B) Cells showing both FKBP51 binding signal (APC/PE-streptavidin) and SAFit-FL signal were sorted for two additional rounds to enrich the population of protein binder scFvs which at the same time enhance SAFit-FL binding. C) Cells showing FKBP51 binding signal (APC/PE-streptavidin) but no SAFit-FL signal were sorted for two additional rounds to enrich the population of protein binder scFvs that inhibit SAFit-FL binding.

To test the influence that each scFv has on the ligand binding to FKBP51, BLI experiments were conducted. Firstly, to set a control measurement, SAX biosensors were loaded with SAFit-biotin and associated with 250 nM FKBP51 and subsequently contacted with 250 nM scFv. For this and subsequent experiments, the FKBP51 binding scFv F12 ($K_D = 762$ nM) was used as a control, as this clone was selected to only bind the protein without any effect on substrate binding or conformational changes on the target protein. As expected, the difference in the biolayer thickness is directly related to the affinity of the scFv to FKBP51 (Figure 6A). To evaluate the influence of each scFv on ligand binding, the SAFit-biotin loaded biosensor was associated with a pre-incubated mix of FKBP51 and a 5-fold excess of each scFv. Here, the layer thickness of F12 was the highest of all, although it is the scFv with the lowest affinity to the protein. However, T32 and the other potential conformation-locking scFvs showed a decreased binding to the SAFit-loaded BLI biosensor when the FKBP51-scFv complex was analyzed (Figure 6B).

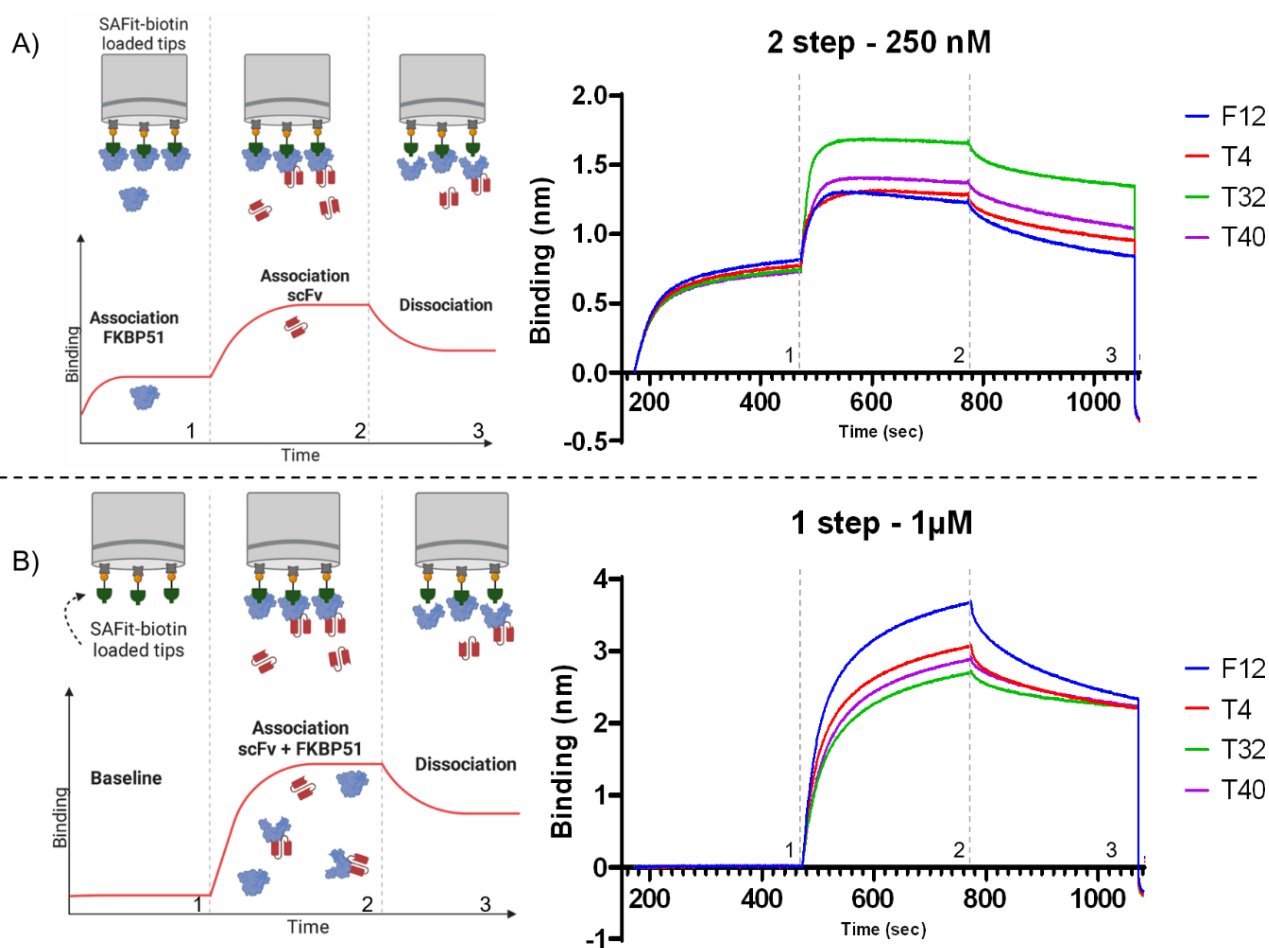


Figure 6. BLI-assisted substrate binding assay. SAFit-biotin was loaded onto SAX biosensors and subsequently associated to A) 250 nM solution of FKBP51, followed by a second association step of 250 nM of each scFv; or B) 250 nM solution of FKBP51 preincubated with 1 μ M of each scFv (5X excess). The two-step association assay (A) resulted in a binding pattern of the scFv that corresponds to the calculated affinity, while the one-step association assay (B) resulted in a higher binding of F12, the low affinity no conformation-locking scFv compared to the T32, T4 and T40, the potential conformation-locking scFvs with higher binding affinities.

In a second test, the F12 and T32 scFvs were tested with a different binding order. SAX biosensors loaded with biotinylated FKBP51 were associated with 1 μ M of each scFv. Once again, this first association presented the

expected binding pattern which corresponds to the binding affinity of each scFv to FKBP51. A second association step with SAFit1 confirmed that this conformation-specific ligand binds with higher affinity to FKBP51 when F12 is bound than when the conformation-stabilizing T32 is bound. Moreover, a DMSO association step was done to discard any effects of the DMSO content in the ligand solutions (Figure 7). Notably, the small molecule SAFit1 or SAFit-biotin produces a signal during BLI experiments that does not correlate to layer thickness, but most probably to light absorption/reflection. This effect is confirmed in Figure S13 by the loading of SAFit-biotin (without protein) which results in a signal of 1.5 nm in approximately 100 seconds of loading.

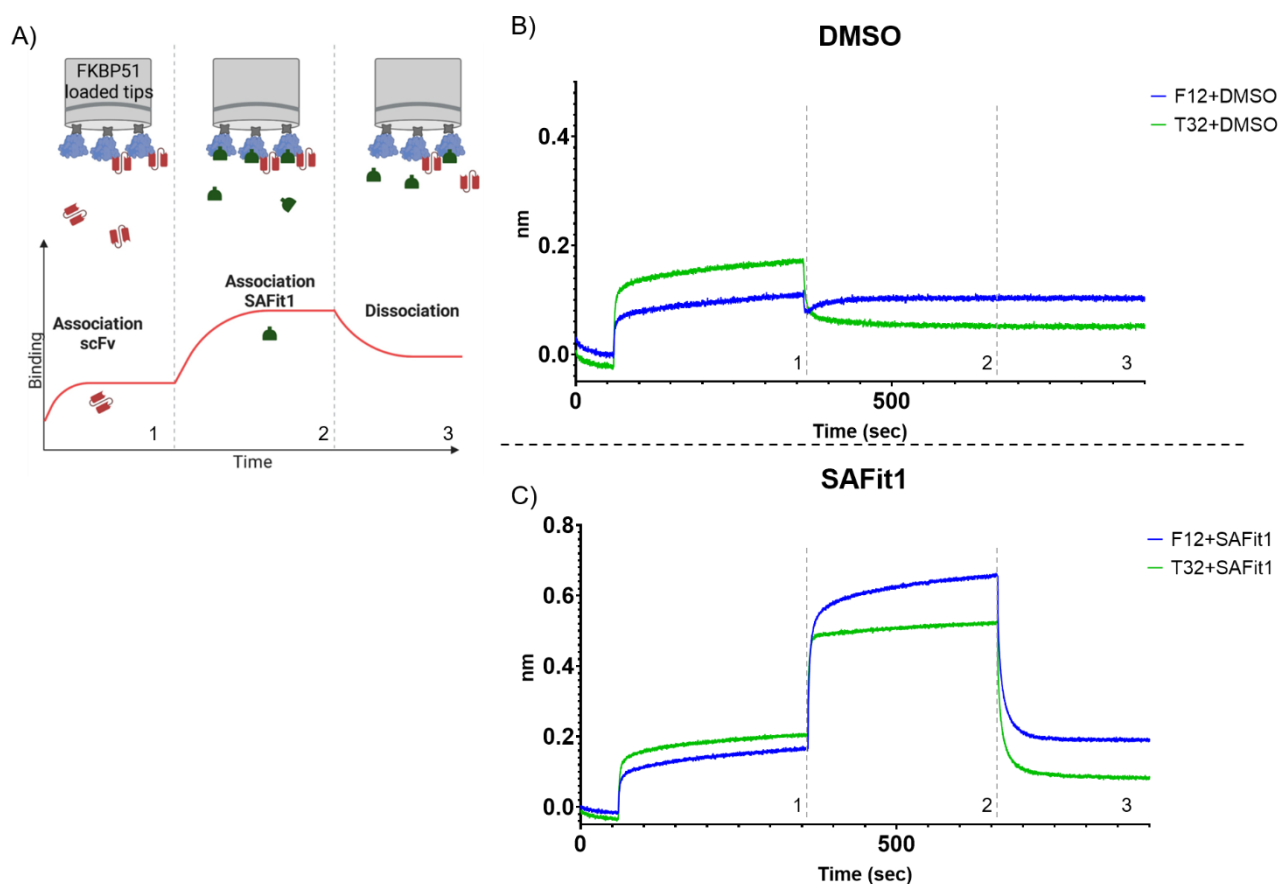


Figure 7. BLI-assisted substrate binding assay. Biotinylated FKBP51 was loaded onto SAX biosensors and subsequently associated to B) 1 μ M of the scFvs, followed by a second association step of DMSO as a negative control; or C) 1 μ M of the scFvs, followed by a second association step of 500 nM SAFit1.

In a third experiment, we aimed to elucidate the effect of T32 on the conformation of FKBP51 in a ligand-bound state by a competitive BLI assay. In the previous experiments, the scFv-FKBP51 complex was first formed and then the ligand binding was measured. Conversely, 500 nM FKBP51 was first incubated with 500 nM of either FK[431] tracer, which binds FKBP51 in the F67ⁱⁿ-conformation, or SAFit1 for 30 min and then, the scFvs were added to a final concentration of 500 nM. The SAX biosensors were then loaded with SAFit-biotin, the biotinylated version of SAFit1 which binds to the F67^{out}-conformation of FKBP51. In the first part of the experiment, the binding of FKBP51 without scFv and with F12 showed no significant difference in the layer thickness in the presence or absence of FK[431] tracer (Figure 8A). Only a subtle decrease in binding was observed. On the

other hand, the FK[431] tracer-bound FKBP51 in the presence of T32 displayed reduced binding to the SAFit loaded tips compared to the complex lacking FK[431] tracer (Figure 8A). The FK[431] tracer binds the F67ⁱⁿ-conformation, which after the possible conformation-locking with T32, was stably bound to the protein (stabilized F67ⁱⁿ-conformation) hindering the binding to SAFit1, a F67^{out}-conformation ligand.

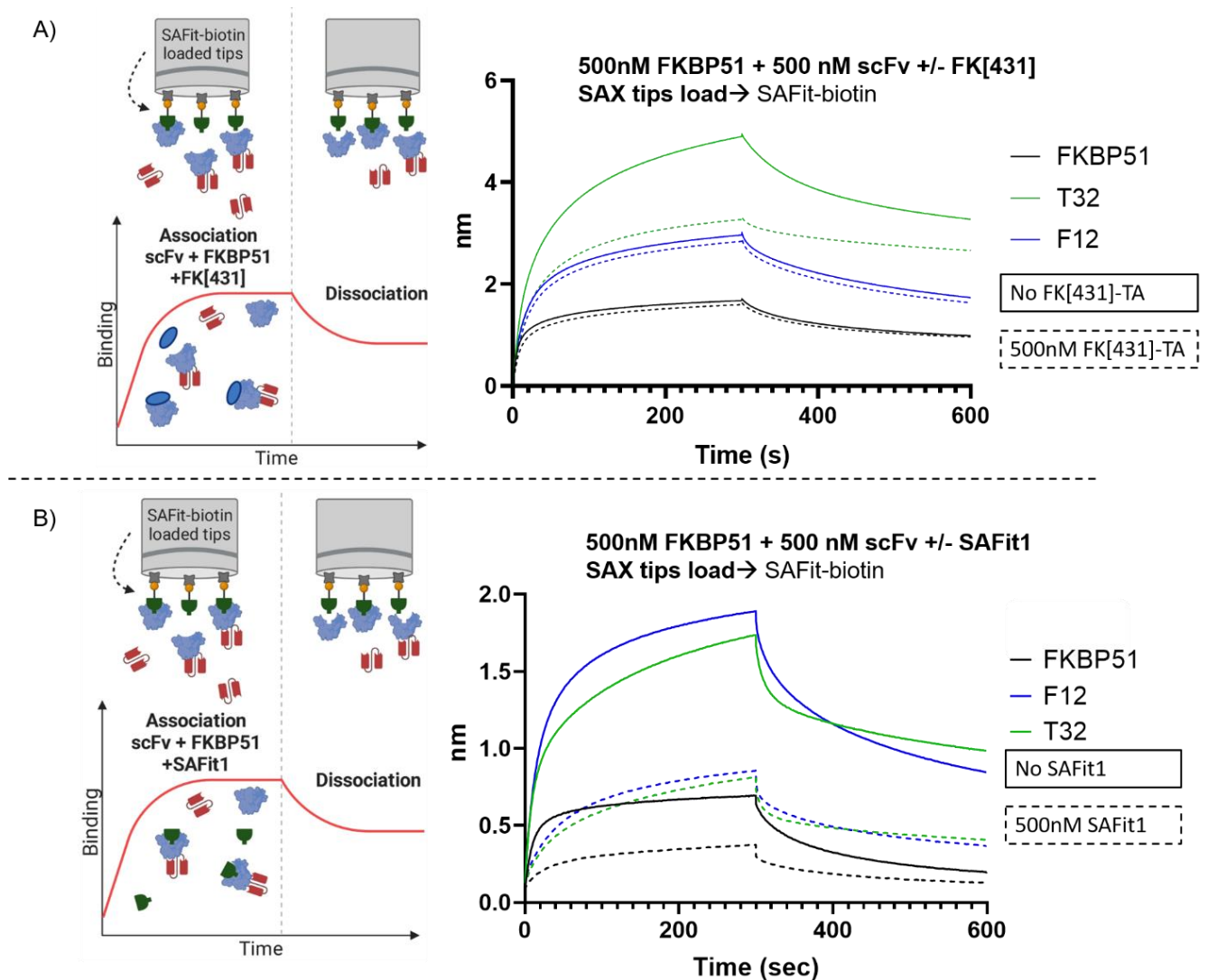


Figure 8. BLI-assisted competitive binding assay. SAFit-biotin was loaded onto SAX biosensors and subsequently associated to a solution with A) 500 nM FKBP51, 500 nM scFvs (F12 or T32) and 0 or 500 nM of FK[431] tracer; or B) 500 nM FKBP51, 500 nM scFvs (F12 or T32) and 0 or 500 nM of SAFit1.

In contrast, when the SAFit-loaded biosensor competed with the SAFit1-FKBP51-scFv complex for the FKBP51 binding pocket, both F12 and T32 presented similar results (Figure 8B), but reduced layer thickness compared to the addition of competitor FK[431]. Because both ligands are virtually identical, competition for the binding pocket is more dynamic than competition with FK[431] tracer, as the binding conformation required for the two SAFit ligands is the same (F67^{out}).

To verify whether the binding of the scFv to the ligand-FKBP51 complex changes depending on which ligand is bound (or to the apo-state), FP experiments were effectuated (Figure S7). This experiment showed that the affinity of both scFvs remained largely unchanged independent of the ligands bound to it, meaning that the different binding profiles to the ligands after scFv binding do not correlate to the ligand-bound conformation of the protein.

A Hydrogen/Deuterium eXchange Mass Spectrometry (HDX-MS) experiment was performed to map the binding epitope of T32 on FKBP51 and analyze the dynamic properties of FKBP51 after T32 binding (Figure 9). The epitope was determined to be in the region between P47-Y57, G82, T96-G100, and L135-E140 (Figure 10A). Moreover, in the region spanning N63 to S70 (colored orange in Figure 10A) at least one amino acid changed its orientation after T32 binding. This was the only region showing an increased deuteration compared to the FKBP51 measurement without T32. This region contains F67 and D68, the two residues responsible for the FKBP51 transient binding pocket formation which facilitates SAFit and macrocyclic ligands binding. The epitope and the identified deuterated region are far away from each other discarding the possibility of a direct contact of the T32 scFv with the N63 to S70 region. Finally, the ColabFold tool of COSMIC2 gateway was used to create a protein-protein molecular docking model of the T32 scFv with the FK1 domain of FKBP51 (Figure 10B) [80]. This model confirmed interactions formed in the region determined by the HDX-MS experiments. The T32 scFv forms polar contacts with E45, D51, K52, D136, D138, and E140 (Figure S16A).

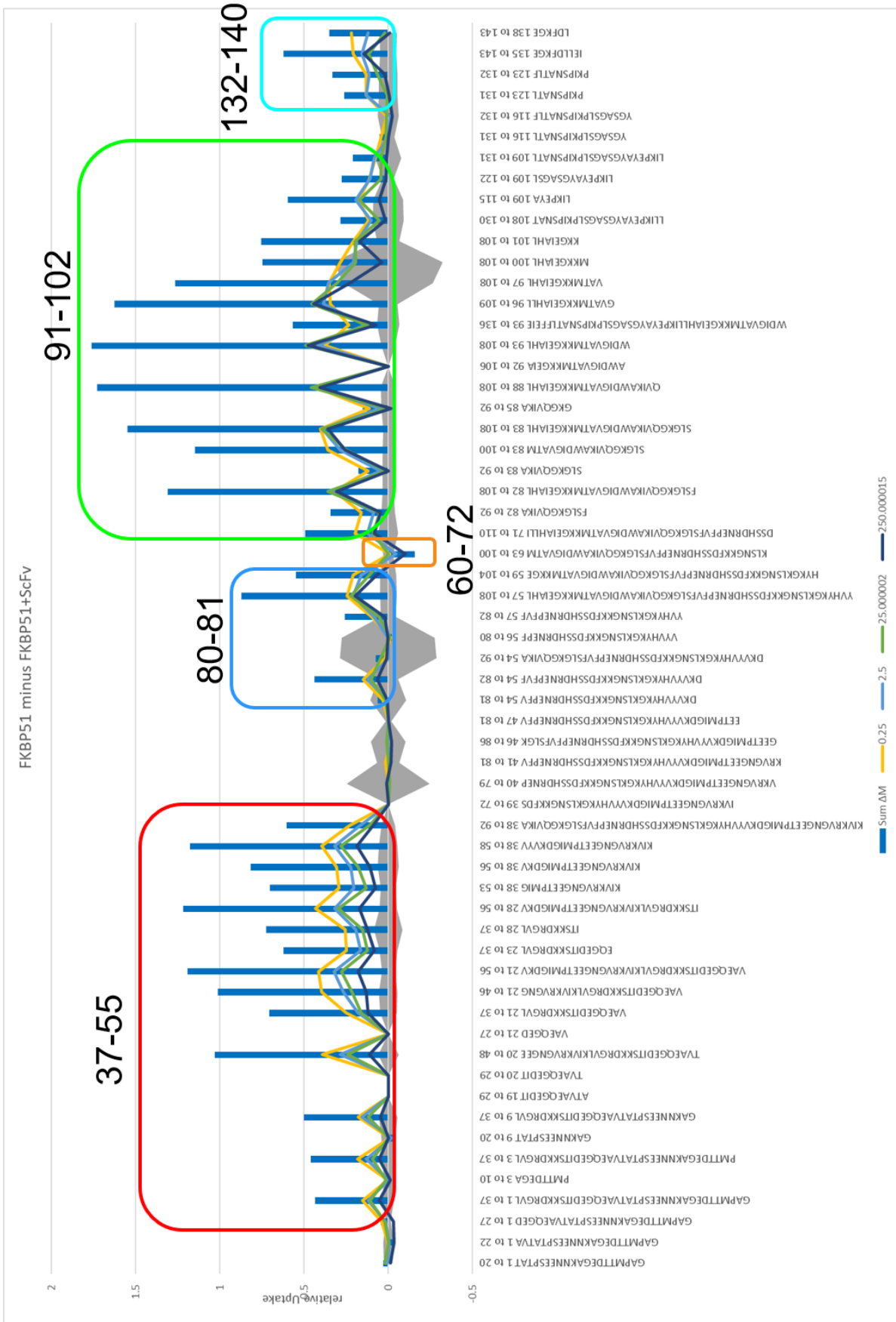


Figure 9. Relative butterfly plot of HDX-MS experiments for FKBP51 minus the FKBP51-T32 complex. These plots show deuterium uptake within a peptide fragment of FKBP51 with and without T32.

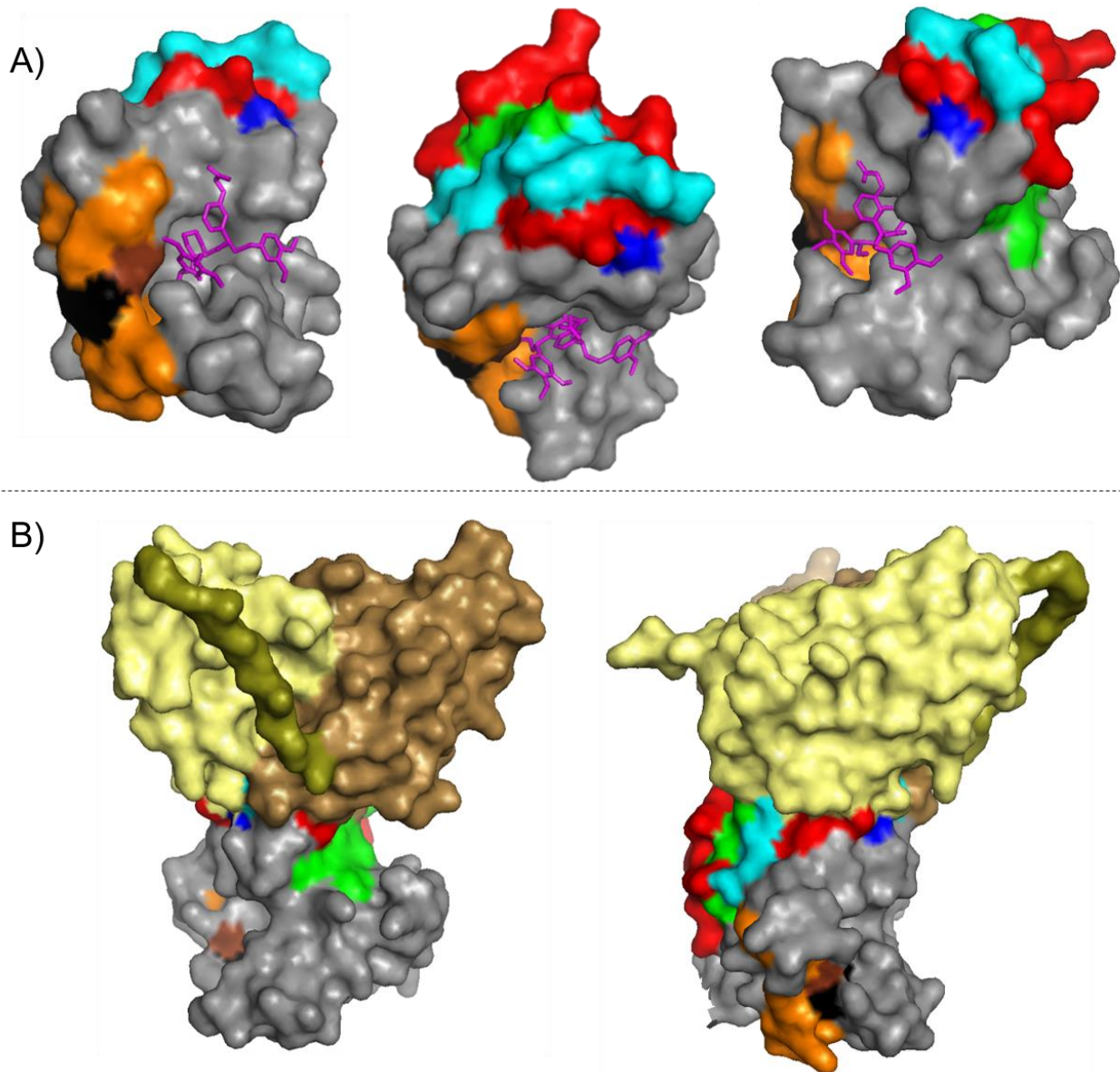


Figure 10. Surface representation of FK1 domain of FKBP51 indicating the determined epitope by HDX-MS. A) FK1 in complex with iFit1 in pink (PDB: 4TW6) showing the epitope region where T32 binds in red, blue, green and cyan (colors correspond to the regions identified in Figure 9). In orange the region with higher deuteration uptake after T32 binding which include residues F67 and D68 in black and brown, respectively. B) The T32-FK1 complex simulated with the ColabFold tool of COSMIC2 [80]. The epitope determined by HDX-MS is illustrated in the same colors, and the T32 scFv binding over a section of the determined region is indicated in pale yellow (V_H), light brown (V_L) and the (Gly₄Ser)₃ linker in olive green.

FKBP51 binding affibodies

With the goal of transferring the work done with the chicken-derived scFvs to an equivalent platform and obtain molecules able to bind with high affinity FKBP51 with the potential to act as conformation-locking molecules, an affibody synthetic library was screened against FKBP51.

A synthetic affibody *E. coli* display library with a diversity of 1×10^{11} cells was generated at the Division of Protein Engineering of the KTH Royal Institute of Technology (Stockholm, Sweden). To obtain high-affinity FKBP51 binders with no effect on ligand binding, the library was screened for two rounds via MACS and four rounds with either FACS or MACS (six rounds in total) using decreasing concentrations of FKBP51 (500 nM and 200 nM) (Figure 3 and Figure 4). After each round, the library output was analyzed by flow cytometry to evaluate the enrichment of an *E. coli* population carrying the genes for affibodies recognizing FKBP51 (Figure 11A). In the sixth round, single clones were sorted into two 96-well plates. Each sample was analyzed by flow cytometry and 96 positive clones from the two plates were sent for sequencing. Nine different affibodies were identified, named A1-A9 (Figure S10). The sequencing results showed a strong enrichment of clone A1, as it appeared in 87 out of 96 samples.

In parallel, a second independent sorting campaign was done with the same initial affibody library. However, the screening strategy changed to a ligand-dependent MACS. Here, the goal was to capture affibodies which bind FKBP51, but at the same time, the bound protein binds with high affinity the SAFit-loaded magnetic beads (Figure 3).

The library was screened for four rounds via MACS, and one last round with FACS (five rounds in total). After each round, the library output was analyzed by flow cytometry to evaluate the enrichment of an *E. coli* population with affibodies that potentially influence allosterically the conformation of FKBP51 and facilitate the binding of SAFit ligand (Figure 11B). On the fifth round via FACS, single clones were sorted into two 96-well plates. Each sample was analyzed by flow cytometry and 96 positive clones from the two plates were sent for sequencing. After comparing all sequences, over 30 different affibodies were found, but only 17 different affibodies were selected to be further analyzed named S1-S17 (Figure S11 and Figure S12).

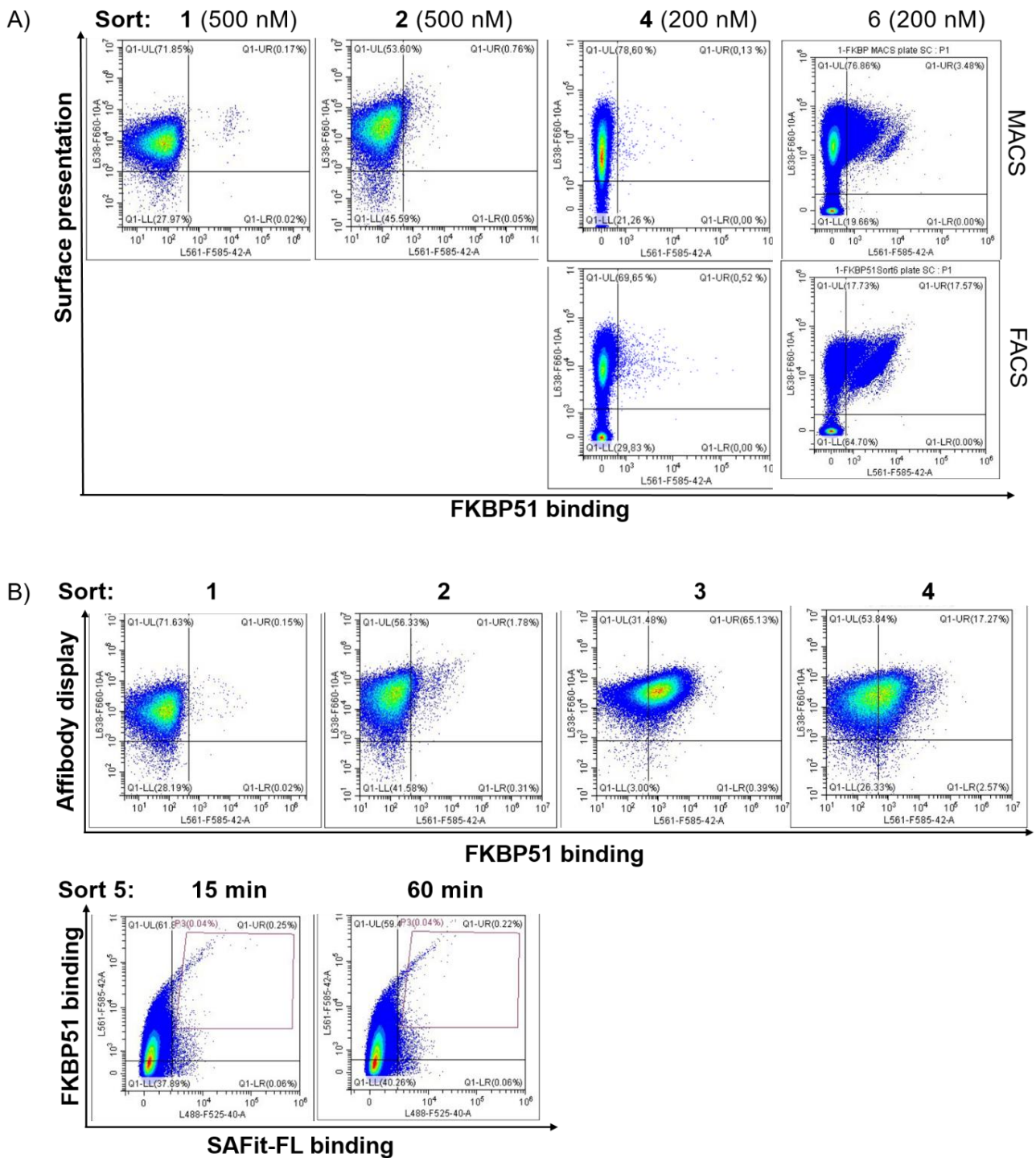


Figure 11. FKBP51-binding affibody *E. coli* display library screening and sorting. A) High-affinity binder screening: cells showing both surface presentation (ABD detection) and FKBP51 binding signal (SAPE) were sorted for six rounds to enrich the population of protein binder affibodies. FACS sorting gate was set to capture approximately 1% of the FKBP51-binding population and used for subsequent sorting rounds; MACS rounds were only controlled but not sorted by flow cytometry. B) Ligand dependent screening: cells showing both surface presentation (ABD detection) and FKBP51 binding signal (SAPE) were sorted for four rounds to enrich the population of protein and SAFit binder affibodies via MACS and controlled via flow cytometry. A fifth round was sorted via FACS to capture approximately 1% of the FKBP51-binding and SAFit-FL binding population.

All identified affibodies were cloned into pET45b+ plasmids (Figure S4), expressed in *E. coli* BL21(DE3), and purified by immobilized metal ion affinity chromatography. However, A5 and A7 were not able to be expressed and purified to be further analyzed. From the ligand-dependent screening, only S2 was successfully expressed. The expression and purification of the other affibodies was unsuccessful as the protein amount was very low, and the elution fraction from the IMAC purification via ÄKTA system contained many other *E. coli* proteins in high concentrations.

A first test showed good binding of A1, A2, and S2, and weaker binding of A3, while the rest showed no measurable binding to FKBP51 (Figure S14). Affinity measurements via BLI from the five affibodies resulted in K_D values of: A1= 24 nM, A2=51 nM, A3=5500 nM, and S2=150 nM (Figure S14). Similarly, affinity measurements via FP resulted in K_D values of: A1= 13 nM, A2=93 nM, and S2=1900 nM (Figure S14). Additionally, the affibody with the highest affinity to FKBP51 (A1) was tested for FKBP52 and FKBP12 binding, resulting in no binding to FKBP12 and a $K_D = >3000$ nM to FKBP52 (Figure S15).

Besides, the affibodies were tested for binding pocket blocking by incubating each affibody in a 5-fold excess with FKBP51. The affibody-FKBP51 complex was then measured via BLI with SAFit-loaded biosensors (Figure 12A). From these results, no apparent blocking of the FK1 binding pocket was observed. In a last experiment, the influence of the affibodies on substrate binding was evaluated via BLI (Figure 12B). Each affibody was added to a final concentration of 500 nM into a preincubated FKBP51-ligand complex with either FK[431] tracer or SAFit1, to then be associated to SAFit-biotin loaded tips. The affibodies identified during the high-affinity screening (A1-3) did not exhibit a clear effect on substrate binding when compared to the samples without affibodies. On the other hand, S2 showed a distinct influence on the association to the BLI tips.

Finally, to determine the binding epitope of the S2 affibody to FKBP51, the ColabFold tool of COSMIC2 gateway was used to create a protein-protein molecular docking model [80]. The model output revealed a possible interaction of S2 with the region of S27, E44-I49, G82-G84, and D91-T96 of FKBP51 (Figure 13). Confirmed polar contacts were found with S27, E44, T46, I49, K88, and A95 (Figure S16B).

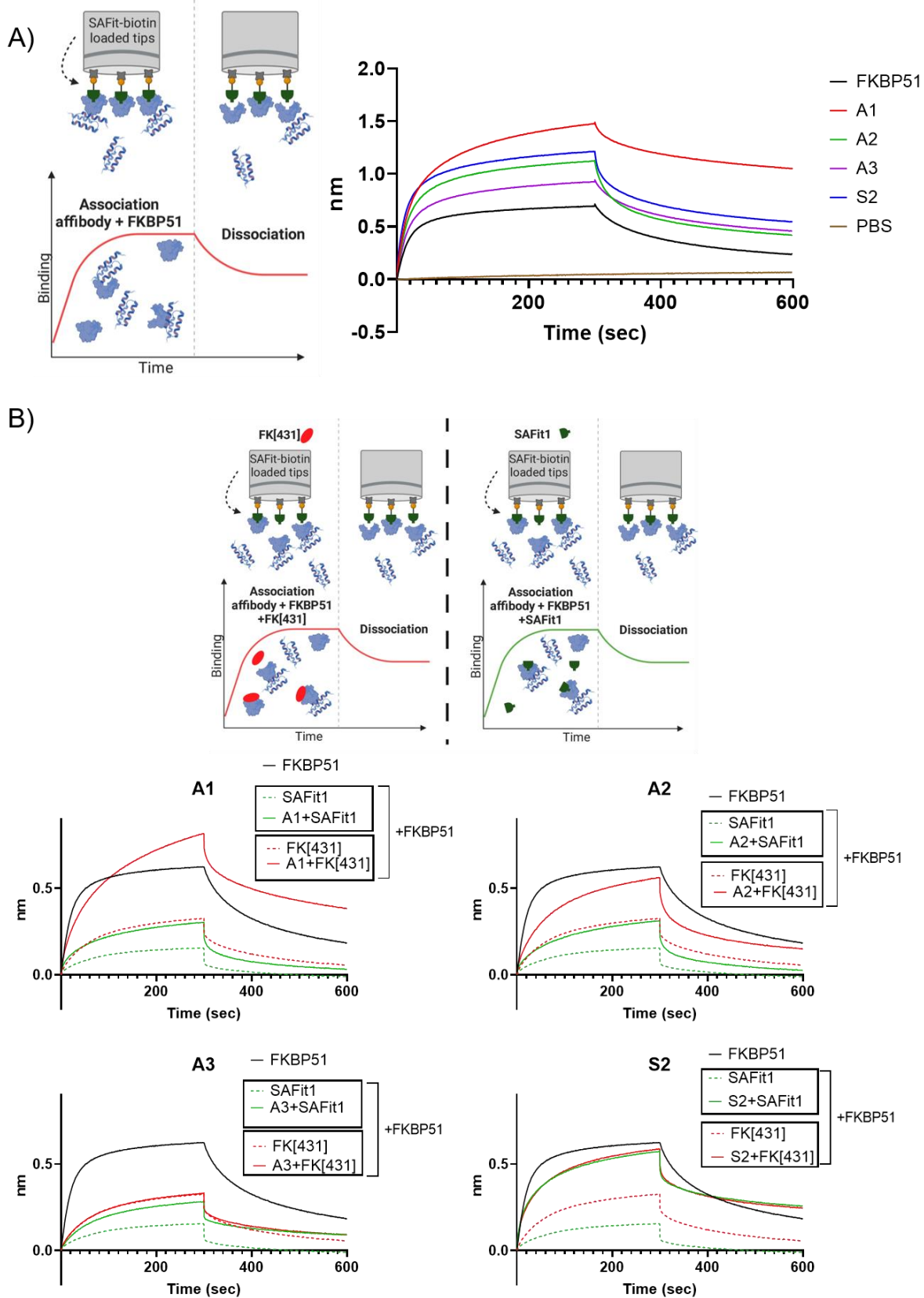


Figure 12. A) BLI assay with a 5-fold excess of affibody to FKBP51 to test the effects on blocking the binding of SAFit-loaded tips B) BLI-assisted competitive binding assay. SAFit-biotin was loaded onto SAX biosensors and subsequently associated to a solution with 200 nM FKBP51, 500 nM affibodies and 0 or 500 nM of FK[431] tracer (red solid lines) or 500 nM of SAFit1 (green solid lines). Dotted lines represent the controls with ligand FK[431] tracer (red dotted lines) or SAFit1 (green dotted lines) but no affibody, and the black line is the control of FKBP binding to the SAFit-loaded tips without affibodies nor ligand.

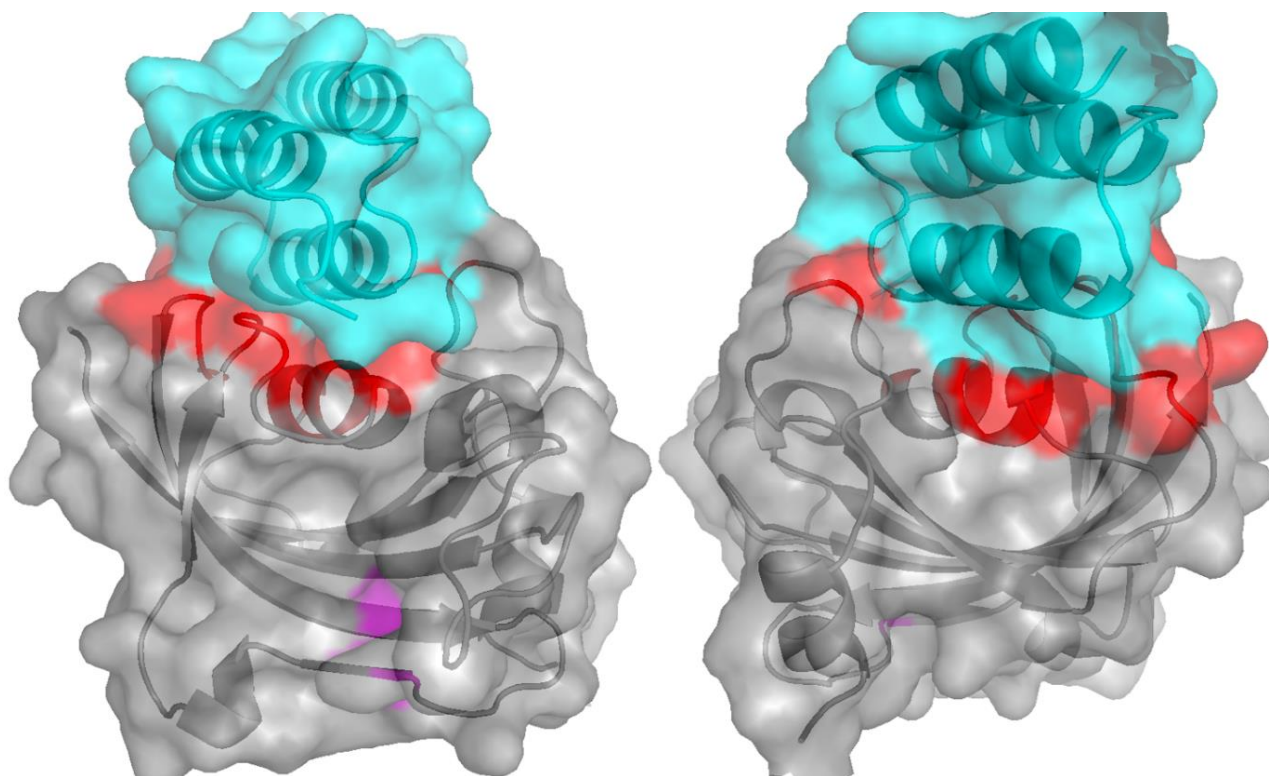


Figure 13. Surface representation of FK1 domain of FKBP51 (gray) in complex with the affibody S2 (cyan) determined with the Colab-Fold tool of COSMIC2[80]. The determined epitope is shown in red and as a reference, F67 is shown in magenta.

Discussion

The FK506-binding protein 51 (FKBP51) has been linked to several stress- and metabolic-related disorders, among others [26–33]. One of the greatest hurdles to creating a molecule able to modulate its activity is the presence of other highly related proteins of the FKBP family, specifically FKBP52. FKBP51 and FKBP52 have a high degree of homology and sequence identity. Moreover, they can both bind the same immunosuppressive drugs FK506 and rapamycin. This is problematic because while FKBP51 is a negative regulator of steroid hormone receptors, FKBP52 has the opposing effect and activates steroid hormone transcription [26, 81]. It has previously been observed that the binding of SAFit-like ligands creates a transient binding pocket of FKBP51. The displacement of phenylalanine 67 from the binding site to an “out” conformation (F67^{out}) is key for the selectivity of this ligand class [47, 82].

In this study, we created a YSD library expressing scFvs derived from the genetic material of a chicken immunized with the human FK1 domain of FKBP51. This library was sorted by FACS to identify scFvs with high affinity to FKBP51 which at the same time, had an effect on the protein conformation to facilitate the binding of fluorescently-labelled conformation-specific tracer SAFit-FL. Besides, we also aimed to identify an scFv able to block the binding pocket of FKBP51 without interacting with other members of the FKBP family.

After five rounds of FACS-based selection using YSD, five different scFvs were identified. T4, T29, T32, and T40 shared the same V_H , while T42 exhibited a unique sequence. Optimal heavy and light chain pairing is necessary for the best affinities, and both chains are codominant in their impact on antigen specificity [83]. Moreover, it has been reported in several studies that V_H - V_L pairing also affects the overall structure of the binding region. Like most proteins, antibodies and antibody fragments are flexible molecules with multiple possible structural conformations. For this reason, the interaction of two domains (V_H and V_L), and subsequent interaction with an antigen, can affect the conformation of the scFvs and antibodies in many ways, which in consequence affects the overall antigen recognition and binding affinity [84–89]. Four scFvs with a shared V_H may be a hint indicating that the V_H is a potent binder with possible conformation-locking properties. However, the different V_L influences in great manner the affinity to the target protein as demonstrated by the FP measurements (Figure S6), and the contact with the epitope may differ as well.

The first BLI measurements confirmed that the layer thickness after scFv binding to the SAFit-FKBP51 fits the data obtained by FP (Figure 6A). The BLI-assisted substrate binding assay where the FKBP51 was incubated with each one of the scFvs showed that F12, the scFv with the lowest binding affinity, was the one that showed the greatest layer thickness, while T32 with a K_D of 29 nM, was the lowest one. In a similar experiment, a SAX biosensor loaded with biotinylated FKBP51, measured a first association step in 1 μ M of the scFvs to then pass to a second association step in 500 nM of SAFit1 (Figure 7B). The results were confirmed once again, the binding of T32 to FKBP51 was stronger than F12 (as suggested by the FP-determined K_D), but SAFit binds better to the F12-FKBP51 complex than to the T32-FKBP51 complex. These results, though contradicting the hypothesis that T32 may have a conformation-locking effect in FKBP51 that facilitates binding of SAFit-like ligands, were complemented with a competitive BLI with two different FKBP51 ligands.

We hypothesize that the conformation-locking of FKBP51 after T32 binding does not necessarily lock the F67^{out} conformation of the protein which is necessary for SAFit-like ligands binding [45], but instead, stabilized the current conformation of FKBP51 at the moment of the interaction (reduced protein flexibility). Data obtained is compatible with a model that upon binding, a high energy barrier is generated that hampers free conversion of conformational states of FKBP51, thereby locking the protein in its current conformer status (Figure 14). During the competitive BLI assay, FKBP51 was preincubated with either SAFit1 (**2**) or FK[431] (**4**) tracer (Figure S5). These two FKBP ligands have different binding mechanisms. The canonical FK[431] binds to the native F67ⁱⁿ conformation of FKBP51, thus binding to FKBP52 and other members of the FKBP family too [90]. In contrast, SAFit1 requires a displacement of the phenylalanine 67 to an outwards conformation; this conformational change is only possible by FKBP51, which is why this ligand family binds selectively to FKBP51 over FKBP52 [45, 46, 90]. After the first incubation, the two different scFvs were added independently to the ligand-FKBP51 complex. The association of these scFv-FKBP51-ligand complexes to SAFit-loaded biosensors corroborated our hypothesis. The FKBP51-FK[431] with and without F12 had little impact on the binding of FKBP51 to the SAFit ligand on the BLI tips. During this association step, the FK[431] tracer was able to freely dissociate from the FKBP51 to then bind the SAFit-loaded biosensors, with a small difference when no FK[431]

tracer was present, being the association slightly better to an unoccupied protein. On the other hand, T32 had a significant effect on the association of FKBP51-FK[431]. The already FK[431]-bound protein had a lower binding to the SAFit loaded tips compared to the non-bound FKBP51 in the presence of T32, demonstrating that either the dissociation of FK[431] tracer is slower or the conformation left by an F67ⁱⁿ binding ligand was not able to shift to F67^{out} due to the interaction with T32.

In contrast, when FKBP51 was preincubated with SAFit1, the SAFit1-FKBP51-scFv complexes had similar behavior for both F12 and T32 bound complexes. Since the fragment of the ligand responsible for FKBP51 binding is the same on both the ligand in solution and the ligand immobilized on the BLI tips, the competition for the binding pocket of FKBP51 was more dynamic. Moreover, because T32 allegedly locked the current conformation of the FKBP51-SAFit1 complex (F67^{out}), the binding to the SAFit-loaded biosensor was facilitated by the already stabilized conformation that is required for binding to this conformation-specific ligand.

With these results, we can then better interpret the findings of the first BLI assays (Figure 6). In this case, T32 appeared to have an inhibitory effect on the binding of the SAFit ligands to FKBP51. Following the evidence from the last experiments, we can now explain this behavior as a locking of the F67ⁱⁿ unbound-state of the protein, which hampered the necessary conformational changes to accommodate the SAFit ligand in the binding pocket of the protein. This phenomenon was not observed after F12 binding or the FKBP51 without scFv.

Compared to FKBP52, the FK1 domain of FKBP51 is a very dynamic protein even in apo-state. NMR analysis of both proteins showed that despite their structural similarity, small differences in the β_3 strand and the β_{4-5} interconnecting loop of FKBP51 make this protein more dynamic and allow it to form a greater number of conformers than FKBP52 [36, 41]. Particularly, residues S70, R73 and, E75 of the β_3 strand revealed a great degree of motion. Besides, cross-strand interactions were identified between Y57 and G59 of the β_2 strand with S70 and D68 of the β_3 strand. Finally, the flexibility of the β_{4-5} loop is mostly due to the two different residues in the whole loop: L119 and S124. Upon mutation of these two residues to the FKBP52 counterparts (P119 and P124), a reduction in motion of the β_{4-5} loop is observed, with an extended effect that reduced the motion of residues in the β_3 strand too [41]. Upon SAFit1 binding, FKBP51 undergoes several conformational changes to accommodate the ligands, being the most prominent, the F67 side chain displacement of the FK1 binding pocket of FKBP51 [51, 82]. Besides, residues K58, K60, F129 in FKBP51 help to stabilize this F67^{out} conformation, while residues spanning from K58 to S62, K66, D68 gained motion to bind SAFit1 [82]. On the other hand, the otherwise flexible β_{4-5} loop is less dynamic in the SAFit1-bound state as it interacts with the ligand and stabilizes its binding [49, 82].

It is important to note that all these residues responsible for the transient binding pocket formation or stabilization of the ligand in the bound state, may be affected by the binding of the T32 scFv to allosterically modulate FKBP51 conformation. In this regard, a plausible explanation for the results obtained in this work is that the T32 obstructs the free motion of the β_{4-5} loop. If β_{4-5} loop flexibility is necessary to accommodate SAFit1 and

the same time allow the F67^{out} motion, hindering this process would reduce the binding efficiency of SAFit1 into the protein as shown in Figure 6. Furthermore, the possibility that the scFv binds preferentially to a ligand-bound protein was rejected by a FP assay (Figure S7), meaning that the change in the layer thickness of the BLI experiments relies only on the effect that the scFv has on the ligand, and not on conformation-selective affinity.

The HDX-MS experiments further confirmed the effect of T32 as an allosteric modulator of the FKBP51 transient binding pocket. The binding epitope of T32 is located mostly on the β_{1-2} , β_4 strands and the C-terminal region of the FK1 domain of FKBP51. These regions are considerably distanced from the K60 to D72 region which was conformationally rearranged allowing for a higher deuteration occupancy of at least one amino acid in the identified region. The epitope region does not comprise amino acids reported to interact with F67 to maintain it in an “In” conformation. Specifically, the F67 phenyl ring which is stabilized under the tip of the β_{4-5} loop (K121-P123) [35]. Hence, this loop is probably still able to move freely to allow the F67^{out} conformation.

Moreover, published NMR experiments have also identified K60, K66, F67, and D68 as highly dynamic residues after analyzing FKBP51 mutants that destabilize the F67ⁱⁿ conformation [14, 51, 91]. These residues fall into the identified region which presented a conformational change after T32 binding. The butterfly plot (Figure 10) provided enough information to narrow down the dynamic region to 12 amino acids. However, because of the pepsin cleaving pattern, the peptides analyzed overlapped in regions where the deuteration signal is greater for the FKBP51 alone (e.g. H56-E101) with the region where deuteration of the FKBP51-T32 complex was higher (K60-D72). This resulted in a reduction of the deuterium intake signal of the FKBP51-T32 complex. The averaged signal was still sufficient to determine a conformational change of the region containing F67 and D68. This experiment suggests a possible conformational rearrangement of the region involved in the sub-pocket creation which allows conformation-specific ligand binding. Due to the design of BLI and FACS experiments, this effect may not be apparent, as the incubation times of the FKBP51-T32 complex with T32 allow an equilibrium of both FKBP51-T32 complex and ligand binding. Moreover, the F67^{out} conformation does not impede FK[431] tracer binding, but only a reduction in the affinity to the ligand which still can bind FKBP51 [14].

To complement the data derived from the HDX-MS experiment, a molecular docking of T32 with the FK1 domain of FKBP51 suggested a binding site which matches the region determined by HDX-MS. The analysis of the model showed polar interactions of T32 with residues E45, D51, K52, D136, D138, and E140 of FKBP51 (Figure S16A). As mentioned before, residues K58, K60, F129, and β_{4-5} loop in FKBP51 are essential for SAFit1 ligand binding [45]. The here presented experiments do not suggest interactions of T32 scFv with these precise residues, which indicates that any possible conformational change that destabilizes the closed conformation of FKBP51, may happen due to allosteric effects after T32 binding. Additionally, T32 is highly selective for FKBP51 over FKBP52 and FKBP12, which makes this scFv not only useful for conformation-locking purposes, but also for biochemical test to differentiate between FKBP51 and other members of the FKBP family.

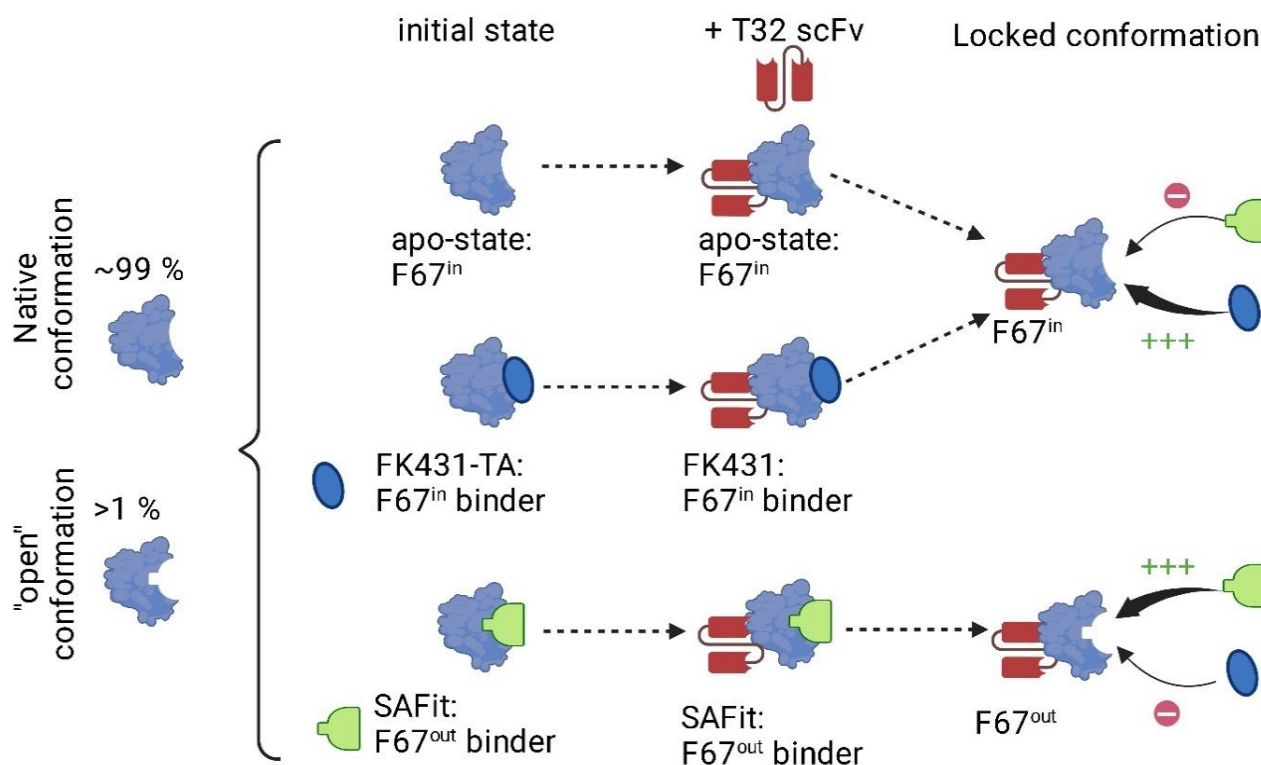


Figure 14. Proposed model scheme of T32 assisted conformation-locking of FKBP51. This model proposes a stabilization of the FKBP51 at the moment of T32 binding, hindering the transition of F67ⁱⁿ to F67^{out}, or vice versa. If T32 binds to the apo- or FK[431]-bound state of FKBP51, F67ⁱⁿ is stabilized, but if T32 binds the SAFit1-bound state of FKBP51, F67^{out} is stabilized. FK[431] and SAFit1 are depicted as blue and green molecules, respectively.

The concept of conformation-locking antibodies is not uncommon and has already been successfully used to enhance the affinity of weak ligands to a target protein by allosterically stabilizing a binding pocket [58], for allosteric amyloidogenesis [92, 93], caspase conformation-specific Fabs [57] and antibody fragments to crystallize a protein in a specific conformation [94].

The screening of affibodies yielded four different molecules able to bind FKBP51. A1, the affibody with the highest affinity to FKBP51 is also selective to FKBP51 over FKBP52 and FKBP12 (Figure S15). The BLI assays showed that the affibodies have no apparent influence on blocking ligand binding, as none of them reduced the binding of FKBP51 to the SAFit-loaded BLI biosensors. A more complex result was obtained from the competitive BLI assay. The incubation of FKBP51 with an excess of FK[431] or SAFit1 followed by a second incubation with the affibodies to then be associated to SAFit-loaded BLI tips delivered different results. FK[431] or SAFit1 bound to FKBP51 without affibodies reduced the binding of the protein to the BLI biosensor. The reported affinity of FKBP51 to SAFit1 and FK[431] is 4 nM and 57 nM, respectively [95]. This is confirmed by the control measurements in our competitive experiment which showed that FK[431] is easier to displace than SAFit1 to bind the SAFit-loaded BLI biosensors (Figure 12B). In the same manner, the FKBP51-ligand-affibody complex has the same behavior when the affibodies A1-3 are bound, only with a higher layer thickness because of the affibody binding. The binding signal was higher for A1 and A2, both exhibiting a better binding affinity than A3, which showed a smaller layer thickness compared to the controls without affibody. However, affibody

S2 has a different effect on ligand binding, as the association to the SAFit tips was identical for the two different FKBP51-ligand complexes.

The S2 affibody was identified when the initial library was screened to obtain molecules that provide an enhanced binding of FKBP51 to SAFit. Normally, it would be expected that the complex with FK[431] dissociates faster from FKBP51 than the SAFit1-FKBP51 complex to bind the SAFit-loaded tips. However, this effect was partially suppressed by S2, which may have a similar effect as the T32 scFv. Upon binding, S2 may help stabilize the conformation of FKBP51 in the bound state with the current ligand, and in consequence, decrease the number of FKBP51 available to bind the SAFit loaded tips, or it locks the F67ⁱⁿ conformation which hinders the binding of SAFit ligands [14]. Alternatively, it might also be possible that S2 influences FKBP51, and that locks the F67^{out} conformation facilitating the binding of SAFit-biotin after dissociation of the FKBP51-SAFit1 complex. A molecular docking of affibody S2 with the FK1 domain of FKBP51 suggested a binding site on regions between the β_1 and β_2 strands, and the α helix of FKBP51. The analysis of the model showed polar interactions of S2 with residues S27, E44, T46, I49, K88, and A95 of FKBP51 (Figure S16B). In the same way as for T32, this molecular docking of the S2-FKBP51 complex does not display interactions with residues directly involved with the formation of the FKBP51 transient binding pocket, which indicates that any possible conformational change of the binding pocket caused by S2 binding, may happen due to allosteric effects.

ScFvs and affibodies are molecules with potential in research and clinical applications. In this work, two different molecules influencing the ligand binding of FKBP51 were identified: T32, a chicken-derived scFv screened via FACS from a YSD library, and S2, an affibody from a synthetic library screened via MACS from an *E. coli* display library. Both molecules show promising results for the conformation-locking of FKBP51, but further testing and characterization is necessary to fully understand their allosteric effects on the protein. The T32 scFv and S2 affibody can be used to stabilize a low-populated FKBP51 conformer and facilitate the screening of novel small molecules for the selective inhibition of FKBP51. Moreover, a set of scFvs and affibodies with high affinity to FKBP51 were identified. This first generation of molecules can be further optimized to improve their affinity to the target protein and can be used in the future as research and characterization tools of FKBP51.

References

1. Huber R (1987) Flexibility and rigidity, requirements for the function of proteins and protein pigment complexes. *Biochem Soc Trans* 15:1009–1020. <https://doi.org/10.1042/bst0151009>
2. Teilum K, Olsen JG, Kragelund BB (2009) Functional aspects of protein flexibility. *Cellular and Molecular Life Sciences* 66:2231–2247. <https://doi.org/10.1007/s00018-009-0014-6>
3. Kumar A, Butler BM, Kumar S, Ozkan SB (2015) Integration of structural dynamics and molecular evolution via protein interaction networks: a new era in genomic medicine. *Curr Opin Struct Biol* 35:135–142. <https://doi.org/10.1016/j.sbi.2015.11.002>
4. Goodey NM, Benkovic SJ (2008) Allosteric regulation and catalysis emerge via a common route. *Nat Chem Biol* 4:474–482. <https://doi.org/10.1038/nchembio.98>
5. Ma B, Kumar S, Tsai C-J, Nussinov R (1999) Folding funnels and binding mechanisms. *Protein Engineering, Design and Selection* 12:713–720. <https://doi.org/10.1093/protein/12.9.713>
6. Hilser VJ, Thompson EB (2007) Intrinsic disorder as a mechanism to optimize allosteric coupling in proteins. *Proceedings of the National Academy of Sciences* 104:8311–8315. <https://doi.org/10.1073/pnas.0700329104>
7. Liu J, Nussinov R (2016) Allostery: An Overview of Its History, Concepts, Methods, and Applications. *PLoS Comput Biol* 12:e1004966. <https://doi.org/10.1371/journal.pcbi.1004966>
8. Nussinov R, Tsai C-J (2015) Allostery without a conformational change? Revisiting the paradigm. *Curr Opin Struct Biol* 30:17–24. <https://doi.org/10.1016/j.sbi.2014.11.005>
9. Monod J, Wyman J, Changeux J-P (1965) On the nature of allosteric transitions: A plausible model. *J Mol Biol* 12:88–118. [https://doi.org/10.1016/S0022-2836\(65\)80285-6](https://doi.org/10.1016/S0022-2836(65)80285-6)
10. Monod J, Jacob F (1961) General Conclusions: Teleonomic Mechanisms in Cellular Metabolism, Growth, and Differentiation. *Cold Spring Harb Symp Quant Biol* 26:389–401. <https://doi.org/10.1101/SQB.1961.026.01.048>
11. Suplatov D, Švedas V (2015) Study of functional and allosteric sites in protein superfamilies. *Acta Naturae* 7:34–45. <https://doi.org/10.32607/20758251-2015-7-4-34-45>
12. McLaughlin Jr RN, Poelwijk FJ, Raman A, et al (2012) The spatial architecture of protein function and adaptation. *Nature* 491:138–142. <https://doi.org/10.1038/nature11500>
13. Xiao S, Verkhivker GM, Tao P (2023) Machine learning and protein allostery. *Trends Biochem Sci* 48:375–390. <https://doi.org/10.1016/j.tibs.2022.12.001>
14. Lerma Romero JA, Meyners C, Christmann A, et al (2022) Binding pocket stabilization by high-throughput screening of yeast display libraries. *Front Mol Biosci* 9. <https://doi.org/10.3389/fmolb.2022.1023131>
15. Huggins DJ, Sherman W, Tidor B (2012) Rational Approaches to Improving Selectivity in Drug Design. *J Med Chem* 55:1424–1444. <https://doi.org/10.1021/jm2010332>
16. Xie J, Zhang W, Zhu X, et al (2023) Coevolution-based prediction of key allosteric residues for protein function regulation. *Elife* 12:. <https://doi.org/10.7554/eLife.81850>
17. Burford NT, Clark MJ, Wehrman TS, et al (2013) Discovery of positive allosteric modulators and silent allosteric modulators of the μ -opioid receptor. *Proc Natl Acad Sci U S A* 110:10830–10835. <https://doi.org/10.1073/pnas.1300393110>
18. Manley LJ, Lin MM (2023) Kinetic and thermodynamic allostery in the Ras protein family. *Biophys J*. <https://doi.org/10.1016/j.bpj.2023.08.010>
19. Dima RI (2006) Determination of network of residues that regulate allostery in protein families using sequence analysis. *Protein Science* 15:258–268. <https://doi.org/10.1110/ps.051767306>

20. Samanta R, Sanghvi N, Beckett D, Matysiak S (2023) Emergence of allostery through reorganization of protein residue network architecture. *J Chem Phys* 158:. <https://doi.org/10.1063/5.0136010>
21. Todd AE, Orengo CA, Thornton JM (2001) Evolution of function in protein superfamilies, from a structural perspective 11 Edited by A. R. Fersht. *J Mol Biol* 307:1113–1143. <https://doi.org/10.1006/jmbi.2001.4513>
22. Wang T, Bisson WH, Mäser P, et al (2014) Differences in Conformational Dynamics between *Plasmodium falciparum* and Human Hsp90 Orthologues Enable the Structure-Based Discovery of Pathogen-Selective Inhibitors. *J Med Chem* 57:2524–2535. <https://doi.org/10.1021/jm401801t>
23. Aleksandrov A, Simonson T (2010) Molecular Dynamics Simulations Show That Conformational Selection Governs the Binding Preferences of Imatinib for Several Tyrosine Kinases. *Journal of Biological Chemistry* 285:13807–13815. <https://doi.org/10.1074/jbc.M110.109660>
24. Hollingsworth SA, Kelly B, Valant C, et al (2019) Cryptic pocket formation underlies allosteric modulator selectivity at muscarinic GPCRs. *Nat Commun* 10:1–9. <https://doi.org/10.1038/s41467-019-11062-7>
25. Moroni E, Paladino A, Colombo G (2015) The Dynamics of Drug Discovery. *Curr Top Med Chem* 15:2043–2055. <https://doi.org/10.2174/1568026615666150519102950>
26. Storer CL, Dickey CA, Galigniana MD, et al (2011) FKBP51 and FKBP52 in signaling and disease. *Trends in Endocrinology & Metabolism* 22:481–490. <https://doi.org/10.1016/j.tem.2011.08.001>
27. Häusl AS, Balsevich G, Gassen NC, Schmidt M V (2019) Focus on FKBP51 : A molecular link between stress and metabolic disorders. *Mol Metab* 29:170–181. <https://doi.org/10.1016/j.molmet.2019.09.003>
28. Hartmann J, Wagner K V., Gaali S, et al (2015) Pharmacological inhibition of the psychiatric risk factor FKBP51 has anxiolytic properties. *Journal of Neuroscience* 35:9007–9016. <https://doi.org/10.1523/JNEUROSCI.4024-14.2015>
29. Scharf SH, Liebl C, Binder EB, et al (2011) Expression and Regulation of the *Fkbp5* Gene in the Adult Mouse Brain. *PLoS One* 6:e16883. <https://doi.org/10.1371/journal.pone.0016883>
30. Stechschulte LA, Sanchez ER (2011) FKBP51—a selective modulator of glucocorticoid and androgen sensitivity. *Curr Opin Pharmacol* 11:332–337. <https://doi.org/10.1016/j.coph.2011.04.012>
31. Maiarù M, Morgan OB, Mao T, et al (2018) The stress regulator FKBP51: a novel and promising druggable target for the treatment of persistent pain states across sexes. *Pain* 159:1224–1234. <https://doi.org/10.1097/j.pain.0000000000001204>
32. O’Leary JC, Dharia S, Blair LJ, et al (2011) A New Anti-Depressive Strategy for the Elderly: Ablation of FKBP5/FKBP51. *PLoS One* 6:e24840. <https://doi.org/10.1371/journal.pone.0024840>
33. Wang L, Pavlov PF, Kumar R, Winblad B (2020) FKBP51-Hsp90 complex as a novel therapeutic target for Alzheimer’s disease. *Alzheimer’s & Dementia* 16:. <https://doi.org/10.1002/alz.042684>
34. Barent RL, Nair SC, Carr DC, et al (1998) Analysis of FKBP51/FKBP52 Chimeras and Mutants for Hsp90 Binding and Association with Progesterone Receptor Complexes. *Molecular Endocrinology* 12:342–354. <https://doi.org/10.1210/mend.12.3.0075>
35. Bracher A, Kozany C, Thost A-K, Hausch F (2011) Structural characterization of the PPIase domain of FKBP51, a cochaperone of human Hsp90. *Acta Crystallogr D Biol Crystallogr* 67:549–559. <https://doi.org/10.1107/S0907444911013862>
36. Hähle A, Merz S, Meyners C, Hausch F (2019) The many faces of FKBP51. *Biomolecules* 9:. <https://doi.org/10.3390/biom9010035>
37. Cioffi DL, Hubler TR, Scammell JG (2011) Organization and function of the FKBP52 and FKBP51 genes. *Curr Opin Pharmacol* 11:308–313. <https://doi.org/10.1016/j.coph.2011.03.013>

38. Sinars CR, Cheung-Flynn J, Rimerman RA, et al (2003) Structure of the large FK506-binding protein FKBP51, an Hsp90-binding protein and a component of steroid receptor complexes. *Proc Natl Acad Sci U S A* 100:868–873. <https://doi.org/10.1073/pnas.0231020100>
39. Kästle M, Kistler B, Lamla T, et al (2018) FKBP51 modulates steroid sensitivity and NFκB signalling: A novel anti-inflammatory drug target. *Eur J Immunol* 48:1904–1914. <https://doi.org/10.1002/eji.201847699>
40. Han J-T, Zhu Y, Pan D-B, et al (2021) Discovery of pentapeptide-inhibitor hits targeting FKBP51 by combining computational modeling and X-ray crystallography. *Comput Struct Biotechnol J* 19:4079–4091. <https://doi.org/10.1016/j.csbj.2021.07.015>
41. Mustafi SM, LeMaster DM, Hernández G (2014) Differential conformational dynamics in the closely homologous FK506-binding domains of FKBP51 and FKBP52. *Biochemical Journal* 461:115–123. <https://doi.org/10.1042/BJ20140232>
42. Wochnik GM, Rüegg J, Abel GA, et al (2005) FK506-binding Proteins 51 and 52 Differentially Regulate Dynein Interaction and Nuclear Translocation of the Glucocorticoid Receptor in Mammalian Cells. *Journal of Biological Chemistry* 280:4609–4616. <https://doi.org/10.1074/jbc.M407498200>
43. Paakinaho V, Makkonen H, Jääskeläinen T, Palvimo JJ (2010) Glucocorticoid Receptor Activates Poised FKBP51 Locus through Long-Distance Interactions. *Molecular Endocrinology* 24:511–525. <https://doi.org/10.1210/me.2009-0443>
44. Bracher A, Kozany C, Hähle A, et al (2013) Crystal Structures of the Free and Ligand-Bound FK1–FK2 Domain Segment of FKBP52 Reveal a Flexible Inter-Domain Hinge. *J Mol Biol* 425:4134–4144. <https://doi.org/10.1016/j.jmb.2013.07.041>
45. Gaali S, Kirschner A, Cuboni S, et al (2015) Selective inhibitors of the FK506-binding protein 51 by induced fit. *Nat Chem Biol* 11:33–37. <https://doi.org/10.1038/nchembio.1699>
46. Kolos JM, Voll AM, Bauder M, Hausch F (2018) FKBP Ligands—Where We Are and Where to Go? *Front Pharmacol* 9. <https://doi.org/10.3389/fphar.2018.01425>
47. Feng X, Sippel C, Bracher A, Hausch F (2015) Structure–Affinity Relationship Analysis of Selective FKBP51 Ligands. *J Med Chem* 58:7796–7806. <https://doi.org/10.1021/acs.jmedchem.5b00785>
48. Feng X (2015) Rational Drug Design and Synthesis of Selective FKBP51 Ligands. Doctoral thesis, Ludwig-Maximilians-Universität München
49. Anderson JS, LeMaster DM, Hernández G (2023) Transient conformations in the unliganded FK506 binding domain of FKBP51 correspond to two distinct inhibitor-bound states. *Journal of Biological Chemistry* 105159. <https://doi.org/10.1016/j.jbc.2023.105159>
50. Voll AM, Meyners C, Taubert MC, et al (2021) Macrocyclic FKBP51 Ligands Define a Transient Binding Mode with Enhanced Selectivity. *Angewandte Chemie - International Edition* 60:13257–13263. <https://doi.org/10.1002/anie.202017352>
51. LeMaster DM, Mustafi SM, Brecher M, et al (2015) Coupling of conformational transitions in the N-terminal domain of the 51-kDa FK506-binding protein (FKBP51) near its site of interaction with the steroid receptor proteins. *Journal of Biological Chemistry* 290:15746–15757. <https://doi.org/10.1074/jbc.M115.650655>
52. Nussinov R, Tsai CJ (2013) Allostery in disease and in drug discovery. *Cell* 153:293–305. <https://doi.org/10.1016/j.cell.2013.03.034>
53. Peracchi A, Mozzarelli A (2011) Exploring and exploiting allostery: Models, evolution, and drug targeting. *Biochimica et Biophysica Acta (BBA) - Proteins and Proteomics* 1814:922–933. <https://doi.org/10.1016/j.bbapap.2010.10.008>

54. McMahon C, Baier AS, Pascolutti R, et al (2018) Yeast surface display platform for rapid discovery of conformationally selective nanobodies. *Nat Struct Mol Biol* 25:289–296. <https://doi.org/10.1038/s41594-018-0028-6>
55. Tanaka T, Williams RL, Rabbitts TH (2007) Tumour prevention by a single antibody domain targeting the interaction of signal transduction proteins with RAS. *EMBO J* 26:3250–3259. <https://doi.org/10.1038/sj.emboj.7601744>
56. Nizak C, Monier S, del Nery E, et al (2003) Recombinant Antibodies to the Small GTPase Rab6 as Conformation Sensors. *Science* (1979) 300:984–987. <https://doi.org/10.1126/science.1083911>
57. Gao J, Sidhu SS, Wells JA (2009) Two-state selection of conformation-specific antibodies. *Proceedings of the National Academy of Sciences* 106:3071–3076. <https://doi.org/10.1073/pnas.0812952106>
58. Davies CW, Oh AJ, Mroue R, et al (2022) Conformation-locking antibodies for the discovery and characterization of KRAS inhibitors. *Nat Biotechnol* 40:769–778. <https://doi.org/10.1038/s41587-021-01126-9>
59. Ahmad ZA, Yeap SK, Ali AM, et al (2012) scFv Antibody: Principles and Clinical Application. *Clin Dev Immunol* 2012:1–15. <https://doi.org/10.1155/2012/980250>
60. Chester K, Pedley B, Tolner B, et al (2004) Engineering Antibodies for Clinical Applications in Cancer. *Tumor Biology* 25:91–98. <https://doi.org/10.1159/000077727>
61. Goldenberg DM (2002) Targeted therapy of cancer with radiolabeled antibodies. *J Nucl Med* 43:693–713
62. Hudson PJ, Souriau C (2003) Engineered antibodies. *Nat Med* 9:129–134. <https://doi.org/10.1038/nm0103-129>
63. Colcher D, Pavlinkova G, Beresford G, et al (1998) Pharmacokinetics and biodistribution of genetically-engineered antibodies. *Q J Nucl Med* 42:225–41
64. Dana Jones S, Marasco WA (1998) Antibodies for targeted gene therapy: extracellular gene targeting and intracellular expression. *Adv Drug Deliv Rev* 31:153–170. [https://doi.org/10.1016/S0169-409X\(97\)00099-9](https://doi.org/10.1016/S0169-409X(97)00099-9)
65. Stipsanelli E, Valsamaki P (2005) Monoclonal antibodies: old and new trends in breast cancer imaging and therapeutic approach. *Hell J Nucl Med* 8:103–8
66. Hudson PJ (1999) Recombinant antibody constructs in cancer therapy. *Curr Opin Immunol* 11:548–557. [https://doi.org/10.1016/S0952-7915\(99\)00013-8](https://doi.org/10.1016/S0952-7915(99)00013-8)
67. Oriuchi N, Higuchi T, Hanaoka H, et al (2005) Current status of cancer therapy with radiolabeled monoclonal antibody. *Ann Nucl Med* 19:355–365. <https://doi.org/10.1007/BF03027399>
68. Tolmachev V, Orlova A, Nilsson FY, et al (2007) Affibody molecules: potential for in vivo imaging of molecular targets for cancer therapy. *Expert Opin Biol Ther* 7:555–568. <https://doi.org/10.1517/14712598.7.4.555>
69. Löfblom J, Feldwisch J, Tolmachev V, et al (2010) Affibody molecules: Engineered proteins for therapeutic, diagnostic and biotechnological applications. *FEBS Lett* 584:2670–2680. <https://doi.org/10.1016/j.febslet.2010.04.014>
70. Barozzi A, Lavoie RA, Day KN, et al (2020) Affibody-Binding Ligands. *Int J Mol Sci* 21:. <https://doi.org/10.3390/ijms21113769>
71. Häggblad Sahlberg S (2011) The effect of a dimeric Affibody molecule (ZEGFR:1907)₂ targeting EGFR in combination with radiation in colon cancer cell lines. *Int J Oncol*. <https://doi.org/10.3892/ijo.2011.1177>
72. Alavizadeh SH, Akhtari J, Badiie A, et al (2016) Improved therapeutic activity of HER2 Affibody-targeted cisplatin liposomes in HER2-expressing breast tumor models. *Expert Opin Drug Deliv* 13:325–336. <https://doi.org/10.1517/17425247.2016.1121987>
73. Frejd FY, Kim K-T (2017) Affibody molecules as engineered protein drugs. *Exp Mol Med* 49:e306–e306. <https://doi.org/10.1038/emm.2017.35>
74. Bogen JP, Grzeschik J, Krah S, et al (2020) Rapid Generation of Chicken Immune Libraries for Yeast Surface Display. In: *Methods Mol Biol*. pp 289–302

-
75. Benatuil L, Perez JM, Belk J, Hsieh CM (2010) An improved yeast transformation method for the generation of very large human antibody libraries. *Protein Engineering, Design and Selection* 23:155–159. <https://doi.org/10.1093/protein/gzq002>
 76. Wang Z, Ravi Kumar N, Srivastava DK (1992) A novel spectroscopic titration method for determining the dissociation constant and stoichiometry of protein-ligand complex. *Anal Biochem* 206:376–381. [https://doi.org/10.1016/0003-2697\(92\)90381-G](https://doi.org/10.1016/0003-2697(92)90381-G)
 77. Walters BT, Ricciuti A, Mayne L, Englander SW (2012) Minimizing Back Exchange in the Hydrogen Exchange-Mass Spectrometry Experiment. *J Am Soc Mass Spectrom* 23:2132–2139. <https://doi.org/10.1007/s13361-012-0476-x>
 78. Neta P, Simon-Manso Y, Yang X, Stein SE (2009) Collisional energy dependence of peptide ion fragmentation. *J Am Soc Mass Spectrom* 20:469–476. <https://doi.org/10.1016/j.jasms.2008.11.005>
 79. Sørensen L, Salbo R (2018) Optimized Workflow for Selecting Peptides for HDX-MS Data Analyses. *J Am Soc Mass Spectrom* 29:2278–2281. <https://doi.org/10.1007/s13361-018-2056-1>
 80. Cianfrocco MA, Wong-Barnum M, Youn C, et al (2017) COSMIC2. In: *Proceedings of the Practice and Experience in Advanced Research Computing 2017 on Sustainability, Success and Impact*. ACM, New York, NY, USA, pp 1–5
 81. Sivils JC, Storer CL, Galigniana MD, Cox MB (2011) Regulation of steroid hormone receptor function by the 52-kDa FK506-binding protein (FKBP52). *Curr Opin Pharmacol* 11:314–319. <https://doi.org/10.1016/j.coph.2011.03.010>
 82. Jagtap PKA, Asami S, Sippel C, et al (2019) Selective Inhibitors of FKBP51 Employ Conformational Selection of Dynamic Invisible States. *Angewandte Chemie International Edition* 58:9429–9433. <https://doi.org/10.1002/anie.201902994>
 83. Near RI, Shi Chung Ng, Mudgett-Hunter M, et al (1990) Heavy and light chain contributions to antigen binding in an anti-digoxin chain recombinant antibody produced by transfection of cloned anti-digoxin antibody genes. *Mol Immunol* 27:901–909. [https://doi.org/10.1016/0161-5890\(90\)90157-U](https://doi.org/10.1016/0161-5890(90)90157-U)
 84. Davies DR, Metzger H (1983) Structural Basis of Antibody Function. *Annu Rev Immunol* 1:87–115. <https://doi.org/10.1146/annurev.iy.01.040183.000511>
 85. Novotný J, Brucoleri R, Newell J, et al (1983) Molecular anatomy of the antibody binding site. *J Biol Chem* 258:14433–7
 86. Narayanan A, Sellers BD, Jacobson MP (2009) Energy-Based Analysis and Prediction of the Orientation between Light- and Heavy-Chain Antibody Variable Domains. *J Mol Biol* 388:941–953. <https://doi.org/10.1016/j.jmb.2009.03.043>
 87. Nakanishi T, Tsumoto K, Yokota A, et al (2008) Critical contribution of VH-VL interaction to reshaping of an antibody: The case of humanization of anti-lysozyme antibody, HyHEL-10. *Protein Science* 17:261–270. <https://doi.org/10.1110/ps.073156708>
 88. Tan PH, Sandmaier BM, Stayton PS (1998) Contributions of a Highly Conserved VH/VL Hydrogen Bonding Interaction to scFv Folding Stability and Refolding Efficiency. *Biophys J* 75:1473–1482. [https://doi.org/10.1016/S0006-3495\(98\)74066-4](https://doi.org/10.1016/S0006-3495(98)74066-4)
 89. Stanfield RL, Takimoto-Kamimura M, Rini JM, et al (1993) Major antigen-induced domain rearrangements in an antibody. *Structure* 1:83–93. [https://doi.org/10.1016/0969-2126\(93\)90024-B](https://doi.org/10.1016/0969-2126(93)90024-B)
 90. Pomplun S, Sippel C, Hähle A, et al (2018) Chemogenomic Profiling of Human and Microbial FK506-Binding Proteins. *J Med Chem* 61:3660–3673. <https://doi.org/10.1021/acs.jmedchem.8b00137>
 91. Lerma Romero J, Meyners C, Rupp N, et al (2023) A protein engineering approach towards understanding FKBP51 conformational dynamics and mechanisms of ligand binding. *PEDS Accepted*

-
92. Dumoulin M, Last AM, Desmyter A, et al (2003) A camelid antibody fragment inhibits the formation of amyloid fibrils by human lysozyme. *Nature* 424:783–8. <https://doi.org/10.1038/nature01870>
 93. Vanderhaegen S, Fislage M, Domanska K, et al (2013) Structure of an early native-like intermediate of β 2-microglobulin amyloidogenesis. *Protein Sci* 22:1349–57. <https://doi.org/10.1002/pro.2321>
 94. Lawson A (2014) Antibody Fragments Defining Biologically Relevant Conformations of Target Proteins. *Antibodies* 3:289–302. <https://doi.org/10.3390/antib3040289>
 95. Nehls T, Heymann T, Meyners C, et al (2021) Fenton-Chemistry-Based Oxidative Modification of Proteins Reflects Their Conformation. *Int J Mol Sci* 22:9927. <https://doi.org/10.3390/ijms22189927>

Supplement

Primers

Table S1. Primers

Primer	Forward (fw) primer 5'-3'
pCT_seq_up	TACCCATACGACGTTCCAGACTAC
pCT_seq_lo	CAGTGGGAACAAAGTCGATTTTGTTAC
VH_gr_up	GGTGGTGGTGGTTCTGGTGGTGGTGGTTCTGCTAGCGCCG TGACGTTGGACGAG
VH_SOE_lo	TCCGCCCCCGACCCGCCGCCCTGAGCCGCCTCCCCGGAG- GAGACGATGACTTCGGT
VL_SOE_up	GGCGGCTCAGGCGGCGGGTTCGGGGGGCG- GAGGGAGCGCGCTGACTCAGCCGTCCTCG
VL_gr_lo	CAAGTCCTCTTCAGAAATAAGCTTTTGTTTCGGATCCTAGGAC- GGTCAGGGTTGTCCC
scFv_chick_his_TEV_NdeI_up	ATATATCATATGATGGCTCACCACCACCACCACCGA- GAATCTTTATTTTCAATCAGGGTCTGCTAGCGCCGTGACGTT GGACGAGTCCG
scFv_chick_SII_TEV_NotI_lo	GAGTGCGGCCG- CATCATCATTTTTTCGAACTGCGGGTGGCTCCATGATTGAAAA TAAAGATTCTCAGACCCTAGGACGGTCAGGGTTG
PALU 87F	ATCGGTGATGTCGGCGATAT
PALU 88R	GCTAGTTATTGCTCAGCGGTG
PALU 103F	AGGAGATATCATATGGTGGATAACAAATTC
PALU 104R	TAGACGAGTCCATTAATGGTGGTGGTGA
pBAD_Fw	ATG CCA TAG CAT TTT TAT CC

Plasmids

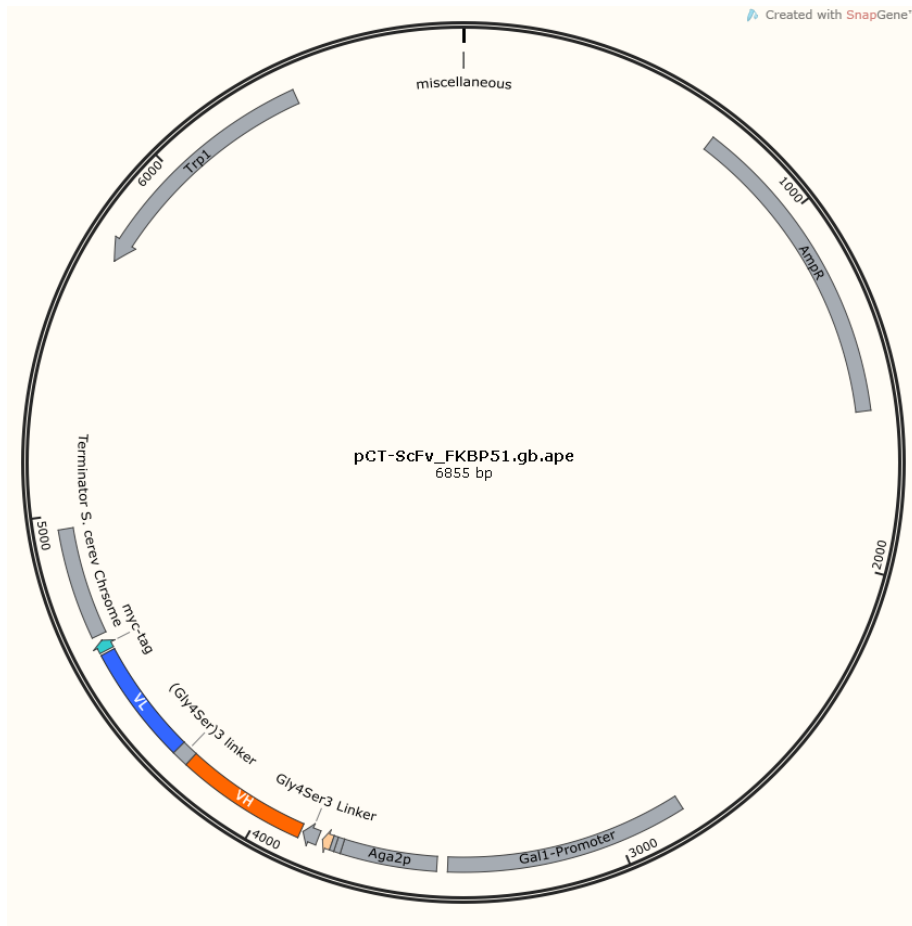


Figure S1. Plasmid map of the Yeast pCT_ScFv vector. The plasmid contains a tryptophan auxotroph gene for yeast selection, an ampicillin resistance gene for bacterial selection, BamHI and NheI restriction sites for gap repair cloning of the gene of interest, an Aga2p gene for the surface presentation of the protein of interest and a Myc-tag to verify the correct protein expression.

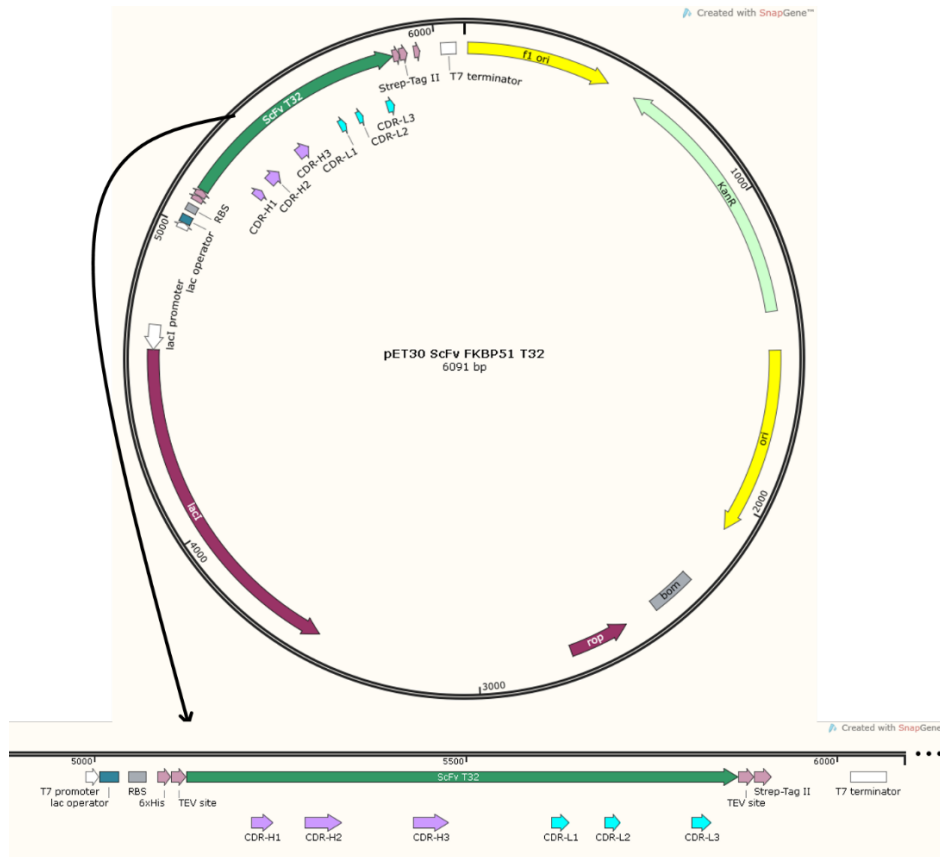


Figure S2. Plasmid map of the pET30_ScFv_FKBP51 T32. The plasmid contains a kanamycin resistance gene for bacterial selection, T7 promoter, and lac repressor gene lacI for IPTG induction of the protein of interest (T32 scFv). Two TEV sites allow the cleavage of the 6XHis and Strep-II purification tags.

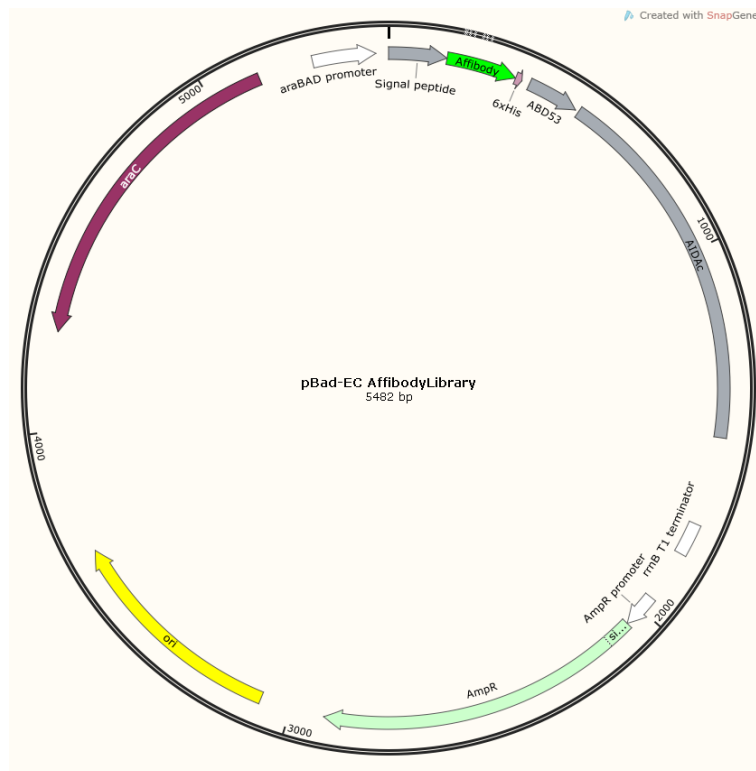


Figure S3. Plasmid map of the pBAD_EC coding for an affibody. The plasmid contains an ampicillin resistance gene for bacterial selection, araBAD promoter, for L-arabinose induction and AIDA transport system to facilitate transportation to the surface



Figure S4. Plasmid map of the pET45b+ for bacterial affibody expression. The plasmid contains an ampicillin resistance gene for bacterial selection, T7 promoter, and lac repressor gene lacI for IPTG induction of the protein of interest with a 6XHis as purification tag.

Ligands and tracers

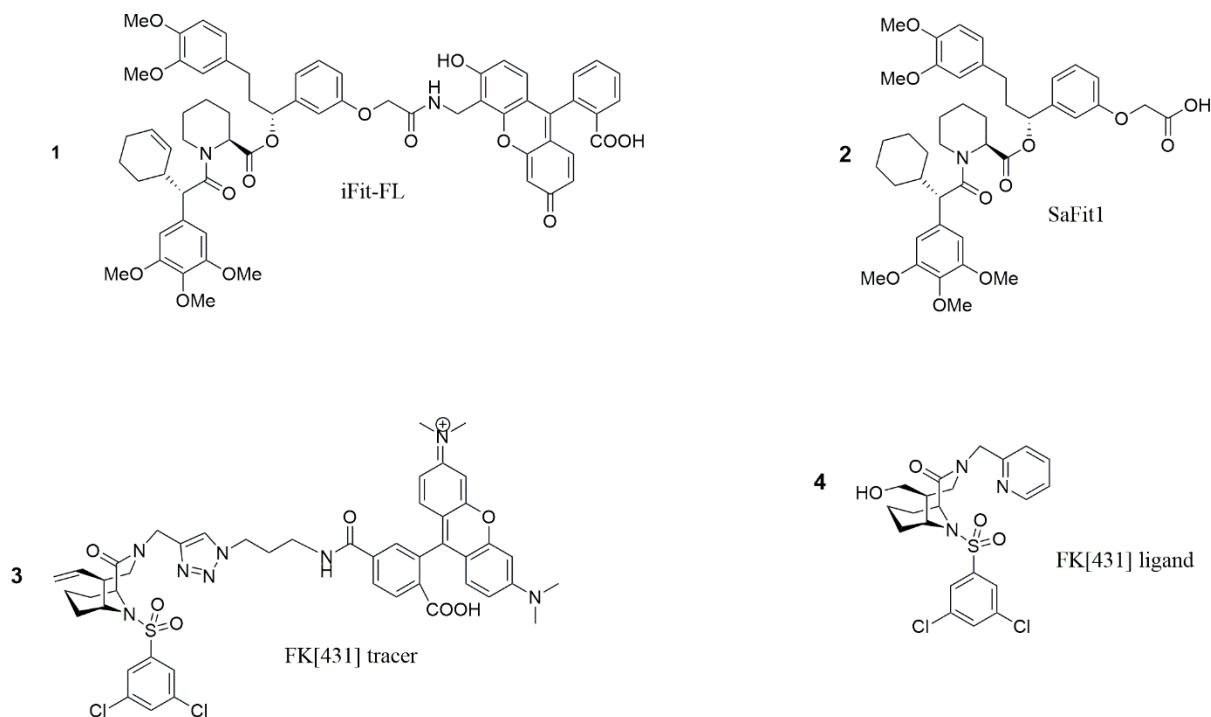


Figure S5: Chemical structure of the FKBP51 ligands and tracers. The FKBP51-selective ligand SAFit1 (2) [45], and its fluorescein conjugated analog of the SAFit-FL (1). Besides, the canonical FKBP inhibitor FK[431] ligand (4) [90] and its TAMRA conjugates tracer (3)

Flow cytometry, fluorescence polarization and BLI

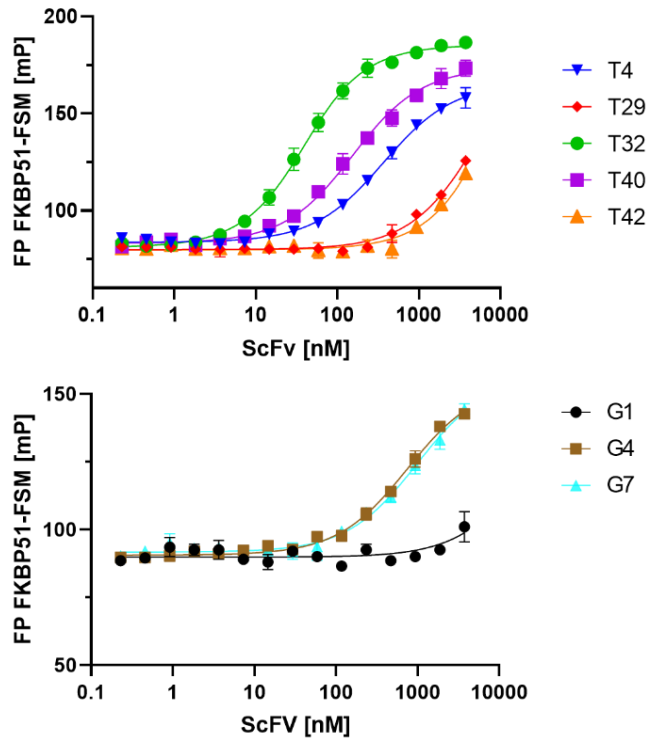


Figure S6. Affinity determination of conformation-locking and FKBP51 binding scFvs via fluorescence polarization

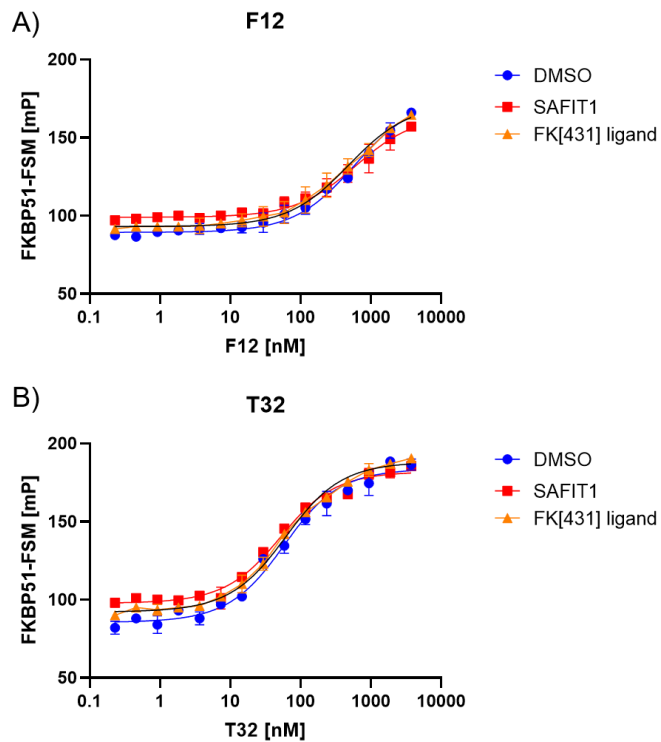


Figure S7. Binding of scFvs to FKBP51-SAFit1 or FKBP51-FK[431] ligand complex via fluorescence polarization

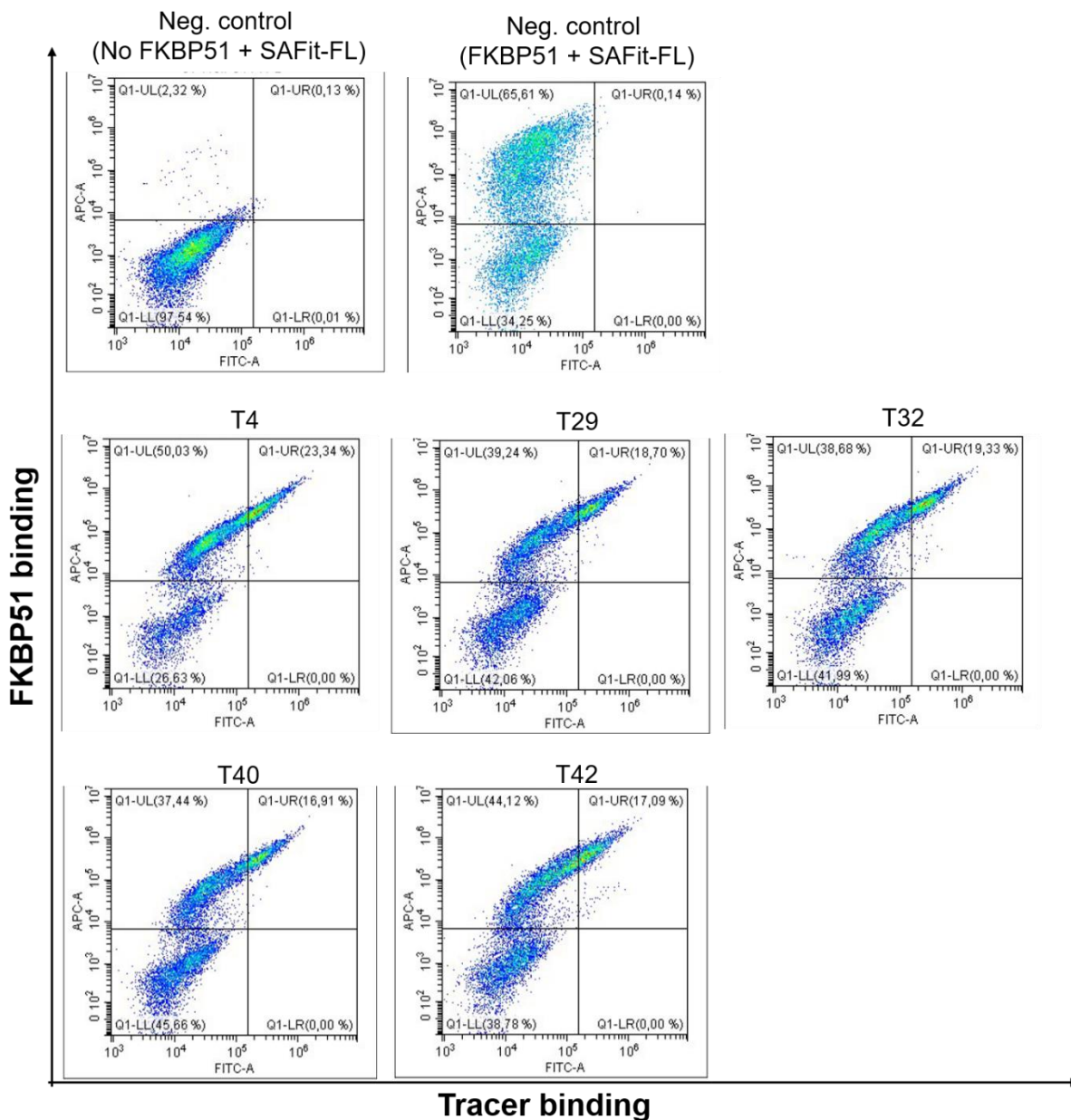


Figure S8. Dot-plots of the scFvs YSD single clones identified from the conformation stabilizing sorting for FKBP51. The data was recorded in a flow cytometer, and the single clones were selected due to the overall population shift into the established gate where cells showing both FKBP51 binding signal (APC/PE-streptavidin) and SAFit-FL signal.

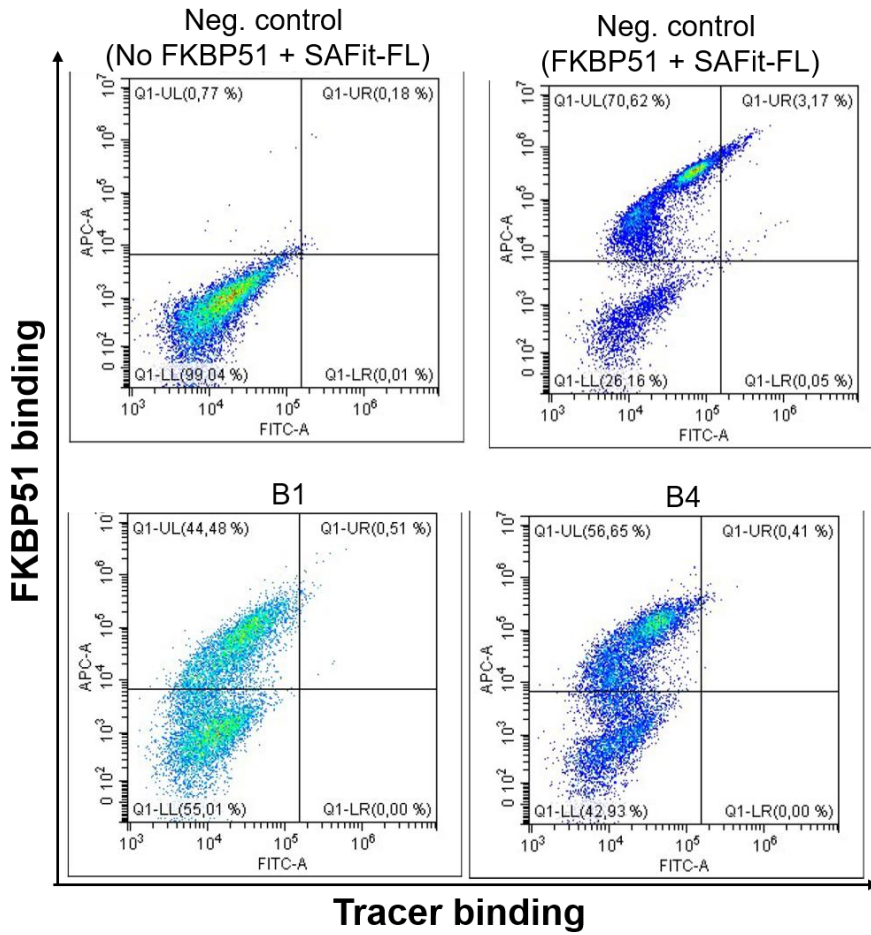


Figure S9. Dot-plots of the scV's YSD single clones identified from the blocking scV sorting for FKBP51. The data was recorded in a flow cytometer, and the single clones were selected due to the reduced population shift into the traced binding quadrant while still presenting FKBP51 binding signal (APC/PE-streptavidin).

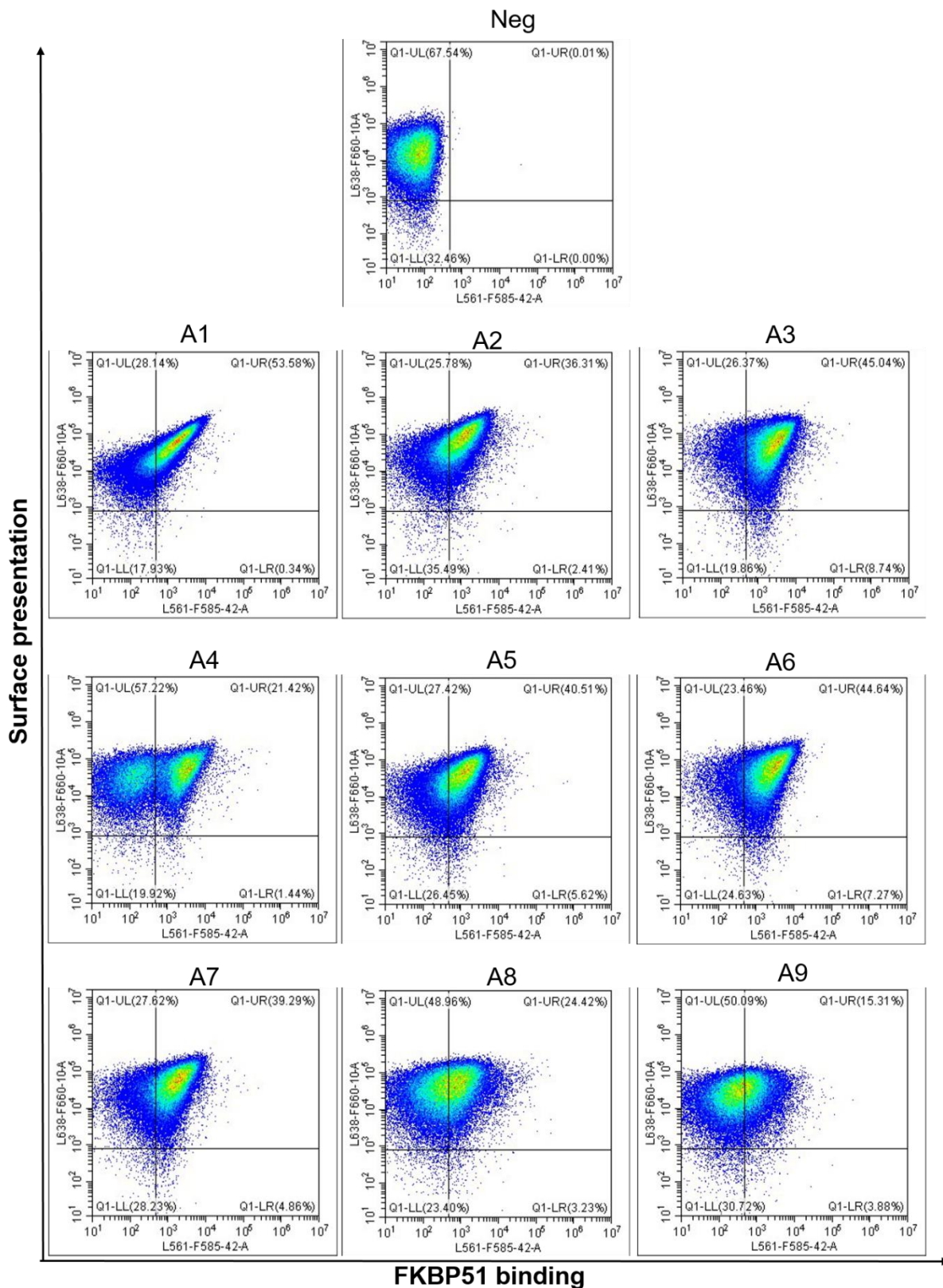


Figure S10. Dot-plots of *E. coli* single clone displaying affibodies found from the high-affinity binders sorting for FKBP51. The data was recorded in a flow cytometer, and the single clones were selected due to the overall population shift into the established gate where cells exhibit both surface presentation (ABD detection) and FKBP51 binding signal.

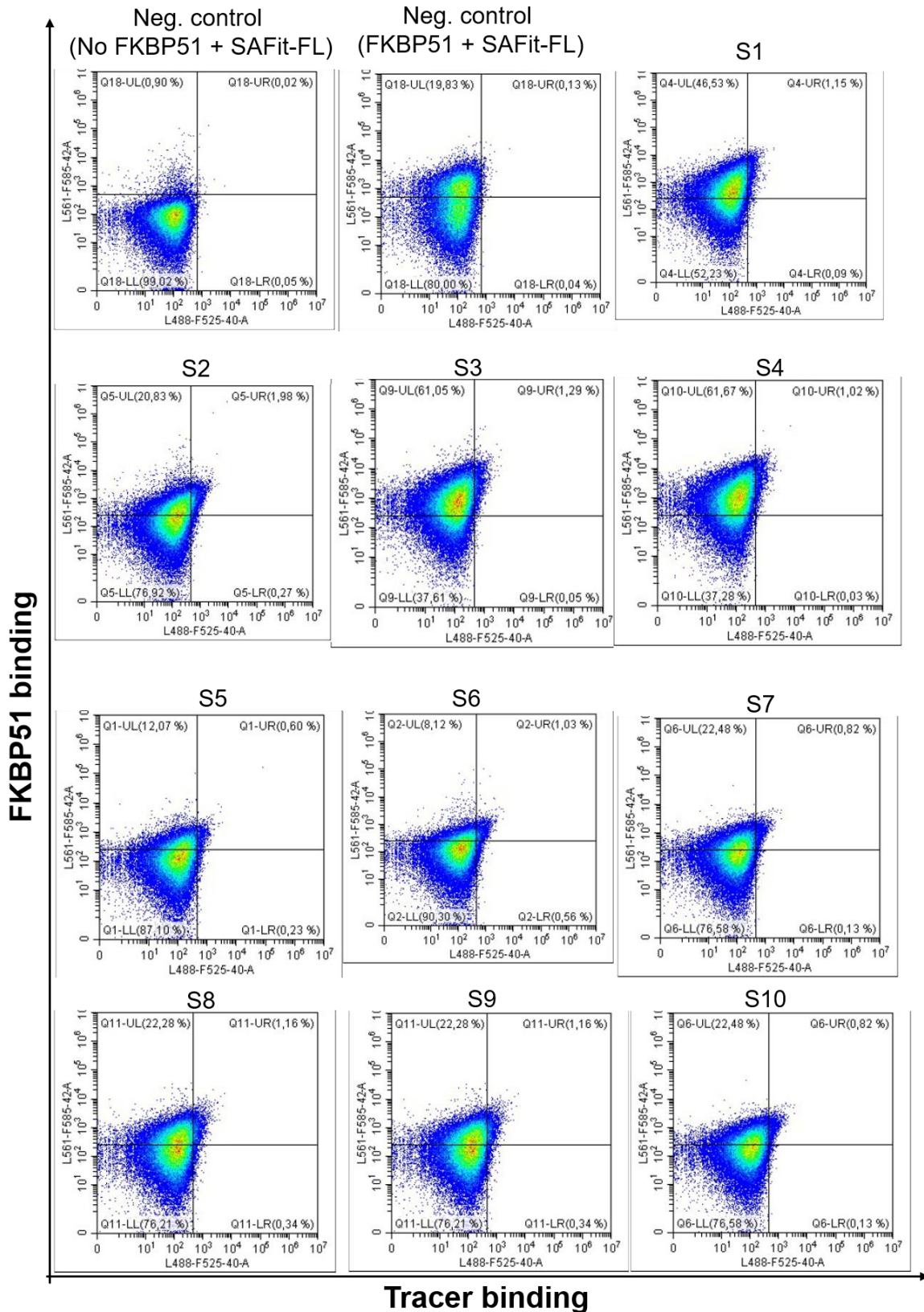


Figure S11. Dot-plots of *E. coli* single clone displaying affibodies found from the ligand dependent selection (1/2). The data was recorded in a flow cytometer, and the single clones were selected due to the overall population shift into the established gate where cells exhibit both FKBP51 binding signal and SAFit-FL signal.

FKBP51 binding

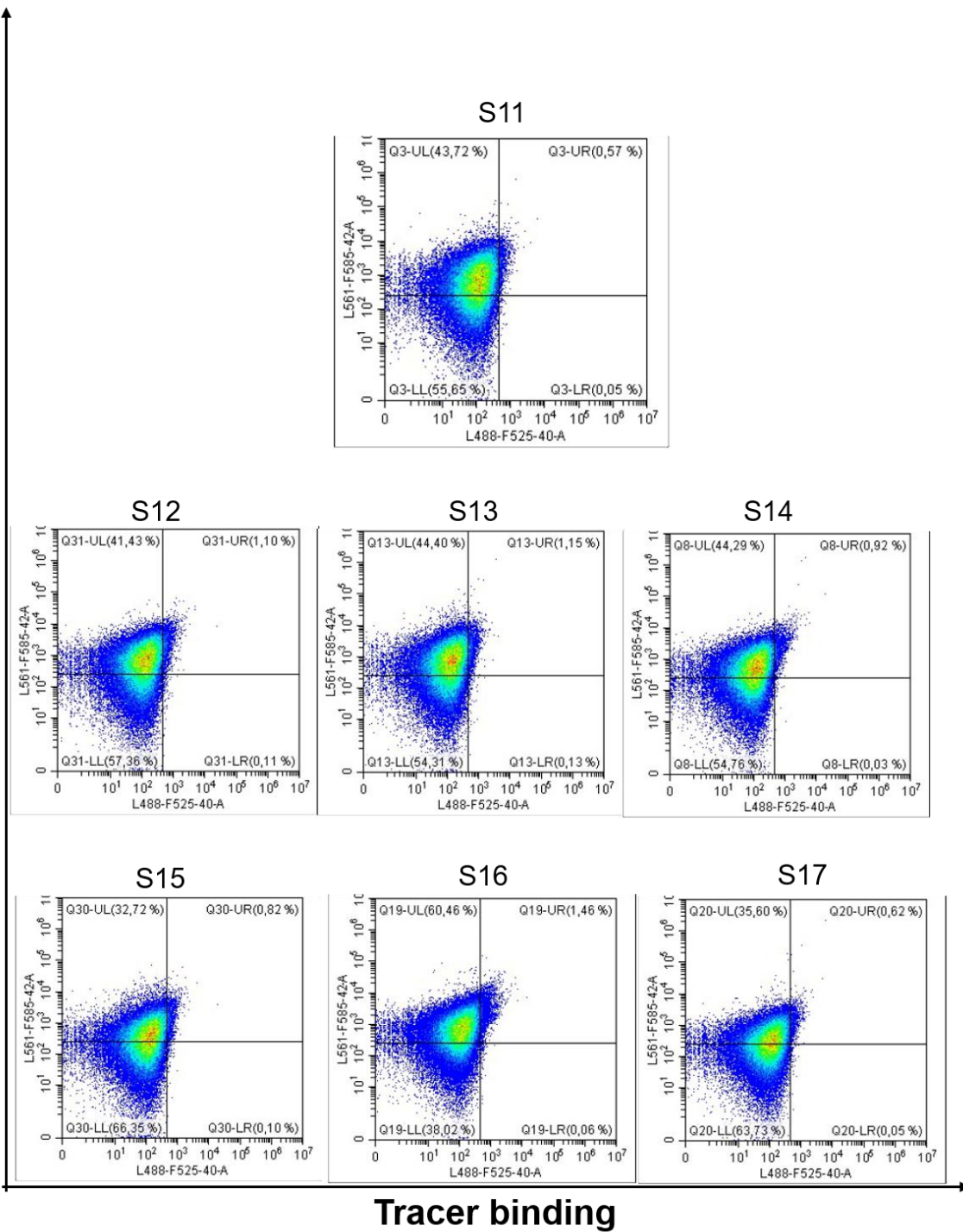


Figure S12. Dot-plots of *E. coli* single clone displaying affibodies found from the ligand dependent selection (2/2). The data was recorded in a flow cytometer, and the single clones were selected due to the overall population shift into the established gate where cells exhibit both FKBP51 binding signal and SAFit-FL signal.

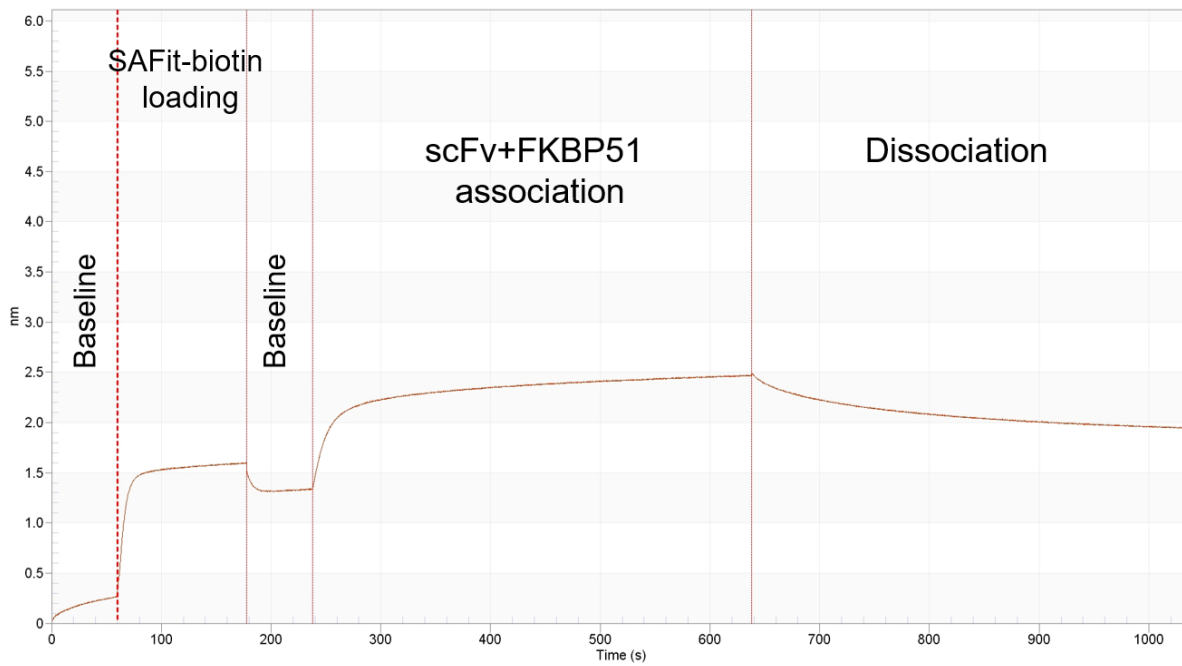


Figure S13. BLI plot demonstrating that the small molecule SAFit-biotin produces a signal on the loading step of the experiment. Layer thickness increases up to approximately 1.5 nm after ~100 seconds after a SAX tip is loaded in 300 nM of SAFit-biotin.

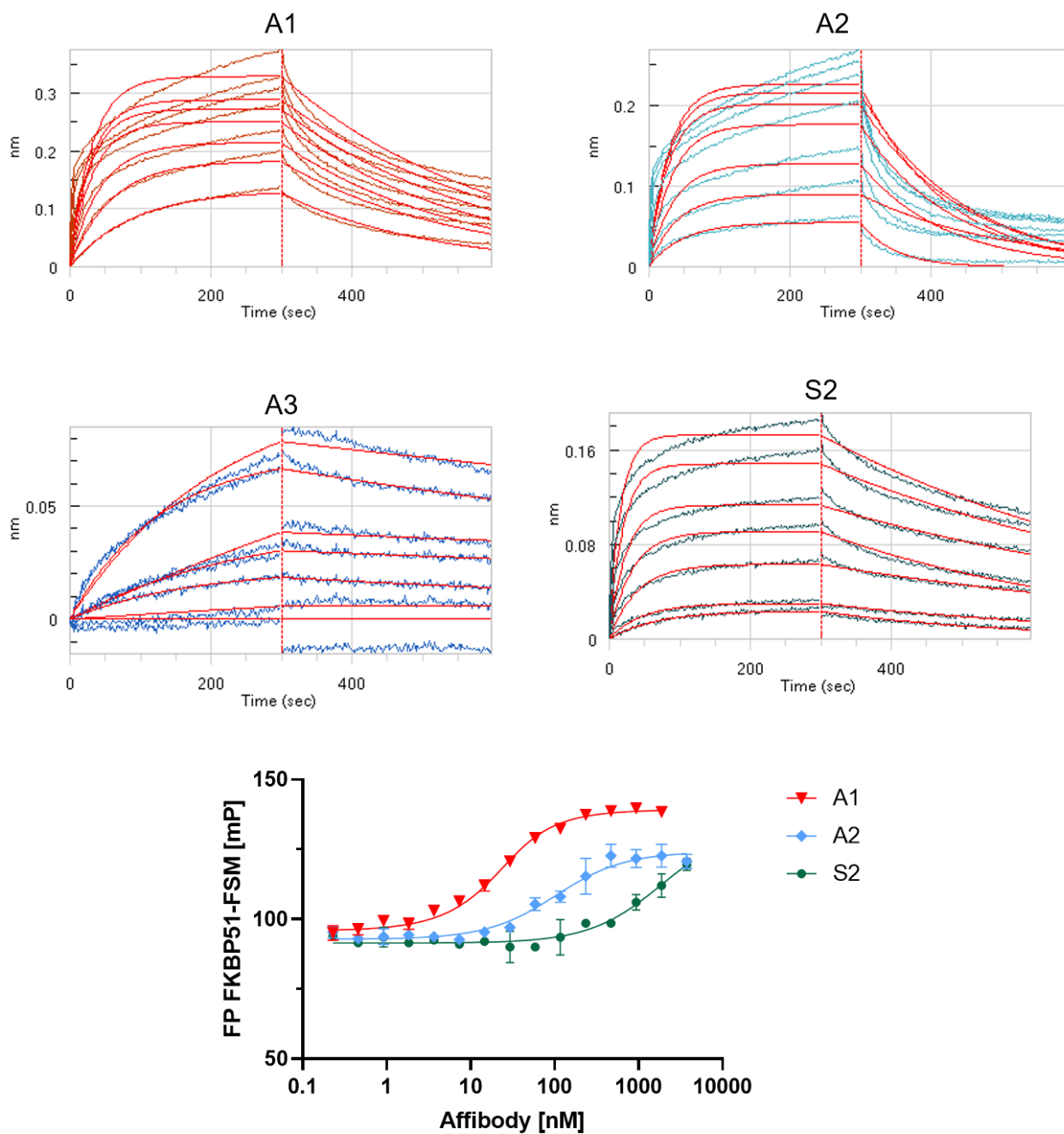


Figure S14. Affinity determination of affibodies via BLI and FP

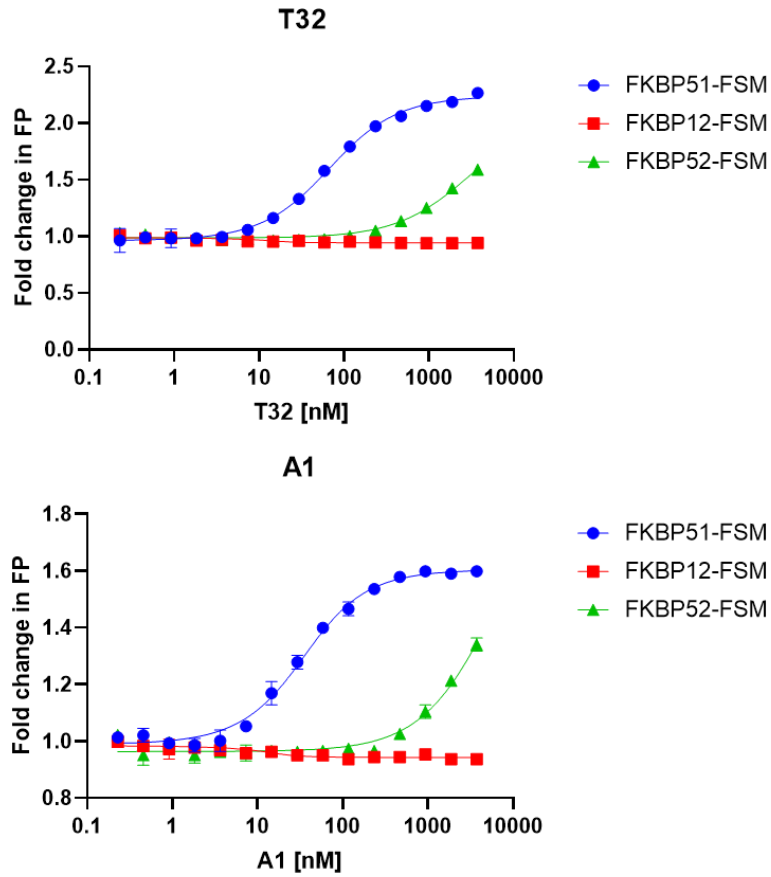


Figure S15. Binding kinetics determination of T32 scFv and A1 affibody to FKBP52 and FKBP12 compared to FKBP51. Both biomolecules are specific to FKBP51 with low or no affinity to FKBP52 and FKBP12

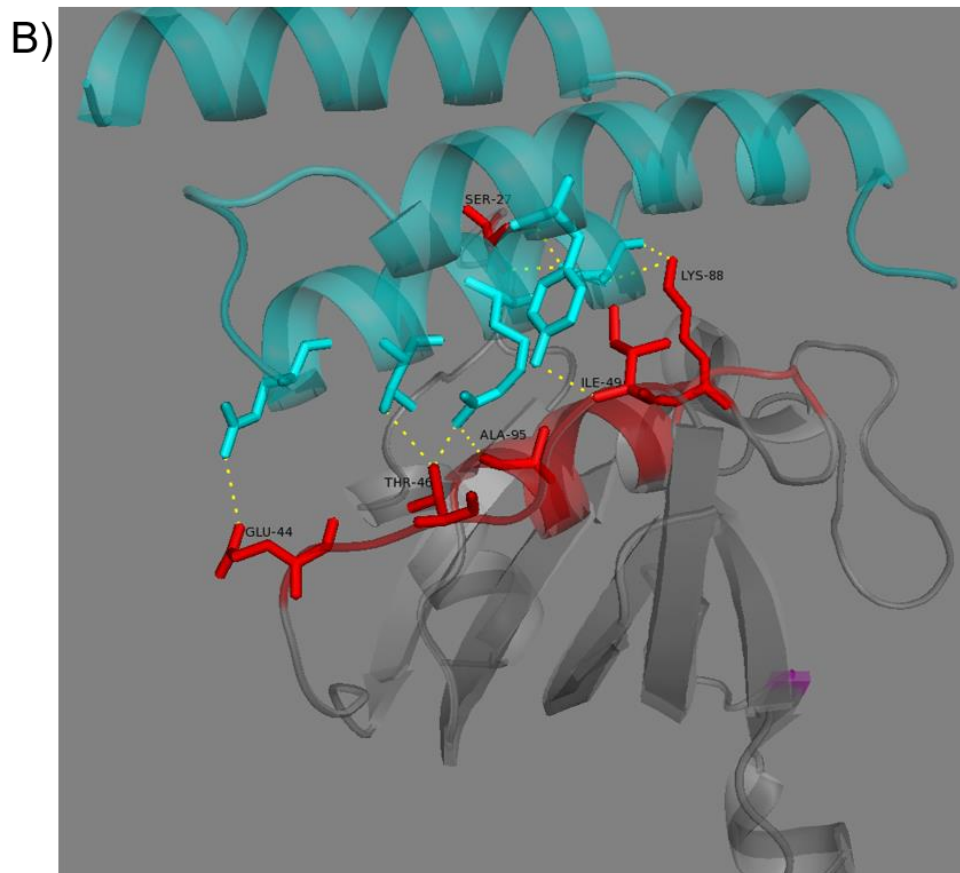
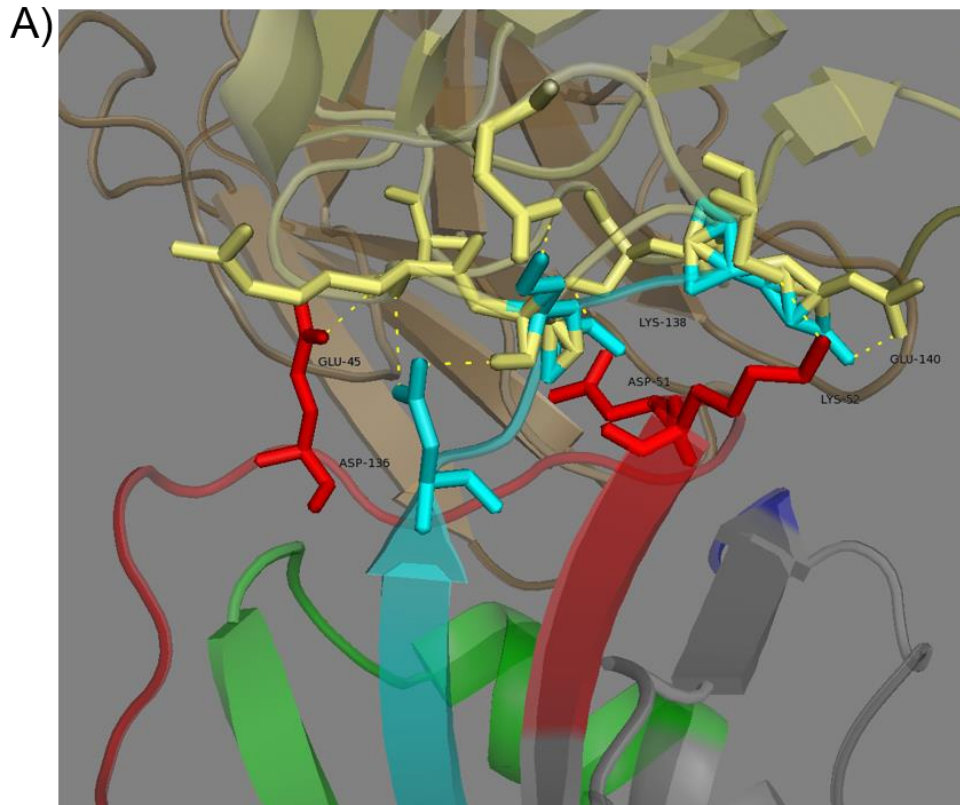


Figure S16. Contact bond residues between the FK1 domain of FKBP51 and A) T32 scFv or B)S2 affibody determined by analysis of protein-protein molecular docking computed with the ColabFold tool of COSMIC2.

5 Acknowledgments

In the following section, I would like to express my deepest gratitude to the extraordinary people who supported and mentored me throughout this journey, enabling me to successfully obtain my doctoral title.

First and foremost, I would like to thank Prof. Dr. Harald Kolmar for allowing me to pursue my doctoral degree in your working group. Thank you for your trust in me during my time in the laboratory, and for your invaluable advice, continuous support, and patience. I appreciate the time and effort you invested in guiding me during my time here. I am especially grateful to you for encouraging me to take the research stay in Sweden. It was an invaluable experience that would not have happened without you.

I would like to offer my special thanks to Prof. Dr. Felix Hausch. All my research was a highly cooperative work between the Kolmar and Hausch working groups, and it would not have been possible without your help, support, and experience. Likewise, I would like to thank Dr. Christian Meyners for your assistance at every stage of my research project in the areas of fluorescence polarization and protein crystallization. I learned a lot from our collaboration and I am deeply thankful for your time and effort.

I would like to extend my sincere gratitude to Prof. Dr. Torbjörn Gräslund and all the people from the Division of Protein Engineering of the KTH Royal Institute of Technology in Stockholm, where I worked as a visiting Ph.D. for three months. Thank you for welcoming me into your lab, for your help and support with my experiments, and for the friendly atmosphere. It was an incredible time that I will never forget!

I am deeply grateful to Dr. Stefania Candela Carrara and Dominic Happel, for your insightful comments and suggestions when I had trouble with my experiments. Your experience and knowledge helped me to find a solution and move my research forward. I had a great time with you in the lab and during coffee or beer breaks after work.

To my colleagues and friends: Dr. Hendrick Schneider, Dr. Simon Englert, Dr. Ataurehman Ali, Dr. Arturo Macarrón Palacios, Dominic Happel, Jordi Pfeifer Serrahima, Dr. Steffen Hinz and Jan Habermann. Thank you for your advice and assistance with my work, but especially for all the fun moments in and outside the lab, happy and sad tequilas, great vacations together, and R6/COD/Overwatch nights.

I would like to express my gratitude to Dr. Sebastian Bitsch, Peter Bitsch, Dr. Jan Bogen, Carolin Dombrowsky, Katrin Schoenfeld, Julia Harwardt, Britta Lipinski, Sarah Hofmann, Alessandro Emmanuello, Ingo Bork, Dr. Adrian Elter, Michael Ullitzka, Felix Geyer, Felix Meiser, Lieke van Gijzel, and the whole AK Kolmar for their support at every stage of my research and for the memorable moments we shared at KWT, PEGS and in the lab.

I would like to thank Dr. Andreas Chistmann for your guidance and introduction to yeast display and FACS operation. Barbara Diestelmann, Dipl.-Chem. Dana Schmidt, Cecilia Gorus, Dr. Olga Avrutina, and Janine Becker, thanks for the organization and assistance in the laboratory and the working group.

To the Bachelor and Master students I supervised, Lisa Reinbold, Nicole Rupp, Janne Kühner, and David Rivic, thank you for your hard work and collaboration. I hope you gained some knowledge from our work together and I wish you all the best in your future endeavors.

Thanks to the Graduate School Life Science Engineering for the funding and organization of all the additional activities, seminars, and courses that contributed to my formation. In the same way, I would like to thank all the PIs and students of the Graduate School LSE and the TRABITA consortium for sharing your interesting research, and for your suggestions or experimental contributions to my project.

Por último, me gustaría agradecer a mi familia Jorge Lerma Nava, Aída Romero Sánchez, Aída Lerma Romero. Gracias por su apoyo incondicional, por motivarme a perseguir mis metas y por todos sus esfuerzos y sacrificios para poner mi éxito personal y profesional por encima de todo. A mi familia y Lyssa Ginther, gracias por su paciencia y por comprender que este reto que consumió mi tiempo y energía durante los últimos tres años era una de mis mayores aspiraciones. No ha sido un camino fácil y estoy muy agradecido de tenerlos a todos a mi lado. No podría haberlo logrado sin su apoyo.

6 Curriculum Vitae

Name: Jorge Alberto Lerma Romero
Birth place: Mexico City, Mexico
Nationality: Mexican

Education

Doctoral student - Technische Universität Darmstadt June 2020 – December 2023
PhD candidate at the Clemens-Schöpf-Institute for Organic Chemistry and Biochemistry under the direction of Prof. Dr. Harald Kolmar.

M.Sc. in Industrial and Pharmaceutical Biotechnology – October 2017- November 2019
Martin-Luther-Universität Halle-Wittenberg
Master thesis completed at the Fraunhofer Institute for Cell Therapy and Immunology under supervision of Prof. Dr. Stephan Schilling: Optimization of expression and stability of antibodies against the β -amyloid peptide. Final grade: 1,2

B.Sc. in Biotechnological Engineering – Instituto Politécnico Nacional – UPIIG (México) August 2015 - January 2016
Bachelor thesis completed at the Universidad de Guanajuato under the supervision of Dr. Gustavo Basurto Islas: Chemical synthesis of nanomaterials and biological tests for Alzheimer's disease treatment

7 Erklärung laut Promotionsordnung

§8 Abs. 1 lit. c der Promotionsordnung der TU Darmstadt

Ich versichere hiermit, dass die elektronische Version meiner Dissertation mit der schriftlichen Version übereinstimmt und für die Durchführung des Promotionsverfahrens vorliegt.

§8 Abs. 1 lit. d der Promotionsordnung der TU Darmstadt

Ich versichere hiermit, dass zu einem vorherigen Zeitpunkt noch keine Promotion versucht wurde und zu keinem früheren Zeitpunkt an einer in- oder ausländischen Hochschule eingereicht wurde. In diesem Fall sind nähere Angaben über Zeitpunkt, Hochschule, Dissertationsthema und Ergebnis dieses Versuchs mitzuteilen.

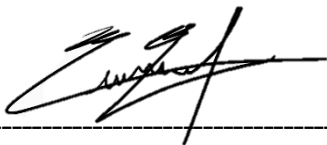
§9 Abs. 1 der Promotionsordnung der TU Darmstadt

Ich versichere hiermit, dass die vorliegende Dissertation selbstständig und nur unter Verwendung der angegebenen Quellen verfasst wurde.

§9 Abs. 2 der Promotionsordnung der TU Darmstadt

Die Arbeit hat bisher noch nicht zu Prüfungszwecken gedient.

Darmstadt, den 08 November 2023



Jorge Alberto Lerma Romero



DECLARATION ON OWN CONTRIBUTION TO PUBLICATIONS

In the following you will find a list of the percentage of publications I have been involved in.

My share in the following publication is 80%.

[1] *Erma Romero, J. A., Meyners, C., Christmann, A., Reinbold, L. M., Charalampidou, A., Hausch, F., & Kolmar, H. (2022). Binding pocket stabilization by high-throughput screening of yeast display libraries. Frontiers in Molecular Biosciences, 9, 1023131. <https://doi.org/10.3389/fmolb.2022.1023131>*


My share in the following publication is 90%.

[2] *Erma Romero, Jorge & Kolmar, Harald. (2023). Accessing Transient Binding Pockets by Protein Engineering and Yeast Surface Display Screening. Methods in molecular biology (Clifton, N.J.). 2681. 249-274. 10.1007/978-1-0716-3279-6_14.*

My share in the following publication is 90% (accepted for publication).

[3] *Erma Romero JA, Meyners C, Rupp N, Hausch F, Kolmar H (2023). A protein engineering approach towards understanding FKBP51 conformational dynamics and mechanisms of ligand binding. PEDS, accepted.*

Date 16.10.2023



Signature of applicant



DECLARATION ON THE REVIEW OF PUBLICATIONS

Prof. Dr. Harald Kolmar
Referee

Prof. Dr. Felix Hausch
Co-Referee

16.10.2023
date

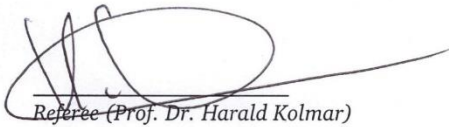
Neither referee (Prof. Dr. Harald Kolmar) nor co-referee (Prof. Dr. Felix Hausch) of this cumulative doctoral thesis were involved in the review of the following publications:

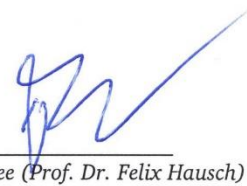
[1] Lerma Romero, J. A., Meyners, C., Christmann, A., Reinbold, L. M., Charalampidou, A., Hausch, F., & Kolmar, H. (2022). Binding pocket stabilization by high-throughput screening of yeast display libraries. *Frontiers in Molecular Biosciences*, 9, 1023131. <https://doi.org/10.3389/fmolb.2022.1023131>

[2] Lerma Romero, Jorge & Kolmar, Harald. (2023). Accessing Transient Binding Pockets by Protein Engineering and Yeast Surface Display Screening. *Methods in molecular biology (Clifton, N.J.)*. 2681. 249-274. 10.1007/978-1-0716-3279-6_14.

[3] Lerma Romero JA, Meyners C, Rupp N, Hausch F, Kolmar H (2023). A protein engineering approach towards understanding FKBP51 conformational dynamics and mechanisms of ligand binding. *PEDS*, accepted.

Date 16.10.23


Referee (Prof. Dr. Harald Kolmar)


Co-Referee (Prof. Dr. Felix Hausch)

